U.S. Department of Energy

OCGEN® MODULE MOORING PROJECT
DE-EE0002650

FINAL TECHNICAL REPORT
February 6, 2015

Ocean Renewable Power Company, LLC
66 Pearl Street, Suite 301
Portland, ME 04101
Phone (207) 772-7707
www.orpc.co

CONTENTS

1. EXECUTIVE SUMMARY 3
1.1 How the Research Adds to the Understanding of the Area Investigated 3
1.2 Technical Effectiveness and Economic Feasibility of Methods or Techniques Investigated or Demonstrated 4
1.3 How Project is of Benefit to the Public 4
2. COMPARISON OF ACTUAL ACCOMPLISHMENTS WITH THE GOALS AND OBJECTS OF THE PROJECT 5
3. PROJECT ACTIVITIES 12
3.1 Task 1: Modeling of Loads on Mooring System 12
3.2 Task 2: Dynamic Stability Analysis 16
3.3 Task 3: Dynamic Analysis of Mooring System Lines 23
3.4 Task 4: Scale Model Testing 29
3.5 Task 5: Geophysical Surveys 34
3.6 Task 6: Cable and Anchor Design 46
3.7 Task 7: Experimental Mooring of a Prototype OCGen® Unit 57
3.8 Task 8: Design of OCGen® Module Mooring System 129
4. PRODUCTS 150
4.1 Publications 150
4.2 Website 151
4.3 Networks or Collaborations 151
4.4 Technologies 151
4.5 Inventions 151
4.6 Other Products 151
5. COMPUTER MODELING 152
6. LESSONS LEARNED 153
7. PLANS TO ADDRESS LESSONS LEARNED 155

FINAL TECHNICAL REPORT

Award Number: EE0002650
Recipient: Ocean Renewable Power Company
Project title: OCGen® Module Mooring Project
Project Investigator: Jarlath McEntee

1. EXECUTIVE SUMMARY

Ocean Renewable Power Company, LLC (ORPC) has successfully completed all tasks of the OCGen® Module Mooring Project (Project).The Project made a significant step in the development of designs, methodologies and practices related to floating and mooring of marine hydrokinetic (MHK) devices. Importantly for ORPC, the Project provided a sound basis for moving forward with a technically and commercially viable OCGen® Power System. The OCGen® Power System is unique in the MHK industry and, in itself, offers distinct advantages of MHK devices that are secured to the seabed using fixed structural frames. Foremost among these advantages are capital and operating cost reductions and increased power extraction by allowing the device to be placed at the most energetic level of the water column.

1.1 How the Research Adds to the Understanding of the Area Investigated

This Project provided an extensive research, design, development, testing and data collection effort and analysis conducted with respect to a positively buoyant, submerged MHK device secured to the seabed using a tensioned mooring system. Although the Project was based on ORPC's OCGen® Power System, it has wide applicability to other MHK systems and other ocean-based technologies, including offshore oil and gas.

Different analytic tools were evaluated for their utility in the design of submerged systems and their moorings. Each of three analytical approaches was evaluated, including basic computation fluid dynamics (CFD), bespoke lumped-parameter modeling efforts, and use of commercial mooring CFD analysis codes. These analytical efforts were supported by a limited scale model test effort. Comparisons of the utility of each approach are provided. Commercial mooring codes offer significant advantages over the other approaches, in that a well developed and validated code offers higher confidence in the analysis results. Scale model testing was shown to have been qualitatively valuable in selected mooring configurations in a rapid and efficient manner.

Deployment and testing of a prototype OCGen® system provided significant data related to mooring line loads and system attitude and station keeping. Mooring line loads were measured in situ and reported against flow speeds. The data set generated was one of the few data sets available for such mooring systems. The data will prove useful for additional validation work of newer design approaches.

1.2 Technical Effectiveness and Economic Feasibility of Methods or Techniques Investigated or Demonstrated

The most important overall measure of the technical and economic effectiveness of the methods and techniques used in the Project was the full demonstration of the stability of the OCGen® device in reversing tidal currents and the efficacy of the tensioned mooring system. There was no doubt after completion of this Project, that the basic design assumptions of ORPC's OCGen® Power System have been technically and operationally proven and that the costs associated with the tensioned mooring system are significantly less than those incurred in ORPC's fixed frame power system, the TidGen® Power System.

Capital costs for the mooring system were proved to be significantly less than for fixed bottom frame systems. Costs of concrete and welded steel anchors were lower than the cost of construction for the tubular space frame structures used for the TidGen® device. While overall masses may be equivalent between the anchors for OCGen® and bottom support frame of the TidGen® device, the mass for the OCGen® anchors was mostly concrete as opposed to high quality steel. Costs of mooring lines were small compared to other project costs.

Installation costs for the buoyancy OCGen® system were much lower than for a piled foundation used for the TidGen® Power System. Installation for the TidGen® Power System would not be expected to be less than ten days of on-water work at the deployment site, with expensive lift and barge assets. Deployment of the OCGen® system took place in two days, with the majority of the assembly work being conducted in protected near shore environments. Actual deployment of the system at the site took approximately six hours.

Combined capital and installation costs for a full scale OCGen® foundation are estimated as $540,000, as compared to an estimated cost for an equivalent TidGen® bottom support frame and foundation piles of $1,100,000.

1.3 How Project is of Benefit to the Public

In addition to the benefits provided to the MHK industry in general, and ORPC in particular, the Project provided benefits to the general public, such as the following:

- Increased general awareness of the potential for generation of electricity from ocean energy resources
- Demonstrated continuing advancements in the commercialization of MHK technologies, making them more likely to contribute to the electricity generation supply in America in the coming years
- Continued awareness of the local economic benefits from the MHK industry through job creation and local spending
- Added to the growing body of knowledge regarding potential impacts of MHK systems to the marine environment, demonstrating once again that there were no known adverse impacts
- Development of a data set for mooring systems for submerged subsea assets
- Confirmation that buoyancy MHK assets are viable and offer a path to reduce levelized cost of electricity (LCOE)

- The Project also provided a site for environmental interaction studies to be performed by third parties

All Project tasks were completed, and the Project objectives were accomplished. The designs, methodologies, practices, testing, data, analysis and lessons learned from the Project are a step forward in the development of the U.S. MHK industry and provide a sound basis for ultimate commercialization of ORPC's OCGen® Power System. Based on the what was learned and demonstrated during the Project, ORPC has determined that the OCGen® Power System has cost and operational advantages over MHK devices supported by fixed structural frames and has the potential of accelerating the commercialization of tidal and ocean current power systems.

2. COMPARISON OF ACTUAL ACCOMPLISHMENTS WITH THE GOALS AND OBJECTS OF THE PROJECT

The goal of the OCGen® Module Mooring Project (Project) was to design a standard mooring system for hydrokinetic devices that will be moored below the surface and above the bottom in reversing tidal environments.

The Project objectives were as follows:

- Develop the analytical models for design of a mooring system for an OCGen® Power System
- Verify these analytical models using scale model testing
- Design, construct and deploy an experimental version of the mooring system in the field
- Monitor the performance and environmental effects of this deployed mooring system for a period of two months
- Remove the test mooring system upon completion of the two-month test period
- Design (but not procure, install or operate) a mooring system for a full-scale OCGen® Power System

Table 2.1 shows a comparison of the Project objectives with the actual accomplishments and variances.

Table 2.1. ***Comparison of project objectives and metrics of success with actual accomplishments***

OBJECTIVES	ACTUAL ACCOMPLISHMENTS	VARIANCES
Develop the analytical models for design of a mooring system for an OCGen® Power System	Developed as planned. Successfully completed 3D CFD analyses for several variants of the OCGen® TGU structure.	None
Verify these analytical models using scale model testing	Scale model testing provided a rapid means of down selecting from a wide variety of mooring line arrangements.	Effort to compile a CFD model to replicate the scale model test was judged to be not valuable
Design, construct and deploy an experimental version of the mooring system in the field	Completed design, construction and deployment of mooring system in field	None

Table 2.1. ***Comparison of project objectives and metrics of success with actual accomplishments***

OBJECTIVES	ACTUAL ACCOMPLISHMENTS	VARIANCES
Monitor the performance and environmental effects of this deployed mooring system for a period of two months (~60 days)	Monitored mooring system for 83 days, June 27 – September 17 OCGen® System operated stationary for 27 days (June 27 – Jul 23) OCGen® System collected data for braked turbine for 2 days (Jul 21 – Jul 23) [Operating State 1] OCGen® turbine rotated for 18 days (Jul 23 – Aug 10) [Operating State 2] OCGen® system operated without turbines for 38 days (Aug 11 – Sep 17) [Operating State 3]	System was installed for 83 days. Data was collected for 58 days
Remove the test mooring system upon completion of the two-month test period (60 days)	Retrieval of the OCGen® system occurred on September 17, 2014.	System was installed for 83 days
Design (but not procure, install or operate) a mooring system for a full-scale OCGen® Power System	Design of the commercial, full-scale prototype was developed.	Additional work is required to fully complete the full scale design.
METRICS OF SUCCESS	**ACTUAL ACCOMPLISHMENTS**	**VARIANCES**
Fabrication of system components	Completed fabrication of system components and final on land assembly in Eastport	None
Delivery and staging of system	Delivered all components and completed assembly of system at the in-water staging area	None
Deployment of system	Deployed prototype OCGen® TGU and mooring system within the specified installation zone and within the specified locational and directional tolerances <u>Location</u> NAD1983 State Plane Mane East Datum	System was deployed seven (7) ft outside the target deployment circle. Orientation was achieved within tolerance.

	Northing 456479.3 Easting 1361307.4 +/- 30 feet <u>Orientation</u> Axis of the turbines to be aligned along the heading 21.5/201.5 degree true +/- 10 degrees	
Balancing of mooring system • Balance mooring line loads to within +/-25% loads of each other • Mooring line loads to within +/-25% loads of predicted load	Mooring lines balanced to +/- 6% Mooring lines predicted to +/- 20% of analysis at max flow	None None
Operation of system with turbines fixed (non-rotating)	OCGen® System collected data for braked turbine for 2 days (Jul 21 – Jul 23) [Operating State 1]	Data of non-spinning turbines collected successfully, which was stated objective. Original intent had been to collect 7 days worth of data in this condition.
Operation of system with turbines rotating	OCGen® turbine rotated for 18 days (Jul 23 – Aug 10) [Operating State 2]	Collected data for a rotating turbine for 60% of lunar cycle. Original intent had been to collect data for at least one lunar cycle

Data collection

Successfully collected data related to following expectations
Three categories of data:

- Has any data collected met the minimum requirements
- Has any data collected met the optimal requirements
- Has supplementary data collected been outside both minimum and optimal requirements adding robustness to our results

The values shown in the table below correspond to the milestones established for the project prior to deployment. Green text indicates that the data collection targets were met, and red text indicates that the targets were unmet.

Green text below indicates data was obtained
Red text below indicates data was not obtained

Measurement	***Minimum Data Ranges Required***	***Optimal Data Ranges Desired***	***Supplementary Data Ranges Desired***
Environment			
Flow Speed	+/- 1.5m/s	+/- 2.1m/s	+/- 2.8m/s Max = 2.5m/s
TGU			
Flow Speed	+/- 1.5m/s	+/- 2.1m/s	+/- 2.8m/s Max = 2.5m/s
Attitude	+/- 10 deg Max pitch = +/- 2 deg	+/- 15 deg Low angle is desirable	+/- 20 deg Low angle is desirable
Heading	+/- 10 deg < +/- 5 deg Low angle is desirable	+/- 15 deg < +/- 5 deg Low angle is desirable. Original expectations were that the system would yaw by a significant amount due to cross currents on the flat end plates. This did not materialize.	+/- 20 deg < +/- 5 deg Low angle is desirable. Ideally, the angle would have been smaller than the 15-20 deg that was predicted. This is believed to be due to a lower cross-flow drag on the system than originally expected.
Turbine RPM	0 to 20 RPM	20 to 40 RPM	40 to 60 RPM
Mooring System			
Mooring loads	20 to 30kN	30 to 50kN	50 to 70kN Max = 60kN
Mooring loads equalization		+/-25% between lines Achieved +/- 6%	
Station Keeping of Mooring Pod			
Translation in Flow Direction 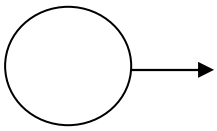	0 to 2.3m Low values are desirable.	2.3 to 4.5m Low values are desirable. Deviation from expectation is due to lower buoyancy pod drag than expected.	4.5 to 6.4m Low values are desirable. Deviation from expectation is due to lower buoyancy pod drag than expected.

Translation in Vertical 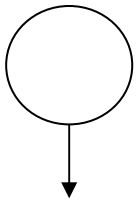	0 to 0.3m	0.3 to 1.2m	1.2 to 2.6m Deviation from expectation is due to lower buoyancy pod drag than expected.
Translation in Axial Direction 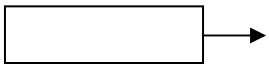	0 to 1.0m Low values are desirable	1.0 to 2.0m Low values are desirable. Deviation from expectation is due to lower buoyancy pod cross flow drag than expected.	2.0 to 3.0m Low values are desirable. Deviation from expectation is due to lower buoyancy pod cross flow drag than expected.

Data analysis	Performed quality checks on data. Processed data to common time base. Processed data to provide plots/data for the following: • Mooring line loads vs. flow speed, non-rotating turbines • Mooring line loads vs. flow speed, rotating turbines • Turbine RPM vs. flow speed, • OCGen® attitude vs. flow speed, non-rotating turbines • OCGen® attitude vs. flow speed, rotating turbines	None
Correlation of data with models	Compared measured data with predictions of OrcaFlex model. Model results to agree to within +/- 25% of empirical data.	None
Removal of system	Completely retrieved system from site. Transported system to shore. Completed detailed inspection of system.	None

Assessment of impacts from system operation	• Assessed the scour behavior around the mooring blocks • Assessed settling behavior of the mooring blocks • Movement of mooring blocks assessed • Inspected the condition of removed equipment to assess any abnormalities caused by system installation and operation	None

Figure 2.1 provides a flowchart of the proposed project process and shows the original intent behind the project structure. As the project developed and as analytical tools were evaluated the process changed to that reflected in the second flowchart (Figure 2.2).

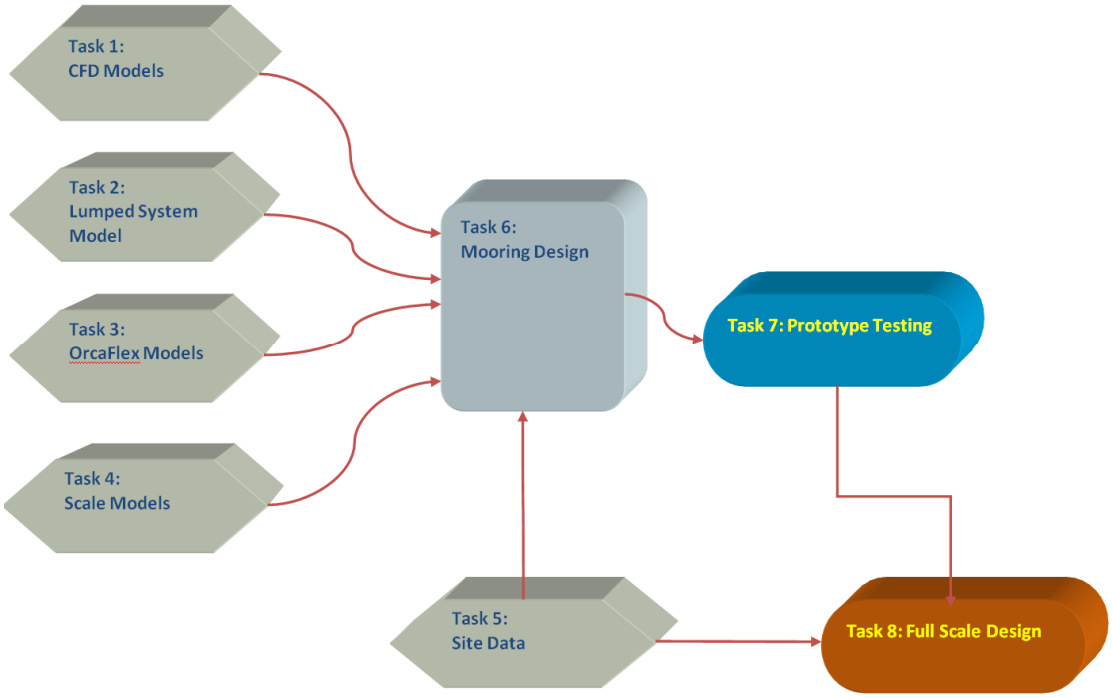

Figure 2.1. Flowchart representing the proposed workflow for the project

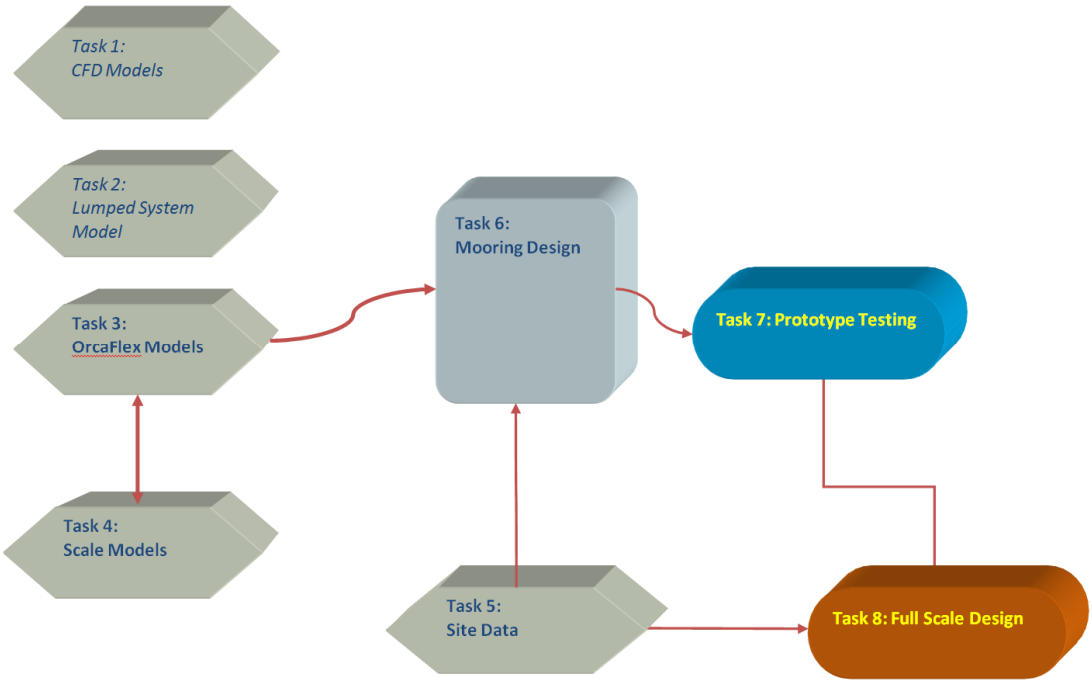

Figure 2.2. Flowchart illustrating the actual workflow for the project, which led to the identification of the optimal software-based design tool, OrcaFlex, to assist with future projects. While Task 1 and 2 efforts did not contribute directly to the detailed designed process in Task 6, they did provide a basis for understanding of the problem, and illustrated general behaviors to be considered.

3. PROJECT ACTIVITIES

Project activities are summarized in Table below showing the Project tasks.

Summary of project activities by task	
TASK	**TASK DESCRIPTION**
1	Modeling of Loads on Mooring System
2	Dynamic Stability Analysis
3	Dynamic Analysis of Mooring System and Lines
4	Scale Model Testing
5	Geophysical Surveys
6	Cable and Anchor Design
7	Experimental Mooring of a Prototype OCGen® Unit
8	Design of OCGen® Module Mooring System
9	Project Management and Report

3.1 Task 1: Modeling of Loads on Mooring System

Original Hypotheses

ORPC proposed to perform numerical modeling of the OCGen® module using computational fluid dynamics to predict the steady state loads and forces generated by the system while in operation. These load values were to be used as inputs into other numerical analysis tools to provide design loads of the mooring system.

Approaches Used

To address the effects of loads on the mooring system, ORPC worked with Blue Hill Hydraulics to develop three dimensional (3D) CFD models of three different unit cell configurations for the OCGen® Power system (Figure 3.1.1). It was recognized that the use of CFD for a 3D problem of this type would potentially be beyond the capabilities of the available Reynolds Average Navier Stokes (RANS) CFD codes, and it was believed that an alternative CFD approach utilizing the Fractional Area Volume (FAVOR™) method would be more computationally efficient. To that end the CFD modeling was performed using the *Flow-3D* CFD software.

Multiple geometries of the OCGen® structure were investigated to understand the effects of the structure on drag and lift forces. As a baseline case a simple, bare structure, without turbines, based on the ORPC Beta turbine generator unit (TGU) system, consisting of tubular elements was modeled first. Two variants of this structure were also modeled. These differed from the base structure in that fairings were added to the major structural element. These changes were made to assess the affect of reduced drag on the structure. The addition of fairings was also intended to provide higher amounts of buoyancy and improved stability for the system. Modelling of these structures using the FAVOR™ approach was efficient and rapid.

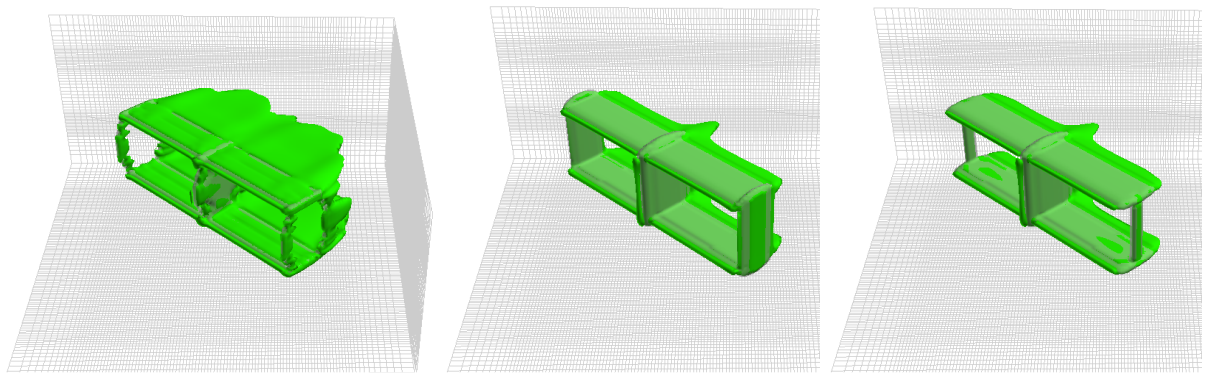

Figure 3.1.1. Velocity iso-surface contours for three different design concepts of the OCGen® module structural cell: Beta TGU, OCGen®-mk1, and OCGen®-mk2. Turbines are not included in these models to simplify the problem

Based on initial findings, ORPC focused efforts on the OCGen®-mk2 configuration, which had lower drag characteristics than the other variations considered (Figure 3.1.2). ORPC expanded the range of parameters to be investigated and generated lift and drag results for a range of pitch and yaw angles. Mesh resolution studies were performed to verify that the predicted force results were insensitive to mesh size.

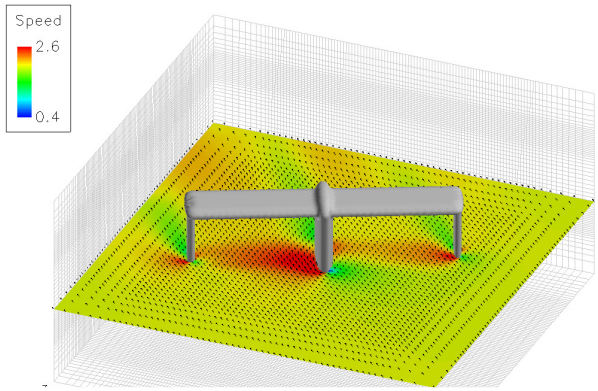

Figure 3.1.2. Velocity results for OCGen®-mk2 structural cell for a yaw angle of 20 degrees

The initial models did not include turbines in order to rapidly iterate towards a desired structure. The model was then expanded to include a turbine. Using the mirror symmetry property, only one side of the OCGen® module needed to be analyzed for the simplified flow condition of zero yaw (Figure 3.1.3). Results were generated for a stationary turbine, for an applied rotation on the turbine, and for a free-wheeling turbine. These results indicated that a more refined mesh size would be required to obtain sufficiently accurate turbine performance utilizing this modelling technique. Greater mesh refinement was required to properly capture the flow behaviour in and adjacent to the boundary layer on a moving foil, and the FAVOR™ approach appeared to offer no significant benefit over RANS codes for this case. To properly model a rotating cross-flow turbine in either RANS or FAVOR®, codes required mesh sizes of the order of the boundary layer thickness, and as such this problem became computationally very

expensive for either CFD approach. For the purposes of rapid iteration, the CFD appeared to be limited to stationary meshs as this stage.

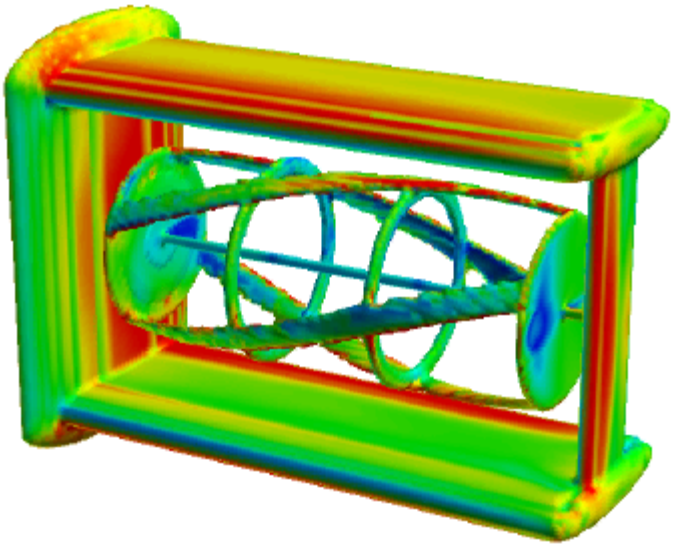

Figure 3.1.3. Half OCGen®-mk2 model with turbine included. The model utilizes a mirror plane of symmetry at the midline of the structure. This limits this model's utility to the case with flow directly from the front of the TGU (zero yaw).

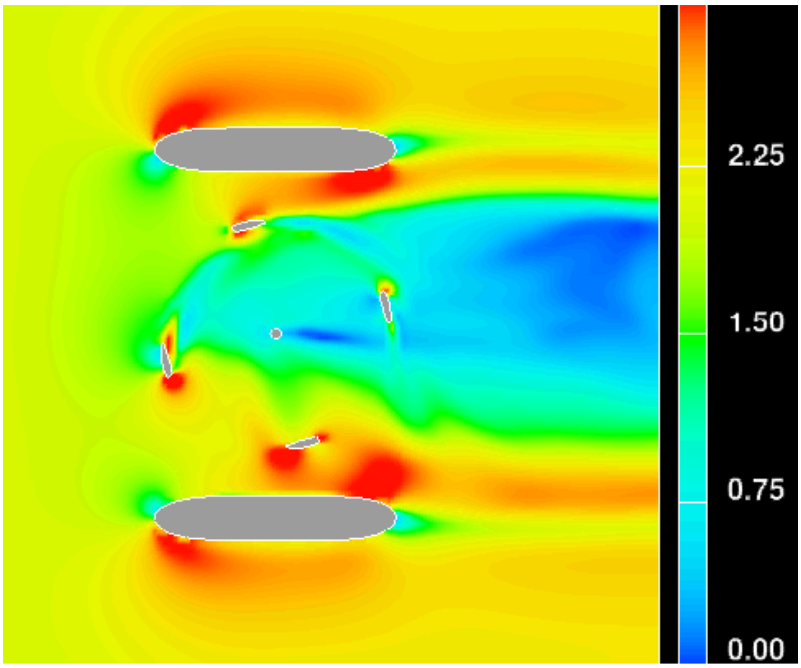

Figure 3.1.4. Computational fluid dynamics models of Mark II OCGen® structure and turbine from Flow3D, showing the velocity fields around the turbine. Mesh refinement studies show this mesh is not sufficiently refined.

From the CFD models of the stationary structures lift, drag and other forces were characterized as a function of flow speed and pitch angles (Figure 3.1.4). This load information was arranged in a format suitable for input into the OrcaFlex model developed under Task 3. Samples of these loads are presented in Figure 3.1.5. Note that there appeared to be a high degree of sensitivity to small changes in pitch angle around 16°. This coincided with flow separation in the model. The ability of this model to accurately track flow separation was suspect, and again depended on mesh refinement.

To develop lift and drag curves for the combined turbines and structure, ORPC analyzed the drag and lift performance of the turbine independently and generated a set of curves predicting this behavior.

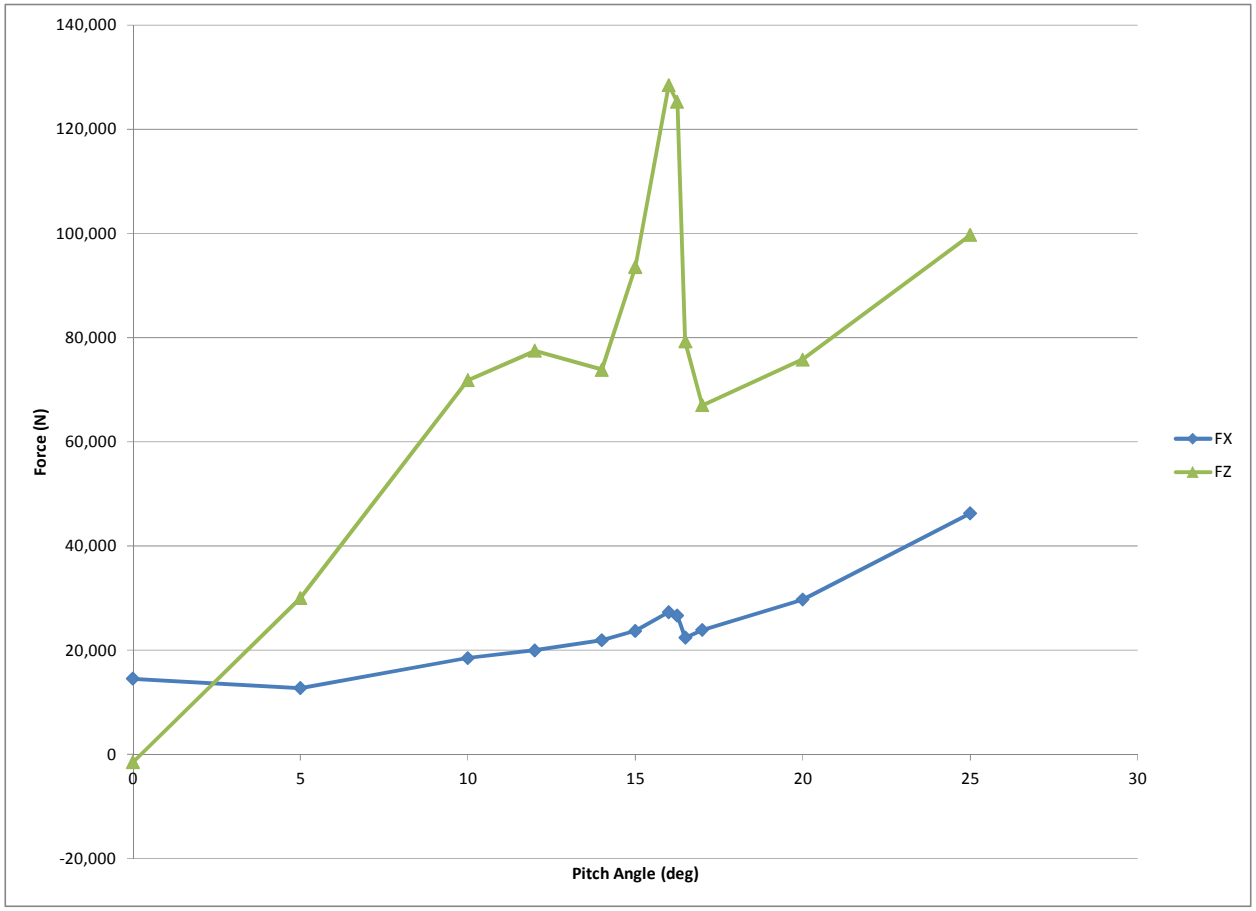

Figure 3.1.5. Lift (FZ) and drag (FX) loads derived from Flow-3D model for various pitch angles. OCGen®-mk2 model with no turbines. Note the sensitivity to small angle variations around 16°, indicating predictions of large changes in loads due to flow seperation.

Problems Encountered

The computational effort required for 3D stationary and rotating meshes using FAVOR CFD codes was large. Mesh sensitivity was noted in several of the CFD runs, which called into doubt the accuracy of the predicted lift and drag coefficients. The extreme sensitivity of the lift forces to small changes in angle of attack at stall also cast some doubt on results. The ability of the CFD codes to accurately and reliably predict behavior for rotating cross-flow turbines was further in doubt.

Departure from Planned Methodology

CFD models were developed as planned. The utility of the CFD models was limited due to the large computational resources required to perform design iterations.

Assessment of Impact on the Project Results

ORPC successfully completed 3D CFD analyses for several variants of the OCGen® TGU structure. Lift and drag forces were efficiently calculated. The effectiveness as a design tool of 3D CFD analysis for moving turbine simulations was less clear. Significant computational resources were required to properly resolve cross-flow turbine physics using either RANS or FAVOR® CFD techniques. The computational effort required meant that CFD tools were unable to rapidly iterate cases. Computational effort required even for stationary meshes was such that this approach was not an effective tool for estimating loads on a mooring system during the design phase. For fully developed concepts, the effort may be warranted. As ORPC was investigating analytical techniques capable of rapid turnaround, and since CFD did not meet these criteria, this approach for predicting mooring loads was not utilized for the rest of the Project.

Impact on the Project consisted of a lower level of confidence in modeling results as the other modeling techniques utilized lumped mass approximations for the flow physics.

In the event that unlimited computational resources had been available for this project, the CFD analyses could have been pursued to the point where accurate force response would have been obtained. There is no reason to believe that any particular CFD technique, whether FAVOR, RANS, or LES would not have provided correct results, but for the particular problem of a rotating cross-flow turbine a RANS or LES approach would probably better model boundary layer effects.

3.2 Task 2: Dynamic Stability Analysis

Mooring a large buoyant device to the sea floor with cables may lead to dynamic oscillation of the system. The Project team created an analytical model to investigate dynamic stability with a lumped parameter six-degree of freedom model of the TGU. This work was performed at University of Washington. The deliverables from this task included a software tool specifically adapted for analysis of floating OCGen® systems capable of predicting loads on the mooring system.

Original Hypotheses

ORPC proposed to develop a six-degree of freedom model of the TGU to determine the stability boundaries of the system under various tidal/current loading conditions. Expected instabilities included large scale oscillation of the system in the water column in any of the six degrees of freedom, up to and including collision with the seafloor.

The system model included the following:

1. Six-degree of freedom rigid body, with the TGU treated as a rigid body with three translational and three rotational degrees of freedom. The equations of motion were developed to include the possibility of large displacements of the TGU.
2. Hydrodynamic forces included the following fluid induced forces:
    i. Added mass and inertia of the accelerating fluid that surrounded the TGU
    ii. Dissipative effects due to lift and drag forces acting on the TGU
    iii. Gravity and buoyancy effects

iv. Current and wave dynamics

3. Tethers/mooring cables for the TGU to be modeled as unidirectional elastic springs
4. Generator forces modeled as periodic forces and moments

The types of analysis to be performed as part of this project included:

1. Modal analysis: The small displacement model was to be used to determine the modal characteristics of the system. This would help the system designer identify suitable operating speeds for the generator, as well as to identify harmful current/wave frequencies.
2. Stability limits: The model was to be used to determine the stability boundaries for the system. In particular, ORPC intended to investigate:
   (a) Types of forces and moments that would lead to system instability; and
   (b) Directions and magnitudes of the current that lead to system instability.

Approaches Used

Faculty and students at the University of Washington, Northwest National Marine Renewable Energy Center, under the direction of Dr. Brian Fabian, developed the lumped system model.[1]

A fixed rectangular coordinate system, denoted by $\boldsymbol{X-Y-Z}$, with origin on the sea floor was used as an inertial reference frame. A fixed-body rectangular coordinate system with origin located at the turbine's center of mass is denoted by $\boldsymbol{x-y-z}$. The coordinate systems are displayed in Figure 3.2.1.

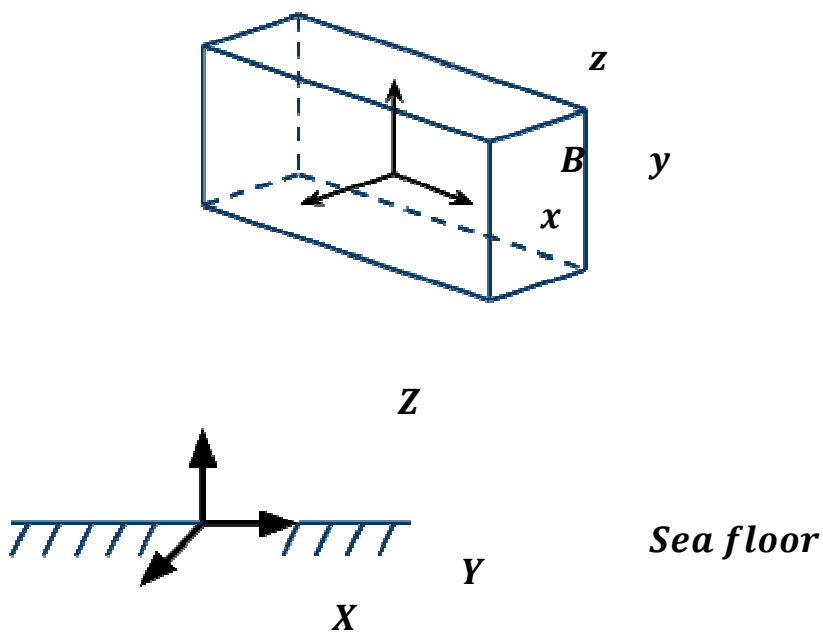

[1] B.C. Fabien, *The static equilibrium of a submerged body with slack mooring*. Nonlinear Approaches in Engineering Applications, L. Dai and R. L. Jazar, (Eds.), Springer-Verlag, 2012; G. DuBuque, *A Lumped parameter equilibrium model of a submerged body with mooring lines* (Master's thesis), University of Washington, Seattle, WA, 2011; T. Nichol, *Numerical modeling of compliant-moored system dynamics with appl ications to marine energy converters*, (Master's thesis), University of Washington, Seattle, WA, 2014; T. Nichol, G. Dubuque, & B.C. Fabien, *Dynamic modeling of compliant-moored submerged systems with applications to marine energy converters*, Proceedings of the Second Marine Energy Technology Symposium, METS2014, Seattle, WA, 2014.

Figure 3.2.1. Inertial and fixed-body coordinate systems

The OCGen® system was modeled as a rigid body with six degrees of freedom that included its position and rotation:

- Position of the center of mass $\bar{\boldsymbol{B}} = \begin{bmatrix} \boldsymbol{B_X} \\ \boldsymbol{B_Y} \\ \boldsymbol{B_Z} \end{bmatrix}$
- Rotation of the body $\boldsymbol{\alpha}, \boldsymbol{\beta}, \boldsymbol{\gamma}$

The three rotation angles, $\boldsymbol{\alpha}, \boldsymbol{\beta}, \boldsymbol{\gamma}$, completely described the body's rotation in 3-dimensional space. The body's final rotation was found by three successive rotations about an axis in the fixed-body reference frame.

A point with coordinates $\bar{\boldsymbol{r}}_{\boldsymbol{1}}$ relative to the body was written with coordinates $\bar{\boldsymbol{r}}_{\boldsymbol{a}}$ relative to the ground with the transform

$$\bar{\boldsymbol{r}}_{\boldsymbol{a}} = \boldsymbol{T}_{\boldsymbol{B}}^{\boldsymbol{G}} \bar{\boldsymbol{r}}_{\boldsymbol{1}}$$

An arbitrary point on the turbine with fixed-body coordinates $\bar{\boldsymbol{P}}_{\boldsymbol{B}} = \left[\boldsymbol{P_{Bx}}\ \boldsymbol{P_{By}}\ \boldsymbol{P_{Bz}}\right]^{\boldsymbol{T}}$ then had the following coordinates with respect to ground, $\bar{\boldsymbol{P}}_{\boldsymbol{G}} = [\boldsymbol{P_{GX}}\ \boldsymbol{P_{GY}}\ \boldsymbol{P_{GZ}}]^{\boldsymbol{T}}$:

$$\bar{\boldsymbol{P}}_{\boldsymbol{G}} = \bar{\boldsymbol{B}} + \boldsymbol{T}_{\boldsymbol{B}}^{\boldsymbol{G}} \bar{\boldsymbol{P}}_{\boldsymbol{B}}$$

The total kinetic energy of the body consisted of both translational and angular velocities. The angular velocities of the body needed to be expressed in terms of the Euler angular velocities $\dot{\boldsymbol{\alpha}}, \dot{\boldsymbol{\beta}}$ and $\dot{\boldsymbol{\gamma}}$, where the dot represents the derivative with respect to time. The angular velocities $\boldsymbol{\omega_{x,}}\boldsymbol{\omega_y}$ and $\boldsymbol{\omega_z}$ of the body about the fixed-body **x, y,** and **z** axis respectively can be found.

The total kinetic energy of the body, $\boldsymbol{T_B}$, was then

$$\boldsymbol{T_B} = \frac{\boldsymbol{1}}{\boldsymbol{2}} \boldsymbol{M}\left(\dot{\boldsymbol{B}}_{\boldsymbol{X}}^{\boldsymbol{2}} + \dot{\boldsymbol{B}}_{\boldsymbol{Y}}^{\boldsymbol{2}} + \dot{\boldsymbol{B}}_{\boldsymbol{Z}}^{\boldsymbol{2}}\right) + \frac{\boldsymbol{1}}{\boldsymbol{2}} \bar{\boldsymbol{\omega}}^{\boldsymbol{T}} \boldsymbol{I} \bar{\boldsymbol{\omega}}$$

$\boldsymbol{I}$ was the moment of inertia in the fixed-body frame.

The weight of the turbine acted at the turbine's center of mass (COM). The origin of the fixed-body frame was located at the turbine's COM for ease of calculations. The turbine's buoyant force acted at the turbines center of buoyancy (COB). The drag and lift coefficients for the turbine for various stream velocities needed to be determined separately.

The model accommodated arbitrary, time dependent body forces and torques, applied at the center of mass of the body. Turbine loads were applied in this manner.

Mooring Lines

The mooring lines were modeled as elastic springs with lumped parameters including weight, buoyancy and drag forces (Figure 2.2). Each line segment was modeled as a spring with an equivalent stiffness **K** defined by

$$K_i = \frac{E_i A_i}{l_i^0}$$

E_i was the modulus of elasticity of the line, A_i was the cross-sectional area and l_i^0 was the unstretched, or free, length. Figure 2.2 displays an example of the lumped parameter model of the mooring lines.

The mass of the lines were modeled as point masses located at the ends of each segment. The kinetic energy of a point mass $m_i$with coordinates $\overline{p}_i = [p_x\ p_y\ p_z]^T$ was then

$$T_i = \frac{1}{2} m_i (\dot{p}_x^2 + \dot{p}_y^2 + \dot{p}_z^2)$$

The potential energy, **V**, of each line segment was

$$V_i = \frac{1}{2} K_i (\Delta l_i)^2$$

where Δl_i was the net deflection of the line segment. The lines were modeled to only support tension forces when the segment was stretched and not compressive forces when the segment was compressed and became slack. To model only tension forces, the net deflection of the line segment was written in a way such that Δl_i equated to zero when the segment became shorter than its original length.

The drag forces from the fluid velocity were modeled to act on each segment of the mooring lines (Figure 3.2.2).

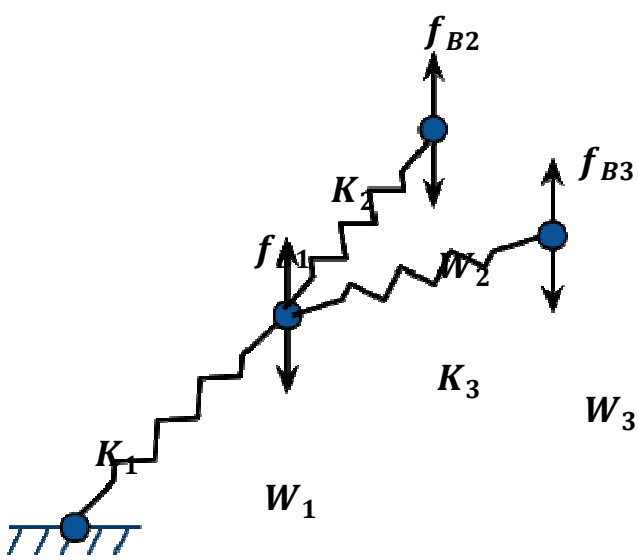

Figure 3.2.2. An example of an elastic lumped parameter model of the mooring lines, showing mooring line elements comprising stiffness, weight and buoyancy. Each individual mooring line is modeled as a set of n springs connected in series. Pinned connections are assumed at the ends of the springs (nodes). Weight and buoyancy of the line segment act at the nodes. Multiple mooring lines may be connected in any manner by connecting at the nodes. In this example, one mooring line is represented by springs K1 and K2, with weight and buoyancy of the line located at the end nodes, and with an additional mooring line, K3, attached at the mid-point of the mooring line.

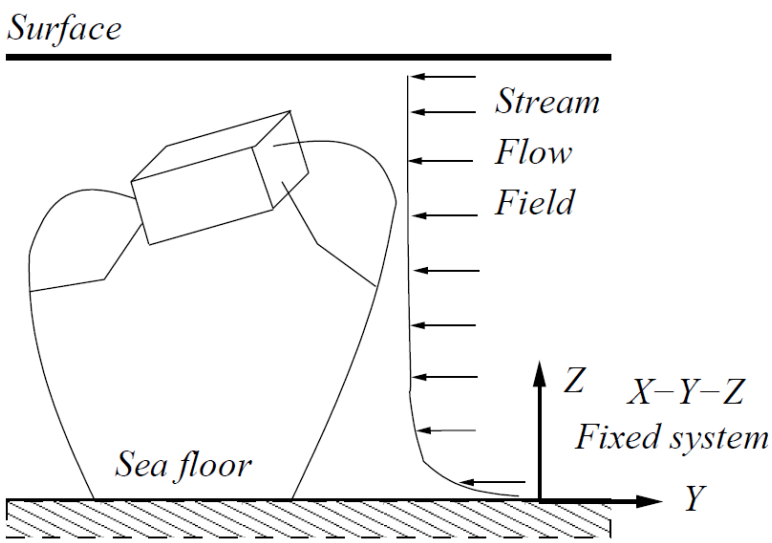

Figure 3.2.3. Schematic of the rigid body system, attached mooring lines, and free stream flow

Using the individual elements already described, a system of equations and constraints is established to describe a particular geometry and loading. The Principle of Virtual Work is used to develop of set of nonlinear equations whose solution provides the equilibrium condition for the system (Figure 3.2.3).

The model was validated by comparison with analytical results for catenary mooring lines (Figure 3.2.4) and run for sample OCGen® type configurations (Figure 3.2.5).

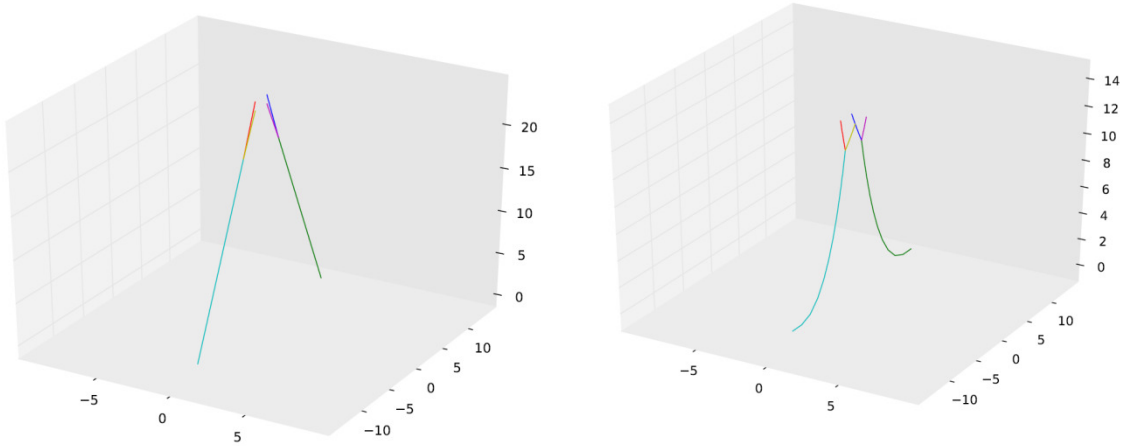

Figure 3.2.4. Initial conditions for a mooring line configuration and results of lumped parameter model showing equilbrium condition.

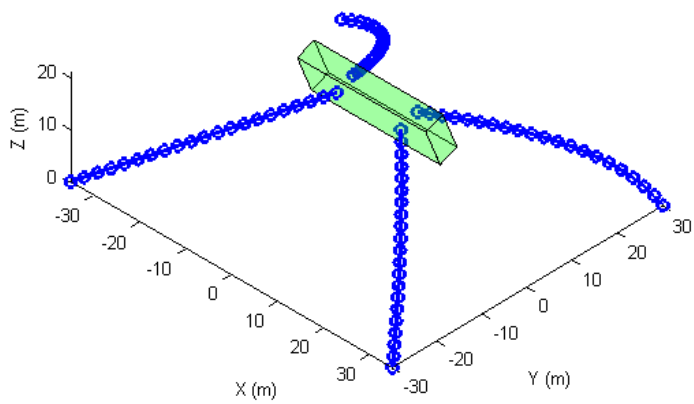

Figure 3.2.5. Model output from lumped parameters analysis model of sample OCGen® four point mooring system with flow induced drag

Problems Encountered

The analytical work proceeded as planned with no issues in the development of the code. The modeling technique was appropriate. The user interface for the analytical model, however, was not intuitive and was cumbersome to use. The difficulties in interacting with the user interface meant that this particular tool was not used to aid in the design of the OCGen® mooring system. In addition, the usual assumptions regarding added mass components needed to be made, and the usual uncertainty in these assumptions existed.

Departure from Planned Methodology

There were no departures from the planned methodology in the development of this analytical tool.

Models of mooring systems were completed and analyzed for static and dynamic load cases. However, the ability to perform modal analyses and other kinds of stability analyses was not included in the code. The complexity of the problem had been underestimated by the researchers. At present, work is

continuing under separate U.S. Department of Energy funding to further develop this mooring analysis code and to implement stability analysis capabilities.

In addition, the tool was not used to aid in the design of the OCGen® mooring system as the user interface proved too cumbersome for a non-expert user.

Assessment of Impact on the Project Results

The development of this analytical tool provided an analytical appropriate means of estimated loads on submerged systems. The lack of a friendly user interface limited the practical utility of the tool and the development of a more user friendly interface for this tool would be beneficial.

This had no impact on project results as alternative means of analysis were identified and used. This alternative is outlined below in Task 3.

3.3 Task 3: Dynamic Analysis of Mooring System Lines

ORPC developed dynamic models of the OCGen® system using a commercially available code, OrcaFlex.

Original Hypotheses

In addition to the previously mentioned approaches which were developed to model the loads and mooring line behavior of the OCGen® system, ORPC also identified commercial codes which already existed for these types of problems. To evaluate the utility of these codes and their applicability to this project, ORPC worked with the OrcaFlex code to assess whether this commercially available code offered advantages in terms of user interface, analytical capability, and general utility as part of the design process. OrcaFlex was used to estimate the mooring line loads for a prototype OCGen® Power System to be deployed in Cobscook Bay, Maine, and for a full scale OCGen® system to be deployed in Western Passage, Maine.

Approaches Used

Work was completed by ORPC to develop a concept for a prototype OCGen® system (Figure 3.3.1). Multiple configurations for the full scale OCGen® TGU were evaluated were down-selected to a passively buoyant system, outfitted with four cross-flow turbines, with a common driveline, undermounted on the buoyancy pod.

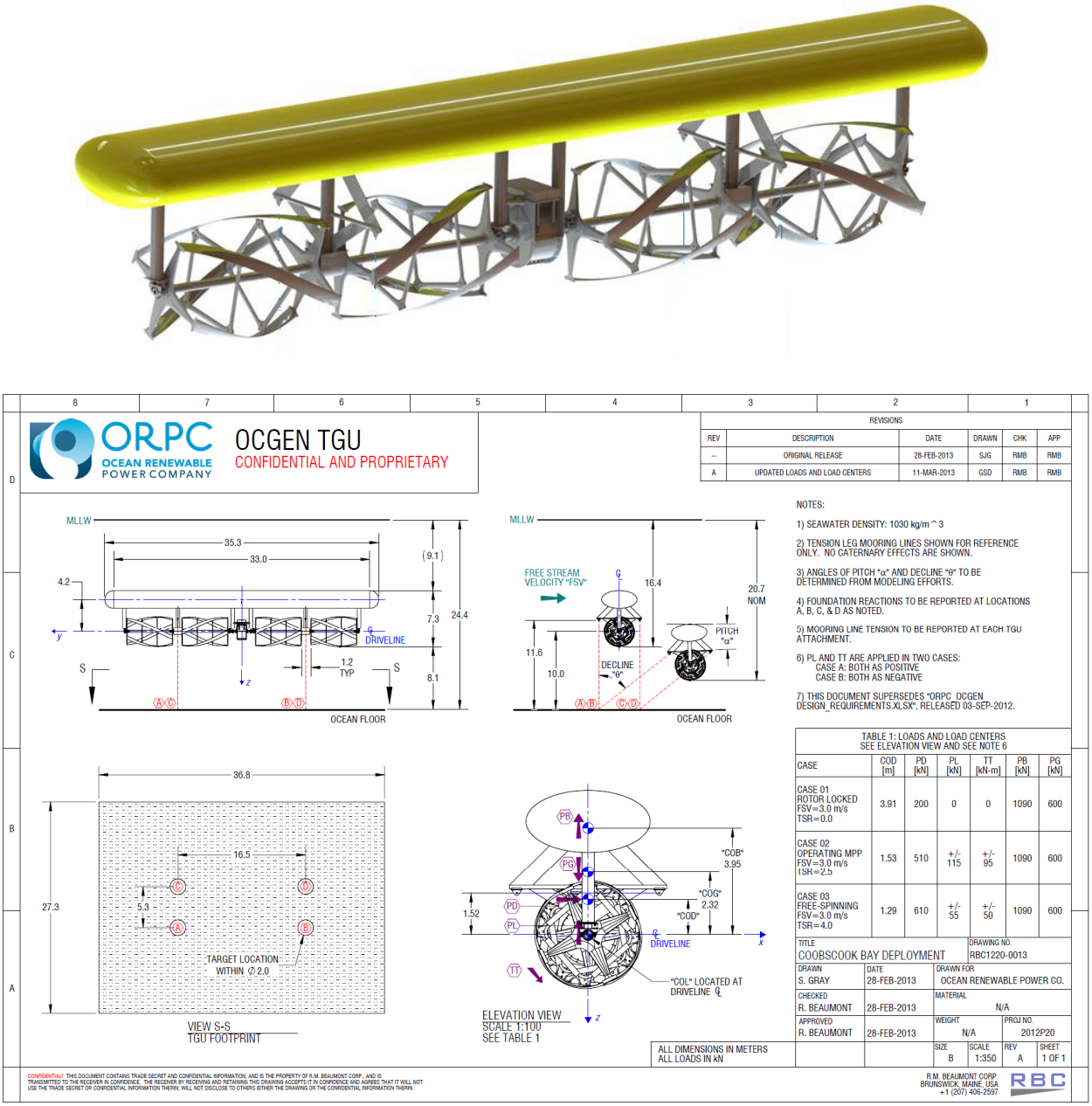

Figure 3.3.1. Isometric and Drawing for Prototype OCGen® Power System

As the rotating turbines cannot be modeled explicitly in lumped system models such as OrcaFlex, a model for the turbines lift and drag coefficients as a function of turbine tip speed ratios were developed using a turbine streamtube model.[2] The streamtube model results for the turbines were used to generate a table of the lift, drag and power coefficients for the turbine as a function of tip speed ratio (Figure 3.3.2).

[2] ORPC OCGen® Design Loads, March 25, 2013, RBC

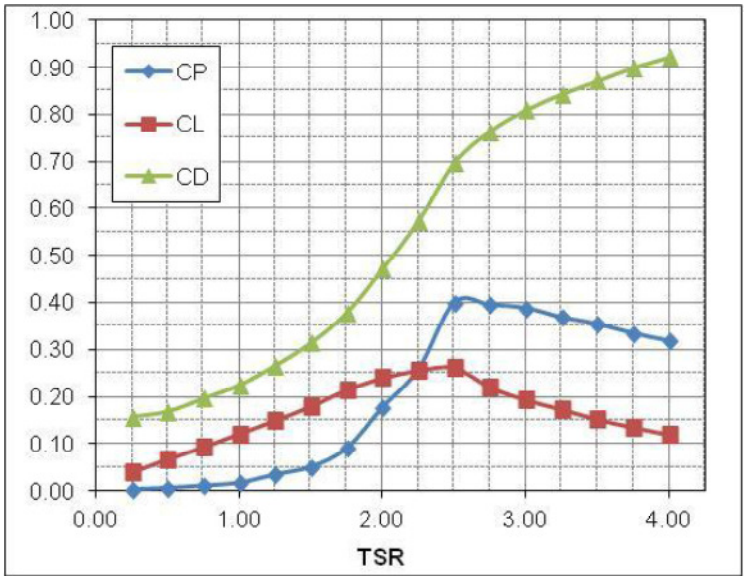

Figure 3.3.2. Streamtube model results for the OCGen® turbines. The plot shows the Coefficient of Power, CP, Coefficient of Lift, CL, and Coefficient of Drag, CD for the turbine as a function of tip speed ratio, TSR

Estimates of mass, center of mass, buoyancy, center of buoyancy, drag and center of drag for for the structure were developed.

For the purposes of the design exercise a reference tidal flow was used as the basis for the fluid loading. This synthetic flow was based on data collected from the Cobscook bay site, scaled by maximum flow magnitude to provide a non-dimensional flow input (Figure 3.3.3).

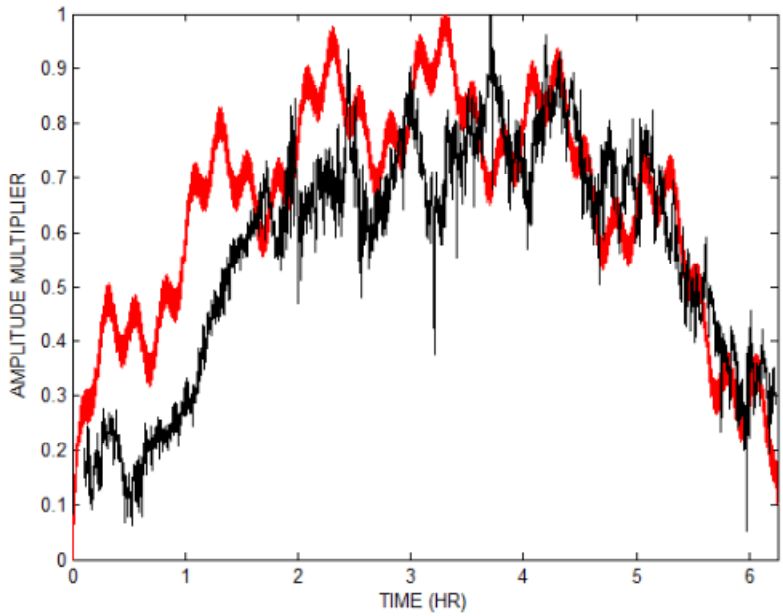

Figure 3.3.3. Non-dimensional reference flow (red), as compared to non-dimensional measured flows, scaled by maximum flow magnitude.

The OrcaFlex design tool proved useful in the early stages of selecting mooring configurations. In combination with the scale model testing (Task 4) different arrangements of mooring lines were implemented in OrcaFlex, and mooring line and device behavior were estimated from the analytical models. Much of this particular analytical effort was performed using the two turbine OCGen® prototype to be deployed in Task 7, but is shown here for the purpose of illustrating the capabilities of OrcaFlex (Figures 3.3.4, 3.3.5 and 3.3.6).

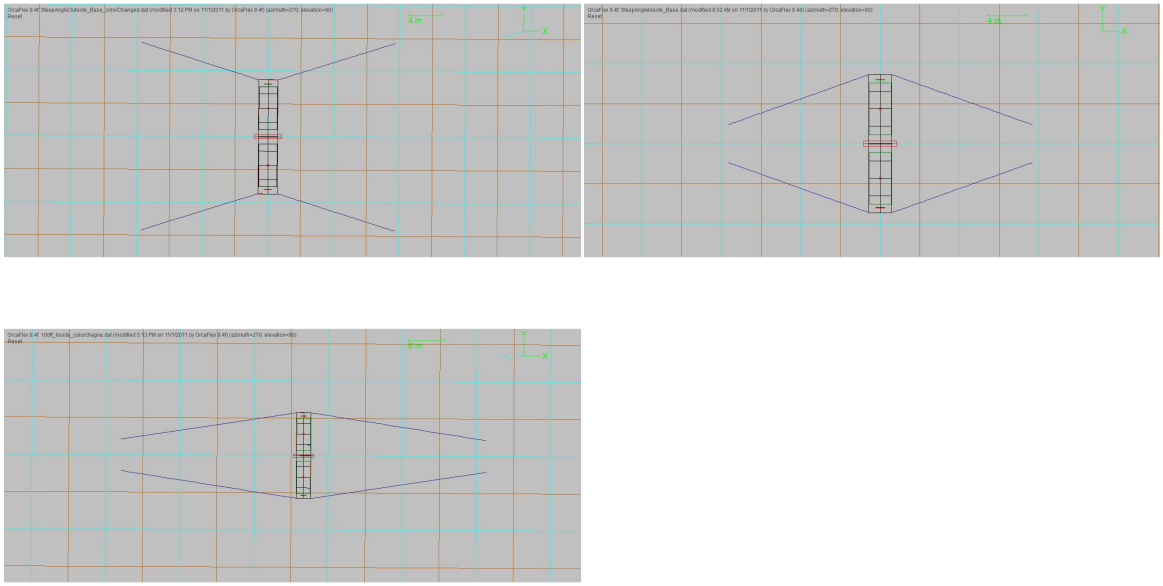

Figure 3.3.4. Three configurations of mooring line arrangement: steep angle outside configuration, steep angle inside configuration, and 100 ft mooring inside configuration

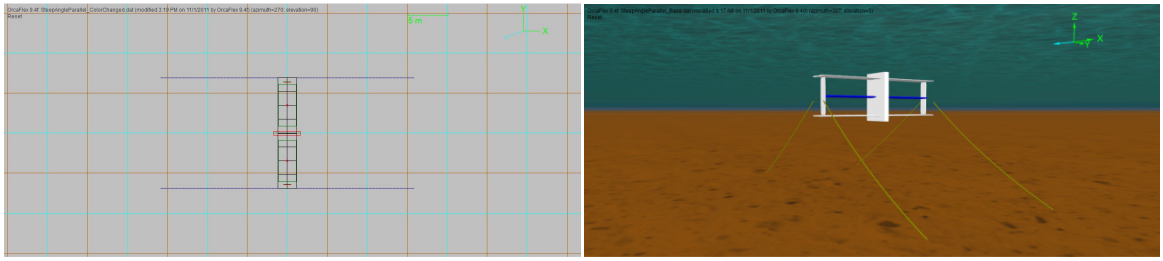

Figure 3.3.5. Steep angle parallel configuration

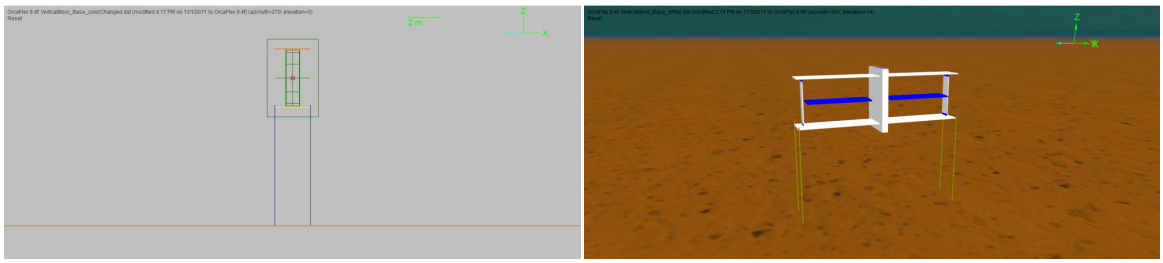

Figure 3.3.6. Vertical tension leg mooring configuration

Analyses of the various mooring configurations were performed for the maximum power condition of the turbine and assuming a chain mooring line.

The various different mooring configurations considered all function similarly in terms of station keeping. However, the level of mooring line load in the various mooring configurations differed in two significant respects between the configurations. At zero water speed, the loads in the mooring lines reflected the net buoyancy of the TGU and the geometry of the lines. If fore and aft mooring lines oppose each, then a horizontal component of force was introduced. This made the base line load in configurations other than the tension mooring line arrangement rather high. For the tension mooring line arrangement the load at zero flow is the net buoyancy of the system, and has no horizontal component.

The second differentiator between the configurations was how well the load was spread between the fore and aft mooring lines as water speed increases. For all configurations, the loads in the forward mooring lines increased and loads in the aft mooring lines decreased. However, for the tension leg mooring configuration, the increase in forward line load and the decrease in aft line loads were more significant than for the other configurations. While this may sound problematic for the tension leg configuration, the maximum load experienced by any one line was actually lowest for the tension leg configuration (Table 3.3.1).

Table 3.3.1 *Comparison of mooring line loads for various chain mooring configurations at 0 m/s and 3 m/s*

Configuration	***Mooring Load V = 0m/s (kN)***	***Max Mooring Load V = 3m/s (kN)***	***Min Mooring Load V = 3m/s (kN)***
Steep Angle Outside Configuration	137.7	154.2	61.6
Steep Angle Inside Configuration	137.7	153.6	59.9
100 ft mooring inside angle	228.9	259.1	177.7
Steep Angle Parallel Configuration	130.3	144.4	54.6
Vertical TLP type mooring	69.6	141.4	9.0

Looking at the station keeping ability of each mooring system, found that the vertical tension leg mooring allowed for the greatest change in depth, but the smallest change in pitch angle. The change in depth is due to the behavior of the system as it rotates about the mooring block as flow speed increases. This may be seen as a potential problem as the tension leg mooring system allows the TGU to move around more in the water column; however the movement is limited (Table 3.3.2).

Table 3.3.2. *Comparison of changes in TGU depth and pitch between the various configurations for 3 m/s*

Configuration	***Max change in depth (m)***	***Max change in pitch (degrees)***
Steep Angle Outside Configuration	0.1	2.0
Steep Angle Inside Configuration	0.1	2.2
100 ft mooring inside angle	0.0	1.7
Steep Angle Parallel Configuration	0.1	2.5
Vertical TLP type mooring	1.2	1.2

Clearly the tension leg mooring configuration provided the smallest footprint. Loads for the tension leg configuration were lower at low flow speeds than for other configurations. Maximum loads were equivalent for a given design flow speed. The tension leg mooring system does allow the TGU to move more in the water column, but the degree of movement was considered acceptable. These findings, combined with the fact that other mooring configurations offered no noticeable advantages in terms of station keeping, made the tension leg mooring configuration extremely attractive. A question remaining to be answered was how loads on the mooring lines transferred into loads on the mooring block itself. This was addressed under Task 6, where the information on the geophysical properties of various candidate sites was considered.

Problems Encountered

While OrcaFlex is outwardly easy and intuitive to use, a deeper examination of the code revealed that many of the input variables required for the analysis are difficult to estimate. In addition to the masses, lift and drag coefficients, geometries, etc., there were additional mass and damping factors required for translation and rotation degrees of freedom, in order to estimate the dynamic impacts of added mass due to water being entrained in the structure. These added mass factors were difficult to estimate for any but the simplest shape, and such estimation became an exercise in the art of engineering. To provide a firmer basis for the understanding of these added mass and damping factors, ORPC performed additional CFD analysis with the AQWA code (Figure 3.3.7). This code was capable of estimating a response amplitude operator (RAO): the frequency domain transfer function from an input spectrum to an output response. For example, an RAO can be used to describe the roll response of a ship to a sea spectrum at a certain heading. In practice, the RAO is a list of amplitudes and phases that are multiplied by the input spectrum. The RAOs, in theory, can be used to provide a better estimate of the added mass and damping factors required by OrcaFlex. However, it was still not transparent how this additional information could be implemented within the model, and hence values for added mass and damping coefficients used in OrcaFlex were still based on previous experience, rather than on the ROA values.

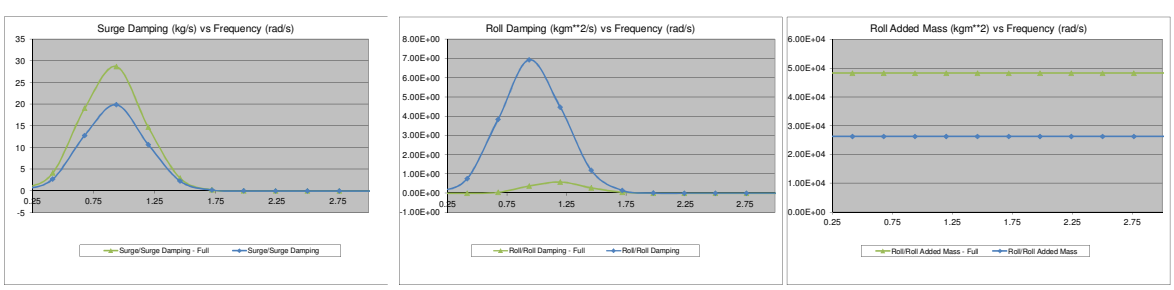

Figure 3.3.7. Sample response amplitude operators obtained by analysis with AQWA

Departure from Planned Methodology

There were no significant departures from the planned methodology.

Assessment of Impact on the Project Results

The utility of the OCRAFlex modeling tool was exceptional. This approach allowed for rapid and apparently accurate iteration of a wide range of mooring line configurations. Model results provided detailed information on TGU station keeping and mooring line loads, which results allowed for selection of a promising tension leg mooring configuration which offered the advantages of low mooring line loads, smallest possible footprint, and acceptable station keeping properties.

OrcaFlex, a commercial code, is an established user community and support, which has been well validated. Based on this, in the future, ORPC will continue to use OrcaFlex for mooring design.

3.4 Task 4: Scale Model Testing

Original Hypotheses

ORPC constructed and tested scale models of the OCGen® unit at the tow tank at the University of Maine. Measurements and visual observations of the behavior of several scale model versions of the OCGen® module were to be made and compared to the results obtained from Tasks 2 and 3.

Approaches Used

A 1/24 volume scaled version of the OCGen®-mk2 design was manufactured by 3D printing. As it initially proved very difficult to print the scaled turbine, it was decided that initial tank tests would utilize a drag cylinder to replicate the the drag forces of the turbine in the OCGen® module.[3] The drag cyclinder was unable to fully replicate the lift and drag loads for a cross-flow turbine but it did provide a qualtitive representation of the turbine.

The decision to perform these tests at 1/24th scale was determined by the dimensions of the University of Maine tow tank. The goal was to keep the model as large as possible, while avoiding blockage effects on the model from the tank boundaries. The University of Maine tow tank is approximately 120 ft long, 8 ft wide, and typically contains about 4 ft of water during normal testing.

The OCGen® 1/24th scale model was constructed from Acura 60 Plastic, and was 23 in. wide, 8 ¼ in. high, and each wing had a chord of 5 ½ in. (Figure 3.4.1).

[3] ORPC: DOE-Scaled Mooring Test A, Curtis Libby, Maine Maritime Academy, May 11, 2011

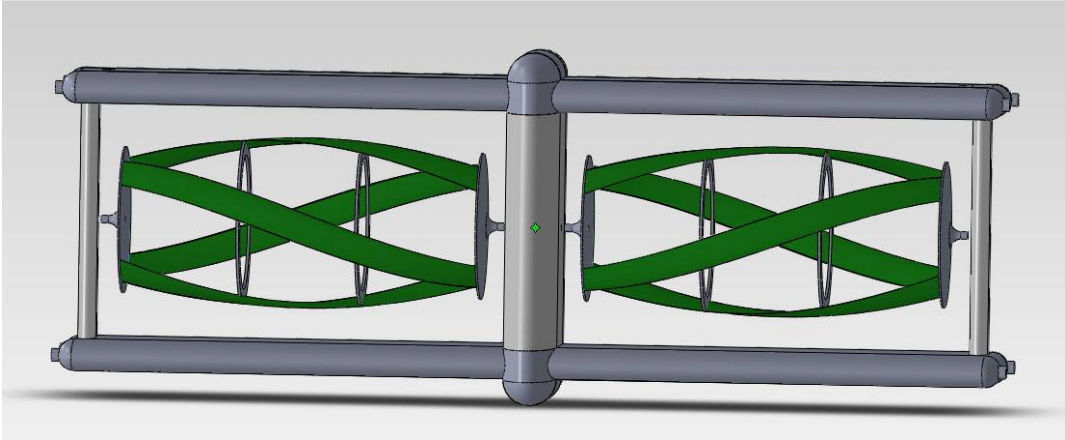

Figure 3.4.1. Scale model for the OCGen® TGU showing turbines. In the initial round of testing the turbines were replaced with a drag cylinder.

In order to simplify model construction and reduce the complexity of the carriage attachments, the model was inverted from the full-scale configuration. With the model inverted, the buoyant force of the full-scale structure was simulated by adding weight to the model.

Floating lines were used to mimic the catenary effects of the full-scale mooring lines. In all tests, the model was located 20 in. from the plate of the towing platform which simulated the seafloor.

Initial Mooring Configurations

Four mooring configurations were initially tested with the drag cylinder: a four point mooring, a two point mooring, and a crossed four point mooring. Schematics of these mooring arrangements are shown in Figure 3.4.2. (Note that the rear mooring lines are not shown for the sake of clarity.)

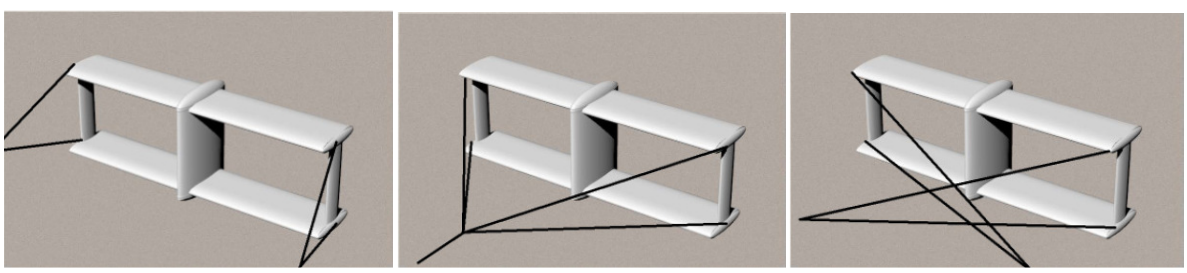

Figure 3.4.2. Three different mooring configurations tested as part of the initial round of scale model testing with a drag cylinder representing the turbines (not shown). From left to right: a four point mooring system, a two point mooring system, and a crossed four point mooring system. The rear mooring lines are not shown.

The four-point mooring system test was the most stable configuration, showing the least amount of vibration and variation in flow path. The two-point connection, which was expected to be very unstable, was found to be stable, with only a slight side to side “bobble” during the higher test speeds. The cross connection mooring test proved to be the most difficult to set up, due to the complexity of making the mooring lines hold the model at a level distance from the tow platform. The crossed design resulted in twisting forces on the structure that could not be corrected with the given test apparatus.

At the conclusion of these initial tests, the two point and four point mooring configurations were recommended for further testing.[4] For the second round of testing turbines were successfully manufactured and replaced the drag cylinder. Mooring line loads were instrumented and loads directly measured. For all tests, video was captured and mooring line tensions were measured to assess the relative performance of the different mooring configurations (Figure 3.4.3 and Figure 3.4.4).

In addition to head on flows, additional testing was performed to simulate a current non-perpendicular to the frontal face of the model by rotating the towing frame by 10° (Table 3.4.1).

Table 3.4.1. *Test matrix for second round of scale model testing*

Towing Speeds	1.0 ft/s 2.0 ft/s 2.5 ft/s 3.0 ft/s
Weight (Acting as buoyancy in water)	Maximum scaled (4.69 lbf) Half maximum scaled (2.56 lbf) Neutral (0.23 lbf)
Mooring Configurations	Two Point – Front to Back Two Point – Side by Side Four Point – 21° Four Point – Inline 90° Four Point – Inline 32° Four Point – Spread 43° Four Point – Spread 60°
Flow Angle of Incidence	0° 10°

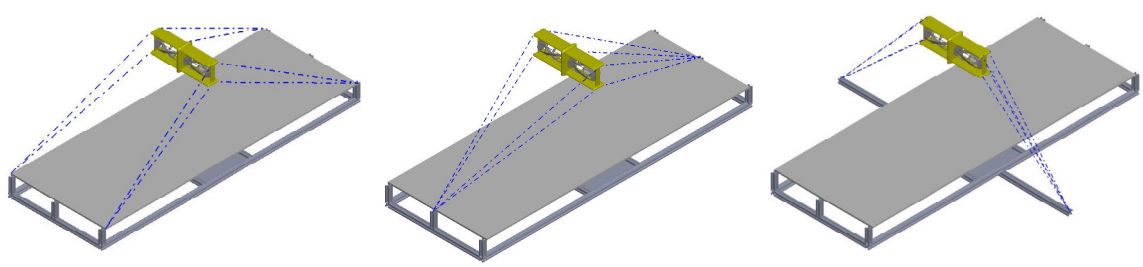

Figure 3.4.3. Mooring line configurations tested in round two of testing. From left to right: A four line mooring system similar to that already tested; a two point fore and aft mooring system; and a two point side to side mooring. In all tests, a scaled rotating turbine was included.

From a qualitative perspective the four point mooring system was by far the most stable of the three types used during the test, confirming first round test results. Angled flow impacted the distribution of

[4] DOE Mooring Tow Tank Report, RM Beaumont Corp, February 2012.

the loading on the lines, causing peak loading in the leading mooring line, but no major impact on the motion of the model.

The front to back configuration of the two point mooring system demonstrated similar behavior to that of the four point configuration in both tensile loads and stability in all but the 10° angled tests. When the flow approached from an angle, the model attempted to pull to the side, causing a rotation about the axis formed by the two mooring points. With nothing to oppose the rotation, this design could prove destructive by driving the structure into surrounding objects and/or the ocean floor. Based on these test results, a two point mooring configuration was not considered for future development.

Some tests were conducted in the two point side to side configuration. During the test, the model rotated about the mooring axis, allowing the model to nearly collide with the towing frame plate ("sea floor collision"). This configuration was not recommended for future model-scale testing.

An additional round of testing on the four point mooring system was conducted, with emphasis on angles between the lines and the vertical (Figure 3.4.4). Of these configurations, the tension leg arrangement had been suggested by the OrcaFlex modeling as a viable candidate.

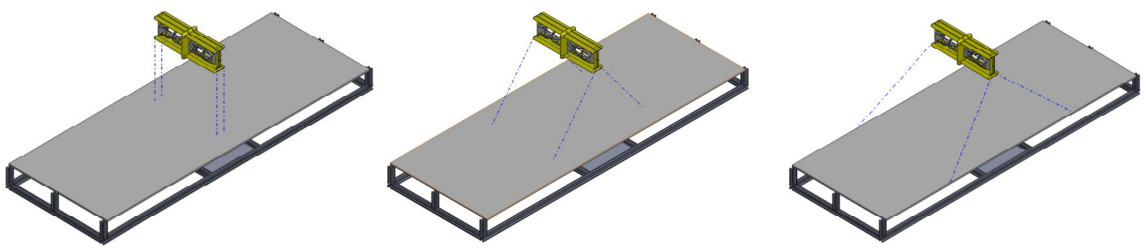

Figure 3.4.4. Additional four point mooring systems tested. From left to right: tension leg mooring (vertical lines), mooring system with lines inline in the flow direction and angled outwards at 32°, and mooring system with lines spread 43° to the vertical in both directions.

All of these configurations tested demonstrated similar loading behavior in the lines, with the vertical tension leg mooring having slightly lower peak values (Figure 3.4.5). The test video revealed that both the Inline 32° and Spread 43° configurations allowed the model to pitch fore and aft, attempting to rotate about the axis of the turbine shaft. For these tests, a cyclic line tension was present, with a frequency of 1.2 Hz. The tension leg mooring did not demonstrate this cyclic behavior. From these tests, the vertical tension leg mooring test proved the most stable overall.

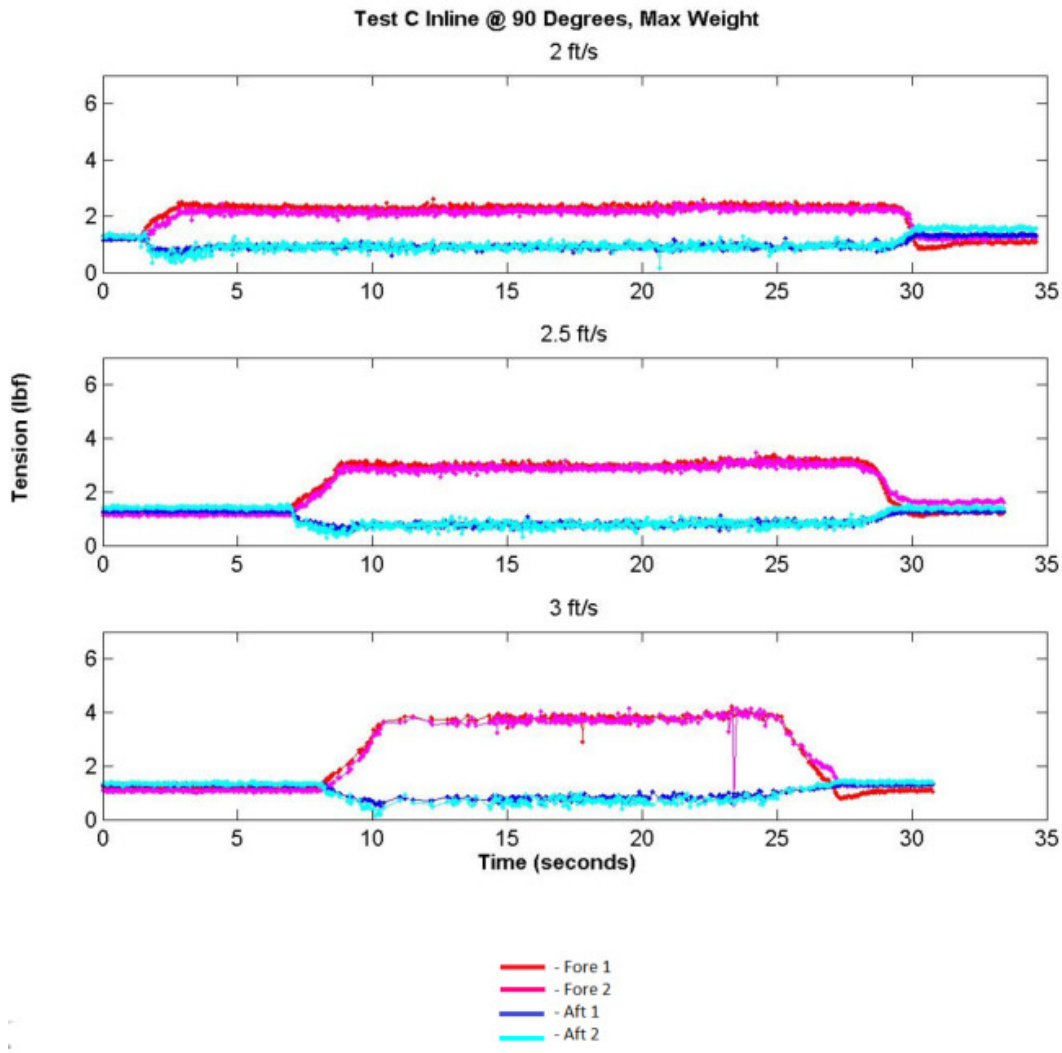

Figure 3.4.5. Tensions in mooring lines of vertical tension leg mooring system. Each subplot shows results for a different flow speed.

Problems Encountered

No significant problems were encountered with the model testing itself. The scale model testing provided a rapid means of down selecting from a wide variety of mooring line arrangements.

Departure from Planned Methodology

Quantitative test data from the model tests was not compared directly with the results from Task 1 (CFD work) or Task 2 (Lumped System Analysis).

The effort to compile a CFD model to replicate the scale model test would have been significant, and since the value of the CFD models were questionable, the work was not judged to be worthwhile.

The scale model test data was not compared with the Lumped System Analysis directly, as the Lumped System model had no apparent means of modeling the tow tank walls.

Additionally, it should be noted that with model testing of the cross-flow turbine it would have been difficult to scale the lift and drag forces produced by the turbine, as Reynolds number scaling was not possible. The size of the model was determined by volume scaling to replicate buoyancy effects. Thus the chord of the turbine foils is small.

Assessment of Impact on the Project Results

The scale model testing provided a rapid means of down selecting from a wide variety of mooring line arrangements, and proved the concept of a vertical tension leg mooring system which was selected as the basis for the full scale design.

The scale model testing provided qualitative data which was extremely useful. The fact that quantitative data from the testing was not directly compared with models did not have an impact on project results, as the scale model load data was not used to design mooring system components.

It was noted in the model testing that the presence of an upper and lower buoyancy section did cause issues when setting up the model due to low initial stability. This input from the scale model testing was considered in the design work for the full scale and proto type OCGen® devices, where only a single buoyancy chamber is used, and where it is placed above the center of mass of the system.

3.5 Task 5: Geophysical Surveys

Original Hypotheses

Local differences in seabed geology provide different degrees of anchoring capability. ORPC determined sea floor conditions commonly found in its areas of operation, and collected this data by means of multi-beam sonar surveys at multiple project sites.

Approaches Used

ORPC performed geophysical surveys of expected deployment areas for the OCGen® technology at several sites over the period of the project. Surveys were performed at two locations (Shackford Head and southwest of Goose Island) in Cobscook Bay, Maine, one site in Western Passage, Maine, and a potential OCGen® site in Cook Inlet, Alaska (Figure 3.5.1 and Figure 3.5.7).

ORPC initially selected the Shackford Head area in Cobscook Bay for deployment of the prototype mooring system and OCGen® TGU. Multi-beam sonar bathymetry data, side scan sonar data, magnetometer data, and sub-bottom profile data had been gathered for this site. The Shackford Head survey was completed in June 2009. However, delays in the project's NEPA review resulted in questions related to the availability of the Shackford Head site, as timing of the deployment could result in potential gear conflicts with local fishermen. At the same time, ORPC continued to gather geophysical, geotechnical and environmental data at the site located to the southwest of Goose Island, which ultimately became ORPC's FERC-licensed Cobscook Bay Tidal Energy Project. A geophysical survey was completed at this site in October 2011 (Figure 3.5.2).

The existing infrastructure (i.e., data cable) and the ability to consolidate ORPC activities within a marked site familiar to local mariners resulted in relocating the OCGen® deployment from Shackford Head to the Cobscook Bay Tidal Energy Project site.

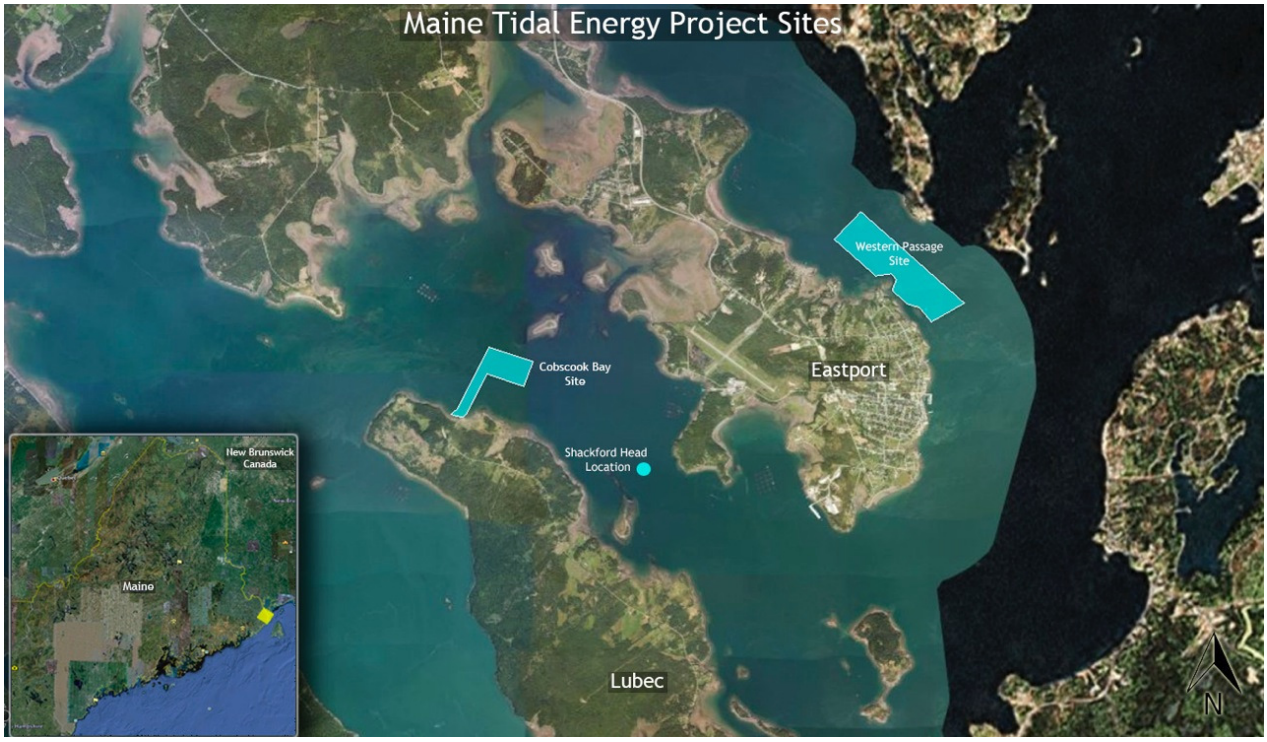

Figure 3.5.1. Location map of Shackford Head in Cobscook Bay, showing Western Passage.

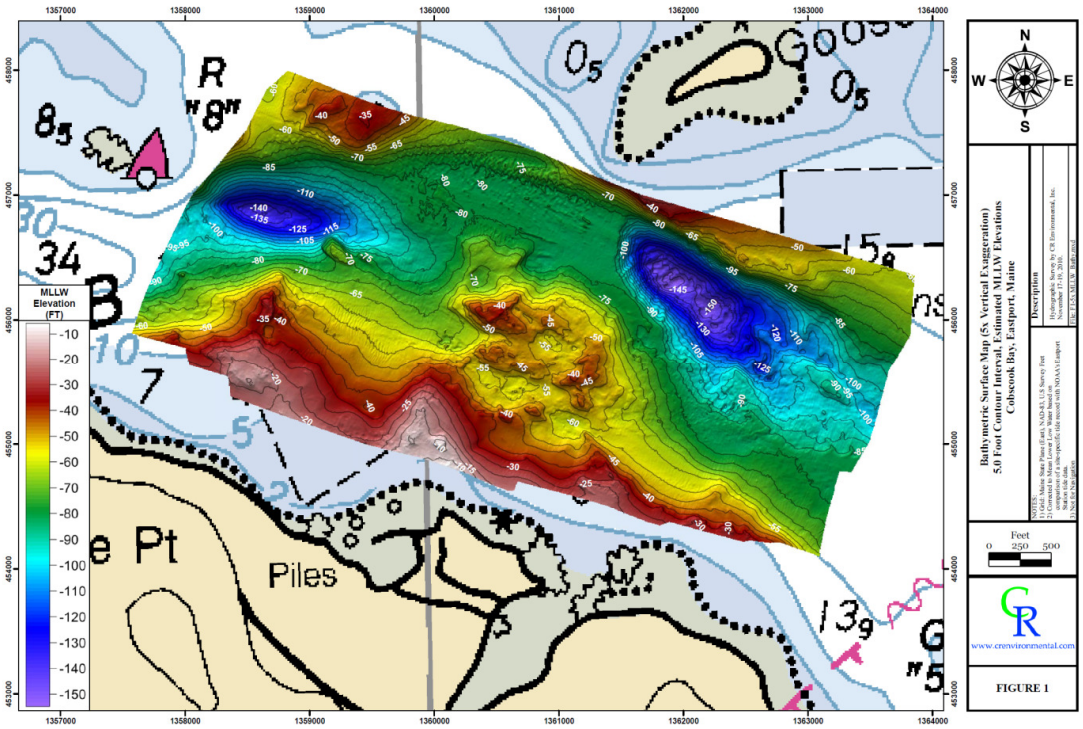

Figure 3.5.2. Bathymetry of OCGen® deployment site, Cobscook Bay, Maine, 2011

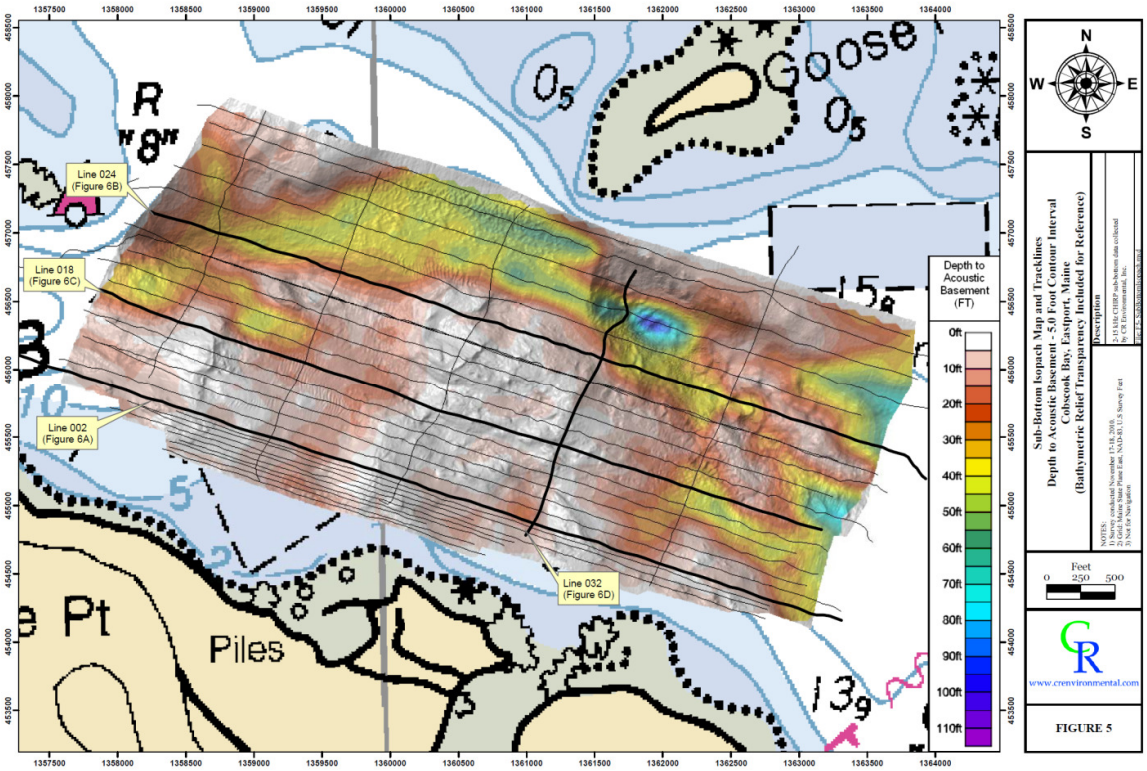

Figure 3.5.3. Estimated sediment thickness, Cobscook Bay, Maine, October 2011.

Findings from the 2011 survey in Cobscook Bay show that up to 50 ft of sediment was to be expected at the deployment site, with a thin cover of gravel, shell and cobble. Adjacent to the deployment site there was little sediment and much exposed rock ledge (Figure 3.5.3).

In addition to the surveys performed in Cobscook Bay, sub-bottom survey work was performed in Western Passage, Maine, to develop an understanding of the sub-bottom at other proposed OCGen® deployment sites.[5] The data collected from this particular survey served as input for the specification document of the full-scale OCGen® mooring design (Figure 3.5.4, Figure 3.5.5, and Figure 3.5.6).

[5] Bathymetric and Geophysical Survey, Kendall Head Western Passage, CR Environmental, March 2012.

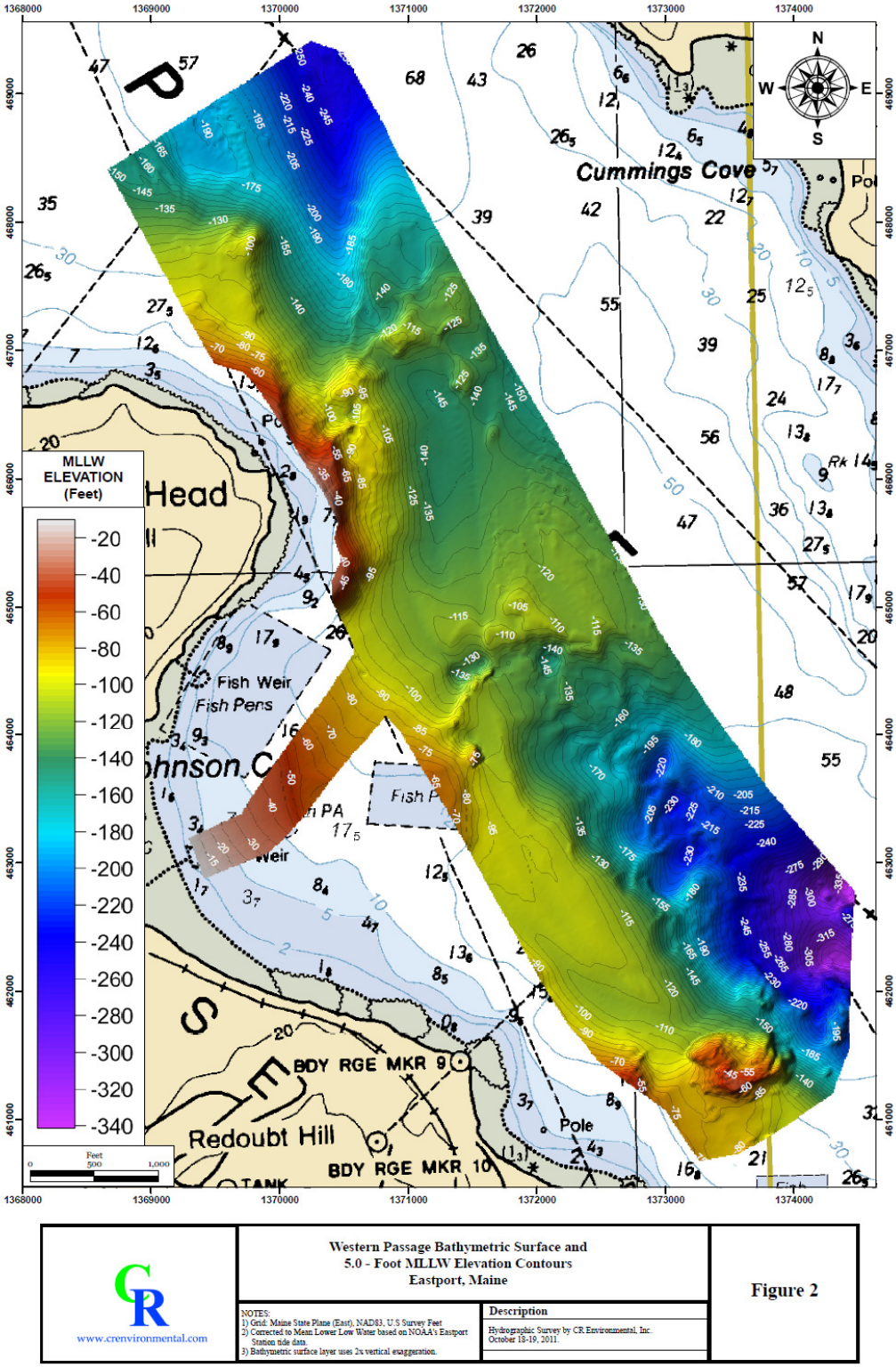

Figure 3.5.4. Bathymetric Surface and elevation contours, Western Passage, Eastport, Maine.

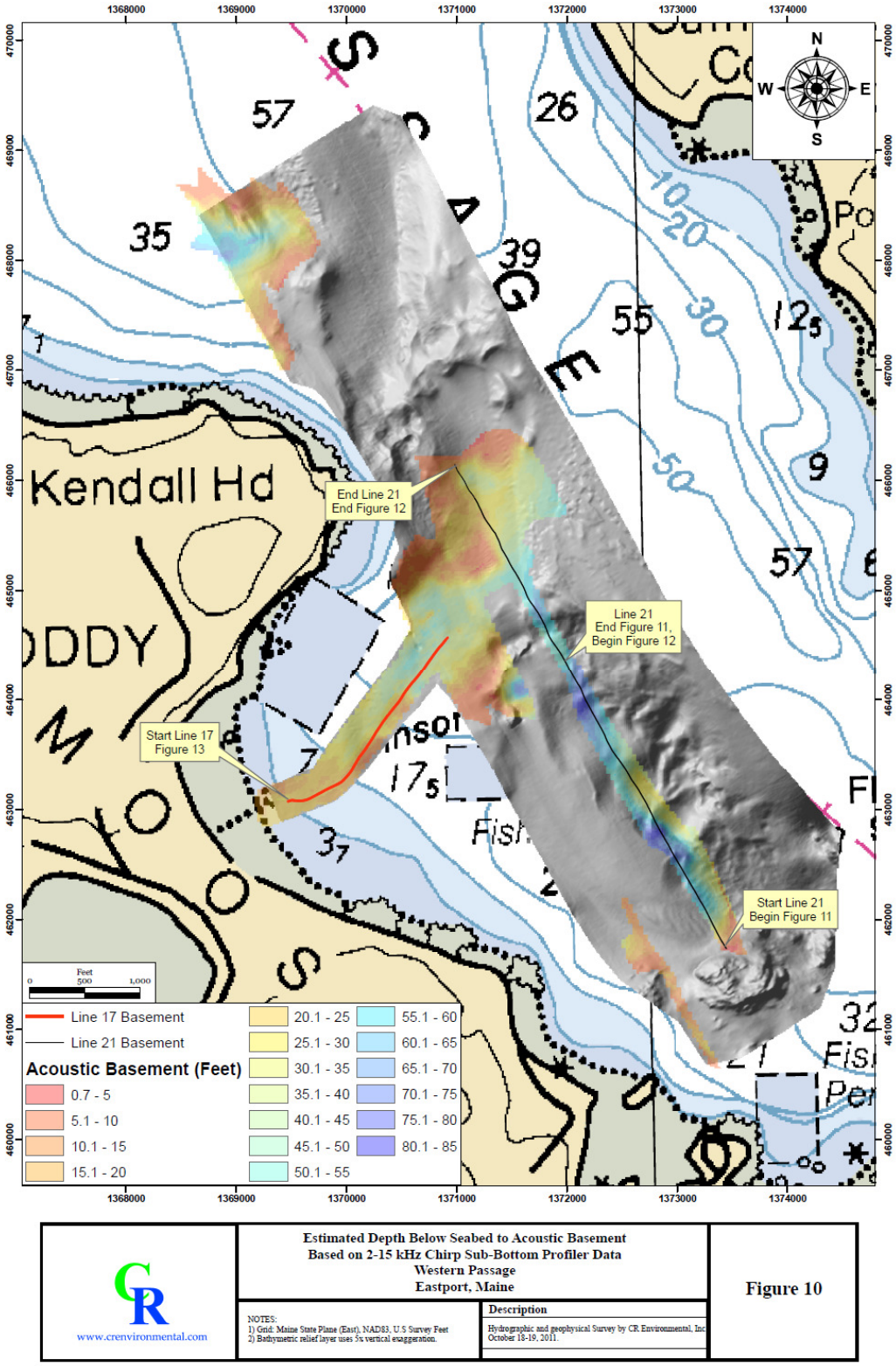

Figure 3.5.5. Estimate depth below seabed to acoustic basement, Western Passage, Eastport, Maine.

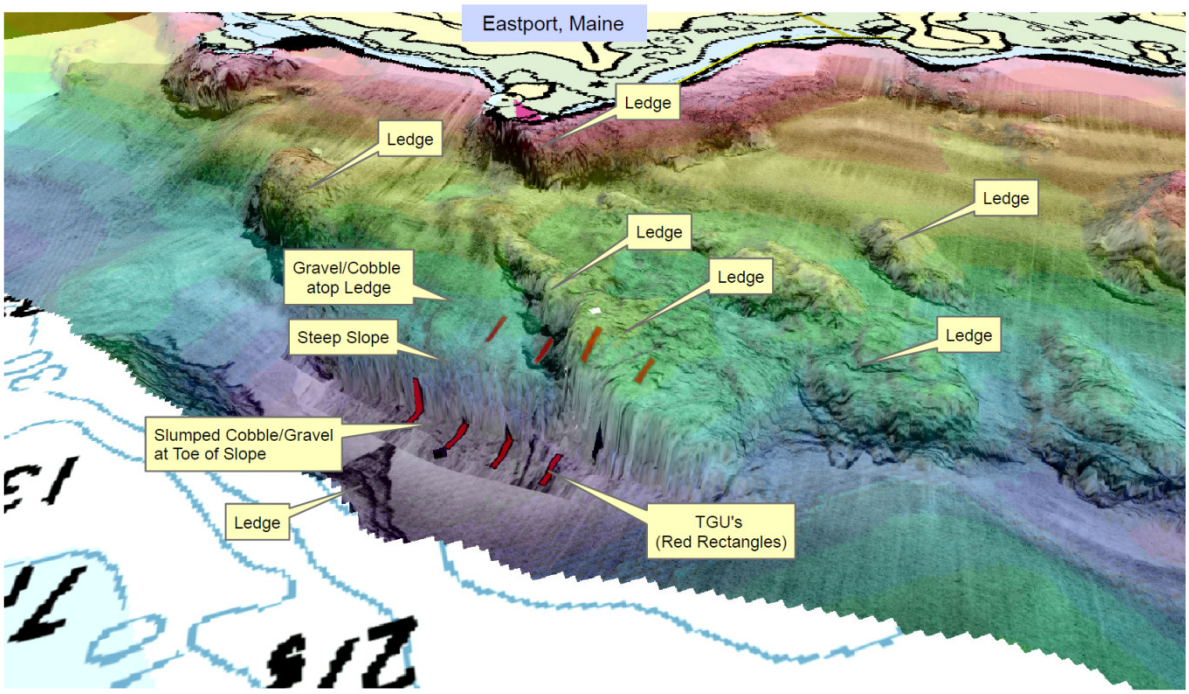

CR www.crenvironmental.com	Oblique 3-Dimensional View to Southwest Proposed Tide Generation Units Western Passage Not to Scale	
	NOTES: 1) Bathymetric data from NOS (survey H12259, 2010). MLLW, Feet. 2) Grid ME State Plane (East) NAD 83, US Foot 3) Side scan sonar data collected by CR Environmental in 2009.	Figure 2

Figure 3.5.6. Proposed OCGen® TGU sites, Western Passage, Eastport, Maine. Sites were selected for their high energy density, based on ADCP surveys and circulation models.

The findings from the survey from Western Passage show a much more challenging site, with depths of up to 340 ft, significant slopes, various slump features at the base of cliffs, and mixed areas of thin sediment and ledge.

To complete the understanding of potential bottom types, a survey was also conducted in Cook Inlet, Alaska, where ORPC holds a FERC Preliminary Permit for the East Foreland Tidal Energy Project (Figure 3.5.7 and Figure 3.5.8).[6]

[6] East Forelands Tidal Energy Power Project, Physical Site Characterization Survey, April 2013

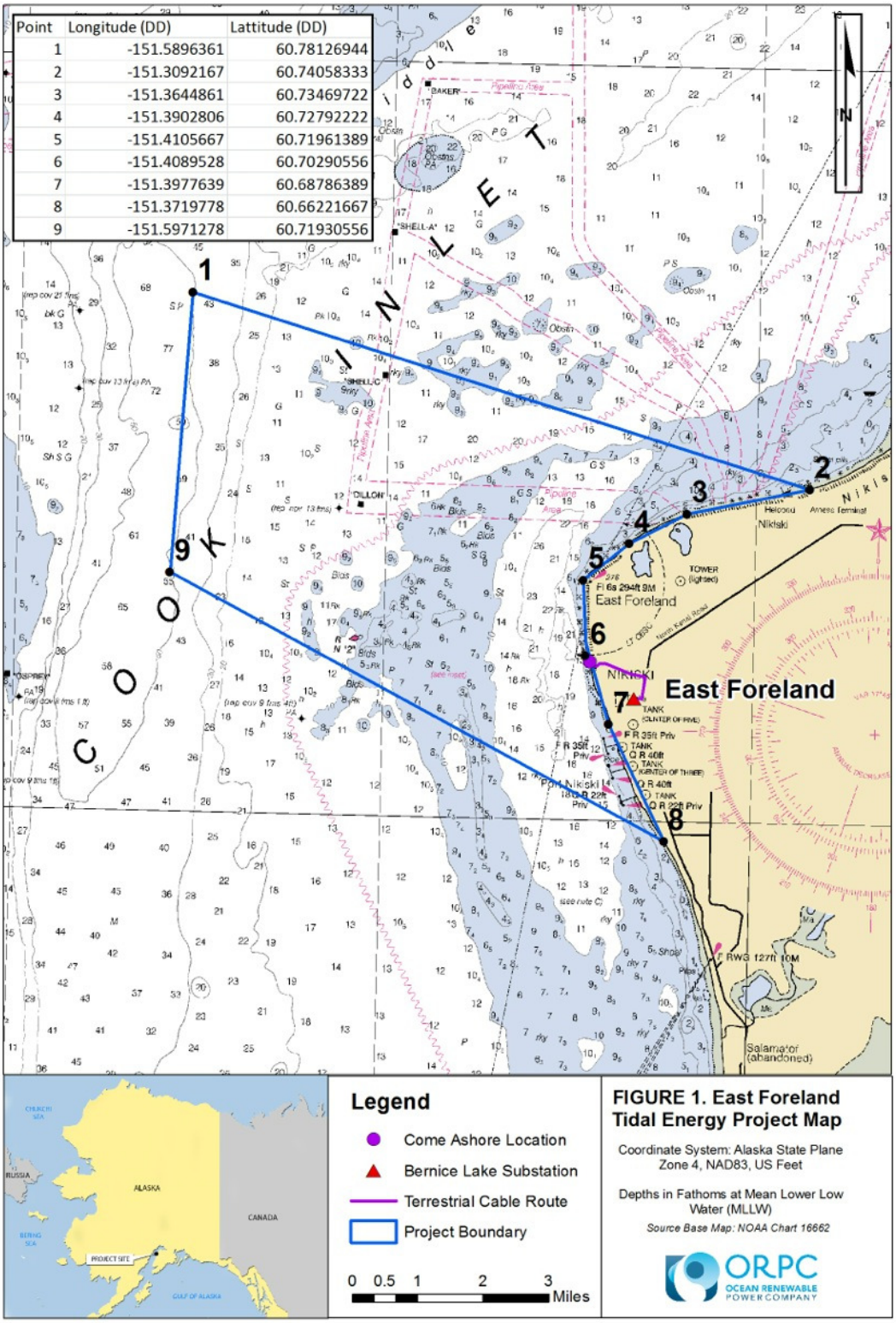

Figure 3.5.7. Cook Inlet Project Area Map

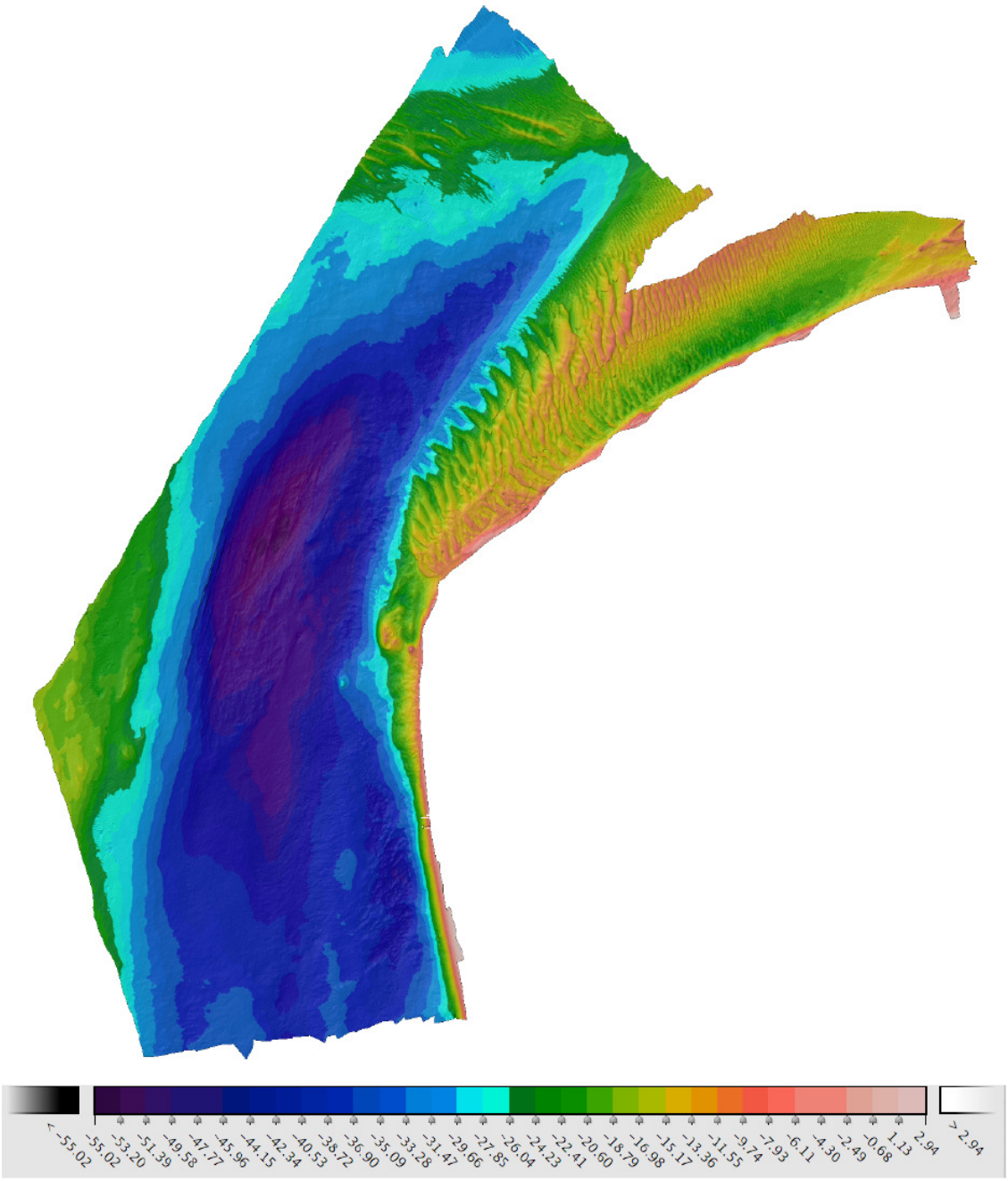

Figure 3.5.8. Bathymetry of Cook Inlet, Alaska site. Depth in meters.

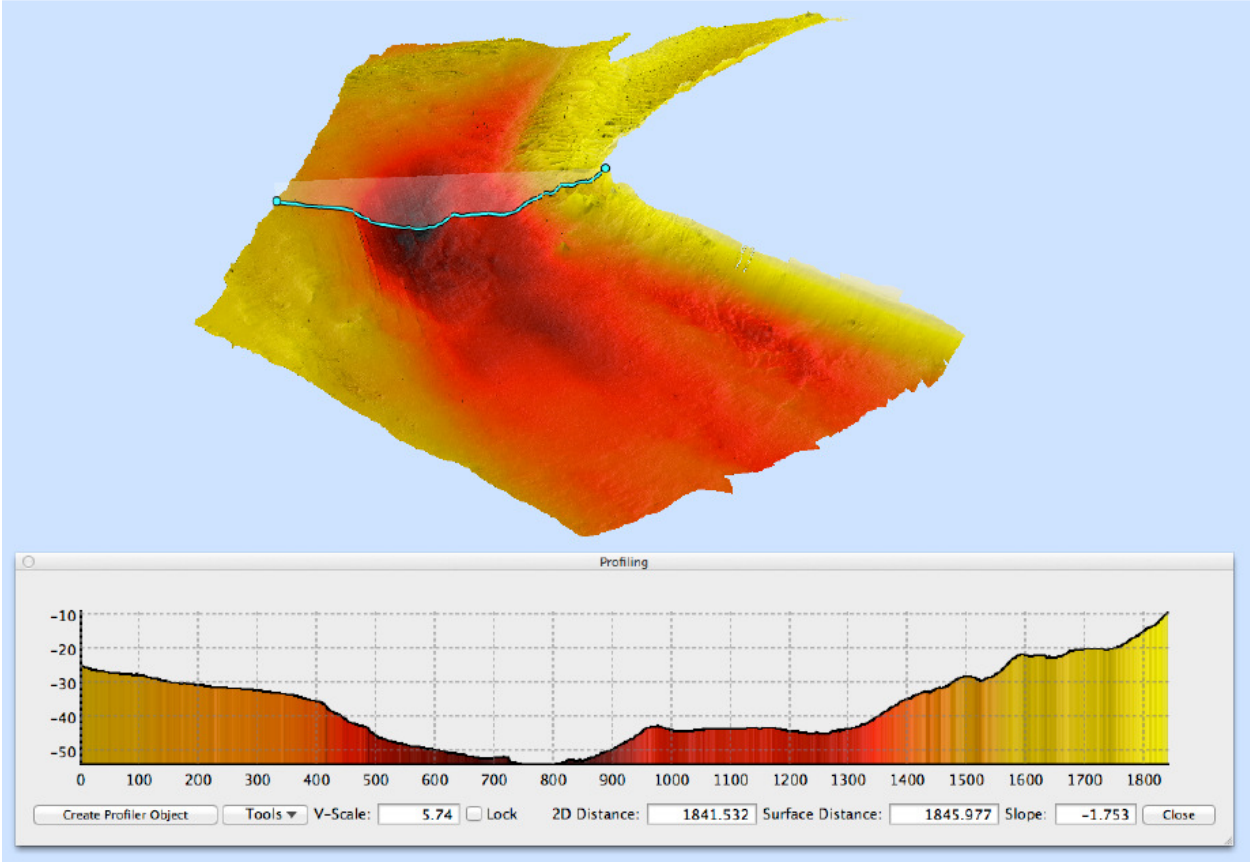

Figure 3.5.9. Sample cross section of bathymetry

Findings from the survey work in the East Foreland of Cook Inlet showed a very different marine geologic environment from that found in Maine, with highly mobile traverse dunes within the northern portion of the project area. The dune placement indicates rapid migration with significant variation over the period of each tide cycle. This shoal zone was surveyed over a period of several days when the vessel could operate in the vicinity at higher tide events. This allowed for significant periods of time between each survey event, and the result is observable in the product surface. The dunes, with sand moving at rapid velocity with the tide, migrate quickly through the dune field. When the vessel was again allowed to return to the shoal area, the dunes had migrated significantly. The dunes are interpreted to be composed mostly of well sorted fine to medium grain sands with other unsorted clasts erratically dispersed beneath the sands, buried at some earlier period and now sheltered from the high current energy (Figure 3.5.10).

Changes to the natural sedimentation patterns due to installation and operation of an MHK device has been an area of concern. For a limited number of devices installed in a large area, no significant changes to flow or sedimentation is expected.[7] As project sizes increases the effect on sedimentation does need to be assessed.

[7] Sandia National Laboratories, Sea Engineering, Inc. (September 2012). Hydrodynamics FY12 Q4 Report, SNL-EFDC Model Application to Cobscook Bay, ME

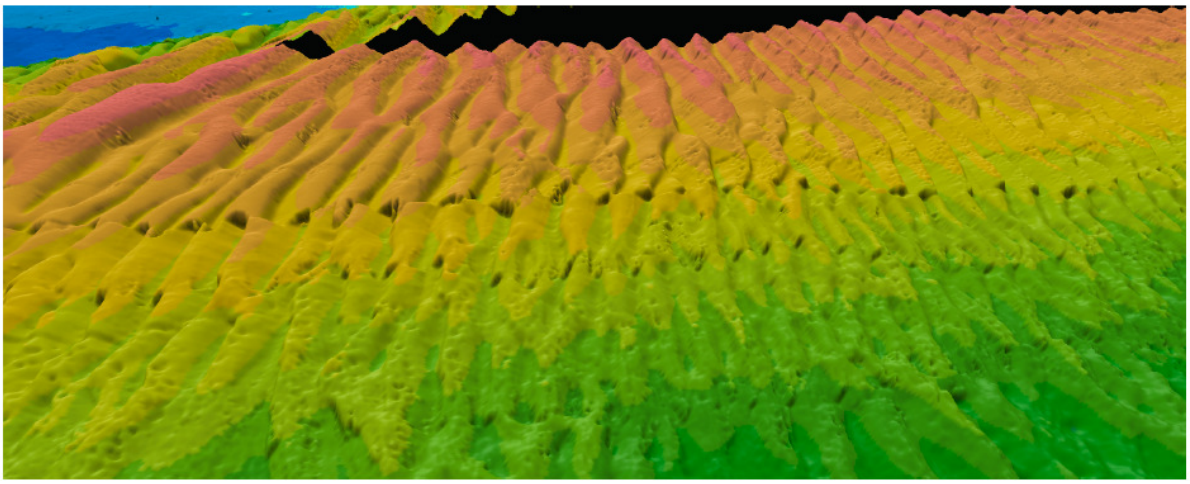

Figure 3.5.10. Separate survey periods (separated by several days) display dunes almost 180° out of phase.

Other areas within the survey site show more stable dunes structures, as well as areas of thin sediment overlaying exposed vertical bedrock ridges.

Problems Encountered

ORPC did not receive a NEPA categorical exclusion until June 2011, approximately fourteen months after the start of the Project Period.

The Shackford Head site had seasonal restrictions related to the local commercial fishery that limited times of the year appropriate for deployment. Considering time required for the NEPA review and the site availability, ORPC requested, and was granted, an eighteen month extension.

The utility of multi-beam survey methods to detect small changes in the bathymetry of the area surrounding the project was limited by the accuracy of the survey. Comparing surveys from different time periods will only be as good as the basic uncertainty in either of the surveys. The degree of change that ORPC was looking for was expected to be in the range of one to two feet. The uncertainty analysis indicated that the uncertainty in the bathymetric survey at the OCGen® location is approximately 2 ft (Figure 3.5.11).

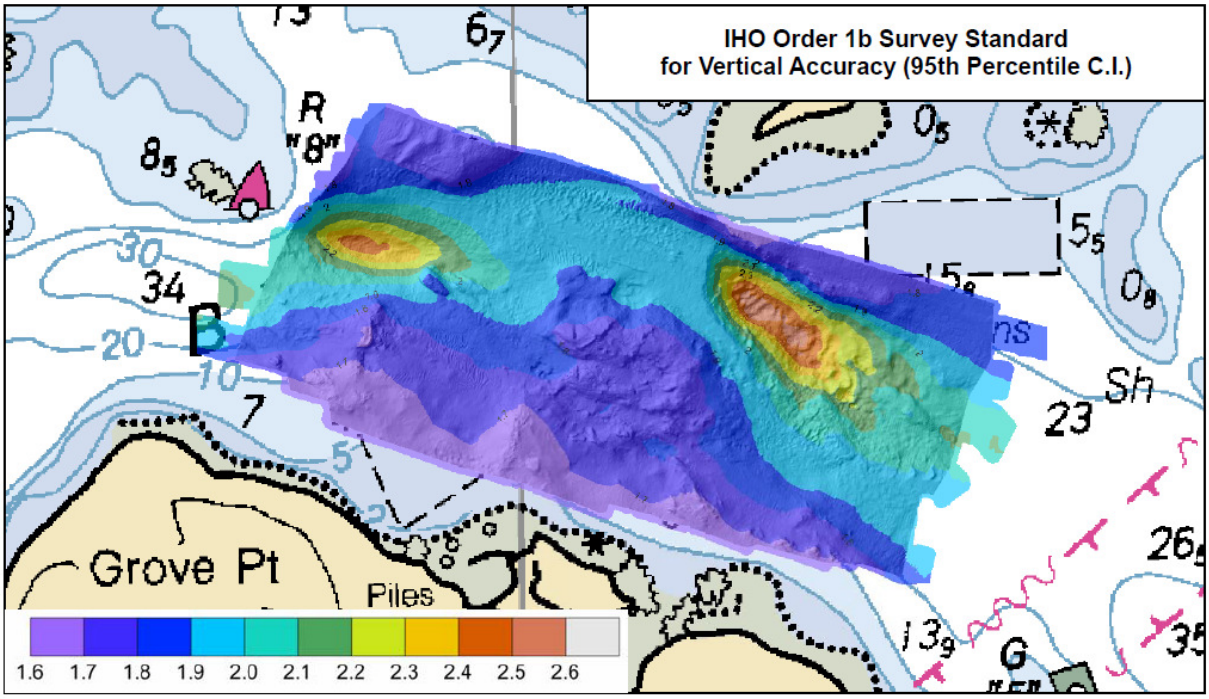

Figure 3.5.11. Accuracy estimates for the multi-beam survey performed in Cobscook Bay. The deployment area was located in the area with 1.9 to 2.0 foot accuracy.

Departure from Planned Methodology

ORPC anticipated that scour depths would be less than 1 ft at any given site. This implied that a multi-beam survey was not sufficiently precise enough to identify the expected changes in the bathymetry. As a result of this finding, ORPC changed the method of geophysical inspection from a multi-beam survey to a dive inspection of the mooring anchors. Reference markers on and adjacent to the anchors were provided, and the relative distance (horizontal and vertical) from the anchors to the markers was monitored at the beginning and end of the OCGen® deployment.

Assessment of Impact on the Project Results

The change in methodology provided more accurate results to quantify vertical changes in seabed elevation and horizontal movement of the anchors.

Review of the typical bathymetry at some potential project sites indicates a wide range of depths over relatively small areas. Use of a tension leg mooring system allows for smaller system footprint and so minimizes the depth variance to be considered. The original mooring concept had been conceived for use in depths of over 30m, but the tension leg concept would be suitable for shallower depth sites, and may also be suitable for surface moored systems.

3.6 Task 6: Cable and Anchor Design

ORPC designed the anchor configuration using the loading information produced by the analytical work provided in Tasks 1, 2, 3, and 4 and the geophysical results obtained in Task 5.

Original Hypotheses

Original concepts for the OCGen® mooring system comprised a buoyant structure moored to the seafloor using a spread leg mooring. This arrangement occupied a significant footprint. Anchors were expected to consist of some variant of an embedment anchor, either high efficiency drag anchors, or helical anchors. Mooring lines were expected to be either chain or synthetic line (Figure 3.6.1).

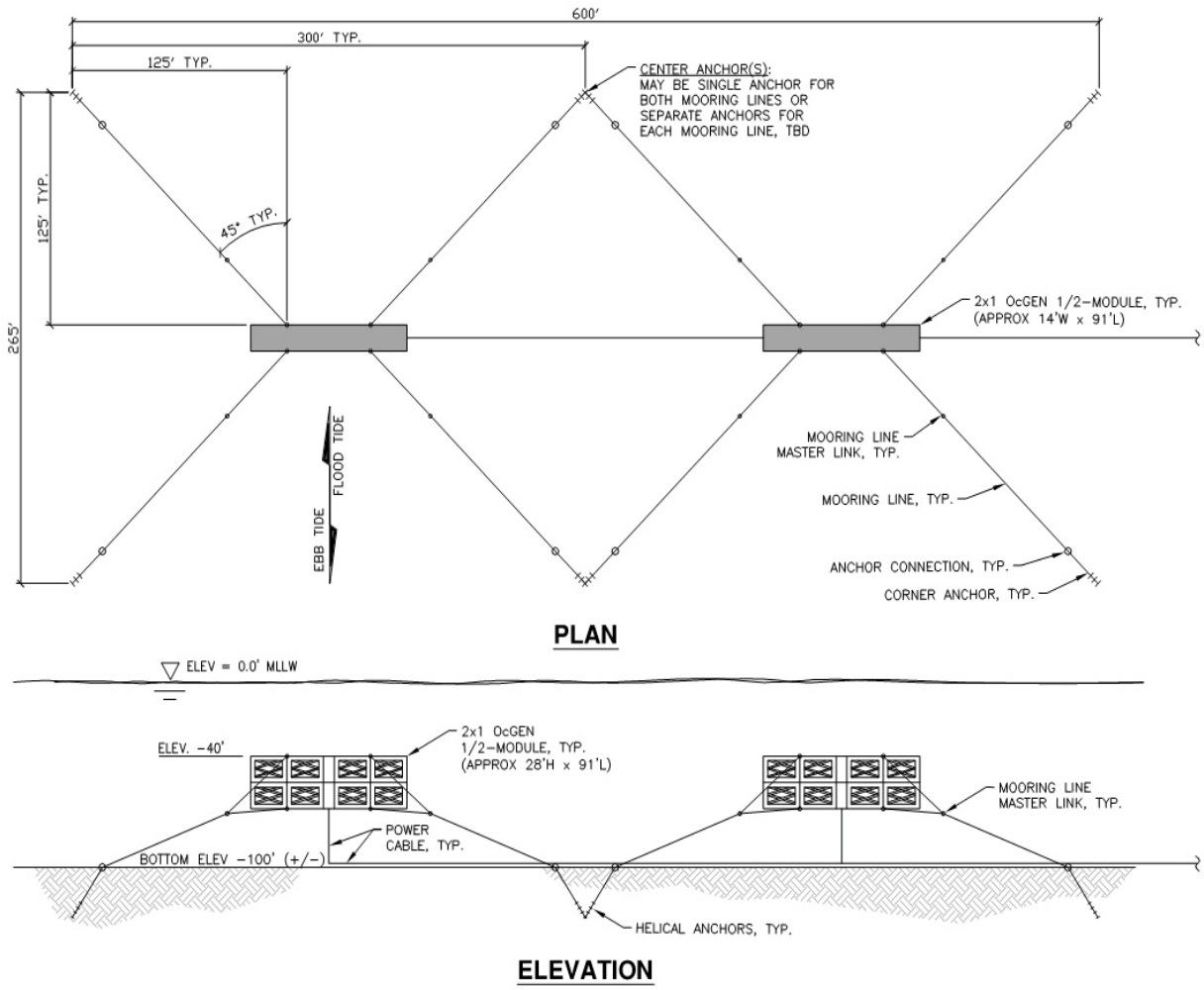

Figure 3.6.1. Original proposed concept for the OCGen® mooring system. The moorings consisted of a spread leg mooring, with embedment anchors

Approaches Used

Assessment of the geophysical information at the various OCGen® deployment sites showed a wide range of bottom types, including gravel, cobble, marine clays, sand-like sediments and exposed rock ledge. The depth of the sediment layers varied widely from site to site and even within each site, creating a significant challenge to the use of embedment anchors as a mooring technology. The site specific conditions implied that the design of the anchors for each and every deployment would be

specific to that deployment. This created many issues, including: documentation of multiple designs, inability to produce or procure anchors in any kind of volume for a given project, a significant amount of uncertainty related to the design life for the mooring as each installation is different, and the requirement for developing different inspection procedures for each mooring in a site. In addition, embedment type anchors may require dedicated installation assets and may also require proof loading before use. The additional cost to the project of such individualization gave cause for concern. A single mooring type, suitable for application in multiple sites, was desirable.

A gravity mooring system, while apparently inefficient in the use of mass, addresses many of the issues mentioned above. For these reasons ORPC decided to focus on the implementation of a gravity mooring system for the OCGen® TGU (Figure 3.6.2).

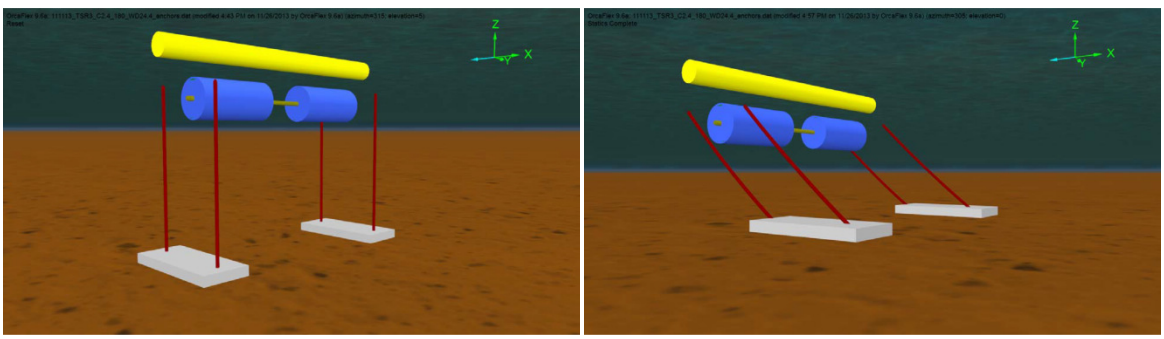

Figure 3.6.2. OrcaFlex schematic of the prototype OCGen® TGU and mooring system

A proper assessment of the loads on the mooring lines required that a full range of operating conditions be examined. Data presented in Task 4 focused on the loads in the mooring lines with the turbines operating. However maximum drag loads for the turbines occurred with the turbine in free-wheel mode, i.e., at maximum RPM. In addition, loads vary depending on the incipient angle of the flow. ORPC investigated the effects of these flow and operating conditions, as well as wave effects, on the mooring loads and on device station keeping.

A studlink chain, 1 -1/4 in., was selected as the first design iteration for the mooring lines (Table 3.6.1).

Table 3.6.1. *Mooring chain specifications*

Mooring Chain				
Type	Studlink, Grade 2			
	Metric		U.S.	
Bar Diameter	0.038	m	1.5	in
Length (attachment to seabed)	10.67	m	35	ft
Wt. / 90-Ft shot (dry)	8.7	kN	1950	lb
Wt./ 90-ft shot (wet)	7.5	kN	1693	lb
Proof Load	582.9	kN	131,000	lb
Break Strength	816.5	kN	183,500	lb
Maximum Installation Load	155.7	kN	35,000	lb
Maximum Operating Load	65.0	kN	14,600	lb
FoS (MBS) with Installation Load	5.2	-	5.2	
FoS (Proof) with Installation Load	3.7	-	3.7	

Using the chain mooring lines a study of the effects of offset flow and variations in turbine operating conditions was conducted using OrcaFlex. The model results are shown below for three different operating conditions: TSR 3 – a freewheel condition with a tip speed ratio of 3; TSR 0 – a non-rotating turbine with tip speed ratio of 0; and TSR 1.5 +L – tip speed ratio of 1.5, with turbine producing power and some additional lift . (Refer to Figure 3.2 above for variation in CD and CL as a function of TSR).

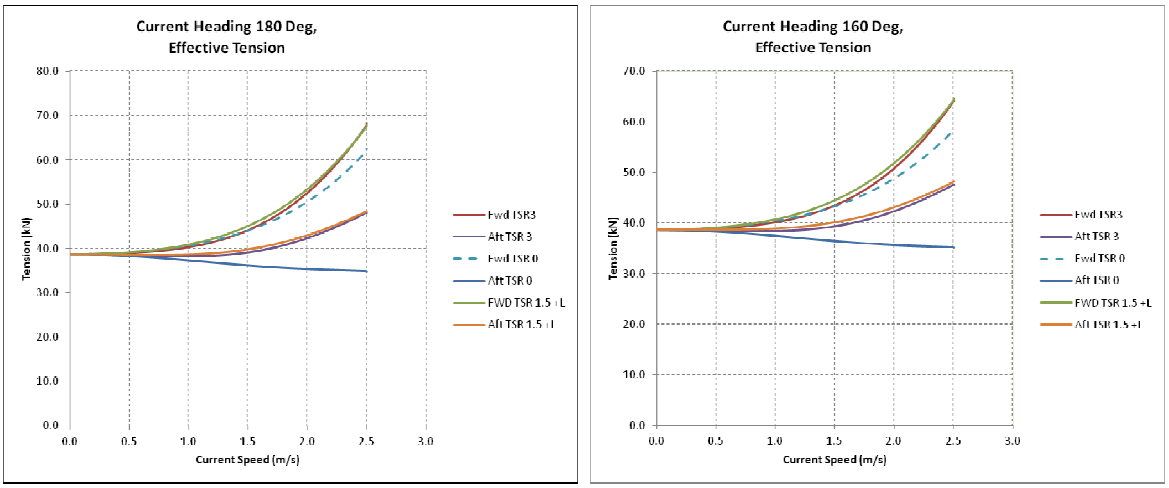

Figure 3.6.3. Mooring line loads for a chain mooring system for dead ahead flows and flows offset at 20°

The plots indicated that mooring line loads do not significantly differ for offset flows from the baseline case.

For the freewheel condition (TSR = 3.0), the loads in the fore and aft lines increased as water speed increased. The freewheel condition was the maximum drag for the turbines.

For the stationary turbine case (TSR = 0) loads in the forward lines increased, and loads in the aft lines decreased as water speed increased. Loads were distributed between the fore and aft moorings.

For the case where the turbine would produce power (TSR = 1.5), the loads tracked the freewheel condition closely.

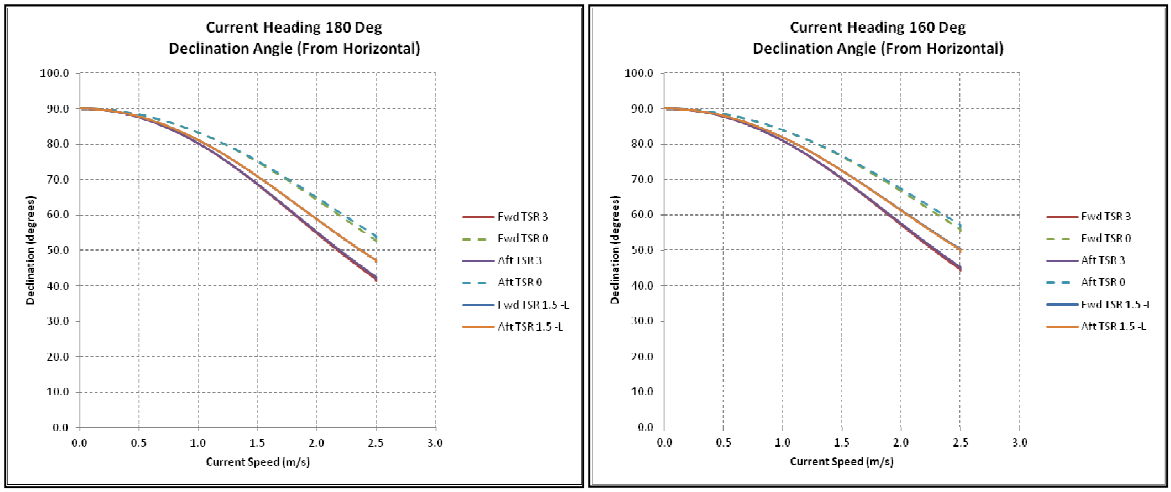

Figure 3.6.4. Declination angle of the TGU as a function of water speed for a chain mooring system

The system acted so that the turbines and the buoyancy pod translated through the water column as the water speed increased. The angle that the mooring line made with the horizontal was significant as shown in Figure 3.6.4. Again, of note, is that the declination angle was not overly sensitive to flow incidence angle. In addition, the declination angle was not particularly sensitive to turbine operating condition. Fore and aft lines tracked each other well in terms of declination angle.

The pitch angle of the TGU remained relatively constant as water speed changes, with a maximum expected change of 1.2°.

The average and maximum wind speed for the Cobscook Bay location was obtained from NOAA weather station PSBM1 – 8410140 located in Eastport, Maine. The maximum wind speed recorded between November 2004 and December 2012 was 50 knots. This value was used for estimating the maximum wave height and period for the site location. The wave height and period can be estimated using the Shore Protection Manual.[8] The U.S. Geological Survey Fetch- and Depth-Limited Wave Calculations applet, which is based on these two equations of the Shore Protection Manuel (SPM), was used to estimate the wave height and period. The equations assume a constant water depth, wind speed, and fetch. The maximum fetch for the location is approximately 6 km. The average water depth across the fetch was assumed to be 30 m. A range of depths were used initially to verify the depth assumption. The results showed very little sensitivity to depth. Using these values the calculated wave height is 1.5m with a period of 3.7s. For a period of 3.7s and wave height of 1.5m, the wave is considered to be a deep water wave. From linear wave theory, the maximum orbital velocity at a depth of 12m is calculated as 0.05 m/s. Compared to the design current of 2.4 m/s, the effect of an individual wave on the current speed was negligible. Therefore, waves were not considered to be a significant load factor for systems such as the OCGen® TGU.

Concerns were raised regarding the ability of the mooring system to tolerate inaccuracies in placement, irregularities on the seafloor, or uneven settling of the anchors. A series of vertical offsets of a single anchor were input into the OrcaFlex model. The Port anchor was assumed to be positioned such that

[8] Shore Protection Manual Volume 1, Coastal Engineering Research Center, U.S. Army Corp of Engineers, 1984.

the forward end of the port anchor was higher than the design position, and the aft end of the port anchor was lower than the design position. The offset amounts are +/- 1 in., +/- 0.5 ft, and +/- 1 ft. An addition case of a 5 degree rotation of the port anchor was also analyzed. The length of the mooring is the same for each leg.

The sensitivity of mooring line loads to small variation in vertical offset was found to be extreme. For a 1 in. vertical offset the mooring line loads were doubled in the aft port mooring line and practically removed in the forward mooring line. The same held true for larger offsets (Figure 3.6.5).

Behavior for angular offsets is also noticeably different, although not as severe as for the vertical offsets.

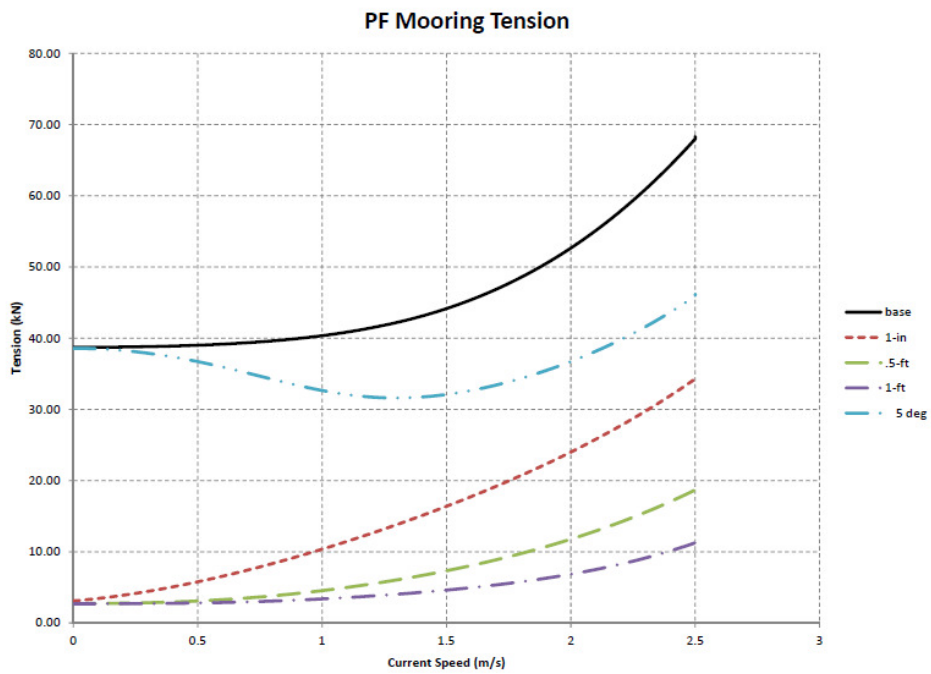

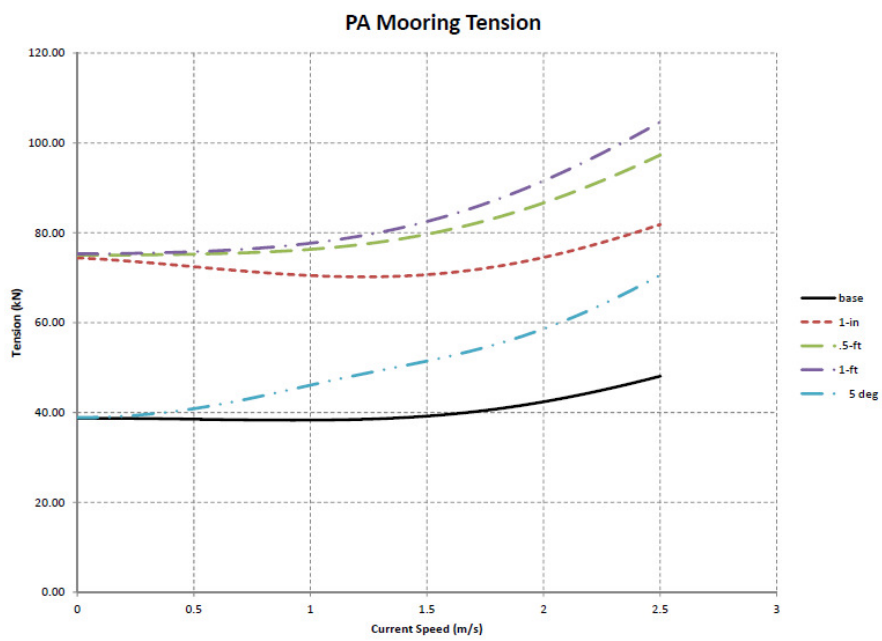

Figure 3.6.5. Sensitivity of the mooring line loads to small changes in anchor position on the seafloor. These results are for a chain mooring for the port side. PF refers to the forward mooring line and PA to the aft mooring line. The port anchor is displaced by various amounts in the vertical direction. A single analysis is also run for a rotation of the port anchor by 5° about the vertical.

Further investigation of this behavior revealed that the root cause was the very high stiffness of the chain mooring line. Small extensions of the tension leg chain mooring result in large load changes. This is aggravated by the relatively small length (<25 ft) of mooring line being considered for this prototype application. A more compliant mooring line was required.

Investigation of the various types of synthetic mooring line available indicate that nylon mooring line is available and is by far the most compliant type of synthetic line.[9]

The OrcaFlex models were adjusted to replace the chain mooring lines with a nylon line. A comparison of the baseline case of nylon versus a chain tension leg mooring line shows that there are only slight force differences between the two cases. Maximum loads are reduced for the nylon mooring line case.

But investigating what happens when the port anchor is displaced 1ft upward on the front and 1ft downward on the rear, research found that while loads differ from the baseline case, the increased compliance of the mooring line allows for better load sharing between fore and aft lines (Figure 3.6.6, Figure 3.6.7 and Figure 3.6.8).

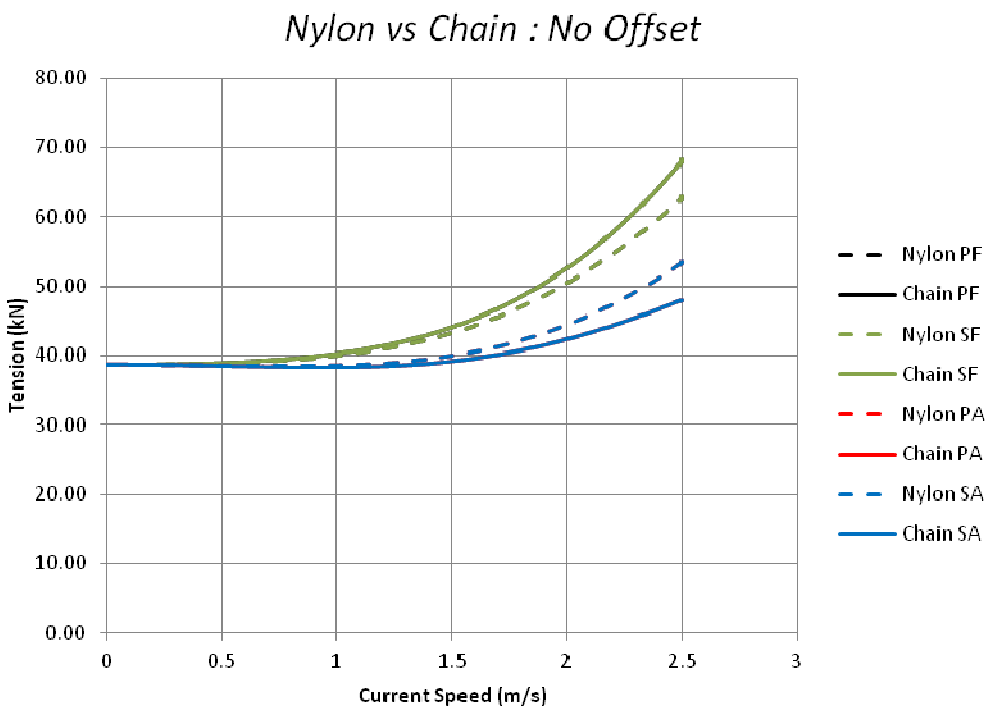

Figure 3.6.6. Tension leg mooring loads for a nylon mooring line and a chain mooring line. Starboard (SB) forces and Port force (PF) overlay each other in this plot.

[9] Guidance on the use of synthetic fiber ropes for marine energy devices, Ifremer reference: RDT CSM 13-232, September 2013

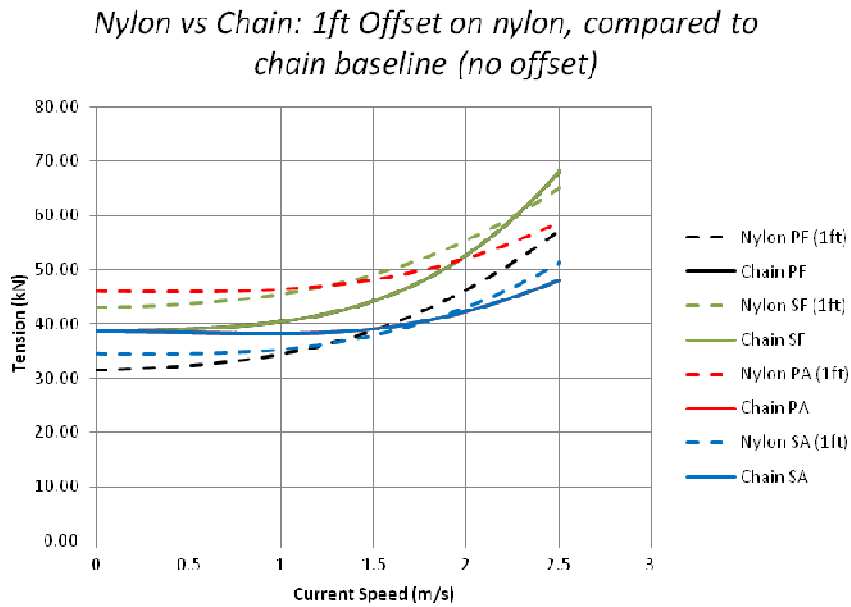

Figure 3.6.7. Mooring line loads for the chain case with no offset are presented and compared with mooring line loads for a +/-1ft offset of the port anchor using nylon mooring lines. Starboard (SB) forces and Port force (PF) overlay each other in this plot for the chain results.

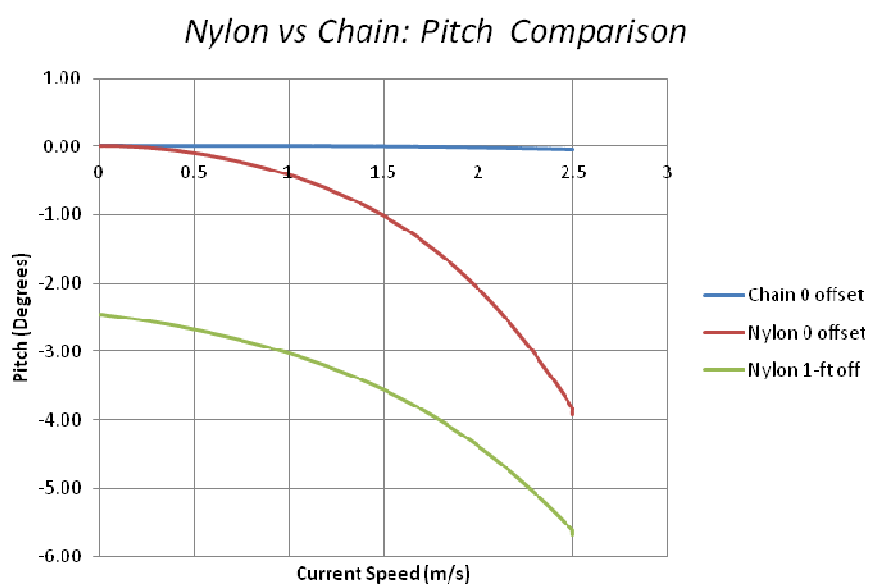

Figure 3.6.8. A comparison of the pitch angle of the OCGen® TGU as a function of water speed for three different cases: the chain mooring system, a nylon mooring system, and a nylon mooring system with a 1 ft offset on the port mooring block.

The additional compliance of the nylon mooring lines, while it improved the load sharing between fore and aft lines in non-ideal situations, did lead to an increase in the pitch angle of the OCGen® TGU itself. This is clear from Figure 3.6.8. Any deviations from ideal placement of the anchors also appeared to have an additional effect on the pitch angle.

ORPC concluded that compliant mooring lines are necessary for the tension leg mooring system to function adequately, especially in the case of relatively short mooring lines as analyzed in this project.

An examination of the literature for synthetic mooring lines[10] showed that fatigue life of synthetic line is predictable once loadings are well understood, and that substantial life can be obtained as long as the lines are handled properly. Primary factors in limiting life cycles include abrasion damage from rubbing on the bottom, and abrasion damage from any sediments or sands collecting between fibers. These failure modes compare favorable with failure modes expected from chain moorings, which are dominated again by abrasion and corrosion. The cost of the synthetic mooring lines and the cost of chain is small in terms of capital costs, but the cost of the synthetic line is favorable in terms of installation and handling costs. Estimated costs for a 25 ft long nylon mooring line for this application was $3,128 each, as compared to the cost of an equivalent rated shot of chain (90 ft) of $1,750. According to the Guidance for synthetic mooring lines:

> Whilst the short and long-term performance of these materials *(synthetics)* is more complex than conventional ferrous materials used in mooring applications, there are distinct advantages to using synthetic ropes instead of steel components including low cost, low mass and an inherent ability to absorb energy.[11]

Vortex induced vibration on the mooring lines is possible for the correct combination of flow speeds, shedding frequencies and mooring line properties. However the natural frequency of the mooring line depends on the length of the line and therefore the issue of VIV needs to be assessed for each individual deployment location, using the specific properties of the line. For the deployment in Cobscook Bay these calculations are reviewed in Task 7.

Moorings

For the test site in Cobscook Bay, the design of the deadweight anchors was performed following the NAVFAC Anchor Design Manual.[12] The anchors capability to resist sliding resulting from long term, short term and cyclic loads determined using recommended safety factors.

Geotechnical information for the site was provided from the geophysical surveys conducted at the site. Not all of the soil parameters required for the design were available, but those that were not available were estimated based on the available soil information. The design parameters utilized are shown in Table 3.6.2.

[10] Guidance on the use of synthetic fiber ropes for marine energy devices, Ifremer reference: RDT CSM 13-232, September 2013

[11] Guidance on the use of synthetic fiber ropes for marine energy devices, Ifremer reference: RDT CSM 13-232, September 2013

[12] Handbook for Marine Geotechnical Engineering, NAVFAC Engineering Service Center, SP-2209-OCN, February 2012. Environmental Conditions

The soil samples taken at the surface are classified as CL in the Unified Soil Classification System. The typical undrained soil friction angle for soil classified as CL from NAVFAC Design Manual 7.02 is 28 degrees and was used in the analysis. The effective cohesion value was not provided in the Geotechnical Data. The typical cohesion value for saturated soils classified as CL was 270 lb/ft^2. The cohesion value was conservatively estimated as 100 lb/ft^2 for use in the analysis. Calculations for the anchor design were conducted by PCCI.[13]

Table 3.6.2. *Site data for design of gravity mooring for OCGen® prototype systems in Cobscook Bay*

Seabed Design Parameters				
	Metric		English	
Seabed Slope	0	deg	0	degrees
Soil Friction Angle	28	deg	28	degrees
Buoyant Unit weight of Soil	890	kg/m^3	55.6	pcf
Effective Drained Soil Friction Angle	0	deg	0	degrees
Undrained Shear Strength	976	kg/m^2	200	psf
Effective Soil Cohesion	488	kg/m^2	100	psf
Coefficient of Friction	0.532	-	0.532	-
Factor of Safety - Long Term Loading	2.5	-	2.5	-
Factor of Safety - Short Term & Cyclic Loading	3.2	-	2.5	

The anchor design consisted of two concrete clump weight anchors. Each anchor has a 1.5-ft high steel skirt surrounding the perimeter with 1.5-ft high steel shear keys. The shear keys and skirt provided additional lateral holding capacity by engaging the soil contained within them. The anchor specifications are provided in Table 3.6.3.

Each of the anchors has attachment points for two mooring lines (fore and aft lines). This offers the advantage of fewer components to install (two anchors versus four) and provides a good control over the mooring line spacing in the fore and aft directions.

Table 3.6.3. *Anchor specifications for OCGen® prototype TGU in Cobscook Bay*

Anchor Design				
	Metric		English	
Concrete density	2401	kg/m^3	150	pcf
Length	7.01	m	23	ft
Width	3.05	m	10	ft
Height	0.61	m	2	ft
Number of Shear Keys	8	-	8	
Skirt Height	0.46	m	1.5	ft
Shear Key Height	0.46	m	1.5	ft
Shear Key Spacing	1.00	m	3.29	ft
Weight in Air	31,752	kg	70,000	lb
Buoyant Weight	18,144	kg	40,000	lb

[13] Ocean Renewable Power Company, OCGEN-2T Technical Design Report, December 31, 2013

An isometric view of the deadweight anchor is provided in Figure 3.6.9. A section of the skirt has been removed in this Figure along the length of the anchor to provide a view of the shear keys. While not shown in the Figure, venting holes are provided in the skirt to allow the water and soft surface soils trapped by the skirt and shear keys to escape as the anchor is placed on the seabed.

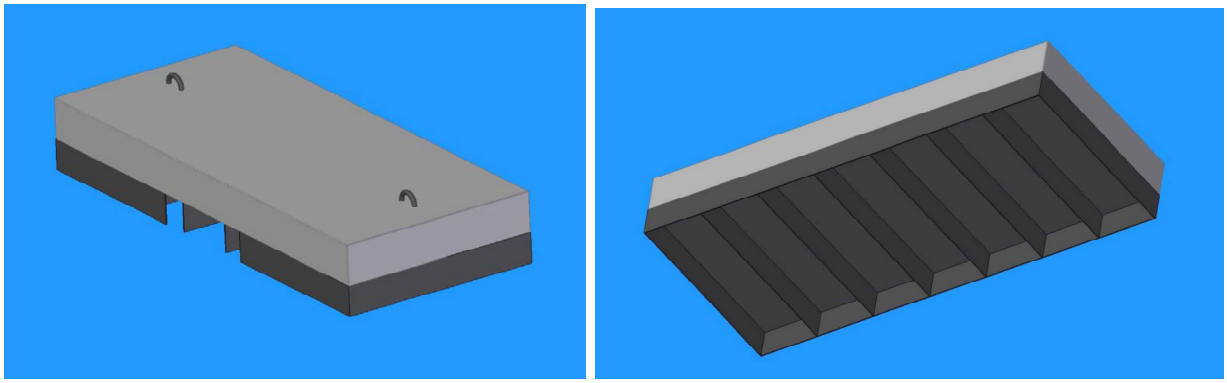

Figure 3.6.9. Isometric views of the anchor blocks

The data and electrical power cable used was intended to be run down one of the mooring line legs and to be attached to the mooring line with strain relief at regular intervals along its length. As such it became a component of the mooring line, rather than its own tether.

Problems Encountered

The only significant problem encountered has already been described above, namely the inability of the stiff chain tension leg mooring system to tolerate any deviation from ideal placement on the seafloor. This was adequately dealt with by use of synthetic line.

Departure from Planned Methodology

None.

Assessment of Impact on the Project Results

None.

3.7 Task 7: Experimental Mooring of a Prototype OCGen® Unit

Original Hypotheses

ORPC's plan was to design and construct a turbine generator unit (TGU) to model the behavior of a full-scale buoyant OCGen® unit tethered in the water column, without a generator or power control electronics. As such, the prototype OCGen® unit would not produce electricity but the turbines would rotate freely. ORPC proposed to design a mooring system, moor the unit to the sea floor, and monitor to determine the effectiveness of the anchoring and cable system. Data would be collected to aid development of the CFD and lumped system models. The unit would be deployed for a two-month period. Instrumentation would make measurements of the strain on the mooring lines, attitude measurement of the TGU, and flow conditions.

Upon completion of the deployment period, the OCGen® and the mooring system were to be removed. Geophysical inspections were to be performed and compared to pre-deployment geophysical surveys to determine if the mooring or operation of the TGU operating over a period of two months had any measurable impact on the sea bottom.

Approaches Used

Work completed in previous tasks allowed ORPC to develop analytical tools for the design of an OCGen® TGU, mooring lines and anchoring system. While multiple design tools were evaluated, the primary design tool used for this work was OrcaFlex, due to its capabilities to analyze a wide variety of situations and arrangements in a time efficient manner.

From the analytical work performed, it was clear to ORPC that the prototype and full-scale OCGen® power systems should comprise the following basic elements:

- Set of cross flow turbines
- Buoyancy pod or chamber arranged above the cross-flow turbines, so that the center of buoyancy of the combined system was above the center of mass of the combined system. This is required for the system to have basic stability, i.e., remain upright.
- Mooring line attachments to be placed on the buoyancy structure at some vertical location between the center of drag of the turbines and the center of drag of the buoyancy pod.
- Set of synthetic mooring lines utilized as tension leg moorings attached from the TGU to the moorings.
- Set of mooring blocks on the seafloor, which obtain their holding power primarily by weight alone.

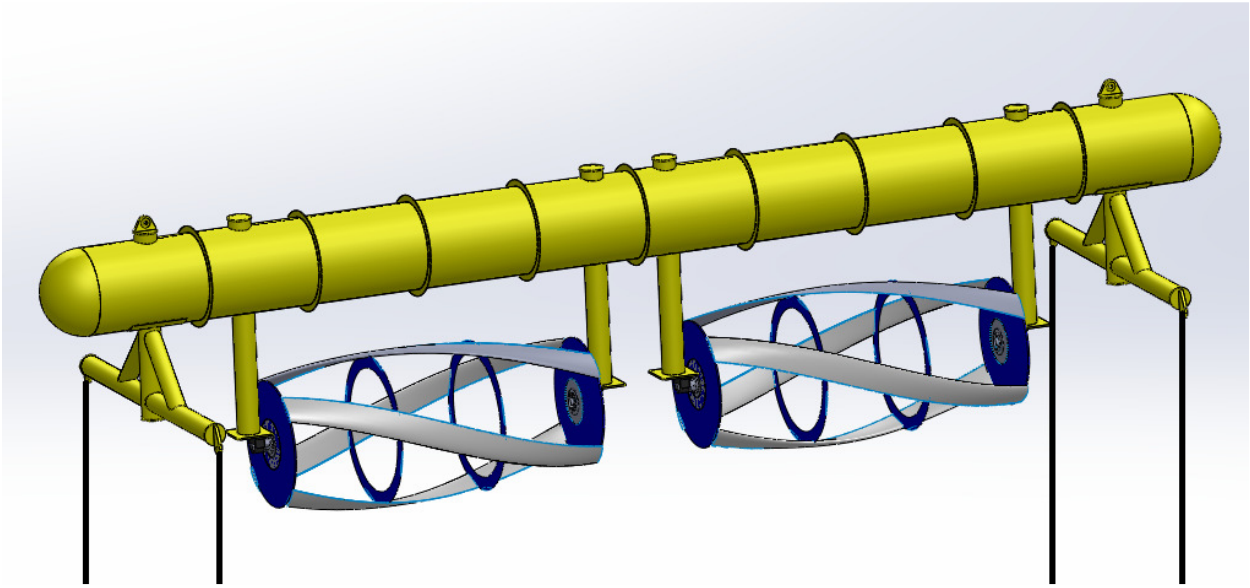

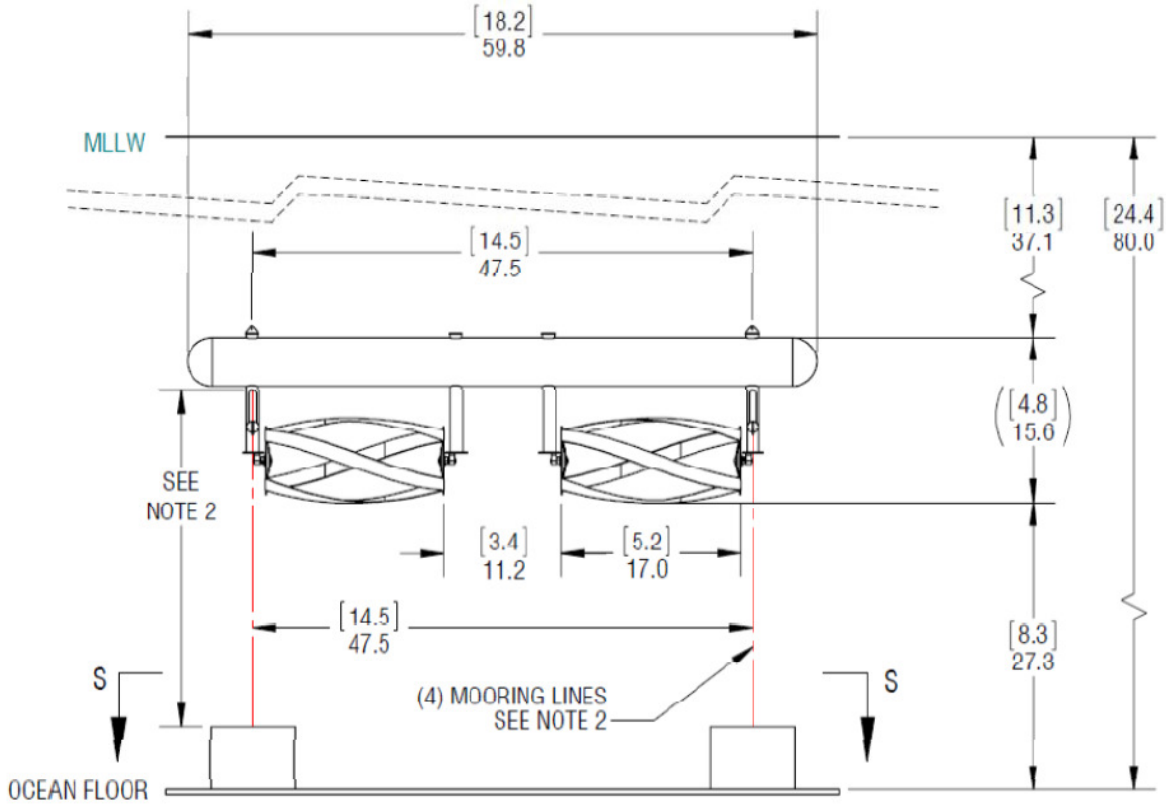

Figure 3.7.1. Prototype OCGen® arrangement, showing an isometric view of the TGU and a general arrangement drawing for the mooring blocks.

With these elements in mind, a conceptual model of the proposed prototype OCGen® Power System was developed. The intent was to construct, deploy, operate, and retrieve this system within ORPC's Federal Energy Regulatory Commission (FERC)-licensed site in Eastport, Maine.

This concept was presented and discussed with the Project's General Contractor (GC), who was to provide services for construction, installation and retrieval of the device. From prior experience with installation, and operation of MHK projects, ORPC was keenly interested in obtaining a fixed price quotation for all the work to be performed by the GC. Primary motivation for seeking such a fixed price contract was to limit financial risk to ORPC. The GC was willing to provide such a fixed price contact, as they were relatively experienced in working on prior MHK projects with ORPC in Eastport. However, in return for providing a fixed price contract, the GC desired that their scope of work also include detailed design and consequent construction of the OCGen® buoyancy pod. This design/build contract was agreed to by ORPC. This in turn, led to changes to the design of the OCGen® buoyancy pod, and its construction details, in an effort by the GC to eliminate perceived constructability issues.

The GC provided significant input into the means and methods of deployment and retrieval. The concept developed for deployment relocated most of the dive work to shallower and more protected waters and thereby limiting dive costs at the deeper deployment site. The prototype OCGen® TGU and buoyancy pod were assembled on land; mated to anchors at a shallow water location; and then transported as an assembled system to the final deployment location, where it was deployed and final data and power connections were made. This innovative approach to deployment was well suited to the OCGen® concept.

The installation site was located in Cobscook Bay, Southwest of Goose Island, as shown in Figure 3.5.1. The location of the deployment in US State Plane 1983 coordinate system, Maine East 1801 zone, NAD83 datum, in US Survey Feet is: Northing 456,514.5, Easting 1,361,250.6

Bathymetry information for this site showed little variation in elevation within the approximate footprint of the turbine. Based on this information, the mooring and anchor design was performed assuming a flat seabed. The water depth at the site is 25 m (82 ft).

Environmental conditions considered for design include the following:

- Water Density – 1025 kg/m^3
- Tide Range ~ +6.7 m, -0.7 m about MLLW
- Mean Current Heading – Ebb 305 degrees, Flood 135 Degrees from North
- Waves – *ignored*
- Minimum distance from OCGen to surface at MLLW – 11.3 m (40 ft)
- Design Depth at Slack Tide MHHW: 18 m
- Design Flow Speed: 2.4 m/s
- Maximum Mooring Decline Angle: 45 degrees
- No power output. Turbine states are free spinning or locked.

Table 3.7.1. *CBTEP HA11-8 Tidal Flow Yaw Angle and Speed*

Cobscook Bay Tidal Energy Site, Flow Yaw Angle and Speed			
LOCATION, TIDE	**ANGLE, MEAN, [deg]**	**ANGLE, STDEV [deg]**	**MAX FLOW [m/s]**
HA11-8, EBB	-55	3	2.40
HA11-8, FLOOD	135	5	2.40
Values obtained from Bin 9, 12.73m above seafloor			

At the intended OCGen® deployment location HA11-8, the tidal flow was known to have a different yaw angle during the ebb and flood tides, as shown in Table 3.7.1. At the maximum flow speed, the flow yaw angle was within one standard deviation of the mean flow angle. The magnitude of the maximum tidal flow shall be taken as 2.4 m/s for the design of the OCGen® prototype.

Regarding the time varying nature of the flow at the Cobscook Bay site Figure 3.7.2 shows normalized real-time data overlaid with an analytical function attempting to match the fundamental frequencies and amplitudes present in the flow. The form and coefficients of this analytical function are given in Table 3.7.2. Note that the analytical function is normalized (maximum value is 1.0), and should be multiplied by the design flow speed. This function is considered representative of the flow at the CBTEP site and can be used for the purposes of performing a rigid body motion analysis.

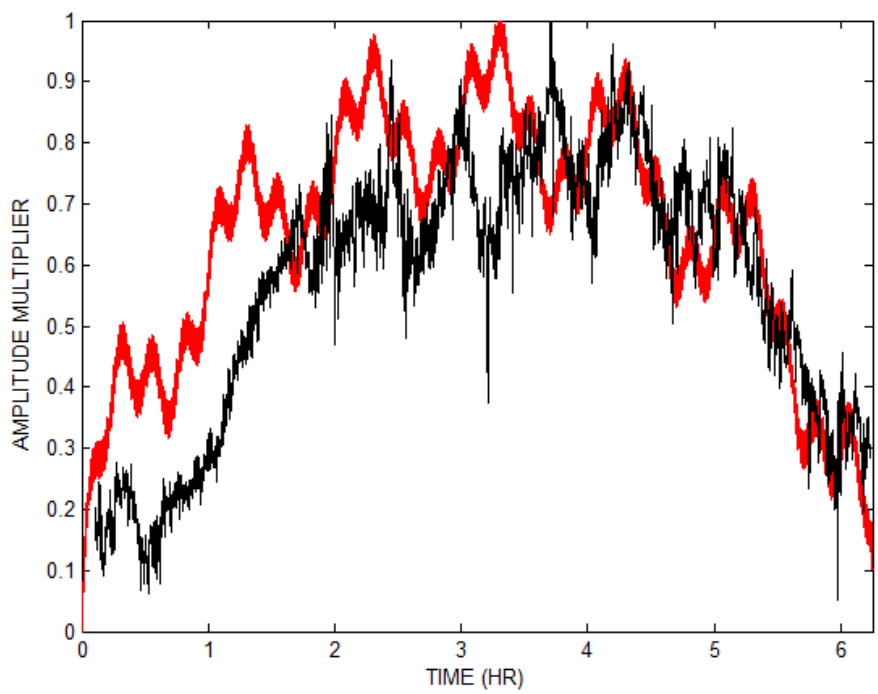

Figure 3.7.2. Analytical function (red) shown with real time flow data (black) collected at site for one tidal cycle.

Table 3.7.2. *Analytical Function for Mean Flow (FSV) at CBTEP HA11-8*

Analytical Function for FSV			
F = A1*sqrt(sin(w 1*t)) + A2*sin(w 2*t) + A3*sin(w 3*t) + A4*sin(w 4*t) w = 2 * pi / T			
AMPLITUDE, A [NORMALIZED]		**PERIOD, T [SEC]**	
A1	0.84	T1	45000
A2	0.10	T2	3600
A3	0.05	T3	900
A4	0.03	T4	60

Design of the TGU

Turbines

The prototype OCGen® TGU utilized an older set of turbines, which was used on the ORPC Beta project. Each turbine comprised four foils, with a 0.46m chord. Turbine length was 5.2m. These turbines were used successfully in multiple deployments of the Beta TGU. They were selected for use in this project in order to reduce project overall costs.

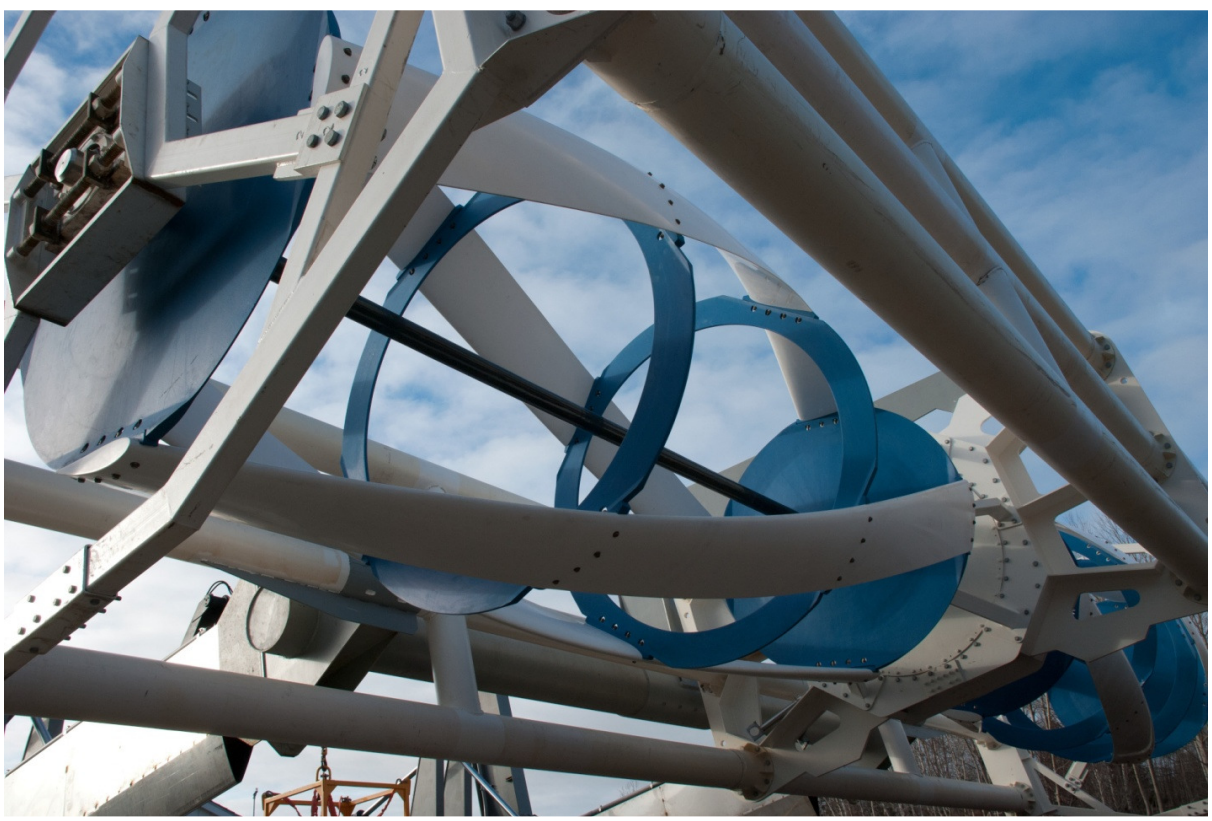

Figure 3.7.3. Beta TGU showing turbines used in OCGen® mooring project

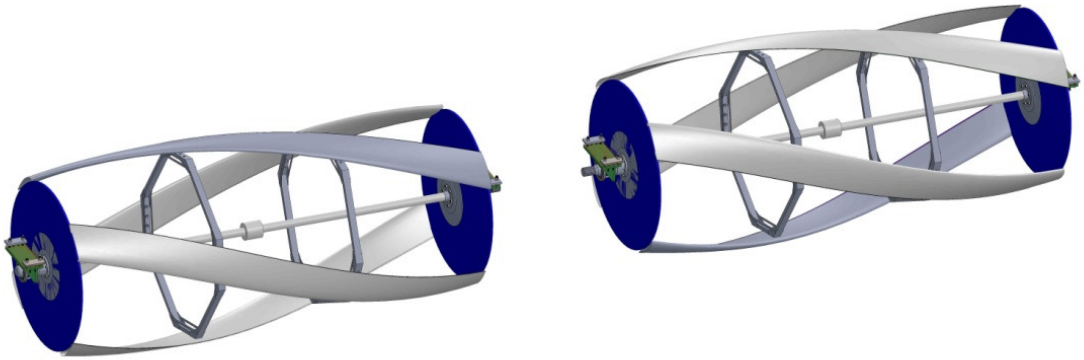

Figure 3.7.4. Beta TGU turbine set. These turbines were reworked for use in the prototype OCGen® mooring test

The turbine foils were constructed from a vinyl ester resin infused structural glass fiber. Foils were hollow. The end discs for the turbines were comprised of a bamboo core covered with a structural glass fiber.

During extended prior operation of these turbines some issues at the intermediate bolted joints arose due to loss of compression in the bolted joint. The composite intermediate rings were replaced with intermediate rings constructed of 304L stainless steel hollow structural steel, and the torque specification for the bolted joint was increased.

Stress analysis of the turbine structure was performed, which indicated high stress points at multiple locations in the stainless steel rings. Additional reinforcing gussets were added to the structure, and resulting levels of stress were deemed acceptable for the purposes of this test.

In addition to the structural additions to the intermediate support rings, the details of the bolted joints at the intermediate support rings were modified to reduce the likelihood of stress relaxation at the joint, with the additional of a new washer to the bolted joint assembly.

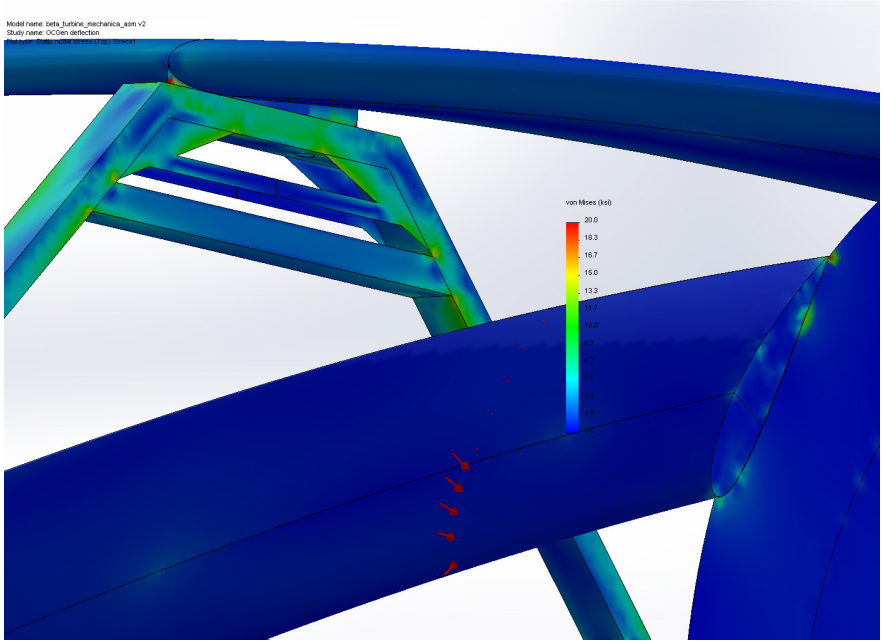

Figure 3.7.5. Von Mises stress on the intermediate rings under turbine hydrodynamic loads. Note that multiple high stress areas of approximately equal magnitude are visible at many of the sharp corners

The turbines were supported on thermoplastic sleeve bearings on each end.

No cathodic protection was provided on the steel elements of the turbines.

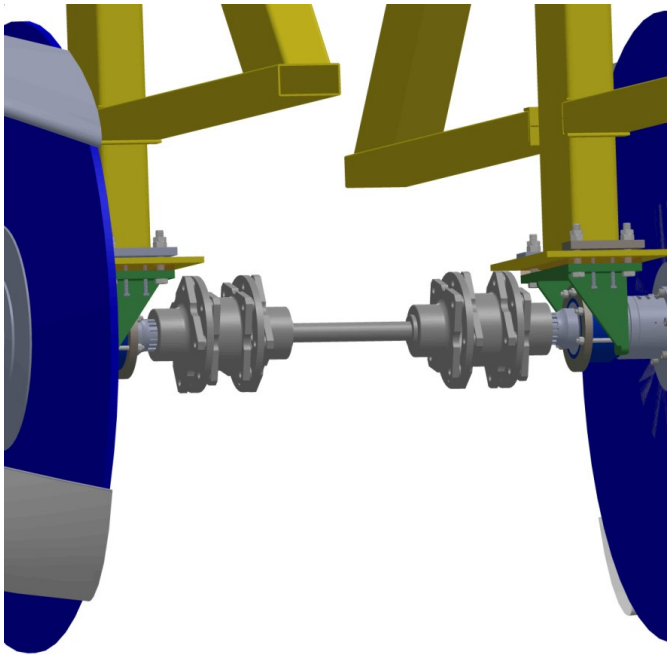

Figure 3.7.6. Flexible couplings and a stainless steel shaft connected the two turbines. A stainless steel shaft was constructed to join the couplings.

Information on lift, drag and power coefficients for these turbines is required for analysis of the loads applied by the turbine to the structure. These data can be presented as a function of the turbine tip speed ratio (Table 7.3).

Table 3.7.3. *ORPC OCGen® 2T Coefficients of Power (CP), Drag (CD), and Lift (CL)*

ORPC OCGen™ 2T TGU Coefficients			
R	[m]	1.1	
ATOT	[m^2]	22.8	
RHO	[kg/m^3]	1030	
TSR	**CP**	**CL**	**CD**
0.00	0.000	0.000	0.370
0.25	0.007	0.117	0.380
0.50	0.017	0.193	0.411
0.75	0.039	0.259	0.471
1.00	0.087	0.317	0.578
1.25	0.185	0.340	0.775
1.50	0.205	0.217	0.926
1.75	0.181	0.159	0.983
2.00	0.155	0.117	1.024
2.25	0.125	0.082	1.058
2.50	0.091	0.050	1.088
2.75	0.052	0.021	1.114
3.00	0.000	0.000	1.137

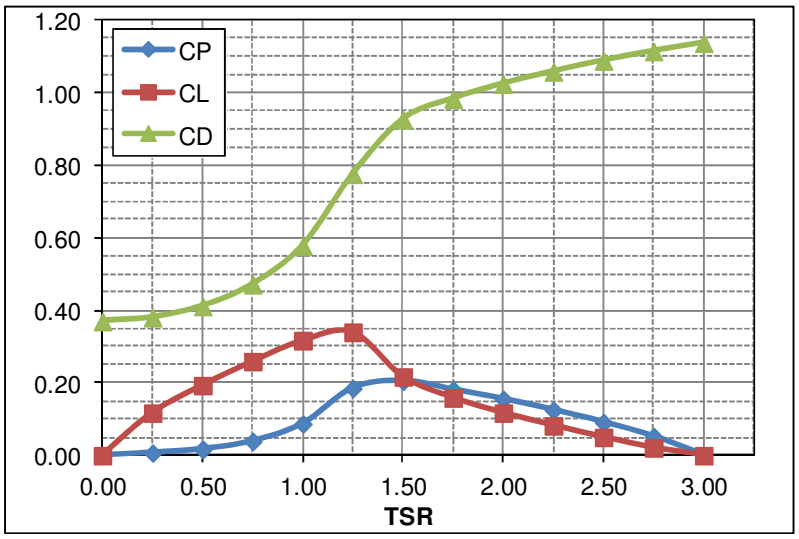

Design of the Buoyancy Pod

The GC desired that their scope of work also include detail design and construction of the OCGen® buoyancy pod. This design/build contract was agreed to by ORPC. This in turn, led to changes to the design of the OCGen® buoyancy pod, and its construction details. These changes in design were primarily intended to allow the GC to construct the buoyancy pod without the need for outside contractors. The evolution of the design is shown in Figure 3.7.7.

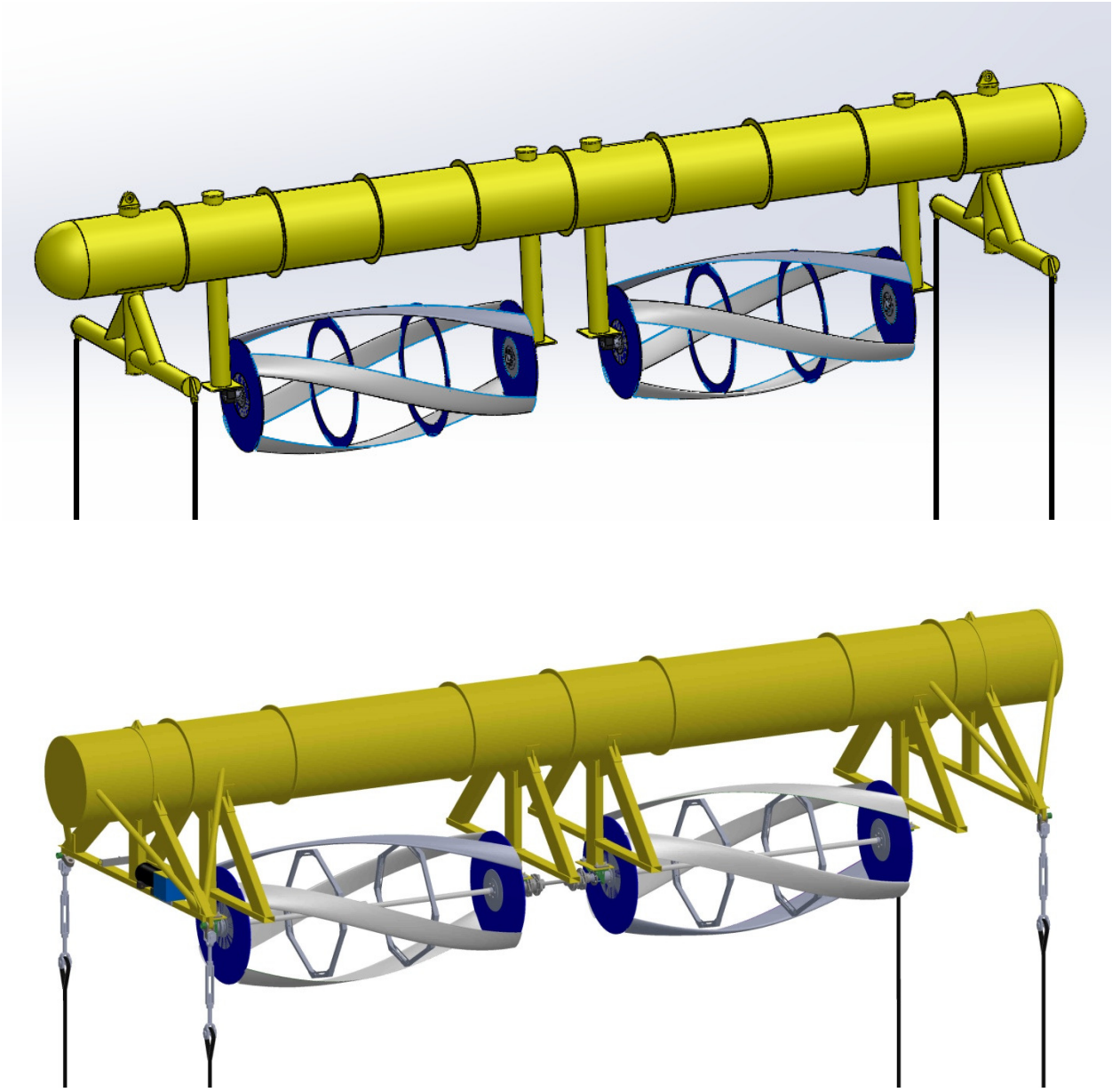

Figure 3.7.7. Design evolution from original concept prototype to as-built unit. The concept had spherical end caps and single vertical supports for turbines and mooring lines. These were replaced at the discretion of the GC by flat end caps and truss structures to reduce construction costs

As can be seen in Figure 3.7.7, major changes were made to the turbine supports and mooring line supports, changing from pipe sections to hollow rectangular steel sections. These changes were intended to reduce the complexity of the welds and remove penetrating welds through the buoyancy pod.

Unlike the full scale OCGen® the prototype, OCGen® does not have internal bulkheads. The weight with the entire pod flooded was still well within the capacity of the deployment catamaran winches, so the need to isolate internal compartments was reduced. Removing the bulkheads eliminated the need for welding on the inside of the shell. However, the lack of internal bulkheads does lead to a higher risk of sinking during operation if a pressure vessel leak occurs.

Stress analysis of the structure for multiple load cases was performed to ensure that the structure was adequate for transportation, installation and operation subsea.[14] For normal operations where all four mooring lines remain intact, all stresses in the connections are lower than the fatigue strength of the carbon steel used. For the case presented in Figure 3.7.8 where a single mooring line parts, there are stresses in excess of the fatigue limit. However, the failure of the mooring line would necessitate retrieval of the unit, in any case.

Corrosion of the metallic components of the buoyancy pod assembly is clearly an issue for longer term deployments. Since the intent of this test exercise was a short term deployment of less than three months it was decided not to provide corrosion protection coatings or cathodic protection on the structures or components. For a long term deployment coatings on the structures and cathodic protection would be necessary.

[14] ORPC FEA of CPM OCGen Buoyancy Pod Design, ORPC Internal Report

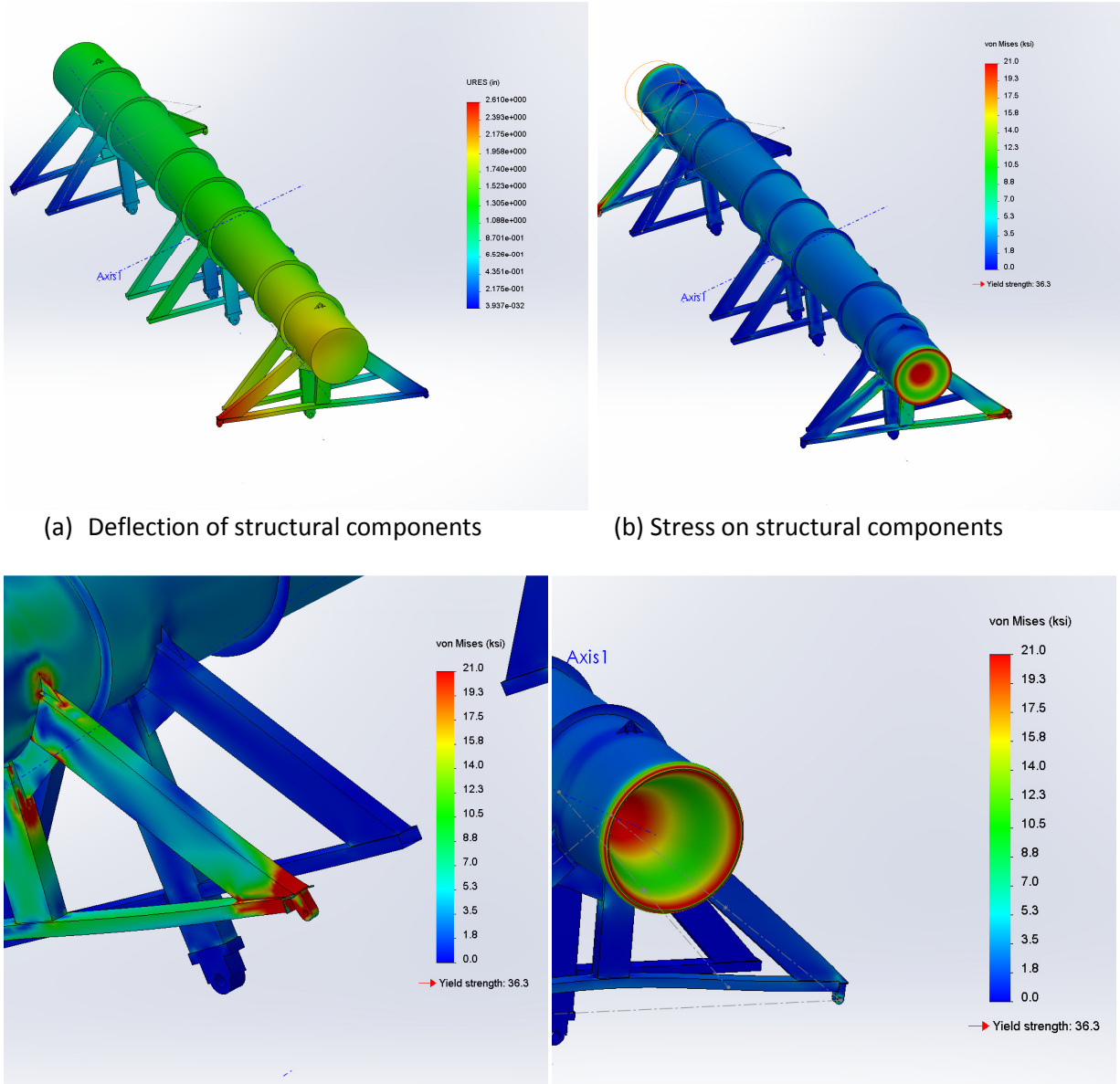

(a) Deflection of structural components

(b) Stress on structural components

(c) View of the mooring line connection

(d) View of the buoyancy pod end plate

Figure 3.7.8. Deflection and stress for the buoyancy pod under operating loads. Loads for this case include, turbine rotation, turbine lift and drag, external pressure loads, and an assumption that one of the mooring lines is completely unloaded, representing a failure condition for the mooring system.

(a) The deflection for the entire system, showing a maximum expected 2.1 in. deflection for this case of a failed mooring line
(b) Von Mises stress for the system. Stresses are below 21ksi for most of the structure expect for local areas
(c) High stresses (>21ksi) are found at the remaining mooring line connections
(d) High stresses (>21ksi) are found on the flat end plates of the buoyancy pod. Spherical end caps would have been preferred. These stresses are quasi-static.

Weights, buoyancies, centers of mass and buoyancy for this case are listed in Table 3.7.4. Expected loads applied are listed in Table 3.7.5.

Table 3.7.4. *Estimates for weights and buoyancy of prototype system*

Component	Weight	Buoyancy	Net Vertical Force	COG	COB
	kN	kN	kN (+) upward	m	m
TGU Structure	90	276	186	2.52	2.83
Turbines	41	10	-31	0	0
Driveline Components	0	0	0	0	0
Entire Structure	131	286	155	1.73	2.73

Table 3.7.5: *Estimates for drag loads on prototype system.*

Maximum current speed	2.4	m/s
Total projected area (turbine)	22.8	m^2
water density	1030	kg/m^3
	TSR	
	0	3
Turbine drag coefficient	0.3701	2.237
Drag Values		
Turbine Drag	25	77
Buoyancy Module Drag	68	68
Bearing Support Drag	9	9
Turbine Lift	0	0
Total Drag (kN)	102	154

Mooring System Modeling

OrcaFlex was used to calculate mooring line tension at the top end of the line for different flow speeds and flow directions.

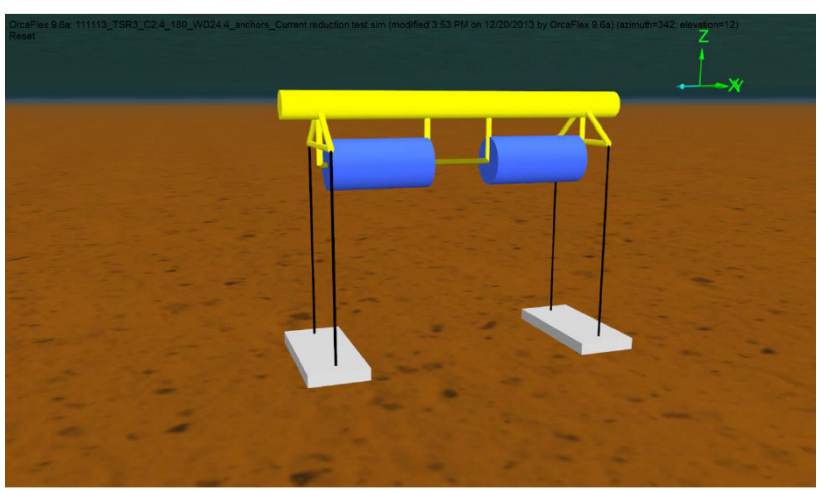

Figure 3.7.9. OrcaFlex model of the prototype OCGen® Power System

Mooring Lines

Based on the loading information obtained from the OrcaFlex models, a mooring line specification was assembled and sent out for quotation. The original mooring line specification was for 2½ in. diameter (60mm nominal) Viking Braidline with a wet breaking strength new of 150,000 lb. Four of these lines were required, and matched lengths were strongly desired. Conversations with the manufacturer of this product indicated that the lead times for delivery of the product was longer than ORPC desired and that it would be difficult to provide the four lines in matching lengths. Length tolerances were expected to be in the order of +/- 3 in.

An alternative manufacturer was approached and the nature of problem explained to them—namely that a very compliant, short mooring line was required. They suggested that ORPC use an oceanographer's brait (http://www.yalecordage.com/oceanographics/brait-plaited/large-brait.html), configured in a four lap, single loop. The lines would be nylon, a compliant material, and wrapped end for end four times, to provide eight lines on each mooring leg. The line was to be steam stabilized to account for the tendency of Nylon to absorb water. The lines would be proof loaded to 7,500 lb. Preload is necessary to "set" the lines and reduce plastic deformation on initial loading. The lines measured 20 ft 6 in. at hand tension and 23 ft 4 in. at 7,500 lb. All lines were measured at 23 ft 4 in. at 7,500 lb, indicating excellent length and load matching between the lines. This particular arrangement of mooring line is actually a common lift sling and was readily available off the shelf. The strength and compliance requirements agreed with the expected loads and these lines were acquired.

Line tensions listed in the Table 3.7.6 were taken at the top end of the line, at the connection point to the structure, where the maximum tension occurred. The maximum mooring line tension found was 64.95 kN, and occurs in both forward lines under a head-on current, with a TSR of 3.0. Since the mooring system and structure are symmetric, the same maximum tension would occur in the two aft lines when the tide flow is reversed through the turbine.

Table 3.7.7 provides the displacement of the model in the X, Y, and Z directions referenced from the starting position of the model. The rotations shown are referenced about the origin of the model. The results show only a slight variation in rotation of the model. The mooring configuration allows very little rotation in yaw. For the most extreme case of a 20 degree offset current, the yaw of the model is approximately half a degree. The maximum roll is less than 1 degree. The maximum movement in the X direction is 8.25 m, resulting in a forward mooring line angle of 43.5 degrees from vertical.

Table 3.7.6. *Tensions in mooring lines for prototype OCGen® Power System*

Case			**Tension (kN) (Top of Line)**				**Mooring Line Declination Angle from Horizontal**			
TSR	speed	Dir	Upstream		Downstream		Upstream		Downstream	
-	m/s	Deg	PF	SF	PA	SA	PF	SF	PA	SA
0	0	-	38.72	38.72	38.72	38.72	90.0	90.0	90.0	90.0
0	2.40	160.00	56.53	56.39	35.02	35.15	57.2	56.5	59.5	58.8
0	2.40	180.00	59.79	59.79	34.70	34.70	54.4	54.4	56.2	56.2
3	2.40	160.00	61.36	60.51	46.25	**46.47**	46.2	45.0	47.3	46.0
3	2.40	180.00	**64.94**	**64.94**	**46.45**	46.45	43.5	43.5	44.8	44.8

Table 3.7.7. *Estimated translations and rotations of OCGen® TGU*

Case			Net Translation			Rotation		
TSR	speed	Dir	X	Y	Z	Roll	Pitch	Yaw
-	m/s	Deg	m	m	m	deg	deg	deg
0	0	-	0.00	0.00	0.00	0.00	0.00	0.00
0	2.40	160	-6.44	0.73	-2.18	0.32	-0.24	-0.43
0	2.40	180	-6.66	0.00	-2.30	0.00	-0.12	0.00
3	2.40	160	-7.87	1.53	-3.58	0.71	-0.24	-0.65
3	2.40	180	-8.25	0.00	-3.85	0.00	-0.12	0.00

Table 3.7.8 provides the maximum mooring loads acting on the anchor connection point. The mooring tension was separated into vertical and horizontal components for use in the anchor design.

Table 3.7.8. *Estimated mooring loads on anchors for prototype OCGen® system*

Case			Mooring Load at Anchor Point							
TSR	speed	Dir	PF (kN)		SF (kN)		PA (kN)		SA (kN)	
-	m/s	Deg	Horiz.	Vertical	Horiz.	Vertical	Horiz.	Vertical	Horiz.	Vertical
0	2.40	160.00	32.92	-39.17	33.36	-38.68	20.06	-21.85	20.45	-21.74
0	2.40	180.00	36.57	-43.03	36.57	-43.03	21.06	-23.26	21.06	-23.26
3	2.40	160.00	43.94	-36.20	44.21	-34.72	32.86	-25.89	33.69	-25.36
3	2.40	180.00	48.46	-36.67	48.46	-36.67	34.29	-24.73	34.29	-24.73

Consideration of vortex induced vibration for this particular mooring line indicates that it is not particularly likely for these line lengths. The shedding frequencies to be expected are less than 6Hz for water speeds of 2.5 m/s, and the fundamental vibration frequency for the mooring line is predicted to be greater than 11Hz.

Design of the anchors

The bathymetry information for this site showed little variation in elevation within the approximate footprint of the turbine. Based on this information the mooring and anchor design was performed assuming a flat seabed. The water depth at the site was 25 m (82 ft).

The anchor design consisted of two concrete clump weight anchors. Each anchor has a 1.5-ft high steel skirt surrounding the perimeter with 1.5-ft high steel shear keys. The shear keys and skirt provided additional lateral holding capacity by engaging the soil contained within them. The anchor specifications are provided in Table 3.7.9.

Table 3.7.9. *Anchor specifications for prototype OCGen® in Cobscook Bay, Maine*

Anchor Design				
	Metric		English	
Concrete density	2401	kg/m^3	150	pcf
Length	7.01	m	23	ft
Width	3.05	m	10	ft
Height	0.61	m	2	ft
Number of Shear Keys	8	-	8	
Skirt Height	0.46	m	1.5	ft
Shear Key Height	0.46	m	1.5	ft
Shear Key Spacing	1.00	m	3.29	ft
Weight in Air	31,752	kg	70,000	lb
Buoyant Weight	18,144	kg	40,000	lb

An isometric view of the deadweight anchor is provided in Figure 3.7.10. A section of the skirt has been removed in this figure along the length of the anchor to provide a view of the shear keys. While not shown in the figure, venting holes are provided in the skirt to allow the water and soft surface soils trapped by the skirt and shear keys to escape as the anchor was placed on the seabed.

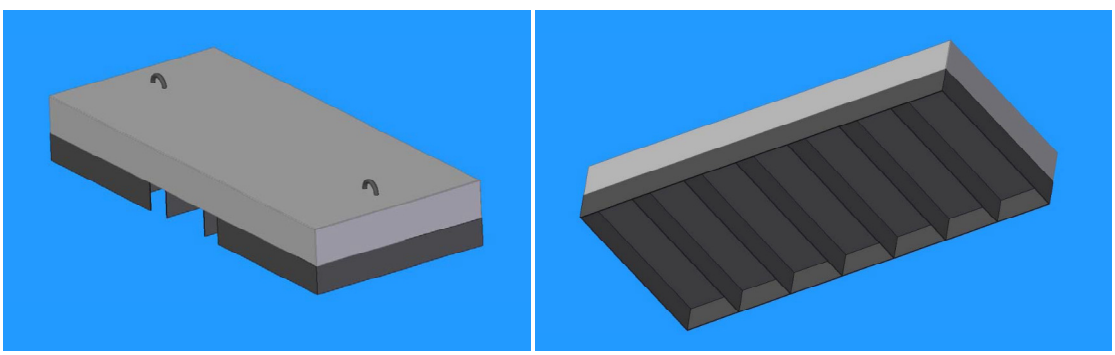

Figure 3.7.10. Isometric views of the anchor blocks

The welded steel construction for the anchors was prefabricated and shipped to Eastport. The concrete was poured onsite.

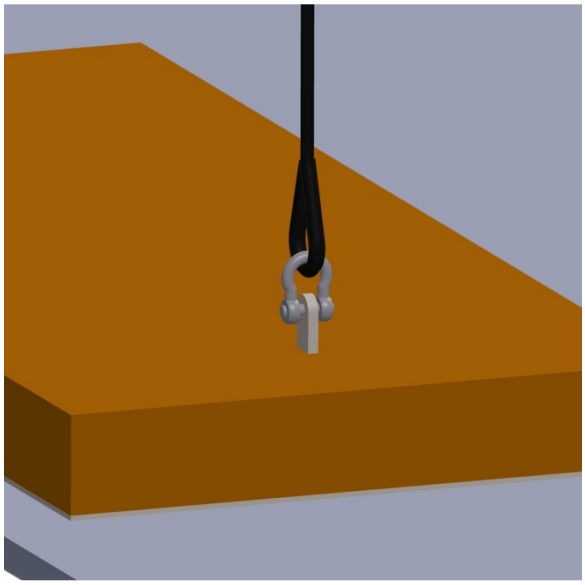

Figure 3.7.11. Connection between mooring block and mooring line. In retrospect, an additional degree of freedom to limit the mooring line sliding fore and aft on the shackle would have been desirable, by the addition of an additional element between the mooring line eye and the shackle

Corrosion of the metallic components of the mooring line assembly is clearly an issue for longer term deployments. Since the intent of this test exercise was a short term deployment of less than three months it was decided not to provide corrosion protection on the structures or components. For a long term deployment, material selection for the shackles and mating components would favor duplex stainless steels rather than the carbon steels used in the prototype.

Modal analysis (PCCI)

OrcaFlex was used to determine the natural frequency of the overall system. The natural frequency was calculated for the model in two static state cases: no current and 2.4 m/s at 180°. The frequencies of the first ten oscillation modes are provided in Table 3.7.10.

The mode shape for mode 1 consisted of rigid body oscillation in the fore and aft direction; mode 2 was oscillation about the vertical axis, and mode 3 is oscillation from side to side.

The shortest period provided the analytic function of current used for design purposes was 60s. The longest modal period calculated for the moored structure was 11.2s. This was much less than the shortest expected period of variation in current of 60s, therefore ORPC expected no dynamic amplification of the oscillations of the turbine due to resonance with the current variations. For flows with shorter periods we expect the length scale of the flow were small enough as to not affect the entire structure simultaneously.

Table 3.7.10. *Modal analysis results for prototype OCGen® TGU*

	2.4 m/s @180 deg		No Current	
	Period (s)	Frequency (Hz)	Period (s)	Frequency (Hz)
Mode 1	9.08	0.1101	11.20	0.0893
Mode 2	5.94	0.1683	7.68	0.1303
Mode 3	5.23	0.1912	6.48	0.1542
Mode 4	1.01	0.9886	1.04	0.9639
Mode 5	0.92	1.0816	1.04	0.9639
Mode 6	0.91	1.0957	1.04	0.9639
Mode 7	0.87	1.1490	1.04	0.9639
Mode 8	0.84	1.1921	1.03	0.9727
Mode 9	0.78	1.2877	1.02	0.9831
Mode 10	0.76	1.3077	1.01	0.9913

Instrumentation provided

The prototype OCGen® system was equipped with instrumentation to collect data from the test. Load cells were located on each mooring leg, attached to the OCGen® buoyancy pod at a swivel joint. Adjustable turnbuckles are used to connect the TGU to the mooring lines. Data cables from the load cells run back to the Prevco subsea electronics housing. Cables from other instrumentation are also feed to the Prevco which provides sensor power and performs signal conditioning.

Data from the unit is consolidated by a RuggedCom network switch and transmitted to shore over an extended ADSL copper network. This copper data cable to shore was previously installed as part of the TidGen® project. Shore station assets from the TidGen® project were also utilized, including the LabView data acquisition system. This approach limited data transfer rates from the system to a maximum rate of 1Hz, with some data channel drop outs at this rate. For the majority of the project a data rate of 0.33Hz was used, with one period of time reporting at the 1Hz rate.

Flow speed data was provided by ADCPs deployed adjacent to the OCGen® TGU. Data sampling rates on these instruments was dictated by the expected length of the deployment and the available onboard battery life.

An additional depth sensor, the HOBO sensor, was included on the system. The data sampling rate was set at a six minute logging interval so as not to exceed the onboard data storage capability of this device.

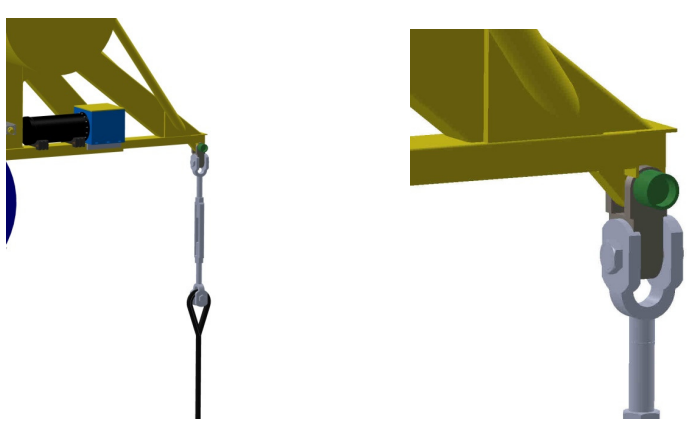

Figure 3.7.12. Prevco instrumentation housing (black cylinder), and load pin and shackle connected to mooring line.

Table 3.7.11. *Measurements made during device operation*

Measurement	***Expected measurement range***	***Instrument***	***Location of Instrument***	***Power Considerations***	***Data considerations***	***Data Collection***
Environment						
Flow Speed	-2.5 to +2.5 m/s	ADCP	Sea floor mounted	battery	Goose Island ADCP • 0.1Hz Lubec ADCP • 0.017Hz	Data collected upon test completion after ADCP retrieval
Flow Direction	0 to 360 degrees	ADCP	Sea floor mounted	battery	Goose Island ADCP • 0.1Hz Lubec ADCP • 0.017Hz	Data collected upon test completion after ADCP retrieval
Water depth	0m to 40m	ADCP	Sea floor mounted	battery	Goose Island ADCP • 0.1Hz Lubec ADCP • 0.017Hz	Data collected upon test completion after ADCP retrieval
TGU						
Flow Speed	-2.5 to +2.5 m/s	Aquadopp	Mounted on TGU	Shore power	Data logged every 3 seconds	Data logged on shore
Depth of TGU	0m to 40m	Aquadopp	Mounted on TGU	Shore power	Data logged every 3 seconds	Data logged on shore
Depth of TGU	0m to 40m	Hobo water level meter	Mounted on TGU	Battery	Data logged every 3 minutes	Data logged on Hobo
Attitude	-20 to +20 degree	Aquadopp	Mounted on TGU	Shore power	Data logged every 3 seconds	Data logged on shore
Heading	0 to 360 degrees	Compass	Prevco	Shore power	Data logged every 3 seconds	Data logged on shore
Turbine RPM	0 to 80RPM	Electro Sensors split collar pulsar wrap Seacon Hall effect proximity switch	Turbine shaft TGU structure	Shore power	Data logged every 3 seconds	Data logged on shore
Mooring System						
Mooring loads	0 to 37.5 tonne	4 x LCM4039 Load sensors	Mooring line	Shore power	Data logged every 3 seconds	Data logged on shore
Mooring movement		Visual inspection	Visual	N/A	Diver inspection	Intermittent data collection based on dive cycles

Deployment

Deployment and retrieval opportunities were identified by assessing the tidal height range to be expected over a given range of dates. Tidal height range acted as a proxy for the length of working window to be expected.

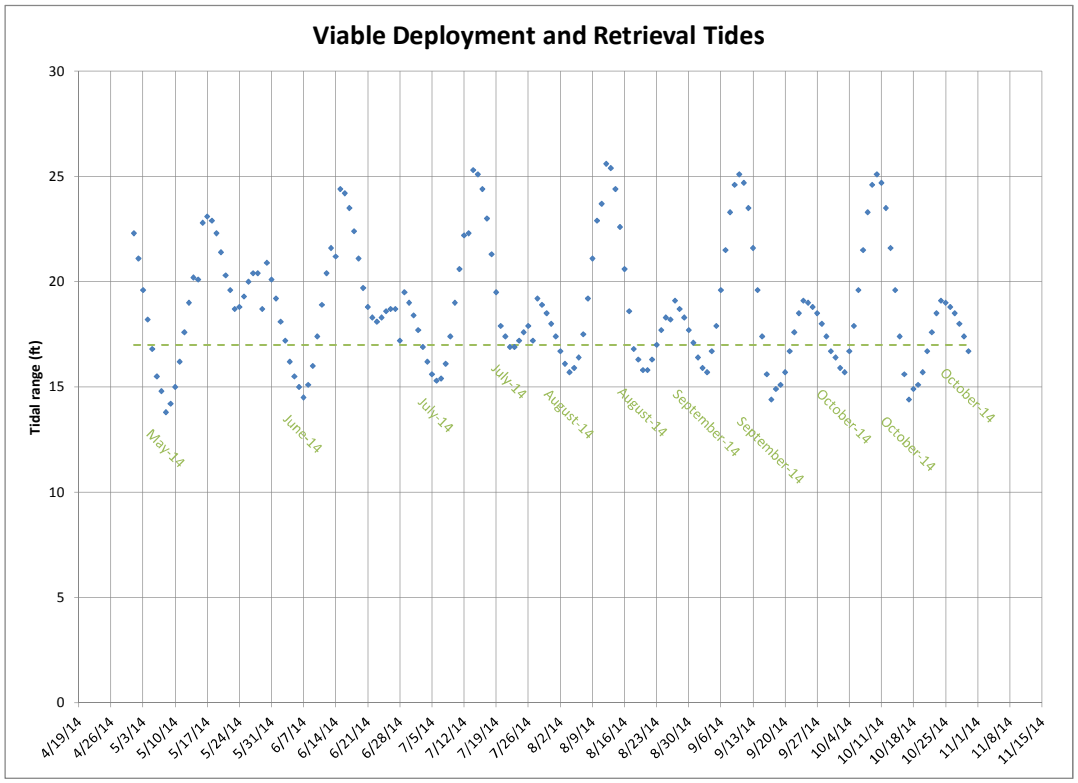

Figure 3.7.13. Tidal height range in Eastport during the Project period. Tide ranges provide an indication of slack water working time. A tidal range of less than 17 ft was selected as a maximum range. Acceptable dates for deployment and retrievals are shown in green.

After assembly of the TGU and buoyancy pod, components were staged for deployment. To stage the components for deployment, the following sequence of events occurred:

- TGU and buoyancy pod were staged on a level surface on support stands.
- Both anchors were moved onto the Eastport Boat School Boat Ramp at low tide by crane.
- At high tide, both anchors were picked by the catamaran lift vessel *Retriever*, and moved offshore to a site with approximately 30 ft depth.
- OCGen® was transported down the boat ramp by Marine Travelift at low tide and placed on stands on the boat ramp.
- At high tide *Retriever* picked the OCGen® off the stands and transported the unit to the site of the anchors on the following low tide.
- At low tide the mooring lines and data cables between the OCGen® and the mooring blocks were made up by divers.
- On the next high tide the entire system was picked by *Retriever*, transported to the deployment site, and set down on the bottom.
- Over the course of the next several days, divers laid data and power cables to the ORPC subsea electrical consolidation puck, and made connections to the OCGen®.

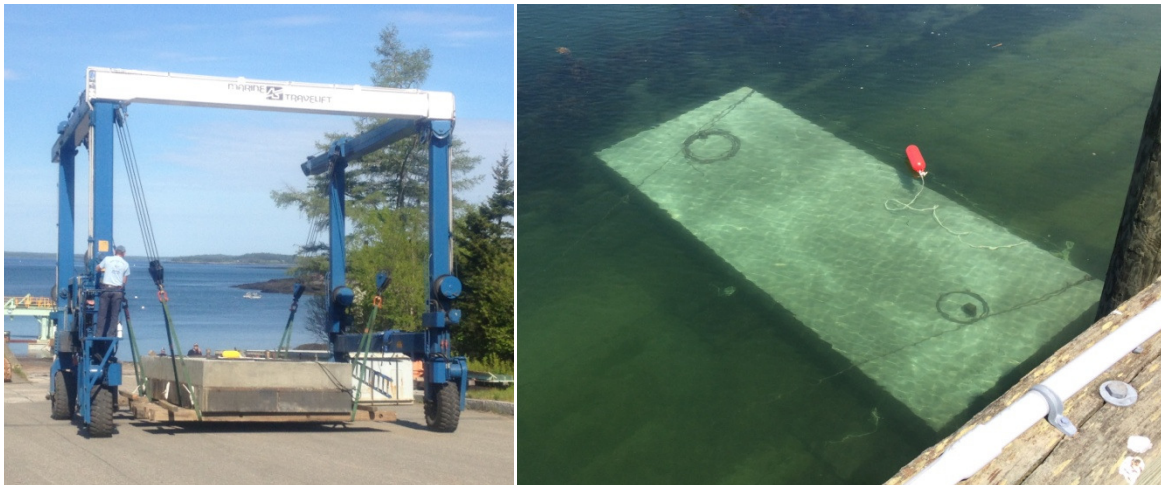

Figure 3.7.14. Anchor being transported down boat ramp (low tide) and anchor underwater at boat ramp (high tide)

Figure 3.7.15. OCGen® system after being picked off boat ramp by Retriever

Figure 3.7.16. OCGen® system in *Retriever* prior to deployment

The sequences of events during deployment are outlined in Table 3.7.12.

Table 3.7.12. *Deployment Schedule as recorded by ORPC representative onsite (27 June 2014)*

Time (EST)	Event	Comments
05:01	Retriever cast off from Boat School Dock	
05:11	Retriever arrives on staging area	
05:14	Start making up with anchors	
05:23	Straight up & down over anchors	Way point recorded. The corner of the area at 44-54.436N 67-1.274. Depth of the area is between 10.8-11.4 meters at MLLW.
05:33	Depth recorded as 33ft by tender boat at 5	
05:38	Divers on board	
05:43	Low water	-0.4 ft
05:43	Eastport side cables in water	
05:44	Lower TGU	
05:44	TGU afloat	Video taken
05:50	Measured depth by skiff is 35 feet	
05:53	Diver in the water	
06:09	2nd diver in water	
06:17	Lubec mooring lines connected	
06:20	All mooring lines connected	
06:32	2nd diver out of water – first diver still in water	
06:44	Diver confirms slack in data cable with visible loops	
07:17	Informed that data cable shackle made up	This was against specific instructions. Based on this information ORPC gave permission to connect data cable ends on this shallow water dive
	Diver informs surface that anchors are floating	
07:36	Diver retrieves dummy plugs, cable connector made up. Dummy plugs examined and looked good. Transferred plugs to D. Speed	
07:45	Crane mats released. Diver out of water. Boat pulling crane mats	
08:01	Of 6 crane mats, 5 are free, 1 stuck under Lubec anchor	
08:12	6th crane mat removed. All clear	
11:37	Coming on station at deployment site. Vessels on station – Retriever, Abaco, Workshorse, TideTracker as safety vessel, and a Border Patrol vessel transiting through site	High water at 11:44, expect slack water to occur approx 20 minutes later

11:53	Maneuvering	
11:55	Preparing to lower TGU	
12:04	Maneuvering	
12:11	TGU lowered to seafloor, touched bottom, raised 5 ft	
12:13	Diver in the water	
12:17	Final approach	
12:19	Lining up range markers with orientation direction	Continuous recording
	Overshooting a little to the North	
12:21	Diver descending to bottom	
		Conversation regarding bottom. "There is a few rocks there but its level". "Little small rocks". ORPC confirms that this is correct.
12:26	Derigging TGU on bottom	Lined up good with range poles. A little to the NW of target. Difficult to get fix as vessel moves faster than GPS update speed
	Both Targets recorded simultaneously Surveyor estimated both GPS read 37 feet to the NW of target site	
12:35	Eastport hook coming out of water	
12:37	Eastport breaks surface	
12:38	Retrieving Lubec hook	
12:40	Diver surfacing	
12:40	Lubec hook out of water	
12:42	Diver on surface	
12:42	Diver on deck	

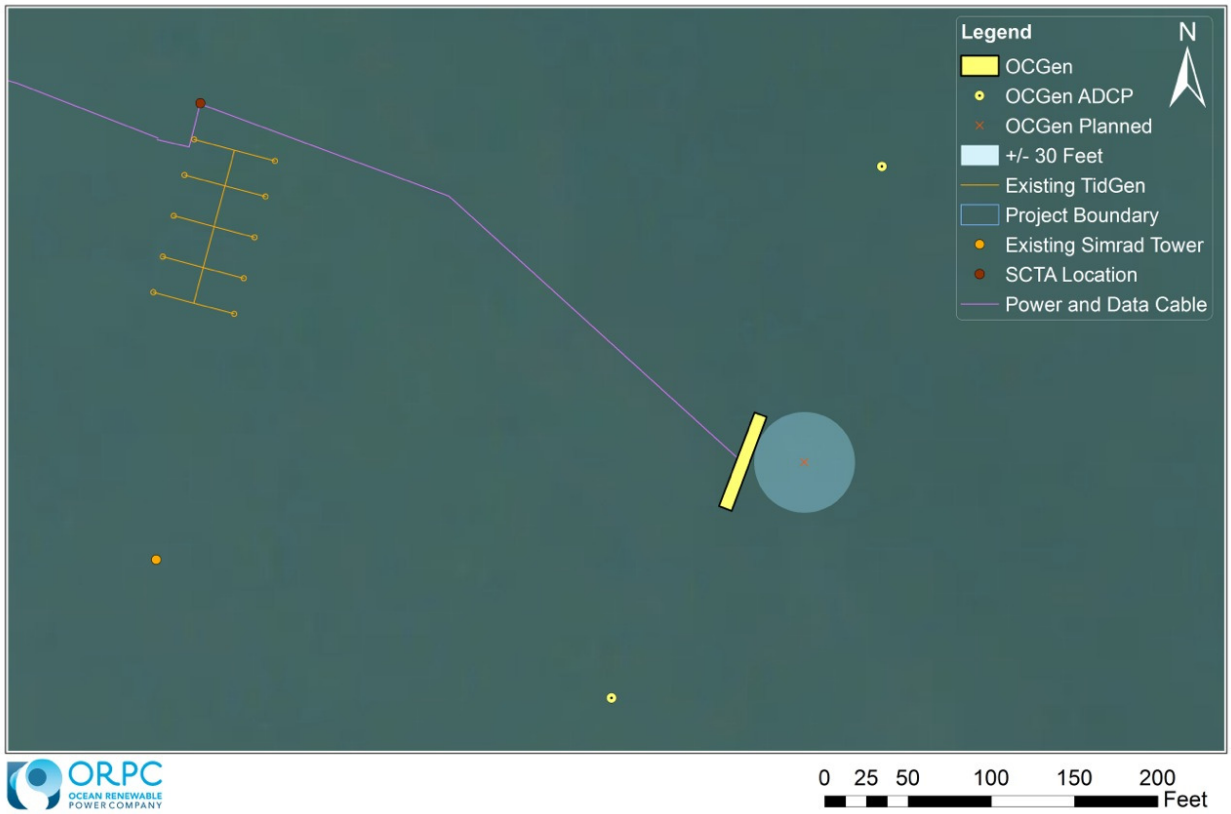

Figure 3.7.17. Installation map showing installed location and position of OCGen® and targeted installation zone

OCGen® TGU deployed position was centered at -67.0446782043025, 44.9096554750793. The deployed location was 37 ft away from the center of the targeted location. The deployment is 7 ft outside the target zone.

Instrumentation issues

Upon making power and data connections to the OCGen® system from shore, the communications system was booted. However, no communications with the OCGen® Prevco were made. There were indications that power was flowing to the instrumentation, but no data signals were returning. Over the course of several weeks, multiple attempts to communicate to the Prevco were made, and all mostly failed, except for one short period of time when communications at a very low data rate were established. Powering off the instrumentation systems broke the communication link and it could not be reestablished.

Review of the diver video of the data cable connection process showed that the diver had been operating in a dirty environment and had difficulties un-mating the dummy plugs in the SCTA puck. However, it appeared that the mating of the data cable and shore cable was accomplished properly.

After failed attempts to recover communications, another dive was scheduled to unplug, clean and replug the data cable connector. Upon reconnection data communications were established on the first try. Examination of the dive video of the data connector seems to indicate that the 16 pin female

connector had been damaged by insertion of the 16 pin male connector in the incorrect angular orientation, punching a 17th hole into the female connector neoprene molding. Thus it appears that the connector was rotated relative to the correct position. This required considerable diver strength to accomplish.

Figure 3.7.18. 16 pin female data cable connector, showing 17th hole punched into inner ring. The inner ring should only have 5 holes.

Upon acquiring data it was noted that one of the flow sensors, the Aquadopp, was not logging water speed, headings or depth. Redundant heading and water speed instruments were mounted on the system, but the Aquadopp was the only depth sensor. To provide depth information ORPC acquired a Hobo pressure logger and attached this to the framework of the TGU during a scheduled inspection dive. The Aquadopp instrument did not report data for the rest of the deployment. Upon retrieval the Aquadopp itself seemed functional, but the communications from the Aquadopp to the Prevco was not functional.

Communications was maintained for the rest of the project except for two periods when the data acquisition system was inadvertently left off. On July 24, 2014, communications with all serial instruments (water speed sensor [Valeport], and heading, pitch, and roll sensors) were lost; however, communications with load cells and RPM sensor was maintained. Due to prior communications faults, the decision was made to let the system run under these conditions for one week rather than rebooting the system and risking another communications loss. After one week without the serial communication link, the system was rebooted and communications were reestablished with these instruments.

Operations

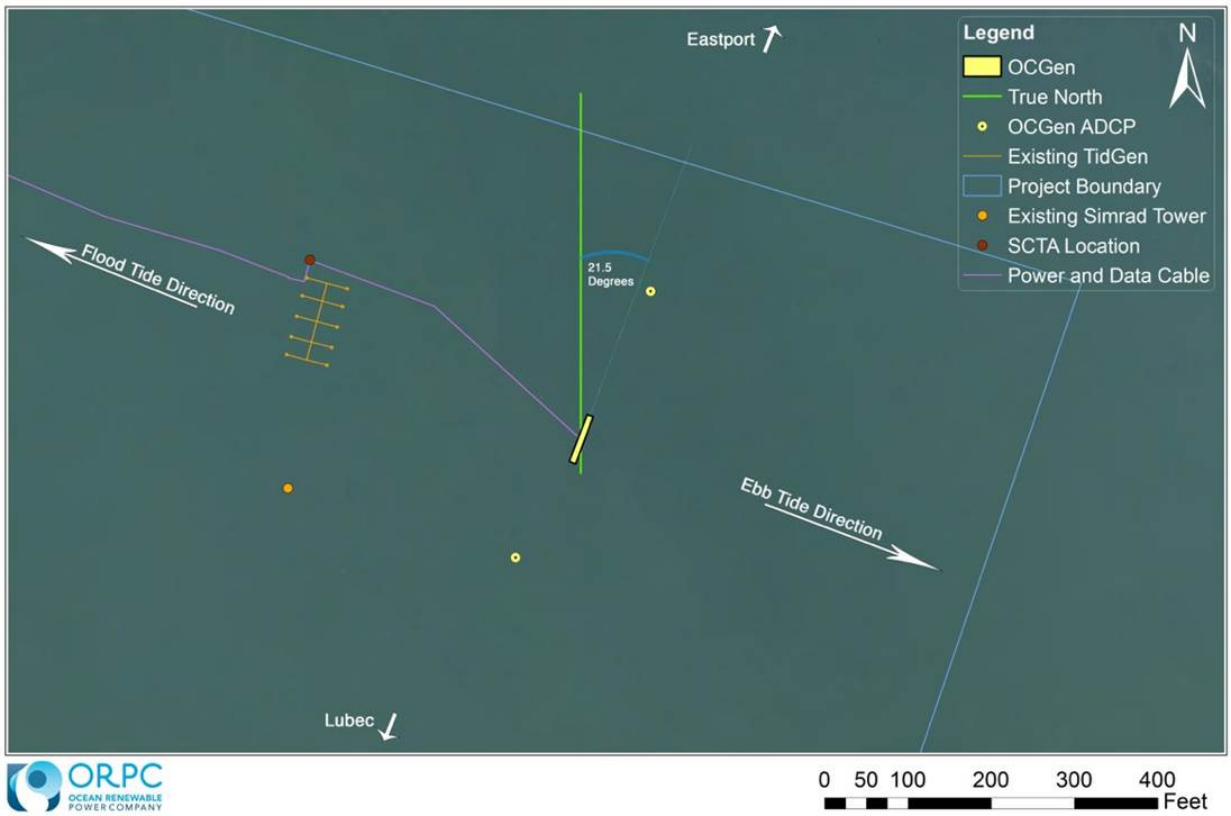

Figure 3.7.19. Map of OCGen® prototype deployment. Maps shows relative positions of TidGen®, ADCPs, data and power cables. In the report text references are made to "Lubec side" and "Goose Island side" of the OCGen®. The "Lubec side" is the southerly end of the TGU and the "Goose Island side" is the northerly end.

Two Acoustic Doppler Current Profiles (ADCPs) were deployed adjacent to the OCGen® prototype. Settings for the ADCPs are listed in Table 7.13.

Table 3.7.13. *ADCP deployments adjacent to OCGen® TGU*

ADCP type	Frequency	Location	Pings/Ensemble	Time/Ping
Teledyne Workhorse	614.4 kHz	Lubec side	60	00:01.00
Teledyne Workhorse	614.4 kHz	Goode Island side	10	00:01.00

In the report text references are made to "Lubec side" and "Goose Island side" of the OCGen®. The "Lubec side" is the southerly end of the TGU and the "Goose Island side" is the northerly end.

Flow Resource at site

Figure 3.7.20 shows ADCP water velocity over duration of project. The figure shows two occurrences of "supermoons" in mid-August and mid-September. The plot has both Lubec and Goose-island side ADCPs overlaid on one another.

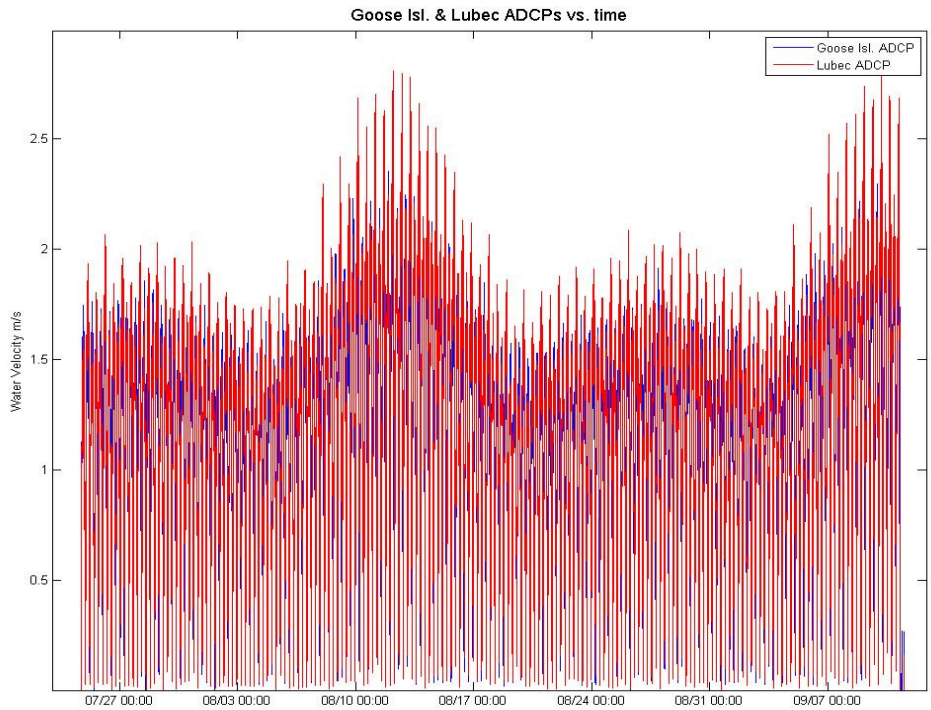

Figure 3.7.20. Flow speed data from the two deployed ADCPs over the course of the deployment. Data was taken from Bin 7 on the Lubec side and Bin 9 on the Goose Island side respectively, both of which are at the turbine hub height. Lubec side ADCP deployment was 2m shallower than the Goose Island side: data from different bins for each ADCP was used.

Flow direction and magnitudes at both ADCP locations

Ebb and flood flows at the site seem to be offset by ~ 5-10°. The direction of the flow changes between both ADCP locations by ~ 20°. There is also more variance on the Ebb tide (blue), in comparison with the more defined flood tide direction.

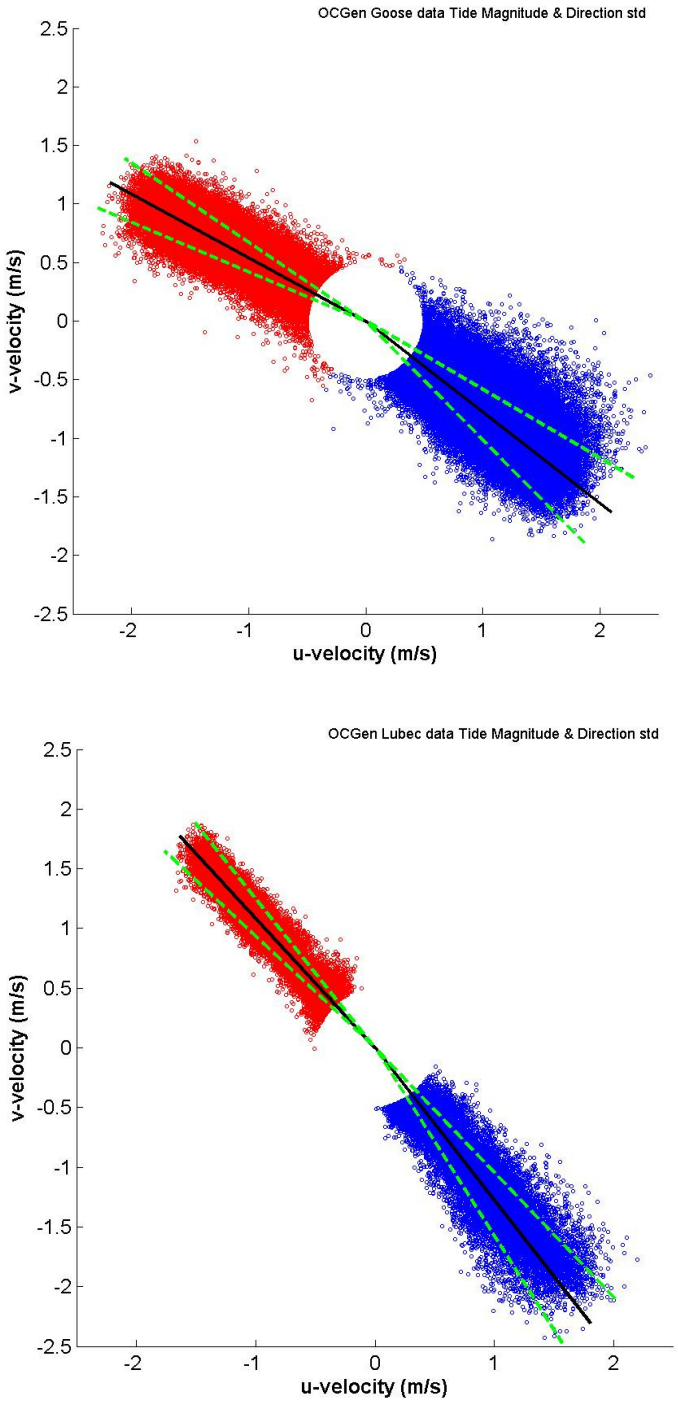

Figure 3.7.21. Ebb and flood flows at the two ADCP deployments at the turbine hub height.

Comparison of ADCP data

As seen in Figure 3.7.22 the magnitude of the flow speed changes between both ADCP locations throughout tide cycles. What is of note here is that there is a variance between both ADCPs on the ebb tides; there is an almost perfect relationship between the flow magnitudes on the flood side, however the ebb tide the flow is noisier and is consistently larger on the Lubec side of the project site.

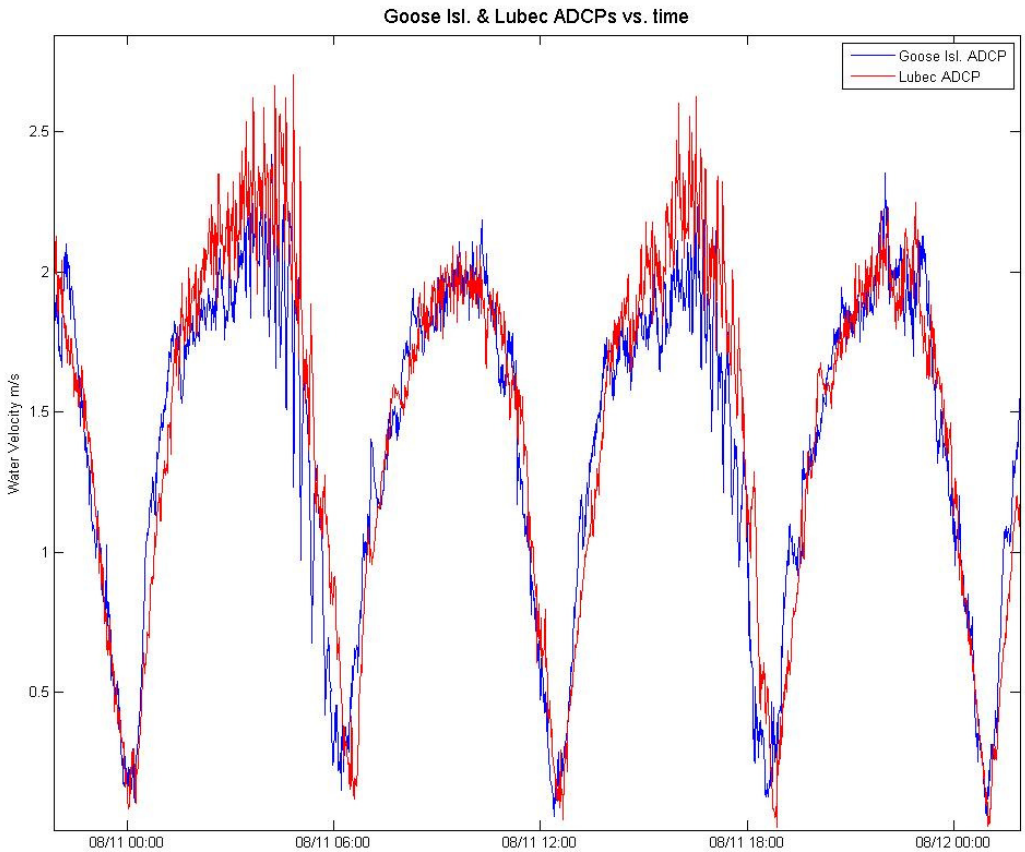

Figure 3.7.22. Water speed data from both ADCPs for July 11, 2014. Note the asymmetry between the ADCPs on the larger ebb tide.

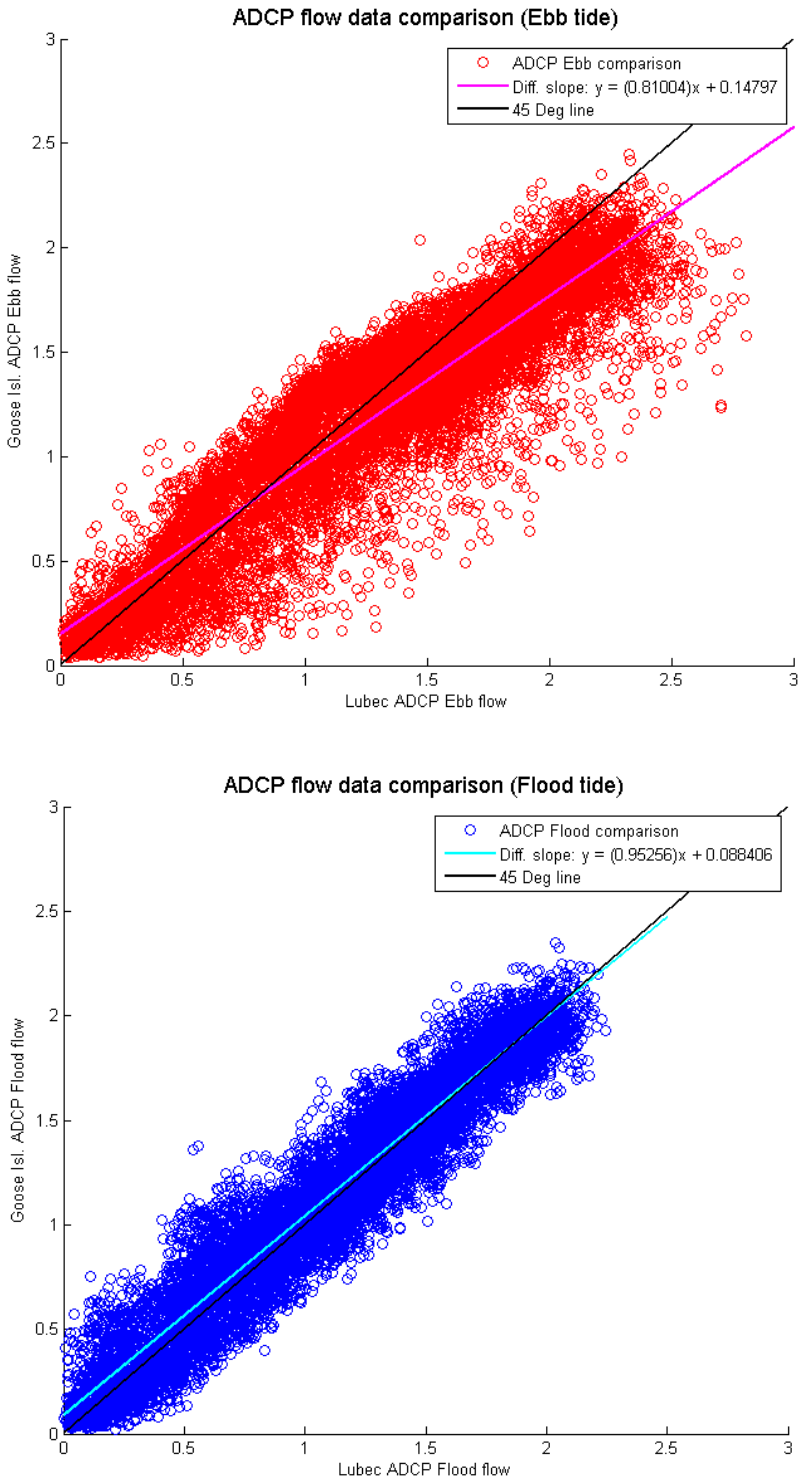

Figure 3.7.23. Comparison of Goose Island ADCP data with Lubec ADCP data. Correlation deviates on the ebb tide, but was good on the flood tide. On both plots a 1:1 correlation is shown as a 45° line.

For the purposes of processing data associated with the TGU itself, an average of the ADCP data was taken, and the resultant flow magnitude was used as the water speed for the remainder of the data processing. Figure 3.7.24 showed the same four tide cycles for both ADCPs but also included the averaged ADCP data overlaid in green.

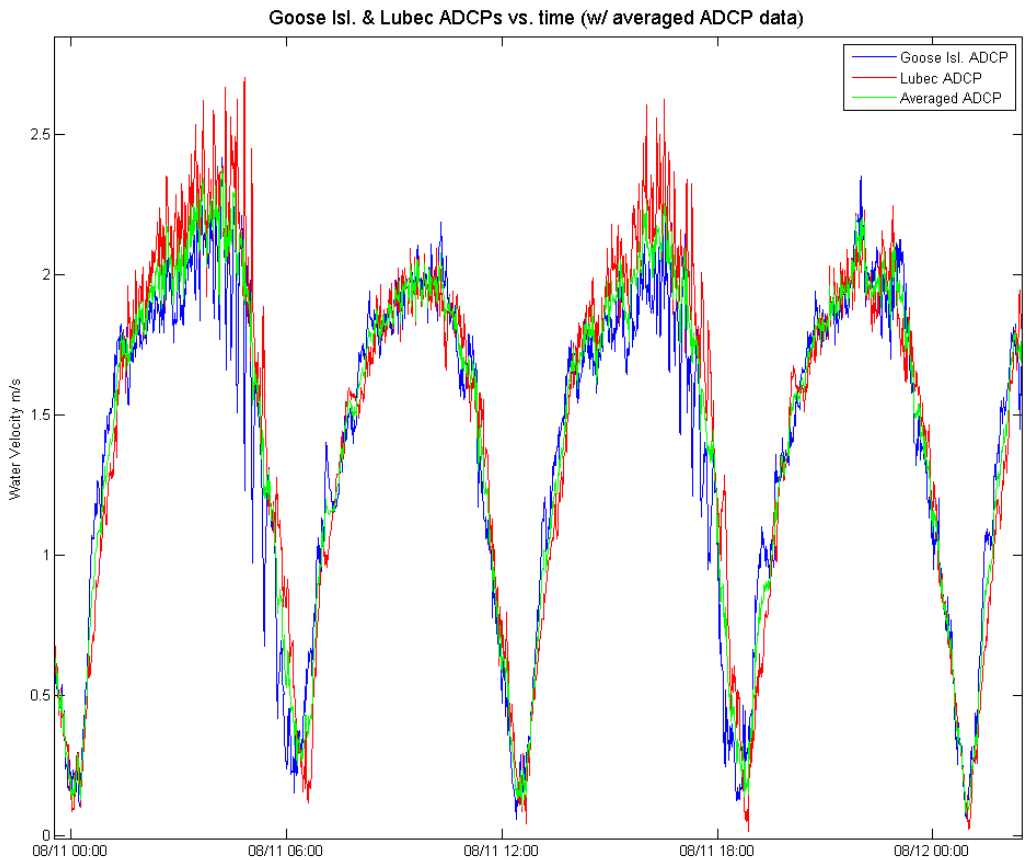

Figure 3.7.24. ADCP data from Goose Island and Lubec ADCPs and the average of both at turbine hub height. Averaged ADCP data is used from this point onwards for the purposes of data processing.

ADCP vs. Valeport Comparison

As the ADCP instruments are self-contained, data from them was not accessible during the project. Instead, the flow data monitored was from a Valeport (electromagnetic flow sensor), which reported flow data at 3 second intervals to ORPC's SCADA system. The Valeport is mounted on the OCGen® TGU and may subject to local turbulence and flow variation around the structure and movement of the buoyancy pod. Figures 3.7.25 through 3.7.26 outline the variance in flow magnitude between the averaged ADCP data and the Valeport flow data. In this case, the ebb tide flow data between the two data sets correlate quite well, however the Valeport appears to measure higher flows than the ADCP on the flood tide.

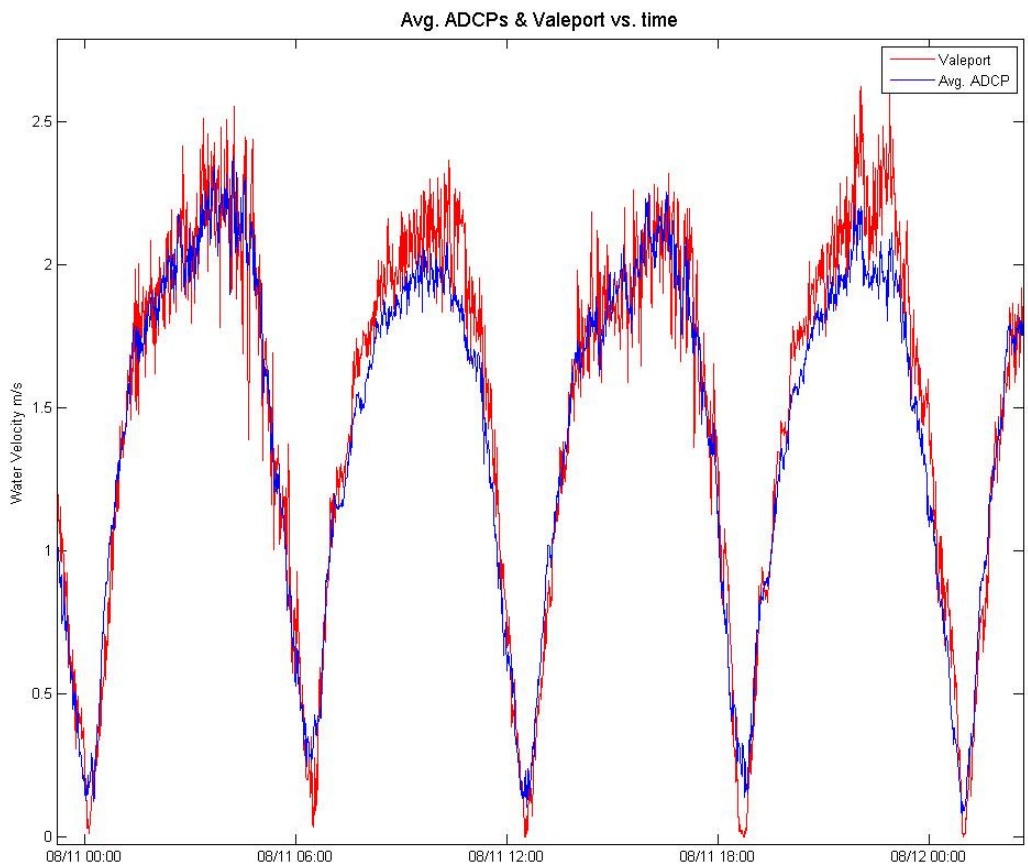

Figure 3.7.25. Comparison of average ADCP data and Valeport data for a sample data set. The Valeport data is collected from an instrument mounted and moving with the TGU

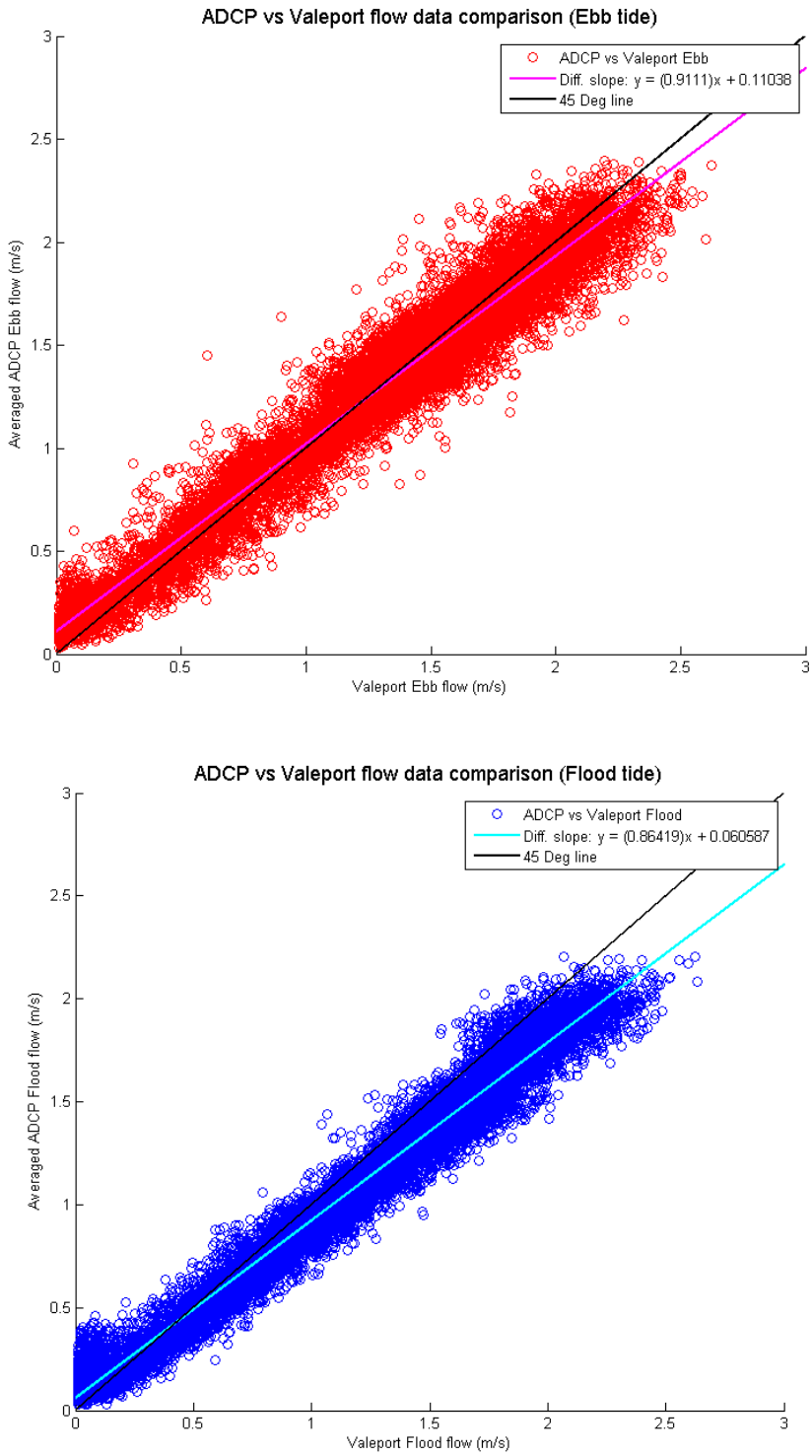

Figure 3.7.26. Comparison of average ADCP data and Valeport data for the full data set. The Valeport data is collected from an instrument mounted and moving with the TGU.

Operating States of System

The system was operated in three distinct states and phases during the deployment. Initial operations involved a period with a brake applied to the turbine to prevent rotation. A second period of operations occurred with the turbine spinning at a rotational speed dictated by the water speed. A third state of operations occurred with no turbines present.

Table 3.7.14 *Operating States of OCGen® TGU during deployment*

Operating State 1	Turbines on structure with brake on	June 27 – Jul 23, 2014
Operating State 2	Turbines intact and spinning	Jul 23 – Aug 10, 2014
Operating State 2	OCGen without turbines	Aug 11 – Sep 17, 2014

OCGen TGU movement throughout project duration

An inertial measurement unit (IMU), located inside the OCGen® Prevco sensor bottle, measured heading, pitch, and roll throughout the duration of the project.

Drop outs in data between July 25 and August 1, 2014 were caused by a loss in communications from serial instruments. ORPC made the decision not to troubleshoot this problem until one week of load, rpm, and flow data had been collected without issue, in order to ensure that any new problems created during troubleshooting did not cause further loss of data. ORPC diagnosed the issue on August 1, 2014. Data rate requests between the Prevco and shore station were too high to be sustained by the internal Prevco communications protocols. When the data rate was decreased, full data transmission began.

The following set of plots show heading, pitch and roll for the OCGen® TGU over the deployment measured by the IMU (Figures 3.7.27-3.7.32). Heading was defined as rotation around the vertical; pitch as rotation around the TGU axis; and roll as rotation around the remaining axis.

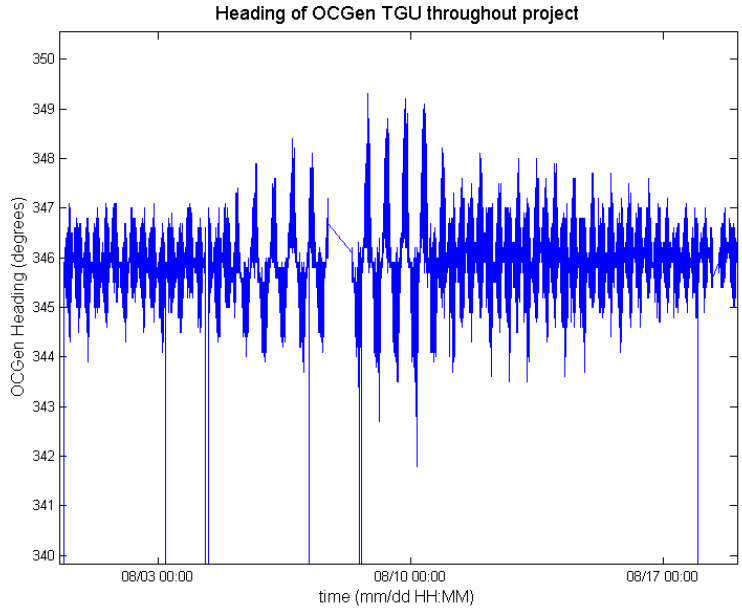

Figure 3.7.27. Heading of OCGen® throughout project. Absolute values have not been adjusted for local magnetic effects of the structure. Of interest here is the relative change of heading, which was small

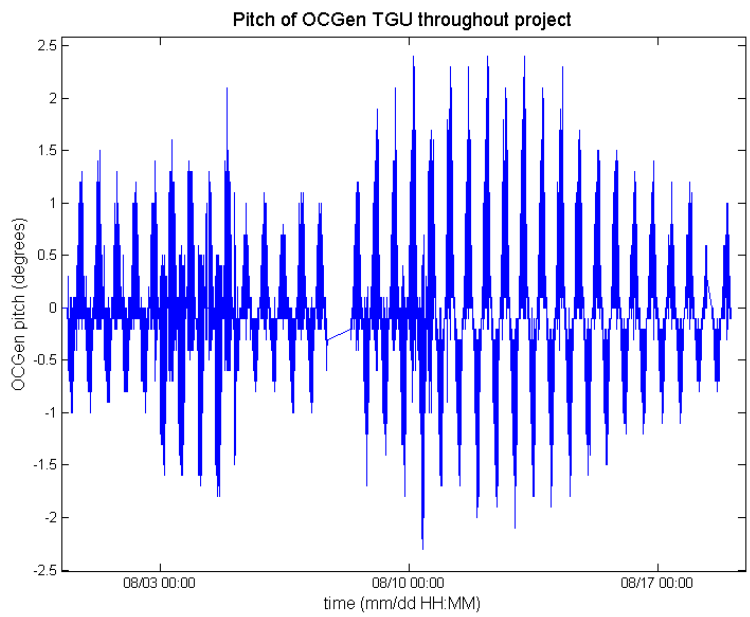

Figure 3.7.28. Pitch of OCGen® throughout project. Pitch is defined as rotation around the buoyancy pod axis. Relatively small changes in pitch are noted throughout the project.

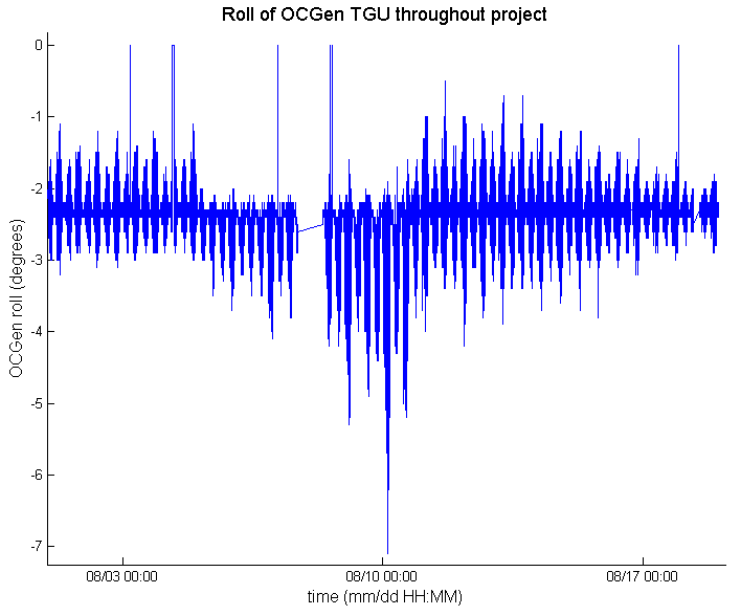

Figure 3.7.29. Roll of OCGen® throughout project. Roll is defined as rotation about the axis orthogonal to the vertical and the pitch axis. Roll events occurred during the test period, with a preference to roll to one side, but in general the angle of roll is low.

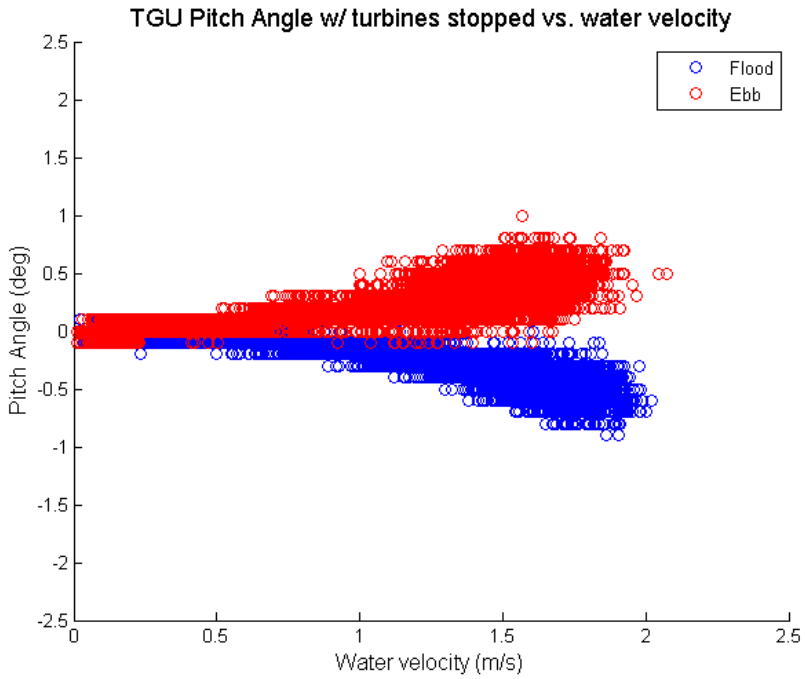

Figure 3.7.30. Pitch of OCGen®, Operating State 1 (turbines stopped), as a function of water speed. Pitch is defined as rotation around the buoyancy pod axis. The figure shows relative symmetry between roll angles for ebb and flood tides.

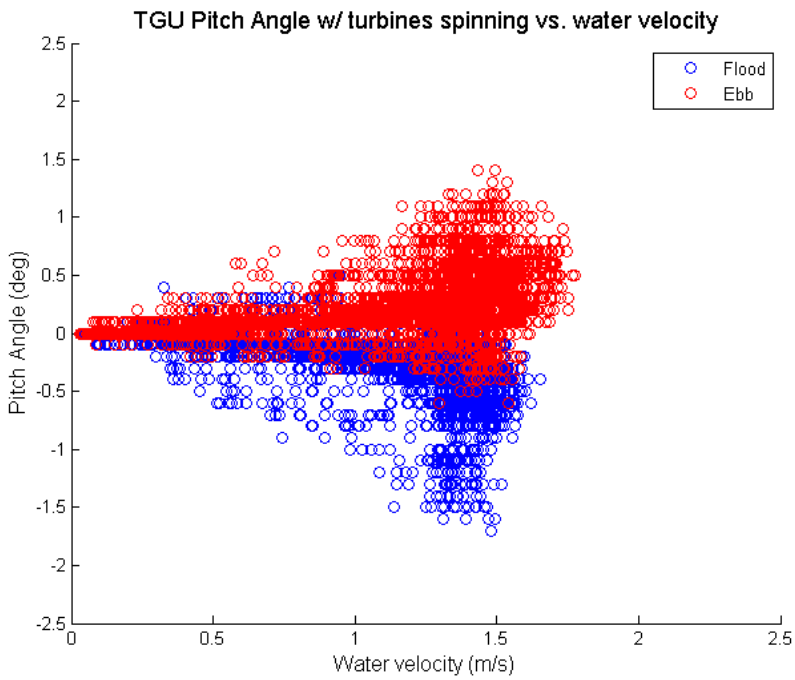

Figure 3.7.31. Pitch of OCGen® Operating State 2 (turbines spinning), as a function of water speed. With the turbines spinning, symmetry was maintained for pitch angle, between flood and ebb tides.

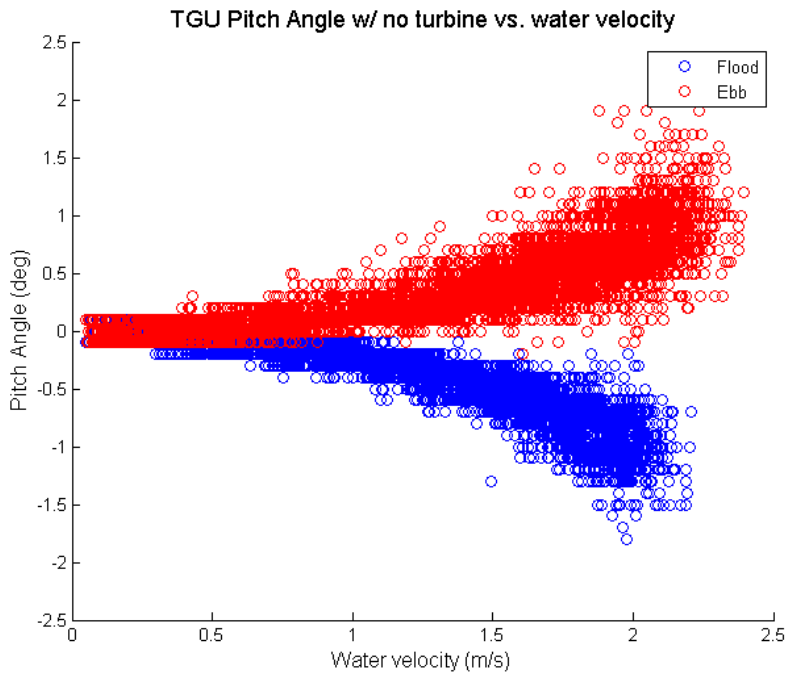

Figure 3.7.32. Pitch of OCGen® Operating State 3 (no turbines), as a function of water speed. Higher pitch angles were noted here, but higher flow speeds were also observed.

Data for slack water events (-0.25m/s < flow speed < 0.25m/s) ORPC concluded that no change in heading, pitch or roll of the TGU occurred for the slack water condition, even though there were significant turbine issues during the week of August 4 through August 11, 2014. Heading at slack changed no more than +/- 0.4 degrees from its average slack heading. Pitch of unit changed no more than +/- 0.2 degrees from its average slack pitch. Roll of unit changed no more than +/- 0.1 degrees from its average slack roll.

OCGen turbine TSR

The condition of the turbines was assessed by plotting the tip speed ratio (TSR) over time. When turbines were fully intact and the TGU was operating under normal conditions, with an average TSR of slightly greater than 2.

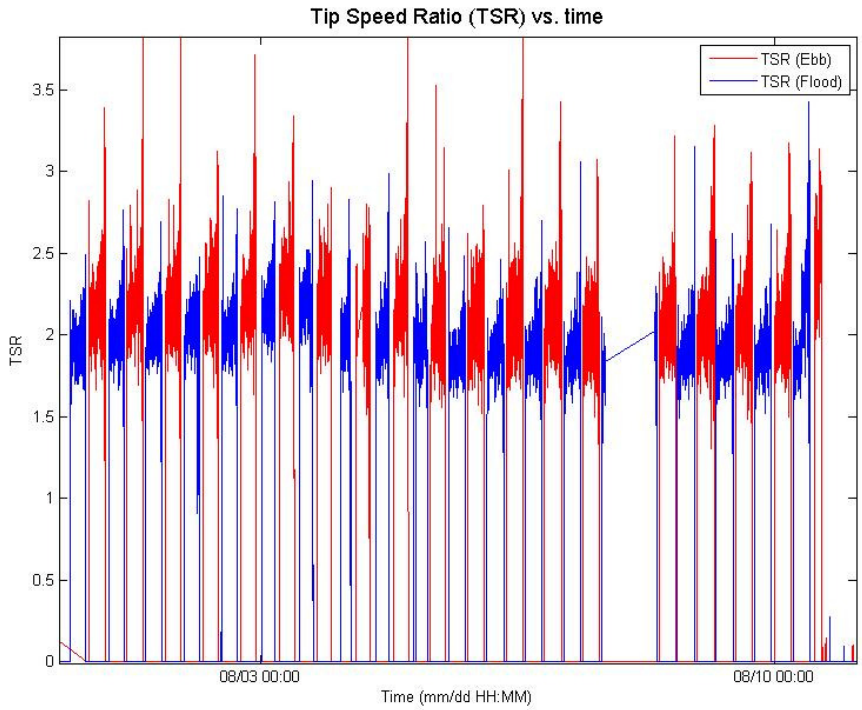

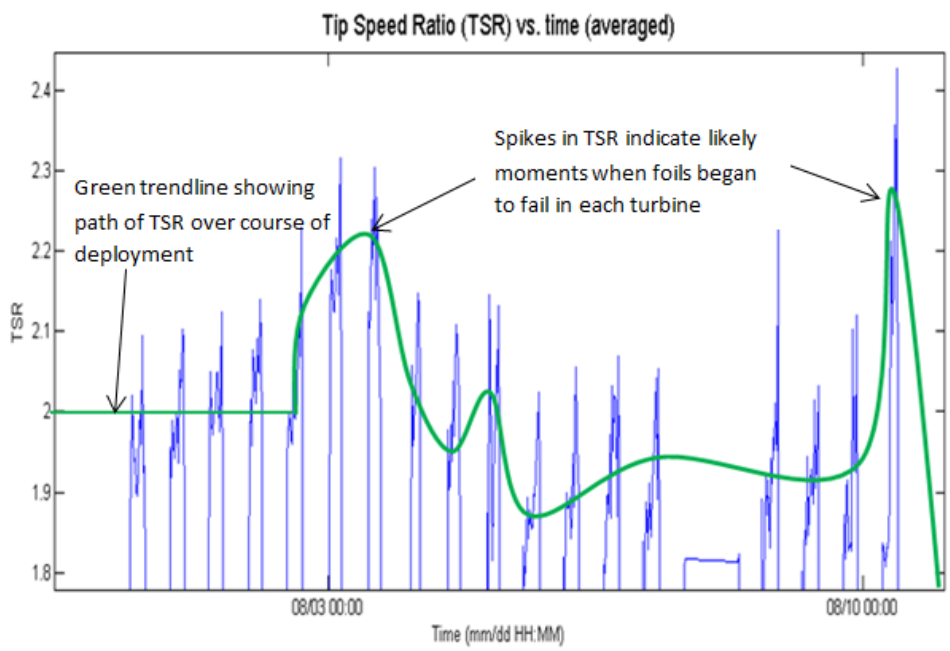

Figure 3.7.33. Tip speed ratio for the turbine during when turbine was turning. The upper chart shows raw data, while the lower chart shows averaged data for TSR and an interpretation of how the TSR changed (green curve).

OCGen® TGU Height

Pressure data from both ADCPs deployed showed a variance in the mean water height with time between the ADCPs. The difference in instantaneous water levels between the two ADCPs reaches a peak of almost 0.4m at certain stages of the tide cycle (Figure 3.7.34). There is an approximately 2.3m difference in depth between the two ADCP locations. This difference in height is shown in Figure 3.7.34, as a mean offset, with the time varying offset shown superimposed on the mean.

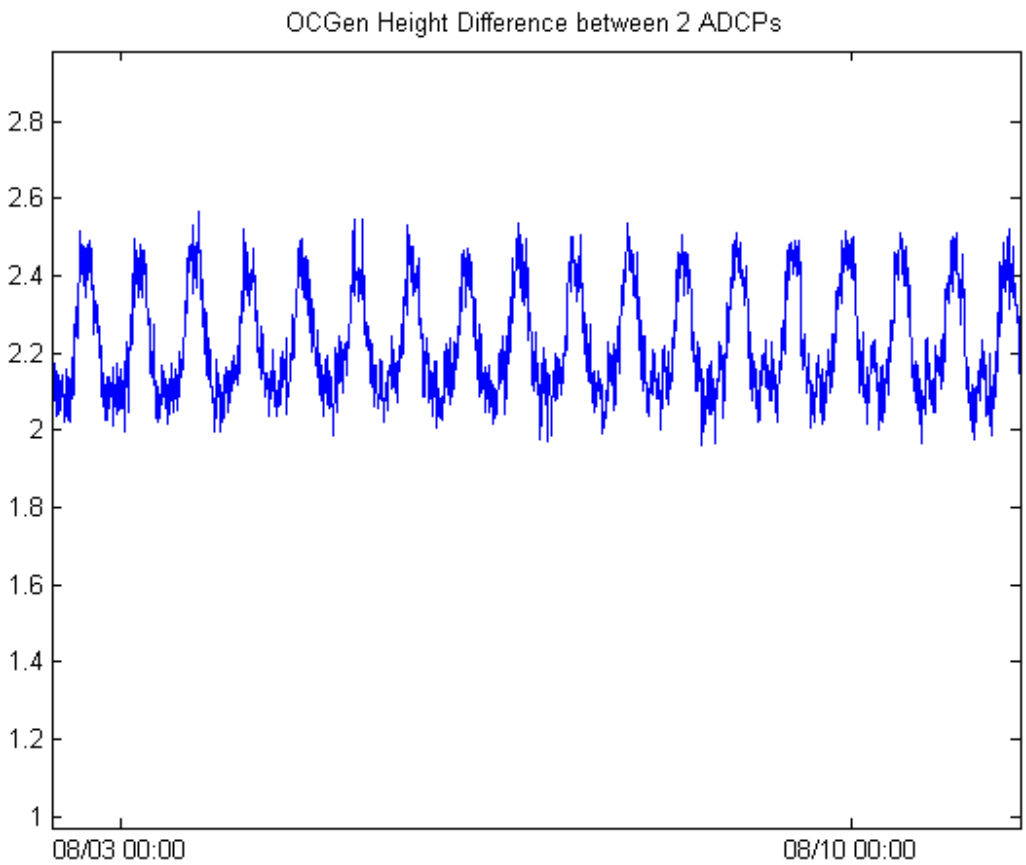

Figure 3.7.34. Difference in water level between the two ADCPs deployed at the project site adjacent to the OCGen® TGU. See Figure 3.7.19 for location of ADCPs.

The height of the OCGen® TGU above the seabed was calculated indirectly using the difference in pressure readings between an onboard pressure sensor, and the averaged pressure sensor reading from the ADCPs. This gave a distance from the ADCP on the seabed to the OCGen® TGU.

In general, a change in OCGen® height of ~1m between slack and peak flows was seen. There was a measurable difference between the height of the system at high water slack and height at low water slack (Figure 3.7.35). This change in height was also reflected in the load cell data where different values are seen for slack water high and slack water low events. The independent load cell data confirms that this behavior is a real behavior and not a numerical artifact of the data processing.

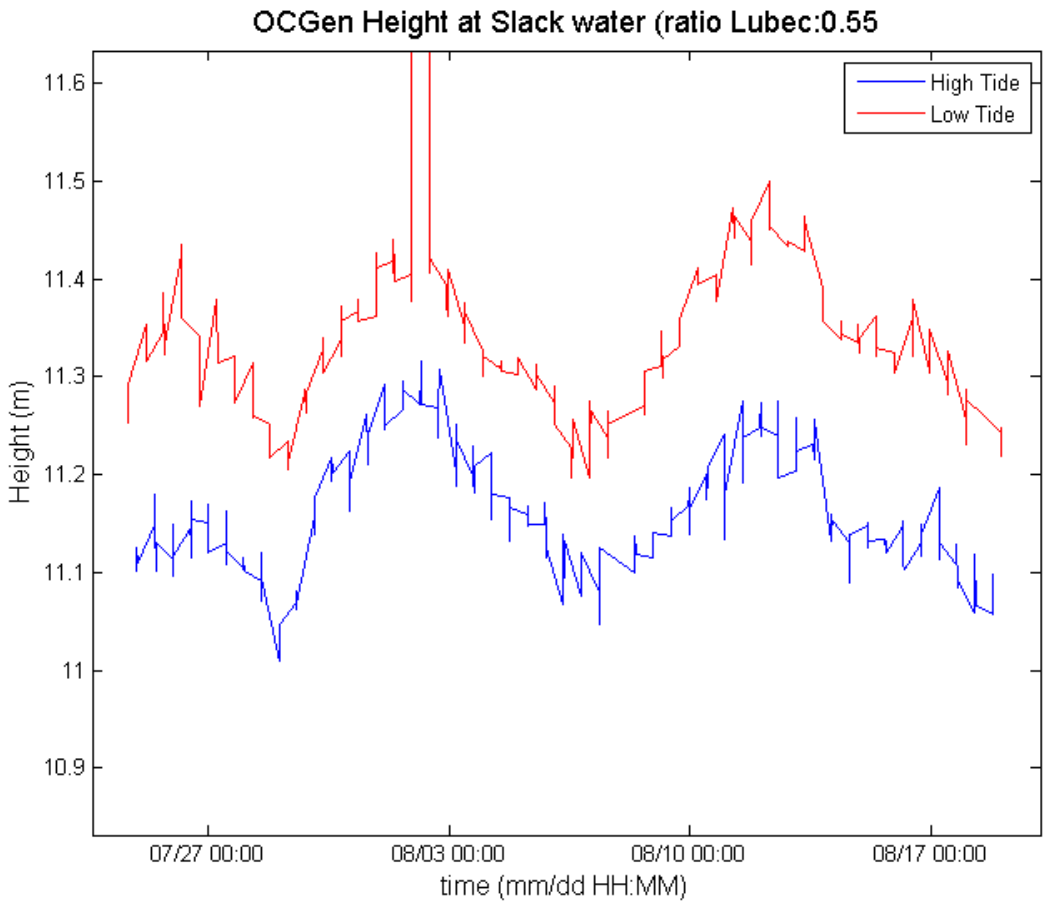

Figure 3.7.35. OCGen® height in the water column showing heights at high and low tide slack water events. Load cell data confirms that different loads occur at the slack high and low water events, confirming that the change in height seen in this chart is a real phenomenon.

Several explanations for this behavior have been proposed, but it has not been possible to confirm which is most likely:

- ORPC noted differences in local water height between the ADCPs previously. A non-uniform water level across the site would influence the methodology used to calculate OCGen® location in the water column.
- Mooring lines may have hysteresis stretching during the ebb tide, leaving the unit higher in the water column at low tide. This theory aligned with earlier graphs, which show that the ebb tide had higher flow magnitudes than the flood.
- Trapped air volumes may have been present in the system, which would have been compressed and expanded by the tide height change.

A plot of OCGen® height as a function of water speed is shown in Figure 3.7.36. Again of note is the behavior at slack water, v = 0m/s. There was a slight but noticeable bi-stable condition in the data, which indicated different OCGen® heights at low and high slack water events.

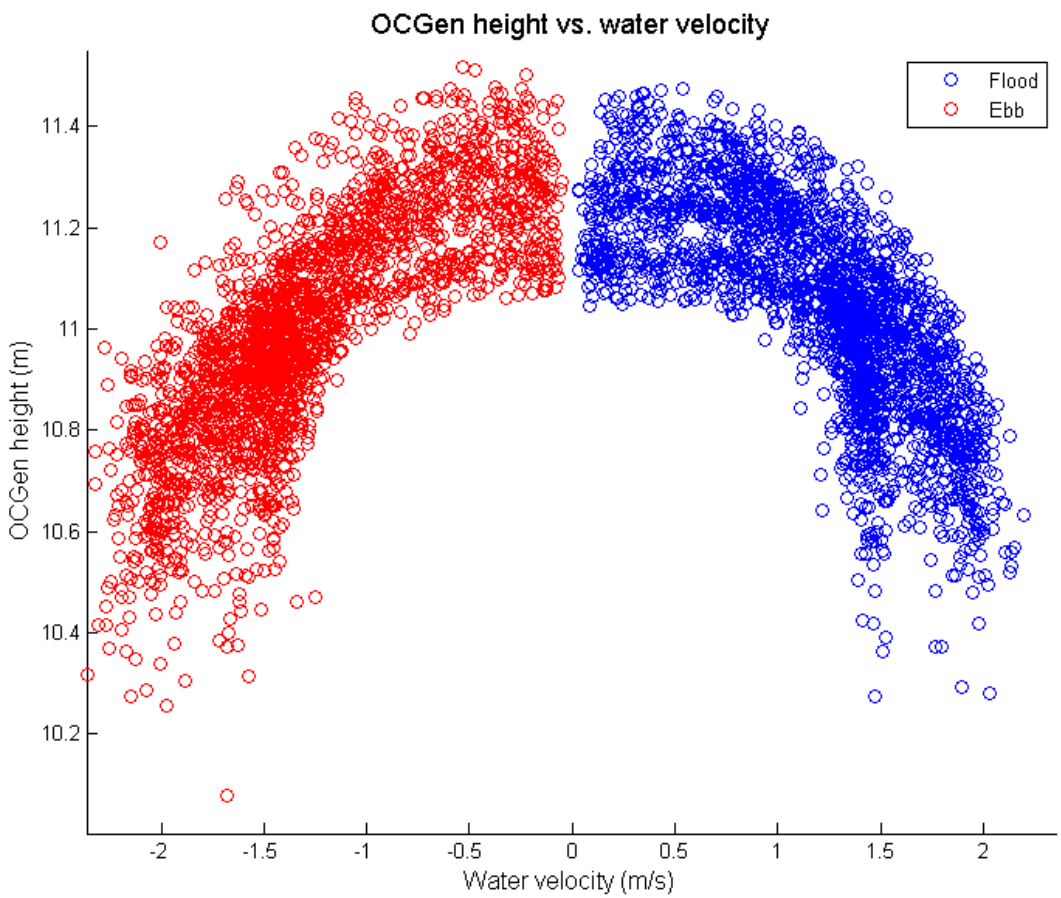

Figure 3.7.36. OCGen® height in the water column for all data. The difference in height between high and low tide slack water events is evident in the bifurcating data at zero water speed.

OCGen® Mooring Line Angle

Mooring line angles, defined as the angle made with the vertical, were estimated from the TGU height data.

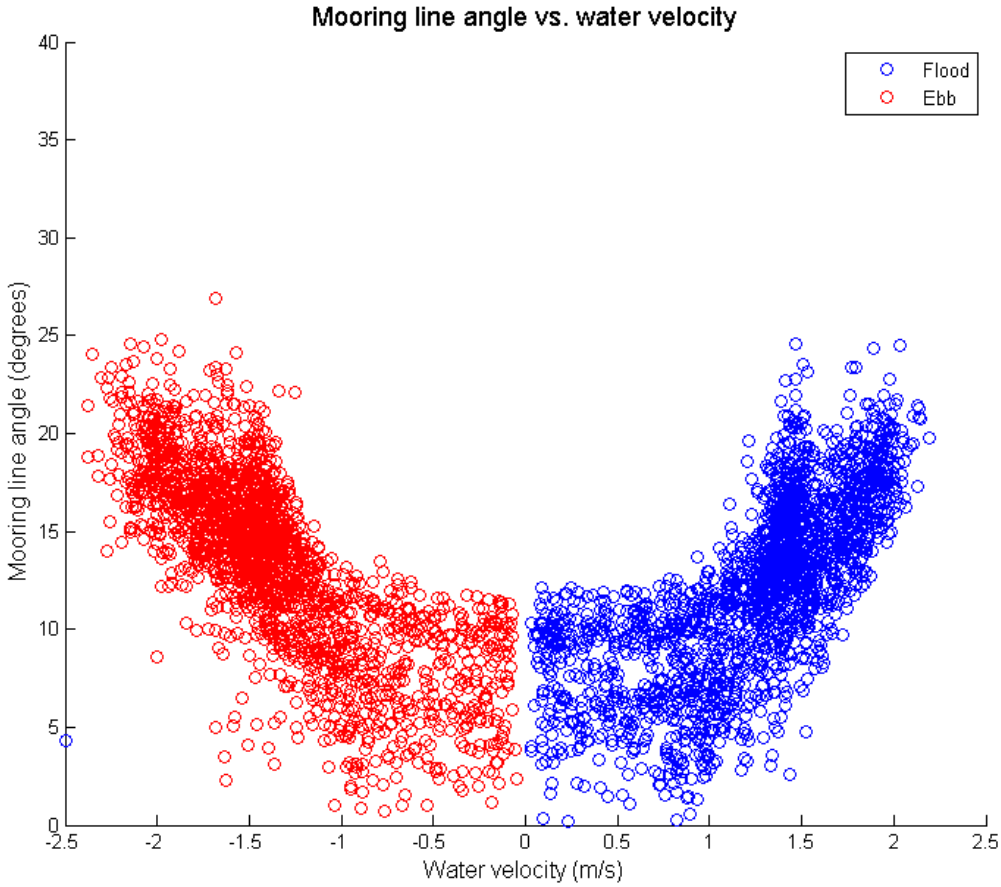

Figure 3.7.37. OCGen® mooring line angles in the water column as a function of flow speed. From the previous plots, height at peak flow speeds appeared to be constant for both ebb and flood tides. The estimated 25° mooring line angle at peak flow was more trustworthy than the angle at slack water.

Mooring Line Loads

Each of the four OCGen® mooring lines was equipped with a load cell, which measured the load experienced by each mooring line at three second intervals. Plots of the loads are presented in various formats.

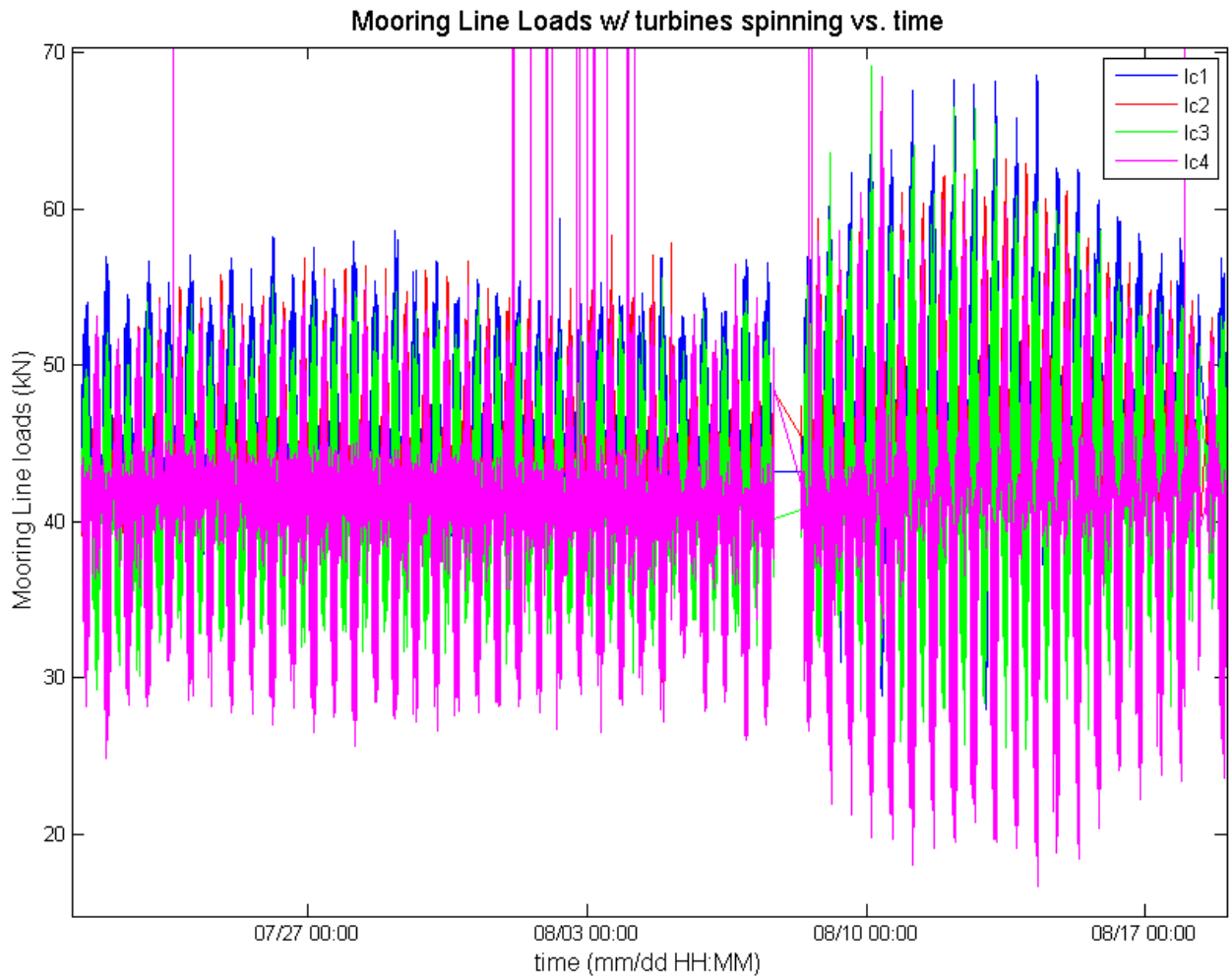

Figure 3.7.38. Raw OCGen® mooring line loads for the full data set. Data spikes are spurious noise and were removed from further data processing.

The large loads on the mooring lines around August 11, 2014, coincide with the "supermoon," which occurred during the project. A snapshot of two tide cycles (Figure 3.7.39) illustrates variation in the load readings. Data for the one second logging periods and the three second logging periods show similar behavior for the loads, and provide an indication that these variations in loads are not noise, but indicate actual load data.

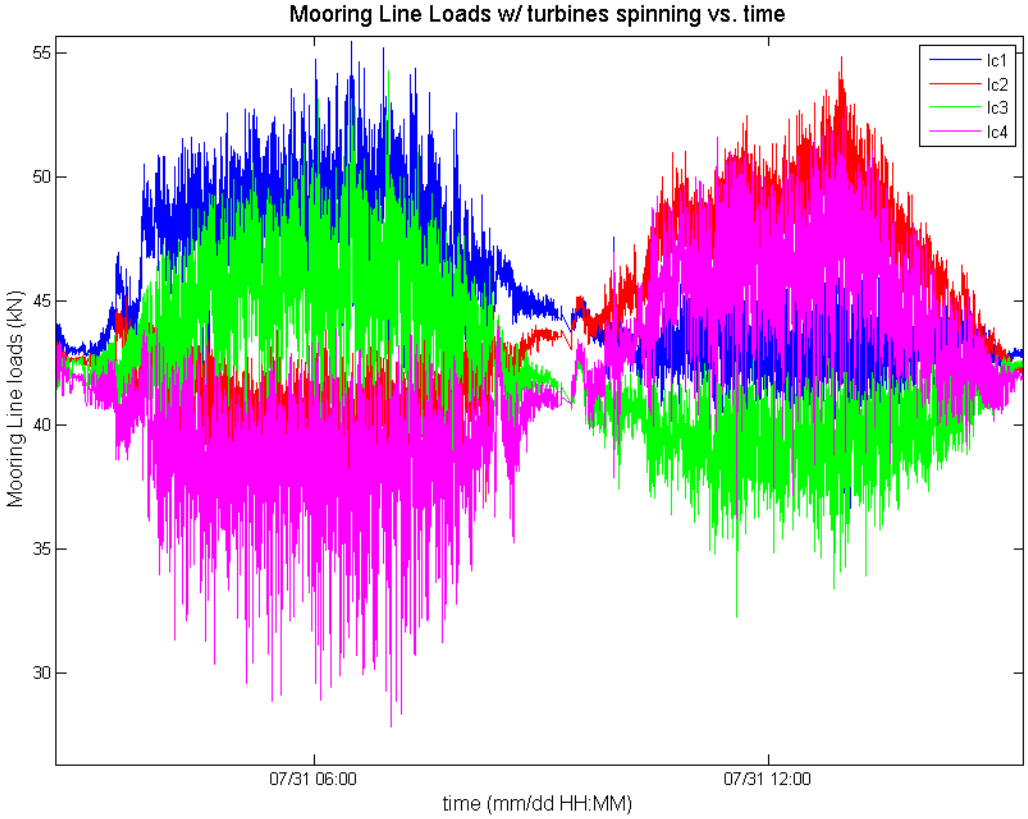

Figure 3.7.39. OCGen® mooring line loads for a tide cycle

Due to variations in this data, plotting load readings over time was not ideal for viewing, so various graphs plotting mooring line load as a function water speed, for both flood and ebb, and during three different operating conditions are presented. It is important to distinguish between the multiple operating states of the system in order to properly present these data.

Along with the raw data plots, averaged data plots are also presented using 3 minute block averages.

In the load cell data, note that loads for the zero flow condition are not equal, indicating difference in mooring line length, probably due to different degrees of mooring block settling at each mooring line.

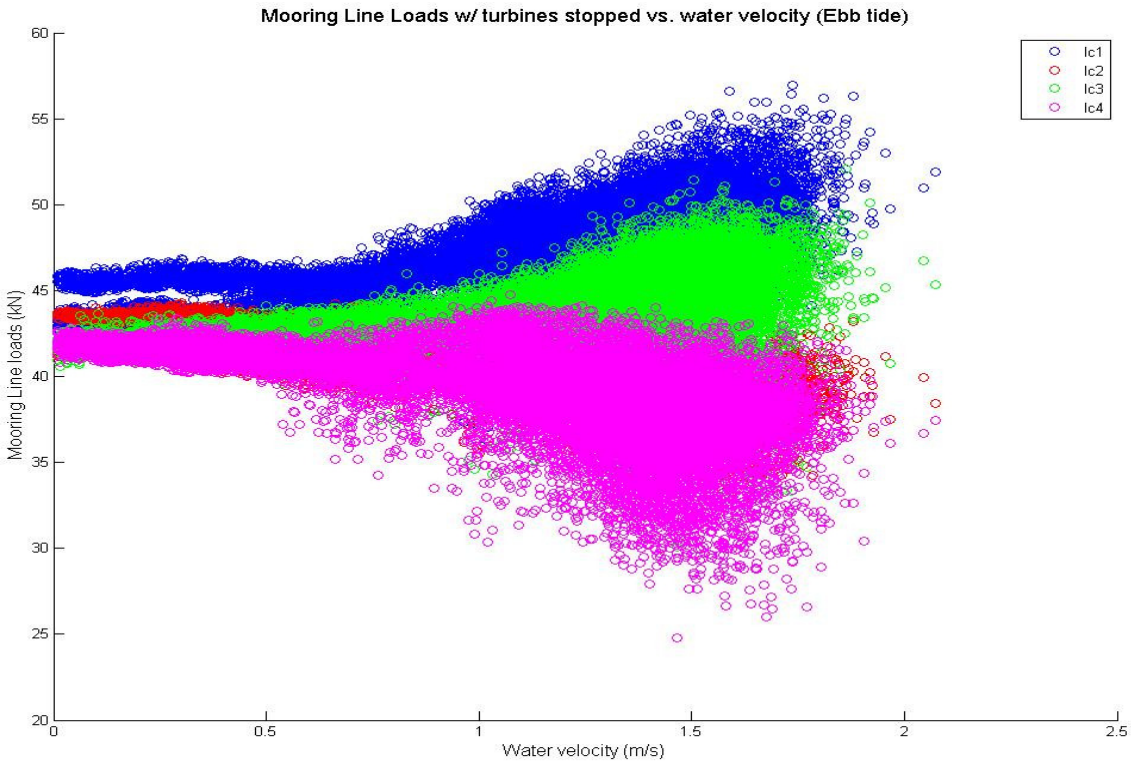

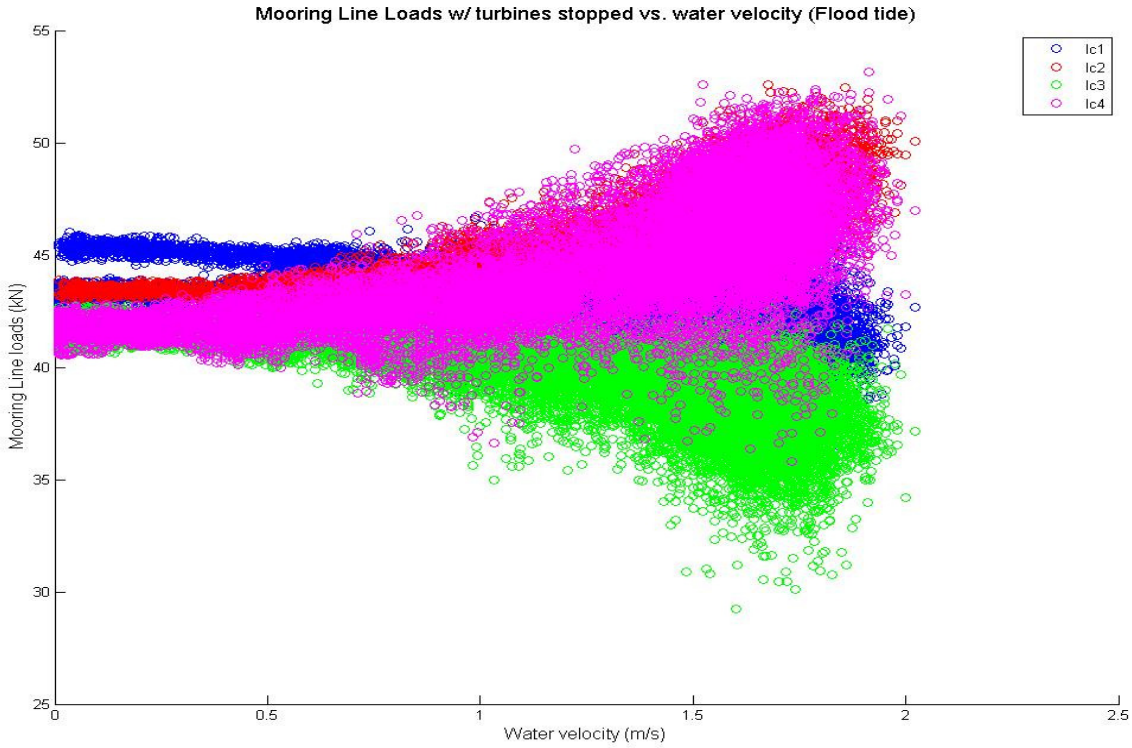

Figure 3.7.40. Raw OCGen® mooring line loads for ebb and flood tides; Operating State 1 (turbines present and not rotating). Note the offset of loads at V = 0m/s. This is due to differences in mooring line lengths, probably due to differences in mooring block settlement at each mooring line.

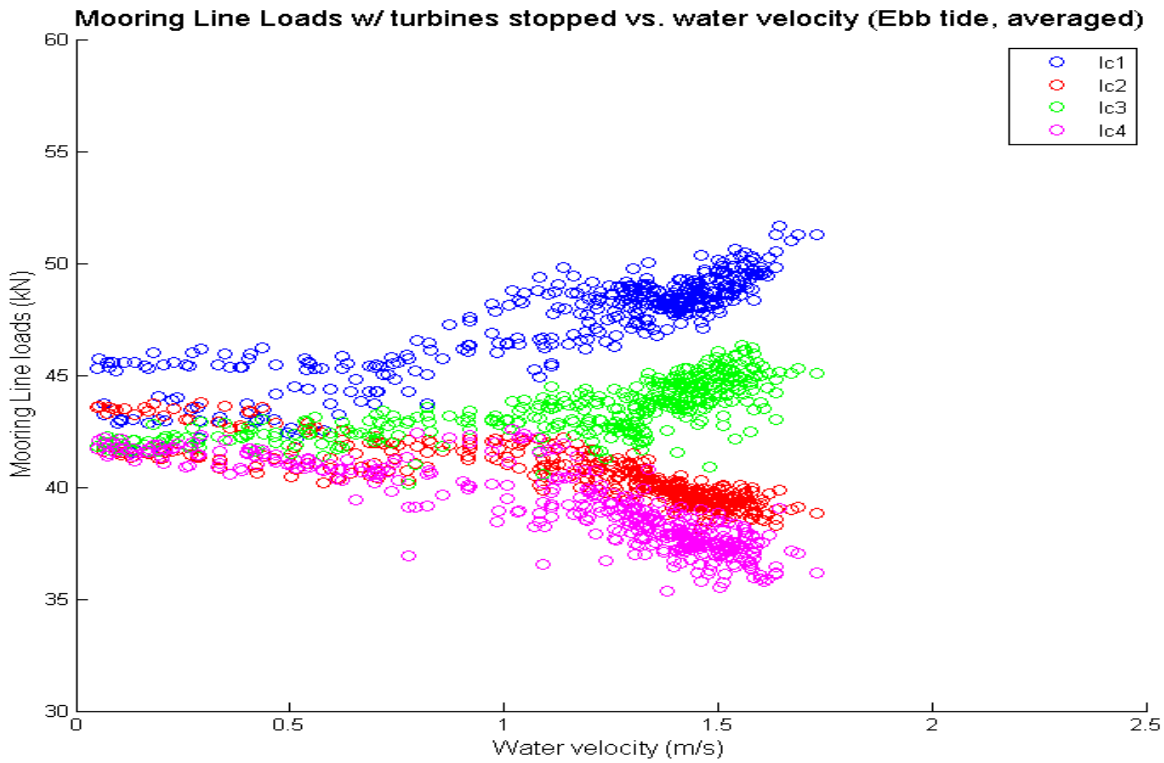

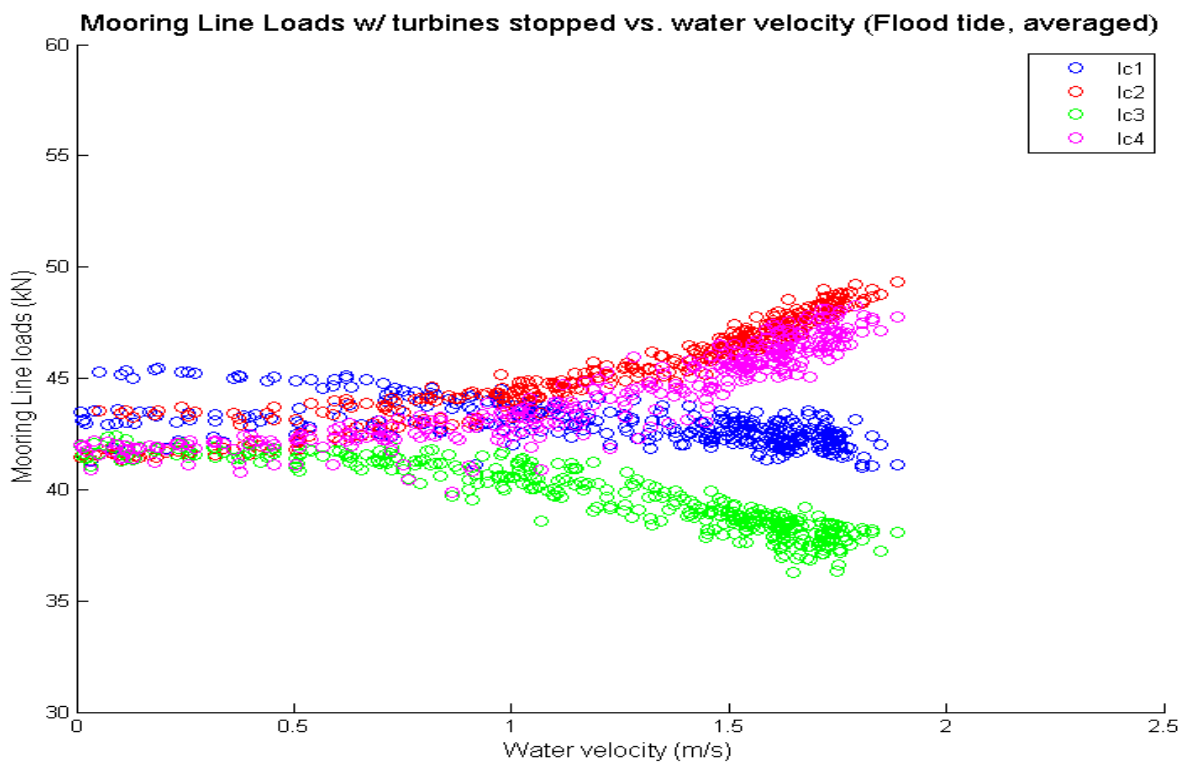

Figure 3.7.41. Averaged OCGen® mooring line loads for ebb and flood tides; Operating State 1 (turbines present and not rotating). Data is averaged in 3 minute blocks.

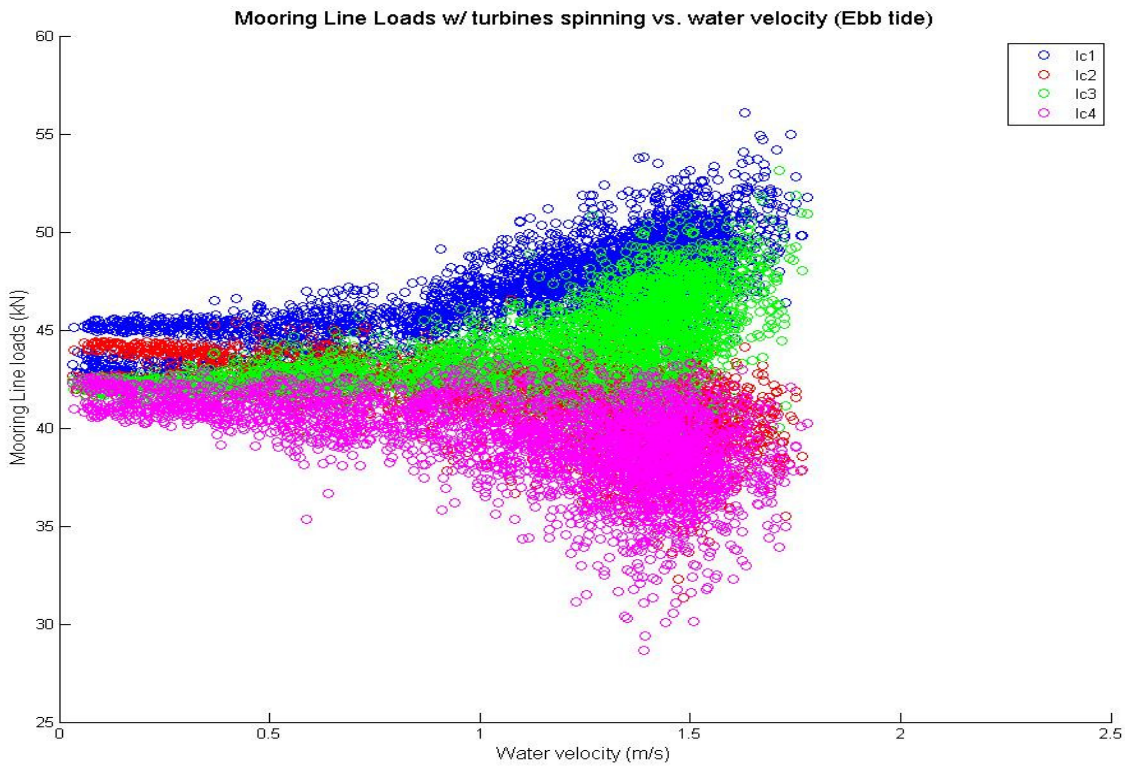

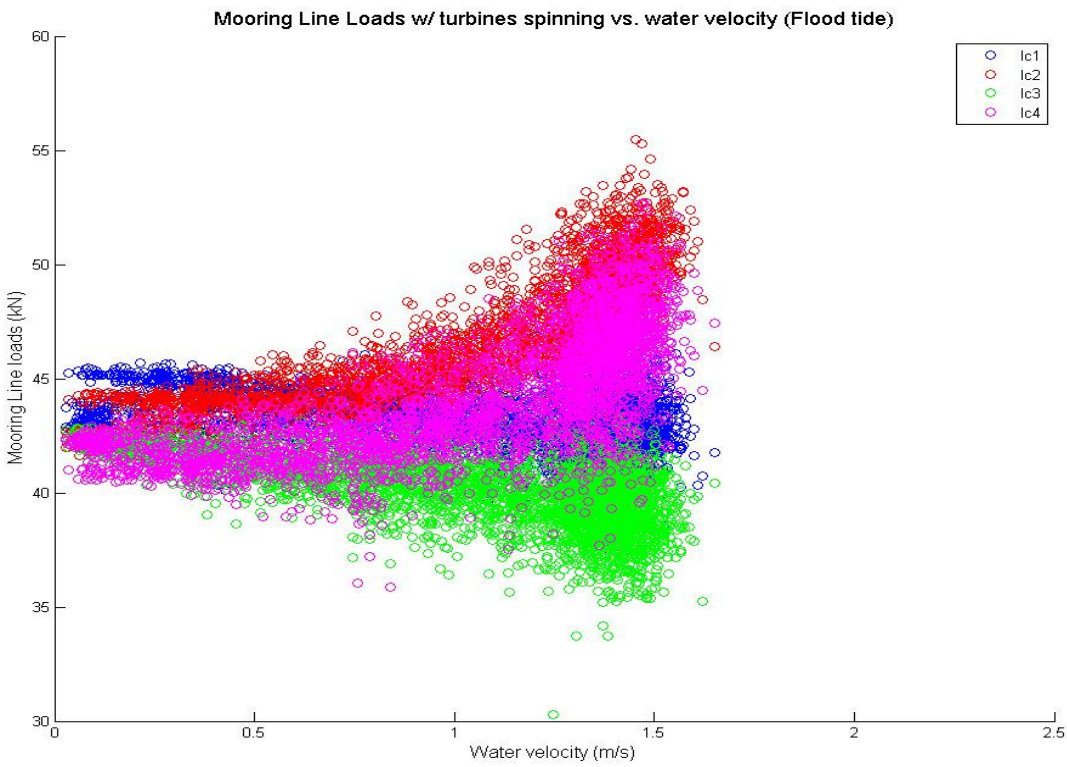

Figure 3.7.42. Raw OCGen® mooring line loads for ebb and flood tides; Operating State 2 (turbines present and rotating).

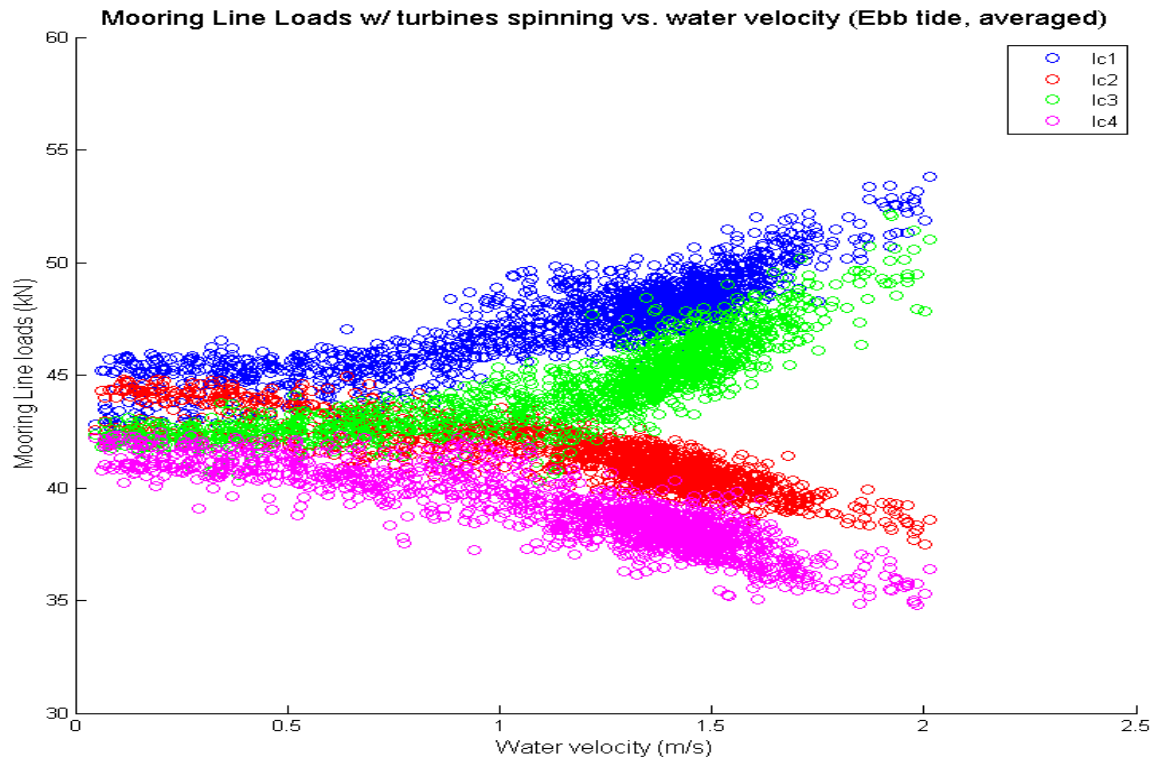

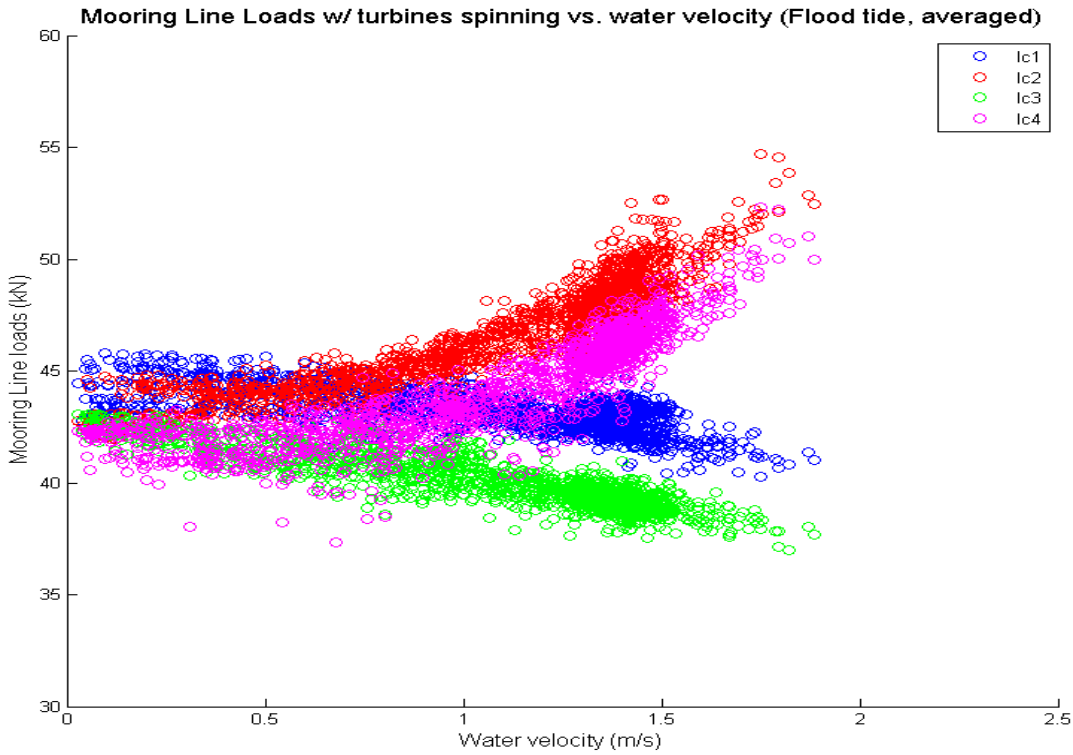

Figure 3.7.43. Averaged OCGen® mooring line loads for ebb and flood tides; Operating State 2 (turbines present and rotating). Data is averaged in 3 minute blocks.

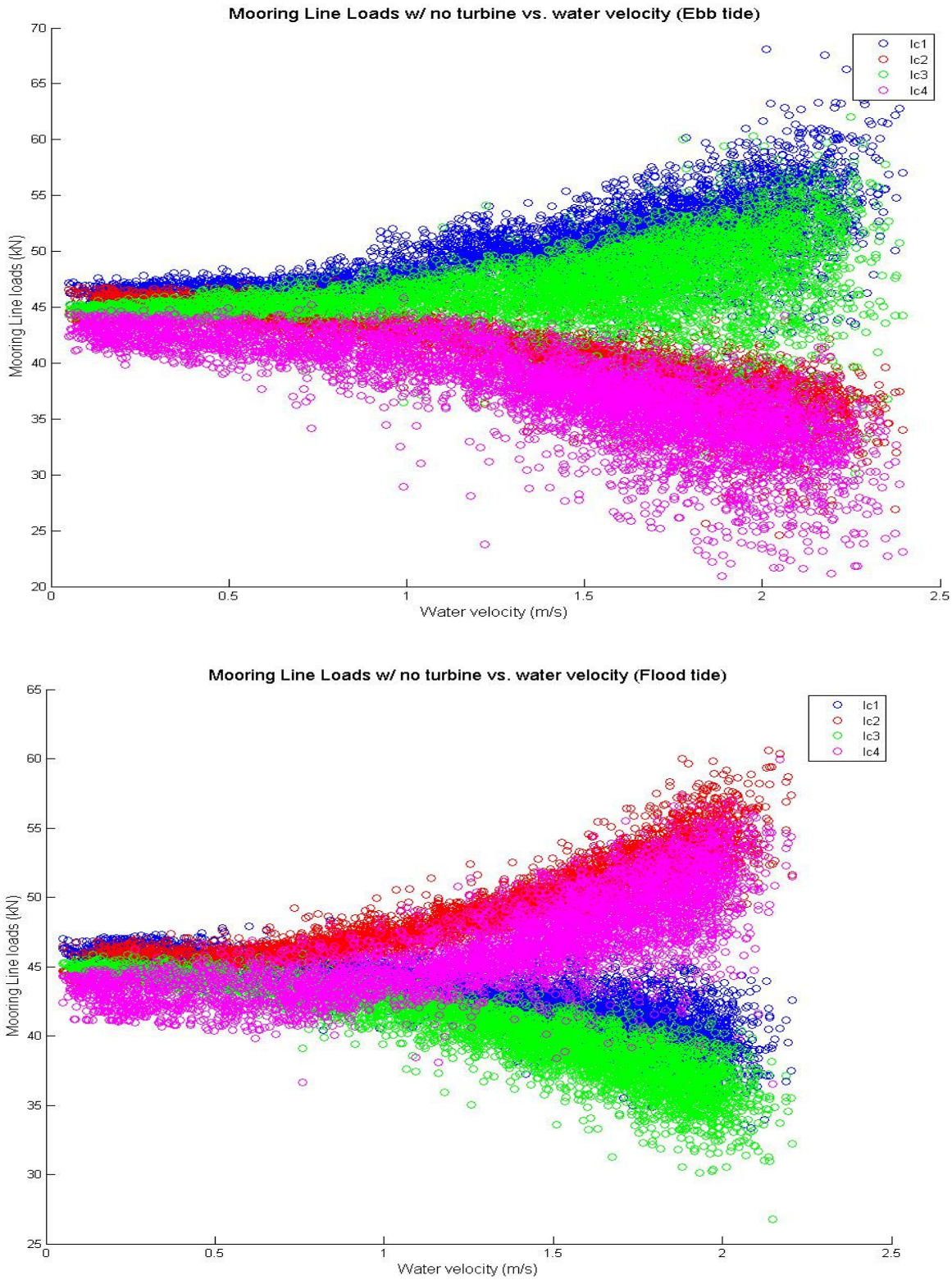

Figure 3.7.44. Raw OCGen® mooring line loads for the for ebb and flood tides; Operating State 3 (turbines not present).

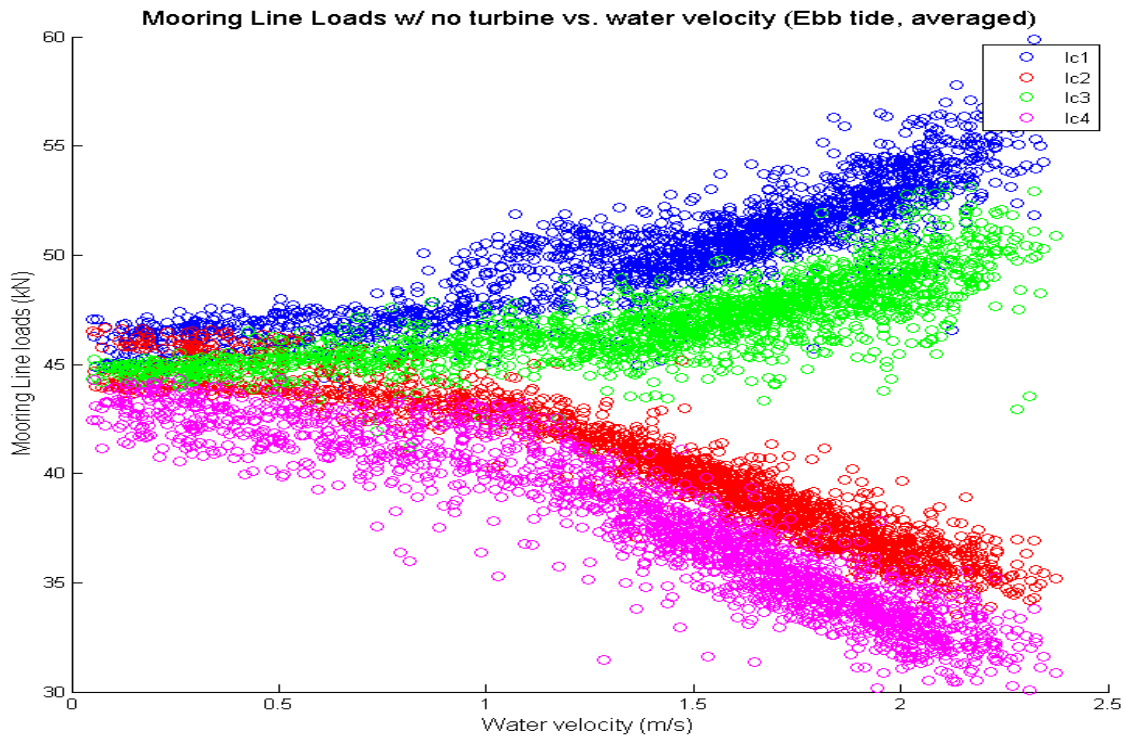

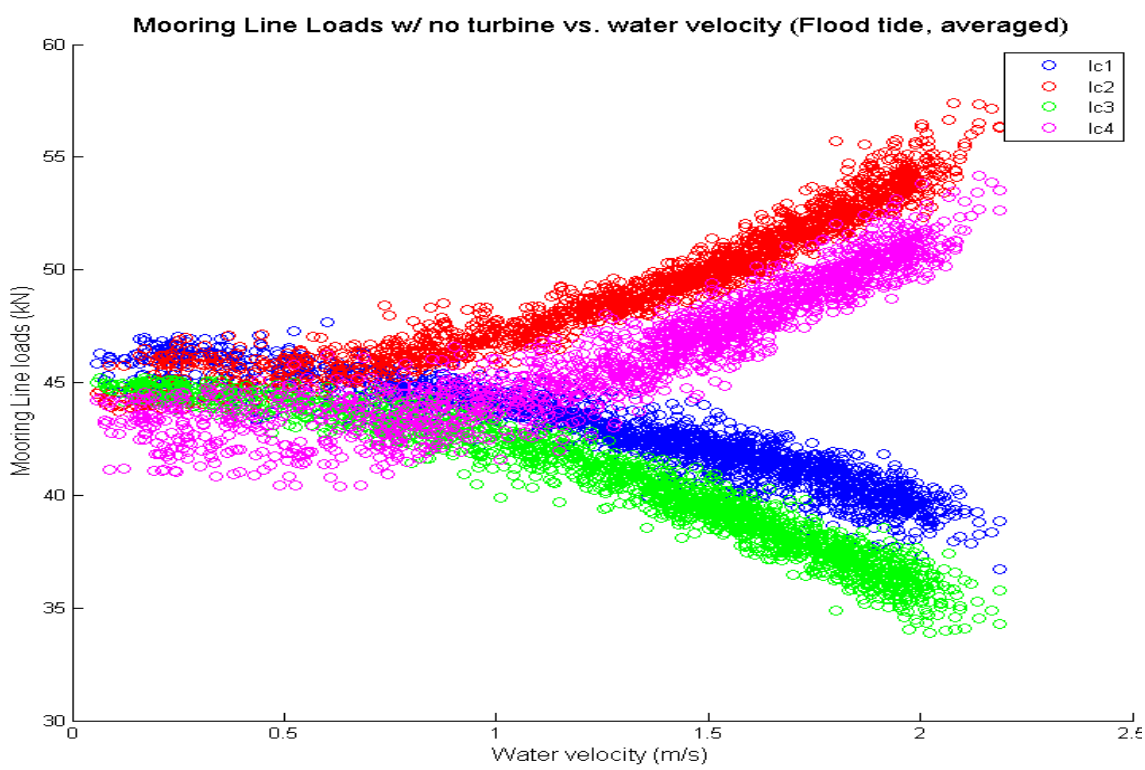

Figure 3.7.45. Averaged OCGen® mooring line loads for ebb and flood tides; Operating State 3 (turbines not present). Data averaged in 3 minute blocks.

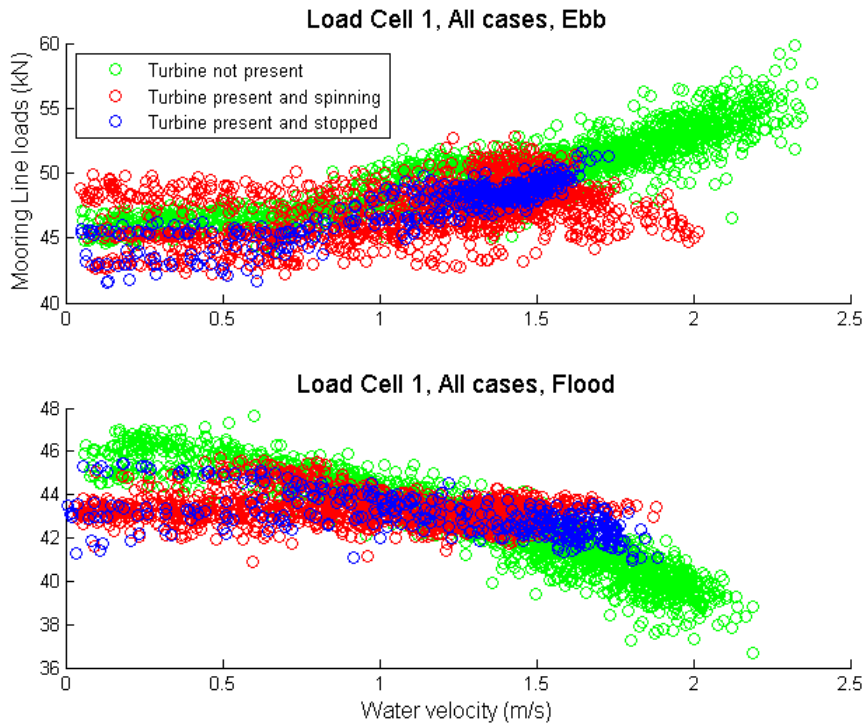

Figure 7.3.46. A comparison of loads for the three operating states for mooring line 1

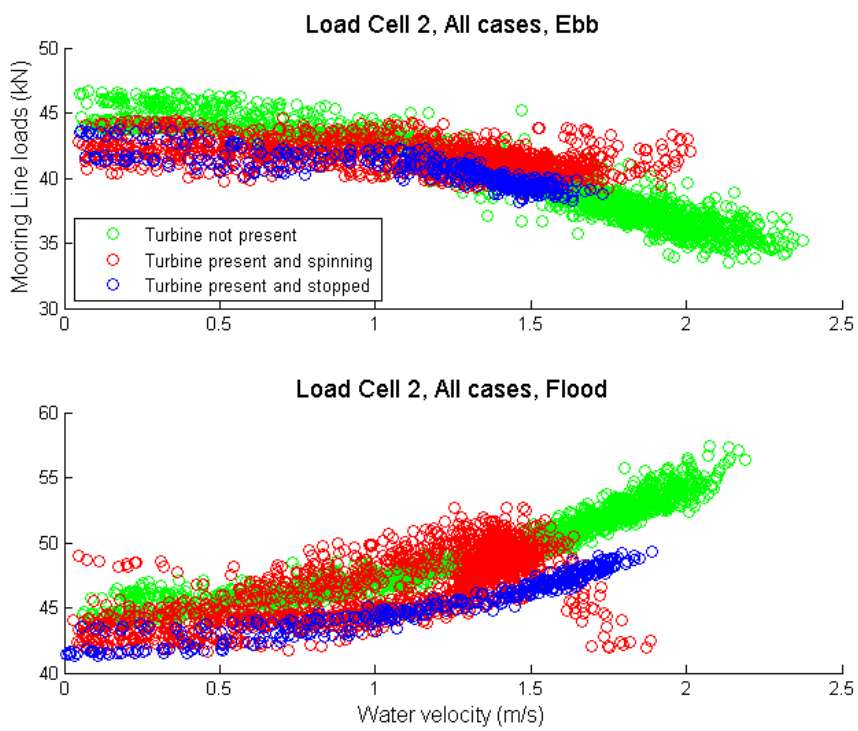

Figure 7.3.47. A comparison of loads for the three operating states for mooring line 2

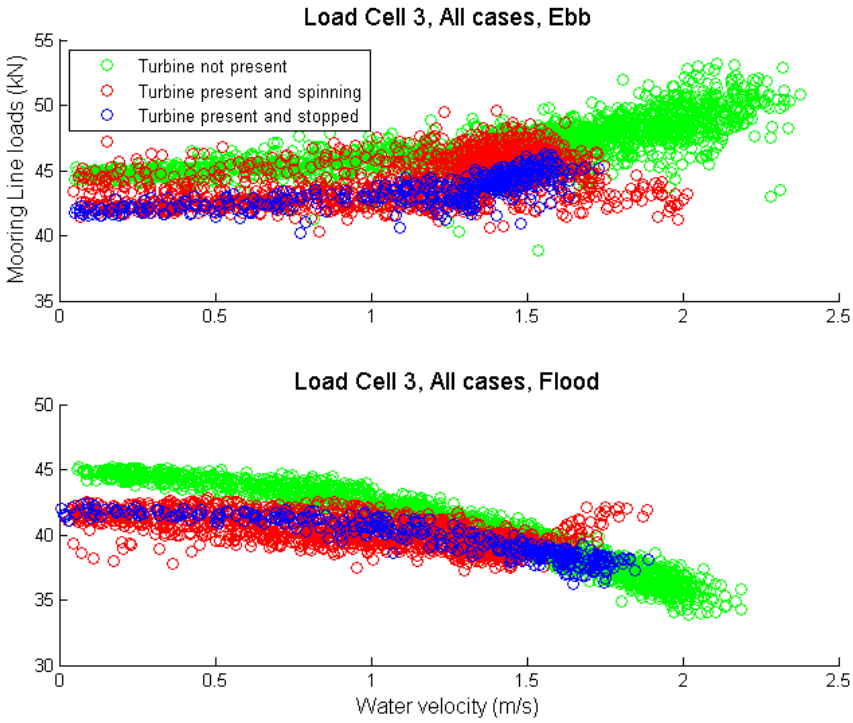

Figure 7.3.48. A comparison of loads for the three operating states for mooring line 3

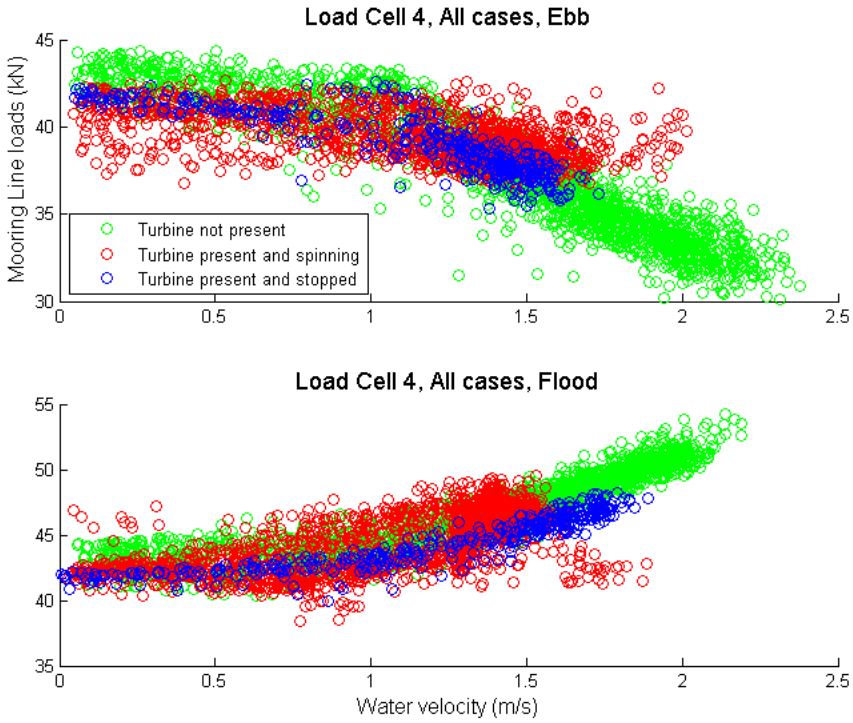

Figure 7.3.49. A comparison of loads for the three operating states for mooring line 4

Examination of the load cell data indicated the following general behaviors for the mooring system:

- Loads on the upstream lines increased with increasing water speed
- Loads on the downstream lines decreased with increasing water speed for this water speed range
- Load behavior was generally the same for all three operating states (turbine braked, turbine spinning, and no turbines)
- Comparison of loads for the mooring lines for the three different operating conditions showed that the loads for each of the operating conditions were not greatly different. This indicated that the loads from the drag of the buoyancy system may be of greater significance than the loads created by operation of the turbine. This implies that models of drag on the turbine may be overestimated.

Mooring Line Loads at slack water

The mooring line loads at slack water should remain constant for the entirety of the project, as the weight of the TGU should not change.

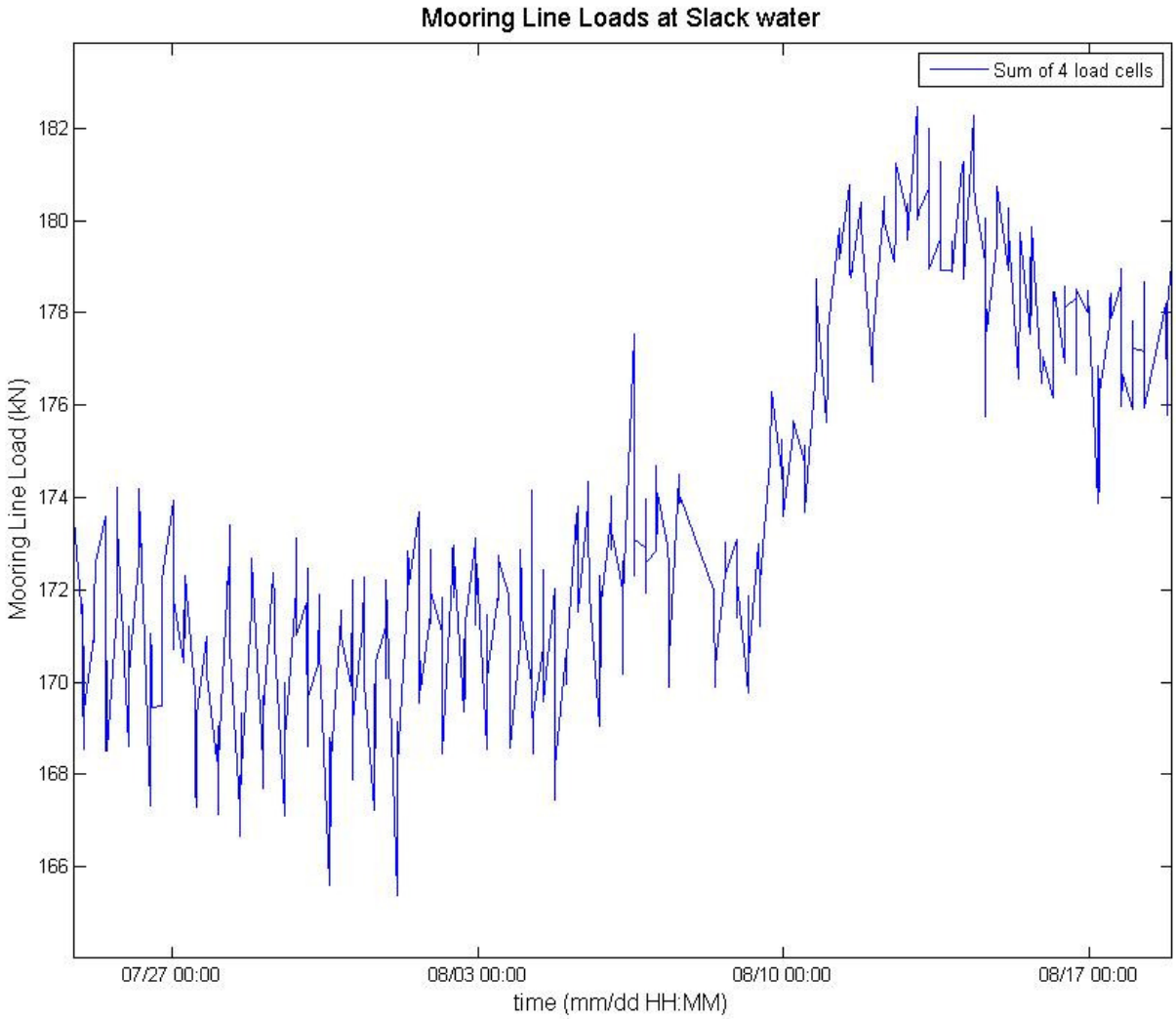

Figure 3.7.50. Sum of the four OCGen® mooring line loads at slack water, measuring the net buoyancy of the TGU.

The loads on the mooring lines show a measurable difference between low water slack and high water slack, indicating in general that mooring loads are lower for low tides. As discussed above an explanation for this behavior has not been established.

The sum of the line loads on each of the two anchors should be equal for both anchors, if the loads of the TGU were distributed equally. However the data show that the Goose Island anchor experienced approximately 3kN higher loads than the Lubec anchor at slack water. (Figure 3.7.48)

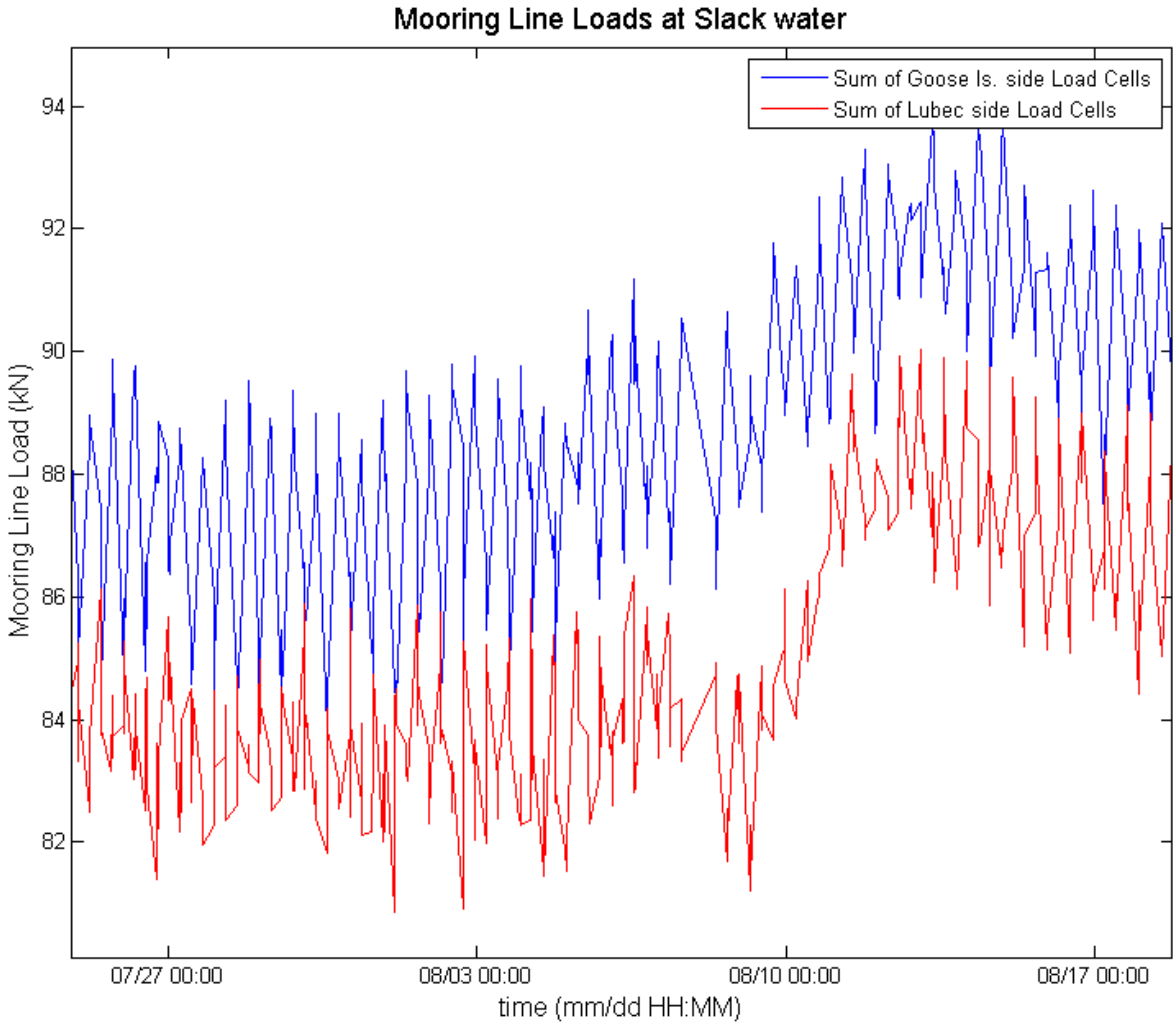

Figure 3.7.51. Sum of mooring lines for each anchor at slack water. The mooring line loads for each of the two anchors are different with more load on the Goose Island anchor.

Retrieval

Retrieval of the OCGen® system occurred on September 17, 2014. The retrieval process was uneventful. Mooring blocks lifted cleanly from the seafloor. The sequence of events for retrieval was the reverse of installation.

During OCGen® retrieval all four mooring line loads were monitored and recorded in order to determine the amount of force required to lift the anchor blocks. Of note is that mooring line loads on lines 2 and 3 were almost identical. These were located at opposite corners of the TGU. Meanwhile, mooring lines loads on 1 and 4 differ from each other and differ from lines 2 and 3. (Figure 3.7.49)

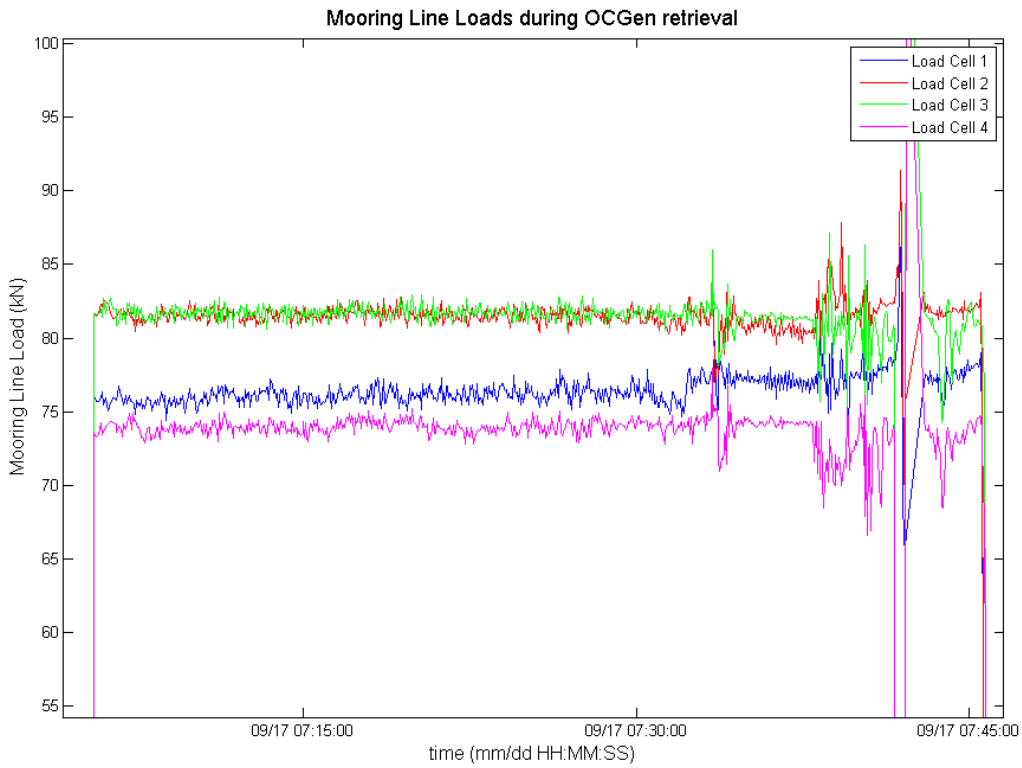

Figure 3.7.52. Mooring line loads during retrieval and transport to shore. Mooring lines 2 and 3 show equal loads. These were on opposite anchors and on opposing sides of the TGU.

Summing the loads on lines 1 and 2, and on lines 3 and 4 gave a measure of the weight of each of the two anchors. The weights of the Goose Island mooring appeared to be higher by several kilo Newtons. Figure 3.7.50.

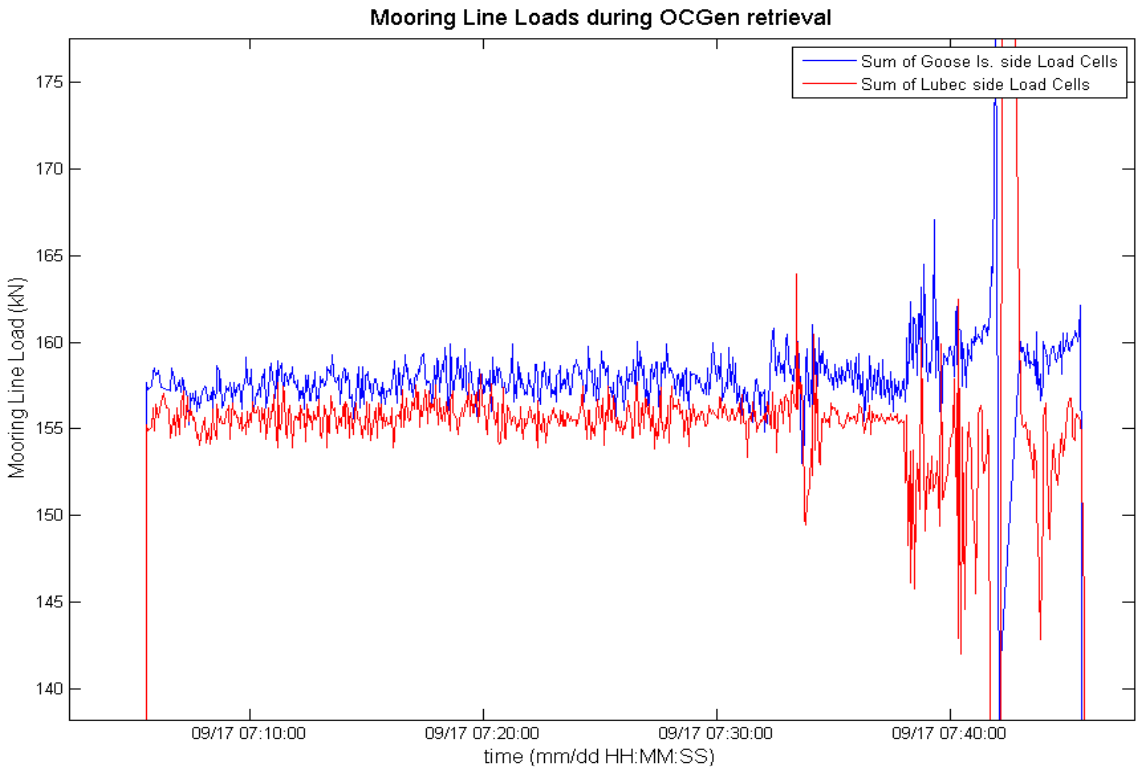

Figure 3.7.53. Sum of anchor loads during retrieval. This represents a measure of the weight of each of the two anchors, which appeared to be slightly different, with the Goose Island mooring approximately 3kN heavier.

Scour Inspection

After installation of the OCGen prototype mooring system (Task 7), video and dive inspections of the mooring system were performed both at the beginning of the installation and just prior to removal. The inspection work was recorded elsewhere.[15]

Findings of the inspection showed that while the anchors were intended to self-embed under their own weight; they did not in fact do so. The anchors remained on top of the seafloor, except for one side of one anchor. Mooring block movement over the course of the deployment was very limited, consisting of 1 to 2 in. of movement on either block.

The fact that the mooring blocks did not self-embed fully and yet that the moorings did not move significantly indicates that the design process for the mooring blocks produced conservative results in this case. The requirement for self-embedment may be relaxed in future design iterations.

[15] OCGen® Module Mooring Project Scour Report, ORCP Internal Report

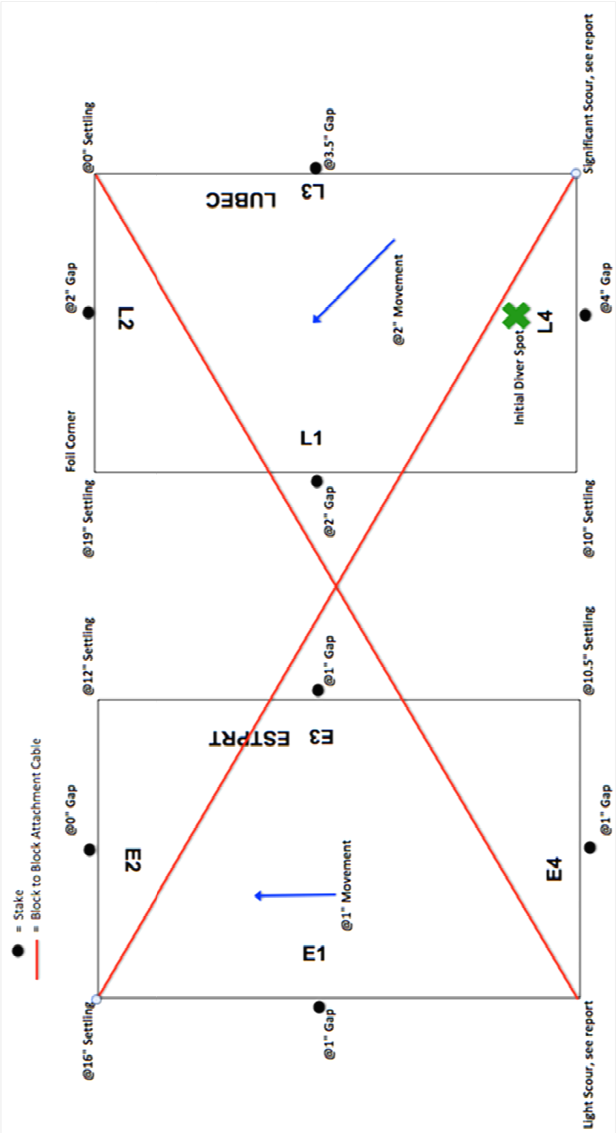

Figure 3.7.54. Results of mooring monitoring during deployment of OCGen® prototype mooring system.

Inspection

Upon retrieval the *Retriever* brought the OCGen® back to the boat ramp where the disassembly and inspection process commenced. Highlights of the inspection include:

- Mooring blocks were completely intact, with the concrete and steel in good condition. Evidence of some degree of settlement into sediment was apparent. Mooring rings were in good condition.
- Mooring line shackles showed some signs of fretting due to movement between the mooring line eye and the shackle. Otherwise they were in good condition.
- The mooring lines showed some signs of abrasion on the protective covering. They also showed some abrasion on the end loops which matched the fretting marks on the shackles.

- The buoyancy pod showed signs of significant general corrosion, but no specific corrosion at the welded joints.
- The buoyancy pod contained positive air pressure when valves were opened
- Instrumentation, wiring and conduit were intact.
- Significant flora was observed in trapped areas inside the instrumentation doghouse.
- The drivelines of the TGU were intact.
- Bearings and couplings were intact and in similar condition to the deployed state.
- Turbine end disc nuts were in an extremely corroded state, but the bolts were still intact.

Figure 3.7.55. OCGen® buoyancy pod after retrieval. Surface corrosion is general but there is no significant material removal or biofouling of structure. Pressure check of the buoyancy pod showed the pod holding pressure.

Figure 3.7.56. Anchor end of mooring line. Abrasion of mooring line covering and mating abrasion marks on shackles. This is likely due to sliding of the mooring line on the shackle during operation. This could have been avoided by the inclusion of an additional degree of freedom at this juncture.

Figure 3.7.57. Unexplained abrasion and some tearing of mooring line covering. This occurred on all four mooring lines at different locations along the length

Figure 3.7.58. End disc carbon steel bolts showing severe corrosion of nuts. Remnants are remains of carbon steel/nylon anti-vibration nuts. These bolts did not fracture or fail but may have been on the verge of failure. This corrosion is not due to electrochemical corrosion as these bolts are not in contact with other metals. Rather, this is due to general corrosion of the carbon steel bolts. No coating or cathodic protection was provided for these bolts.

Mooring Line Stiffness

Mooring lines were brought back to the suppliers and stiffness of the mooring lines was measured. All four lines showed similar stiffness and initial length, indicating the properties of the line did not change as a result of the deployment. Lines were saturated when tested.

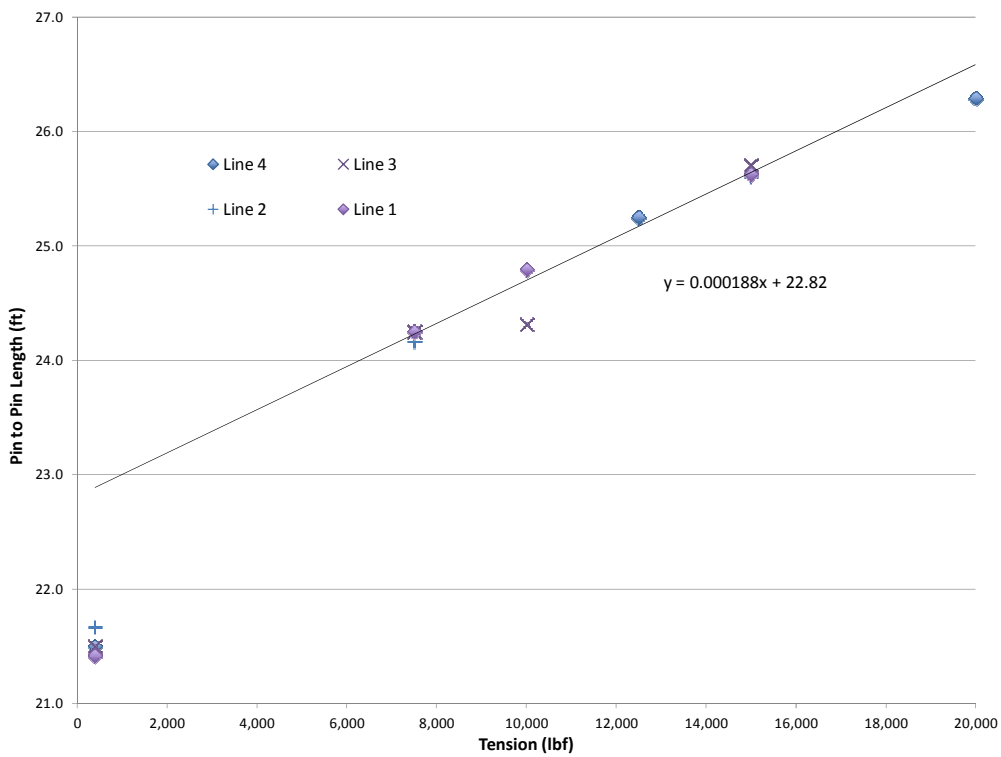

Figure 3.7.64: Lengths of mooring line as a function of applied load for all four mooring lines, as tested at the manufacturer's facility after deployment. Data for the initial load set values (< 2,000lbf) were removed for the curve fit.

From this work the compliance of the mooring lines was measured as 0.188 ft/kip with an zero load length of 22.8 ft. The stiffness of the line is the inverse of the compliance, and was equal to 77.5kN/m.

Comparison of experimental data with models

A comparison of empirical results from the deployment and analytical results predicted by design tools was made.

Some calibration of the OrcaFlex models was required in order to provide a reasonable match between the model results and the data. This calibration is primarily related to the load difference between the mooring lines at slack water. These load differences are most probably related to differences between the height of the moorings off the seafloor, and are modeled as such in OrcaFlex.

Table 3.7.15. *Offsets for OrcaFlex. Negative offsets represent a raising of the anchor point by the increment noted. A positive offset indicates a lowering of the anchor point.*

Mooring Line	No Turbine (m)	With Turbine (m)
#1	-0.305	-0.415
#2	-0.265	-0.385
#3	0.22	0.29
#4	0.28	0.31

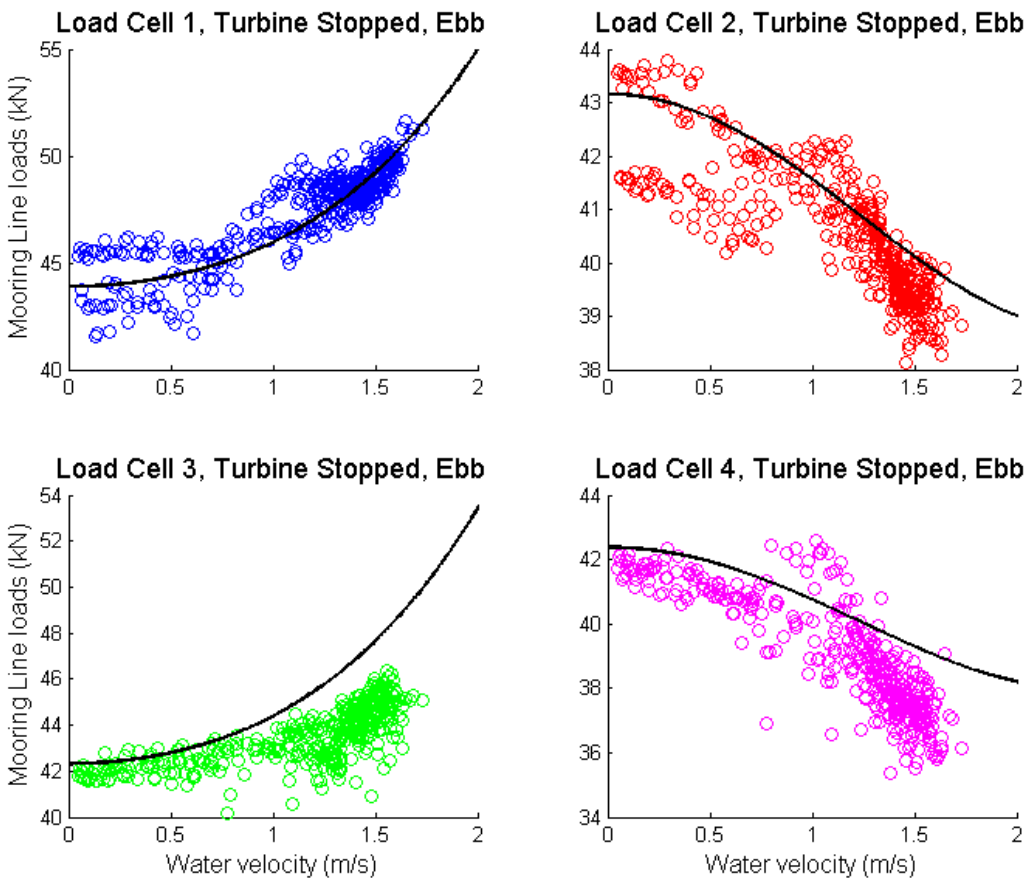

Figure 3.7.65. Operating State 1 (Turbine stopped). Mooring line loads are compared for all four mooring lines with the OrcaFlex results for the ebb tide. Data are averaged over three (3) minute time intervals. Black lines represent the OrcaFlex results.

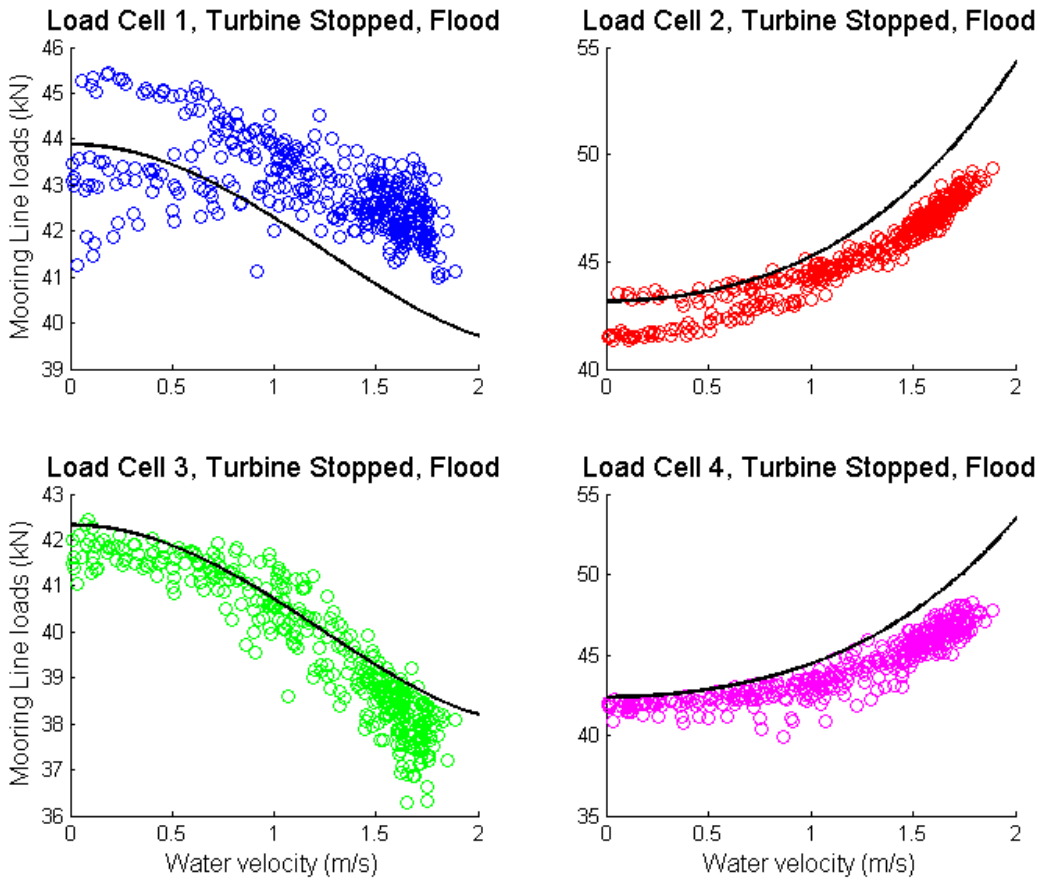

Figure 3.7.66. Operating State 1 (Turbine stopped). Mooring line loads are compared for all four mooring lines with the OrcaFlex results for the flood tide. Data are averaged over three (3) minute time intervals. Black lines represent the OrcaFlex results.

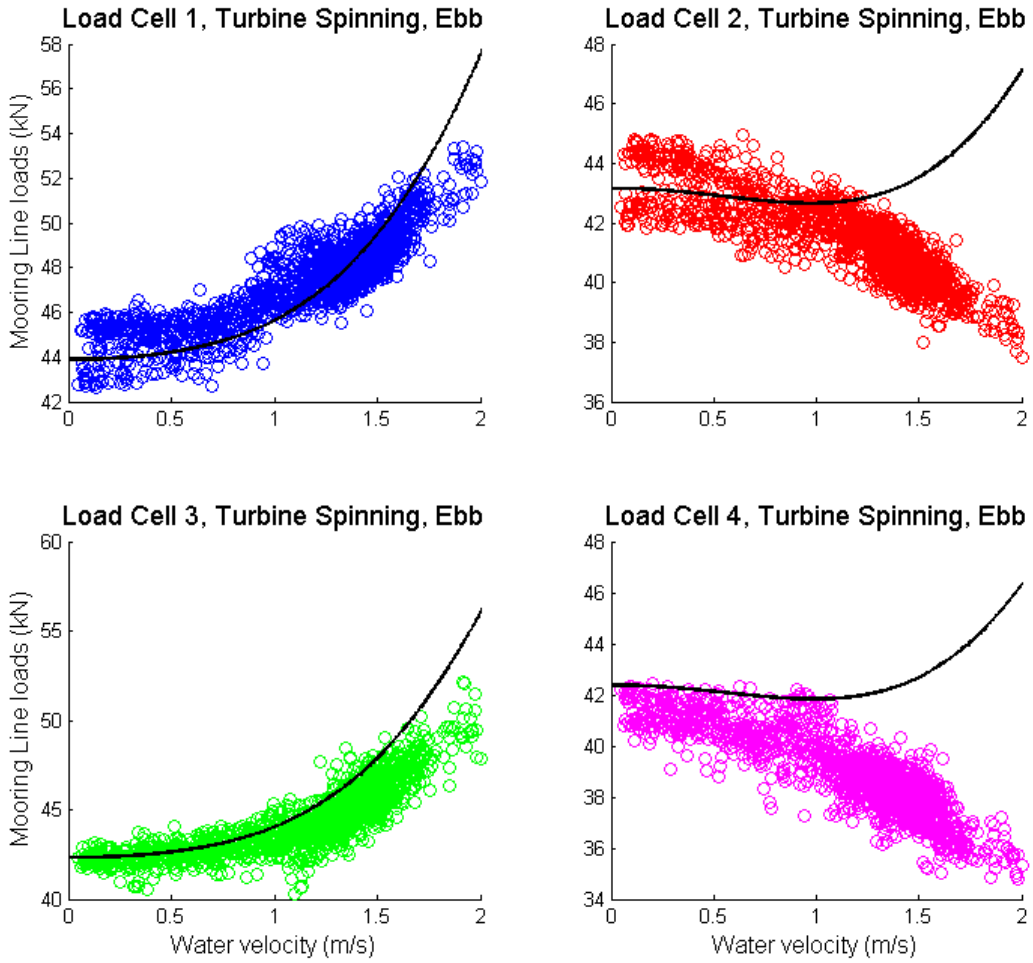

Figure 3.7.67. Operating State 2 (Turbine spinning). Mooring line loads are compared for all four mooring lines with the OrcaFlex results for the ebb tide. Data are averaged over three (3) minute time intervals. Black lines represent the OrcaFlex results.

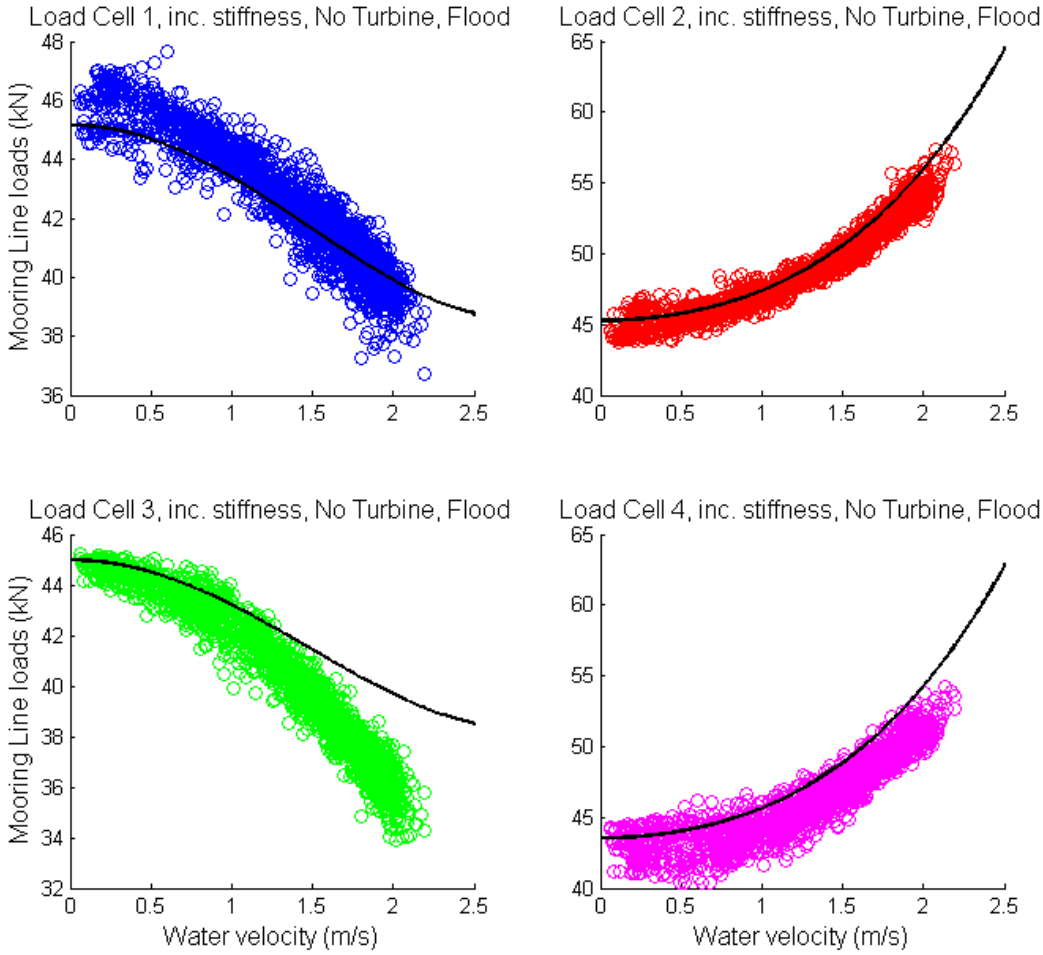

Figure 3.7.68. Operating State 2 (Turbine spinning). Mooring line loads are compared for all four mooring lines with the OrcaFlex results for the flood tide. Data are averaged over three (3) minute time intervals. Black lines represent the OrcaFlex results.

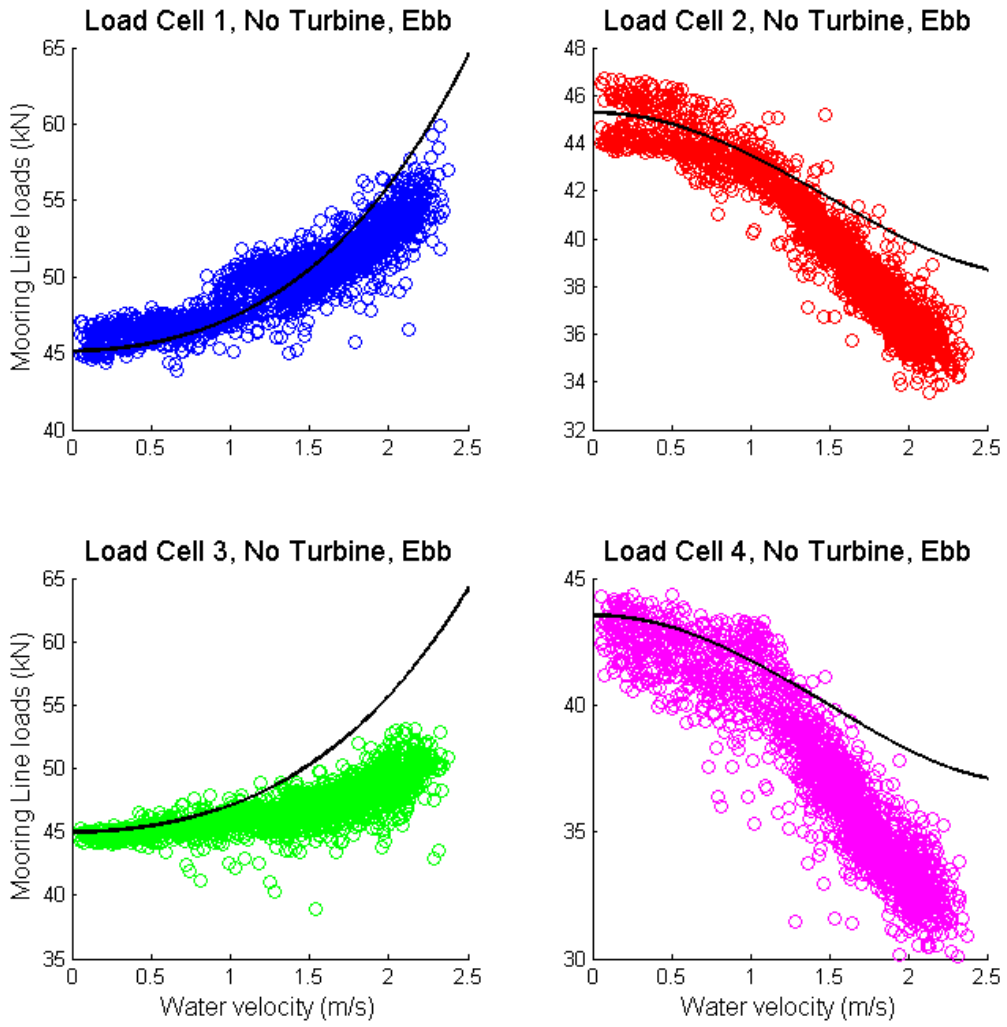

Figure 3.7.69. Operating State 3 (Turbines not present). Mooring line loads are compared for all four mooring lines with the OrcaFlex results for the ebb tide. Data are averaged over three (3) minute time intervals. Black lines represent the OrcaFlex results.

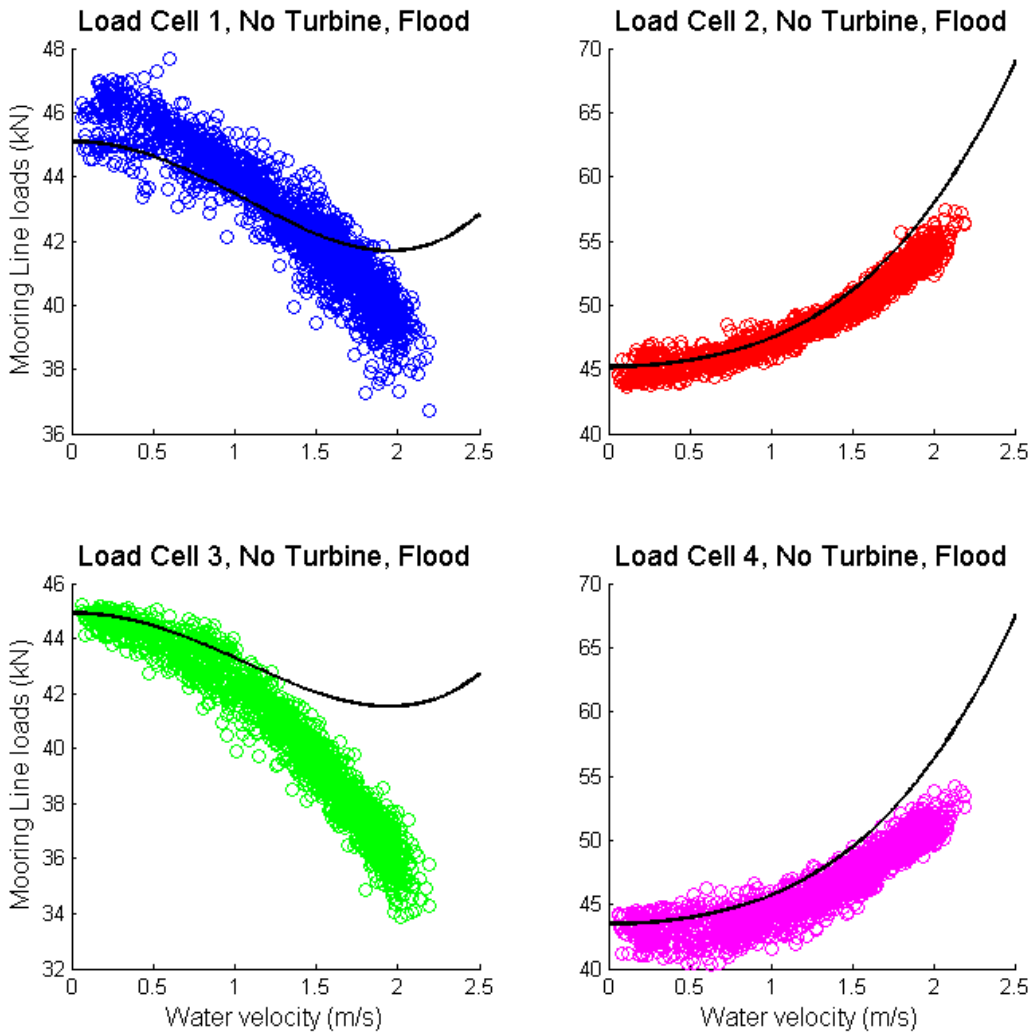

Figure 3.7.70. Operating State 3 (Turbines not present). Mooring line loads are compared for all four mooring lines with the OrcaFlex results for the ebb tide. Data are averaged over three (3) minute time intervals. Black lines represent the OrcaFlex results.

In general the correlation between measured load and predicted load for the upstream, mooring legs was good. Correlation between the OrcaFlex results and the measured downstream legs was weaker. The OrcaFlex models predicted an increase in mooring line loads with increasing water speed, and this increase is not seen in the data. The increase in loads, as predicted by OrcaFlex, is due to the increase in line extension required on the aft line as the TGU translates further with increased flow speed. This deviation seems to indicate that the OrcaFlex model for the mooring line is more compliant than was actually the case during deployment.

Frequency Response of System

An attempt to discern a frequency response from the various data signals was made. Fast Fourier Transforms were performed on the data for the period of September 8 through September 10, when data rate was highest at 1Hz.

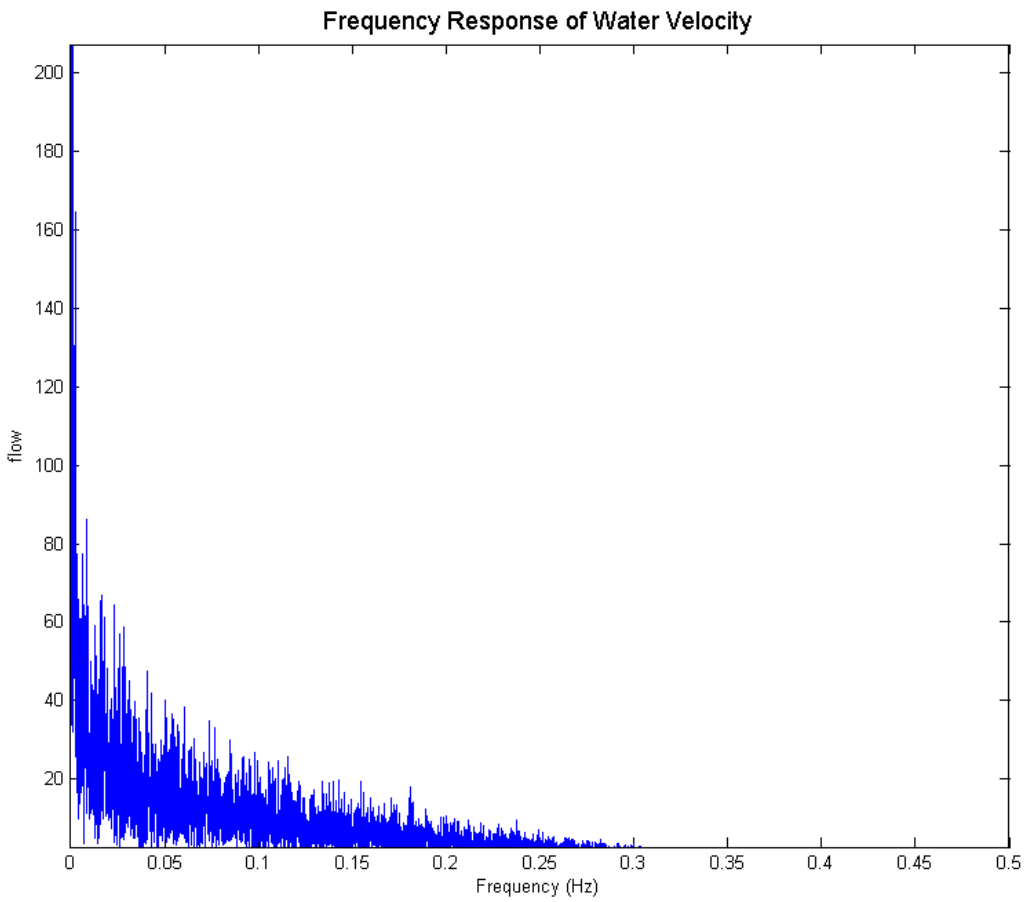

Figure 3.7.71. FFT of the water speed data from the Valeport for the period of September 8 through September 10, 2014. No significant frequency response is noted.

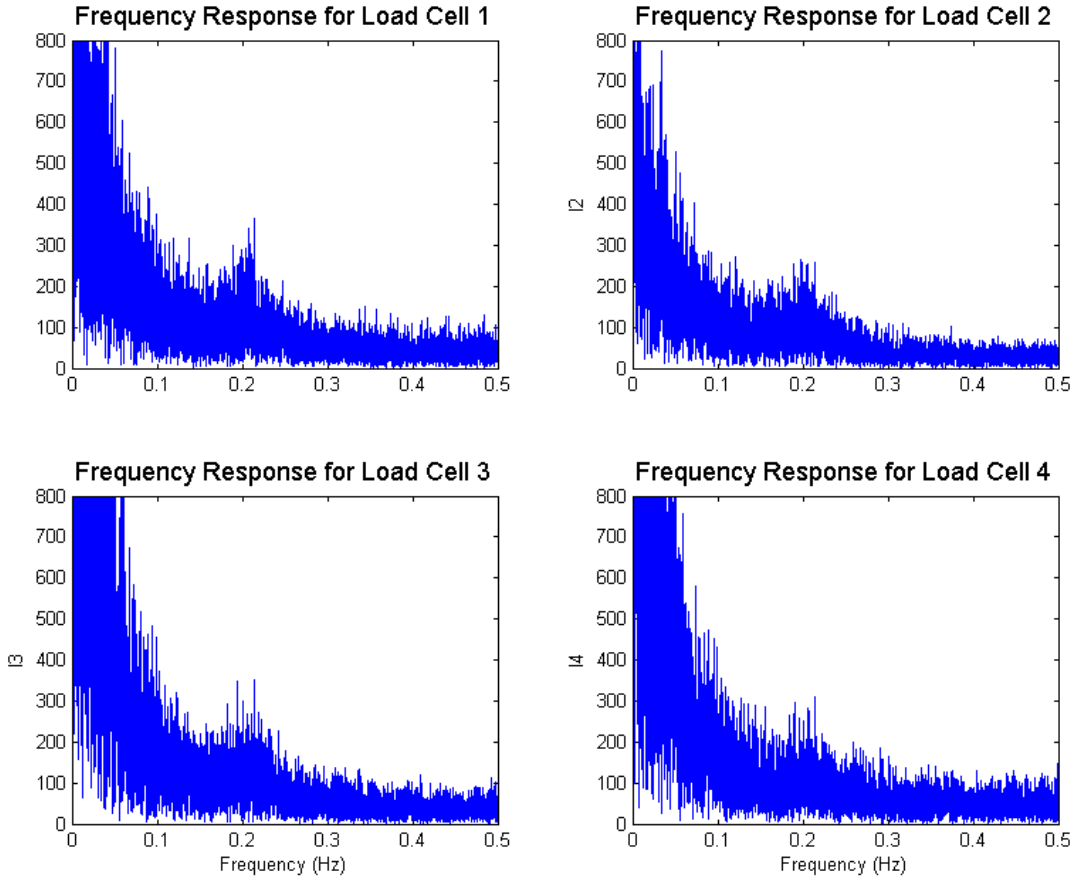

Figure 3.7.72. FFT of the loads for each mooring line for the period of September 8 through September 10, 2014. A frequency response is noted in the vicinity of 0.2Hz. The response at 0.8Hz is the mirror image response inherent in the FFT technique.

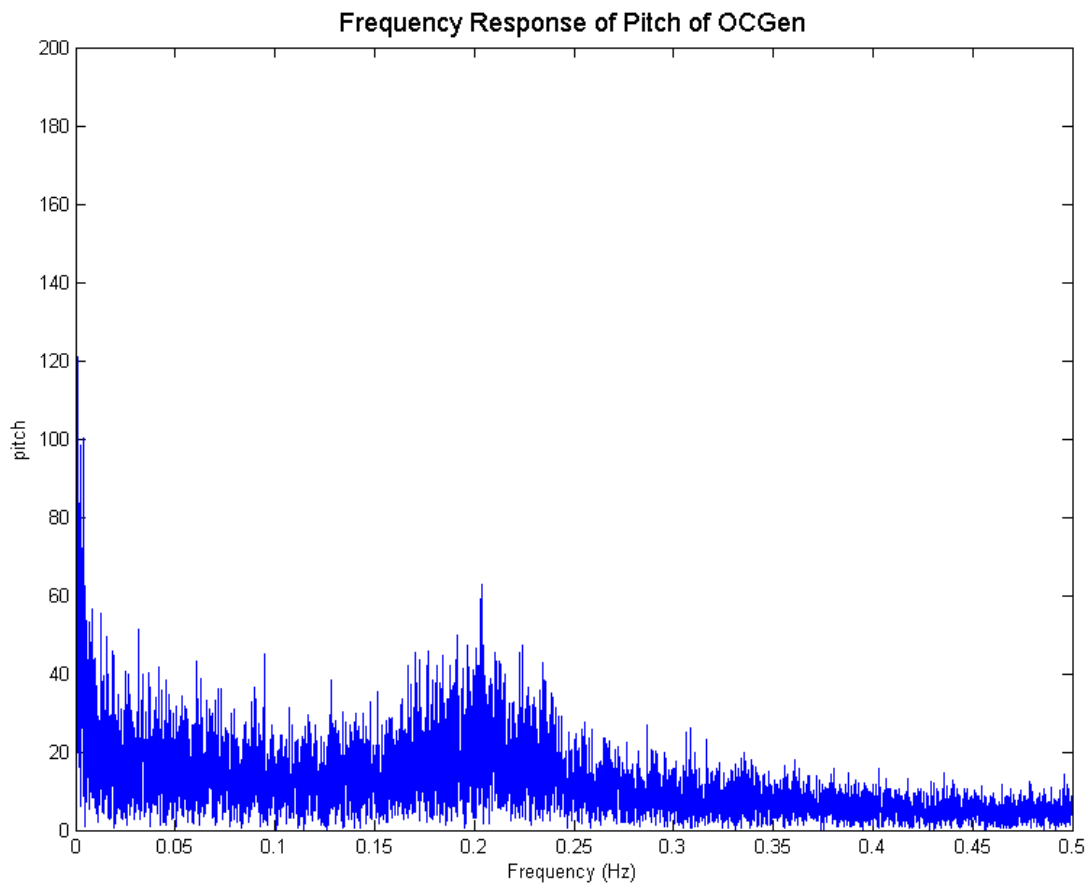

Figure 3.7.73. FFT of the TGU pitch during the period of September 8 through September 10, 2014. A frequency response is noted in the vicinity of 0.2Hz. The response at 0.8Hz is the mirror image response inherent in the FFT technique.

A significant frequency response at 0.2Hz is noted in the mooring lines and in the pitch of the TGU. No other data streams produced a notable frequency signal using this technique. The modal analysis for the system presented earlier shows a Mode 3 response at 0.2Hz. The modal shape for this resonance is for the TGU to sway side to side, and would be excited by off-axis flows.

Problems Encountered

- Instrumentation
  - The loss of communication with the Aquadopp instrument and the consequent loss of depth, water speed, and heading data was problematic.

- Data rates were low
  - Data rates were limited to a maximum of 1Hz due to limitations associated with the data acquisition system. Faster data rates would have been desirable for this deployment.

- Data Connectors
  - The subsea data connector was damaged and mated incorrectly by the diver, impeding communications with the deployed TGU. This was fixed, but the female data connector was compromised.

- Corrosion
  - Generalized corrosion was severe.
  - Local corrosion was severe.

- Mooring Line Abrasion
  - The inclusion of an additional degree of freedom at the connection of the mooring line to the shackles would have relieved the need for the mooring line to slide on the shackle and so reduced the abrasion at this connection
  - The use of alternative sheaths for the mooring line would have improved abrasion resistance for the lines

Departure from Planned Methodology

Loss of data from Aquadopp led to reliance on the Hobo water level sensor for information with which to calculate OCGen® TGU position in the water column.

Assessment of Impact on the Project Results

- No impact

3.8 Task 8: Design of OCGen® Module Mooring System

Original Hypotheses

Upon evaluation of the results from the tow tank tests and experimental mooring test, ORPC completed the designs of a full-scale OCGen® system. Procurement, installation and operation of the full-scale OCGen® Power System, however, was not within this Project Scope and was not funded under this DOE Project. The results and lessons learned from this Project will, however, be incorporated into the OCGen® design before a full scale OCGen® system is ultimately build, installed and tested.

Approaches Used

After a thorough review of applicable codes and standards, ORPC commenced the design of a four turbine, full-scale OCGen® module, to be deployed in Western Passage, an inlet in the Bay of Fundy located between Eastport, Maine, USA and Deer Island, New Brunswick, Canada. Western Passage is characterized by tidal flows of 3.0 m/s and water depth of 100 m, and will serve as a good test site for eventual OCGen® deployments in the ocean currents of the US Gulf Stream, Cook Inlet, Alaska, and other deployment sites under development or consideration by ORPC.

The full-scale OCGen® module is a four-turbine, horizontal axis device designed to extract energy from tidal currents in both ebb and flood cycles, or in the case of deep water ocean currents, from unidirectional ocean currents. The OCGen® device consists of an elliptical buoyancy pod mounted above a TGU containing four horizontal axis turbines connected by a single driveline to an underwater generator in the center of the TGU. The OCGen® device is attached to four tensioned mooring lines that position the device at a predetermined distance above, and secure it to, the seabed. The mooring lines are attached to clump weight anchors that rest on the seabed.

Design alternatives to the baseline OCGen® TGU were considered in order to improve performance and reduce loads with the goal of reducing overall costs and increasing return on investment. A costing model was created to assess the baseline and alternative concepts. These alternatives included the "FatHub" (Figure 3.8.1) to decrease drag loads at the expense of decreased performance, and the "Diverter" (Figure 3.8.2) to increase performance at the expense of increased drag loads by use of upper and lower fairings. These alternatives are discussed at length in another report.[16] These design studies concluded that the “FatHub” concept was unlikely to be beneficial, and that the “Diverter” concept showed no significant benefits over the baseline design presented here.

[16] ORPC OCGen® 4T and 2T, Design Summary, January 4, 2014, RM Beaumont Corp.

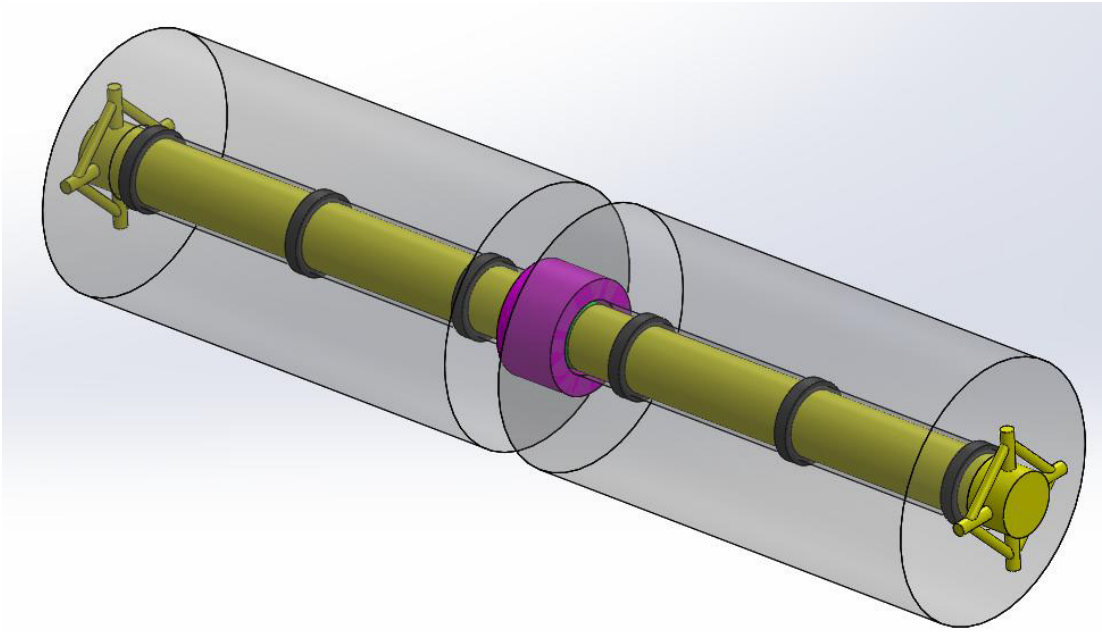

Figure 3.8.1. "FatHub" concept drawing. The central shaft was used to provide buoyancy for the system. Turbines are represented as cylinders in this sketch.

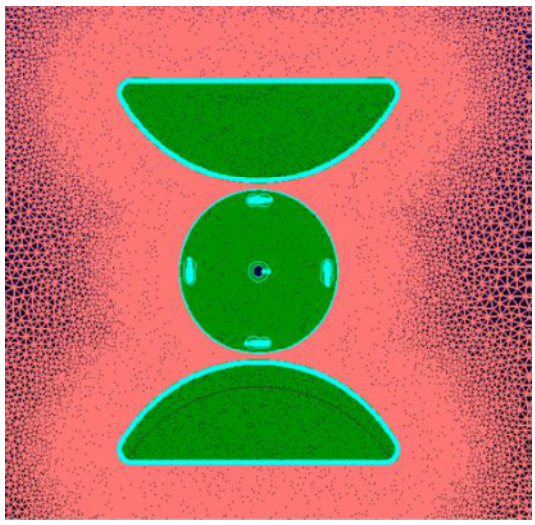

Figure 3.8.2. Cross-sectional sketch for "Diverter" concept, which consisted of upper and lower fairings close to the turbines. This was similar to original OCGen® concepts, but suffers from low initial stability making handling at sea difficult.

ORPC also explored concepts that included a lifting body instead of a buoyancy pod and a single point mooring with a swivel attachment. Based on initial conversations with the mooring design firm, PCCI Inc., it was decided that a single point mooring would present undue challenges in this application. There also existed no effective passive lifting body shape, other than an elliptical profile, for a bi-directional (tidal) flow. For these reasons, an elliptical-shaped buoyancy pod was chosen as the best path forward.

From the previous work performed, it was determined that the full-scale OCGen® device should comprise the following basic elements:

- A TGU consisting of a set of cross-flow turbines connected by a single driveline to an underwater generated located at the center of the turbines, all mounted within a TGU chassis.
- A buoyancy pod or chamber arranged above and connected to the TGU chassis in which the cross-flow turbines are mounted, so that the center of buoyancy of the combined system was above the center of mass of the combined system. This was required for the system to achieve basic stability, i.e., remain upright.
- Elliptical faring covering the cylindrical buoyancy pod
- Mooring line attachments to be placed on the buoyancy structure at a vertical location above and between the center of drag of the turbines and the center of drag of the buoyancy pod
- Set of synthetic mooring lines utilized as tension leg moorings attached from the buoyancy structure to the moorings
- Set of mooring blocks on the seafloor which obtain their holding power primarily by weight alone.

The baseline OCGen® design concept (Figure 3.8.3) consisted of a cylindrical buoyancy pod serving as the pressure hull and an elliptical fairing serving as the hydrodynamic hull. Material selection for the cylindrical buoyancy pod will most likely be limited to carbon steels. Coatings for the carbon steel will most probably be epoxy based marine paints, combined with cathodic protection. Biofouling paints may be required to limit the accumulation of marine growth. Epoxy resin composite materials will mostly likely be utilized for the fairing. As the fairing is exposed to moving water, it is less likely that antifouling paints will be required.

The device will be secured to the seafloor with four tension legs. The driveline consists of four cross-flow turbines of patented ORPC design and a permanent magnet generator at the center, all rotating together in the same direction on a common driveshaft. The primary loads on the mooring system are the drag, lift, and torque loads from the driveline components, the structural drag of the pod, and the static buoyancy load.

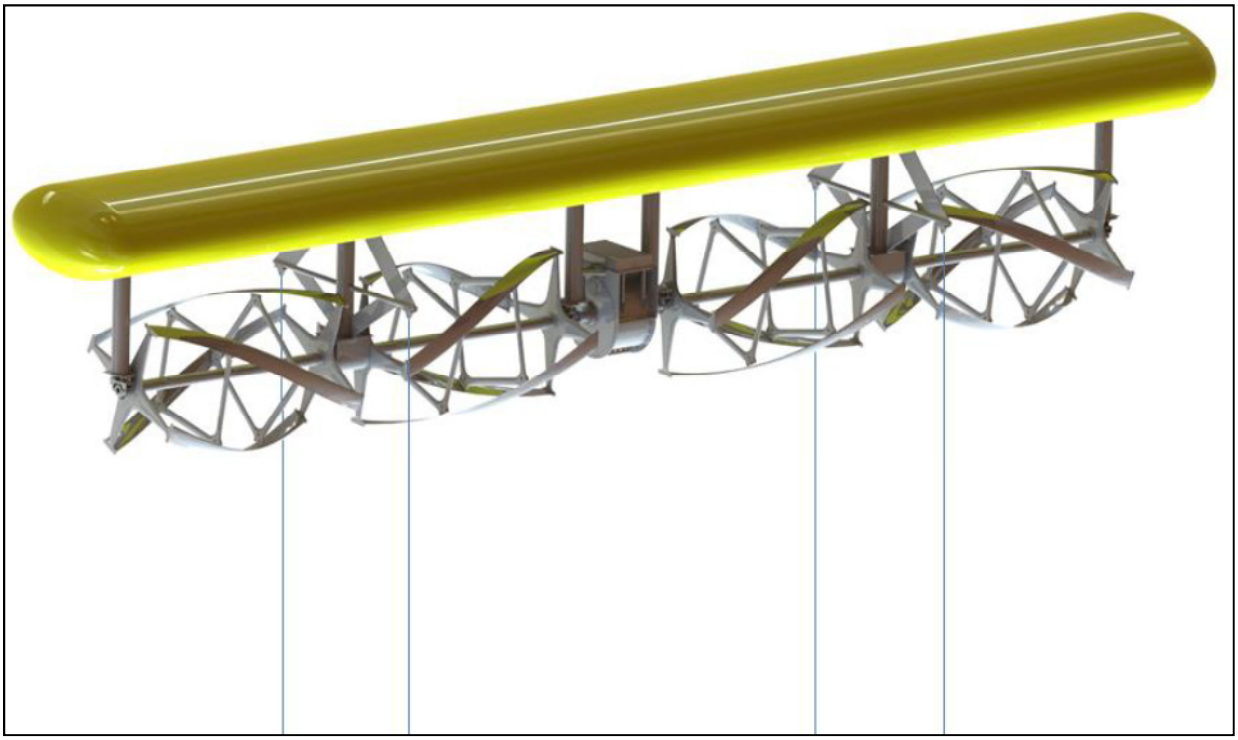

Figure 3.8.3. Baseline OCGen® design concept

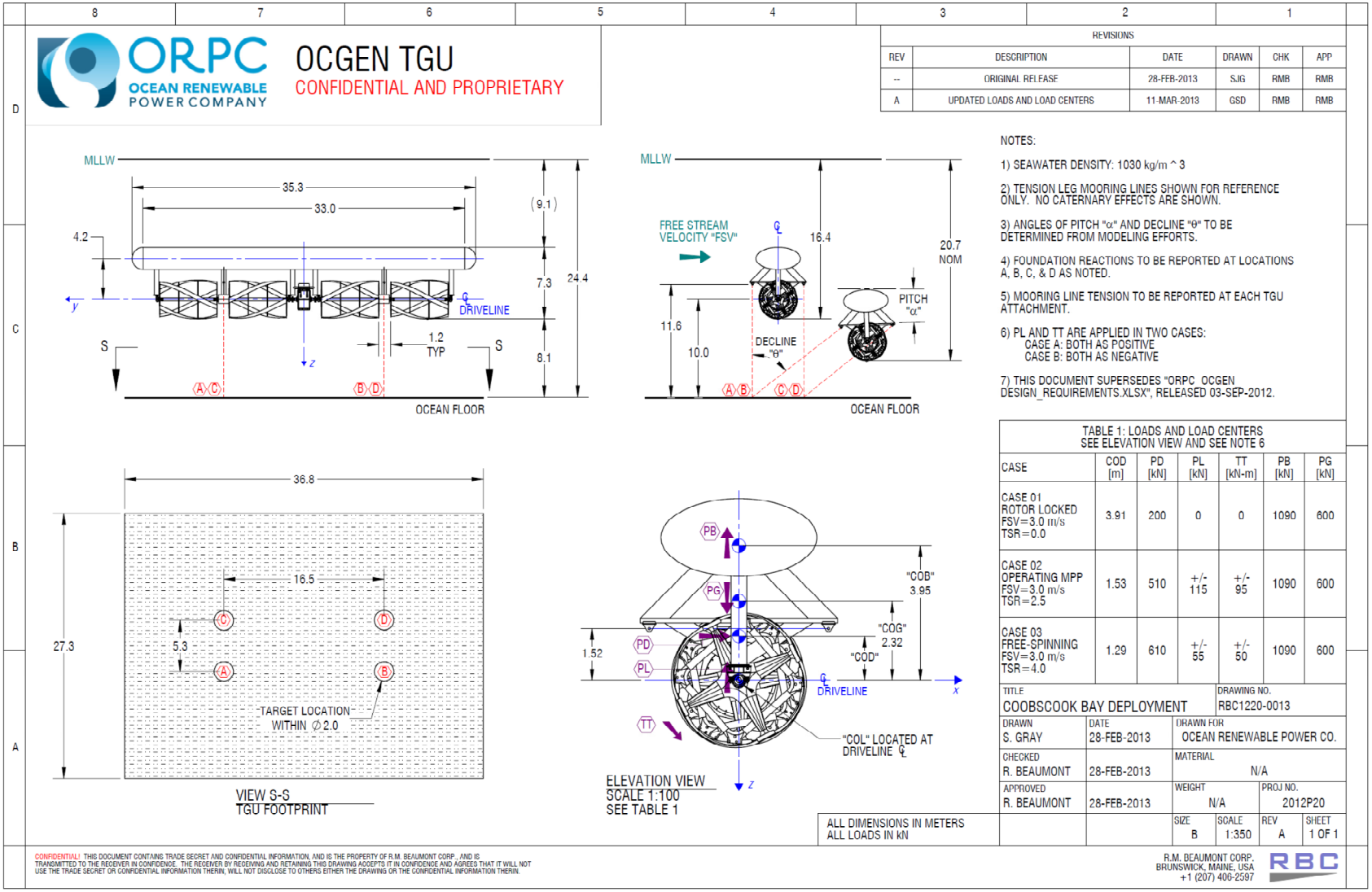

Figure 3.8.4. OCGen® layout

Design Conditions and Turbine Loads

At the Western Passage site, the following bullets summarize the key design conditions. The design depth at slack tide was the depth measured from the mean higher high water (MHHW) mark to the bottom of the buoyancy pod. The design flow speed was chosen by ORPC based on data from ADCP deployments. The maximum mooring decline angle was chosen as 45° to limit the declination depth during operation.

- Design Depth at Slack Tide MHHW: 50 m
- Design Flow Speed, FSV: 3.0 m/s
- Maximum Mooring Decline Angle: 45°
- Power Rating: 150 kW

During operation, the OCGen® device moves along an arc-path defined by the tension leg geometry (Figure 3.8.4). Tension was maintained on all four legs during all operational conditions. As the tension in the fore and aft legs changed, the device took on a pitch angle, which changed the lift and drag characteristics of the elliptical fairing, as shown in Table 3.8.1.

Table 3.8.1. *Lift and drag coefficients and forces as a function of pitch angle for the baseline OCGen® 4t elliptical fairing*[17]

Drag and Lift Loads on Elliptical Fairing				
h	[m]	1.93		
c	[m]	3.86		
b	[m]	34.15		
Ap	[m^2]	131.85		
Af	[m^2]	65.92		
AR Ellipse	[unitless]	2.00		
AR Planform	[unitless]	8.85		
FSV	[m/s]	3.00		
ALPHA [deg]	**CL**	**CD**	**LIFT [N]**	**DRAG [N]**
-10	-1.091	0.713	-666757	217934
-9	-0.983	0.705	-600662	215444
-8	-0.874	0.698	-534383	213208
-7	-0.766	0.691	-467942	211229
-6	-0.657	0.686	-401358	209509
-5	-0.548	0.681	-334652	208050
-4	-0.438	0.677	-267844	206853
-3	-0.329	0.674	-200955	205921
-2	-0.219	0.672	-134004	205255
-1	-0.110	0.670	-67012	204855
0	0	0.670	0	204721
1	0.110	0.670	67012	204855
2	0.219	0.672	134004	205255
3	0.329	0.674	200955	205921
4	0.438	0.677	267844	206853
5	0.548	0.681	334652	208050
6	0.657	0.686	401358	209509
7	0.766	0.691	467942	211229
8	0.874	0.698	534383	213208
9	0.983	0.705	600662	215444
10	1.091	0.713	666757	217934

Bulkheads were incorporated into the buoyancy pod. The bulkheads allowed for survival of the device in a damaged state arising from shell puncture, leak due to corrosion, or a leak due to an improperly sealed or gasketed penetration. Also, the bulkheads could be used to create fully flooded compartments, which may be used to offset buoyancy during deployment. Fully flooding avoids the risk of sloshing when partially filled.

[17] Hoerner, S. F. (1975). *Fluid Dynamic Lift.* Bricktown, NJ: Hoerner Fluid Dynamics.

A positive internal pressure (PIP) design was also considered. The pressure difference across the shell would be zero when in operation at depth. In concept, the goal of the PIP would be to eliminate the buckling criterion from the design and sizing of the structure. The shell would be designed for a PIP equal to the maximum hydrostatic pressure experienced during operation, or for a smaller pressure with the difference supplied by pressurized make-up air or nitrogen gas during deployment. At a minimum, a system would be required consisting of a source of pressurized gas and a sensor network for monitoring and control of the PIP. The cost savings with this approach would only be realized by accepting a higher level of risk, as the PIP system adds an additional single point of failure. The baseline design of the buoyancy pod did not include the PIP system.

The use of various types of foam was investigated as a means of passive buoyancy. Structural considerations led to a focus on synthetic foams. However, the required structural properties to fully resist buoyancy necessitated the use of high density syntactic foams which while buoyant underwater are quite heavy in air. The use of such foams added significant mass to the system and was rejected based on consideration of onshore lift capabilities and logistics.

The baseline design evolved to include a composite fairing to reduce the drag coefficient of the buoyancy pod. The final fairing was elliptical in shape and mounted to the external stiffeners. In intermediate design iteration, an elliptical buoyancy pod was considered, though quickly rejected as a viable option due to diminishing returns with required shell thickness. The laminate thickness and material for the fairing was finalized to determine weight and cost, though the detail design of the connection to the sub-structure has not been finalized. Expertise with the engineering and fabrication of composite-to-steel connections is required to complete the detail design of the fairing.

The major components of the TGU are itemized below in Table 3.8.2. The net weight and buoyancy for all components, along with load centers for these loads are shown.

Table 3.8.2. *Buoyancy, weight, and load centers for OCGen® Power System*

ORPC OCGen™ TGU Components				
COMPONENT	**WEIGHT [kN]**	**BUOYANCY [kN]**	**COG[1] [m]**	**COB[1] [m]**
Fairing & Stantions	85	43	4.19	4.19
TGU Structure	281	993	3.65	4.14
Generator	120	8	0.00	0.00
Turbines	72	37	0.00	0.00
Driveline Components	42	5	0.25	0.25
Net	600	1086	2.32	3.95
[1] All distances measured vertically upward (-z) from the driveline CL				

The turbine operating loads included turbine drag, lift, and torque. The value of these loads was determined by the non-dimensional coefficients of drag (CD), lift (CL), and power (CP), given a value for FSV and tip speed ratio (TSR) (Table 3.8.3 and Table 3.8.4).

Table 3.8.3. *ORPC Baseline OCGen® 4T Coefficients of Power (CP), Drag (CD), and Lift (CL)*

ORPC OCGen™ TGU Coefficients			
R	[m]	2.0	
ATOT	[m^2]	96	
RHO	[kg/m^3]	1030	
TSR	**CP**	**CL**	**CD**
0.00	0.000	0.000	0.152
0.25	0.002	0.039	0.157
0.50	0.005	0.067	0.169
0.75	0.010	0.093	0.197
1.00	0.016	0.121	0.225
1.25	0.034	0.149	0.266
1.50	0.050	0.180	0.315
1.75	0.090	0.215	0.379
2.00	0.177	0.240	0.472
2.25	0.258	0.256	0.573
2.50	0.400	0.262	0.697
2.75	0.395	0.220	0.764
3.00	0.388	0.193	0.809
3.25	0.368	0.173	0.843
3.50	0.354	0.152	0.871
3.75	0.334	0.135	0.899
4.00	0.318	0.119	0.921

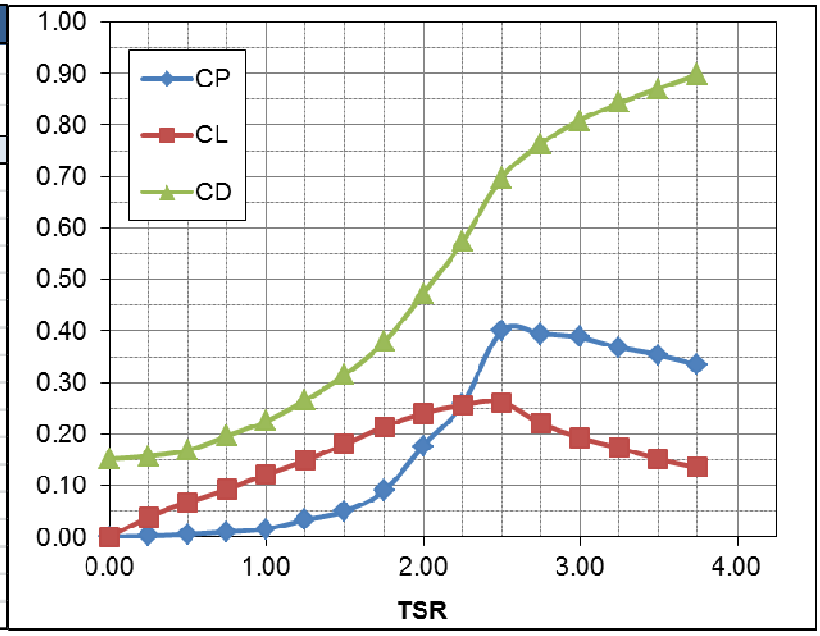

Table 3.8.4. *ORPC baseline OCGen® turbine drag, lift and torque for various flow speeds and operating conditions*

Current Velocity (m/s)	TSR 0 Drag (kN)	TSR 0 Lift (kN)	TSR 0 Torque (kN-m)	TSR 2.5 Drag (kN)	TSR 2.5 Lift (kN)	TSR 2.5 Torque (kN-m)	TSR 4.0 Drag (kN)	TSR 4.0 Lift (kN)	TSR 4.0 Torque (kN-m)
0	0	0	0	0	0	0.0	0	0	0.0
0.25	0	0	0	2	1	1.0	3	0	0.5
0.5	2	0	0	9	3	4.0	11	1	2.0
0.75	4	0	0	19	7	8.9	26	3	4.4
1	8	0	0	34	13	15.8	46	6	7.9
1.25	12	0	0	54	20	24.7	71	9	12.3
1.5	17	0	0	78	29	35.6	102	13	17.7
1.75	23	0	0	106	40	48.4	139	18	24.1
2	30	0	0	138	52	63.3	182	24	31.4
2.25	38	0	0	174	66	80.1	231	30	39.8
2.5	47	0	0	215	81	98.9	285	37	49.1
2.75	57	0	0	261	98	119.6	344	44	59.4
3	68	0	0	310	117	142.4	410	53	70.7
3.25	79	0	0	364	137	167.1	481	62	83.0
3.5	92	0	0	422	159	193.8	558	72	96.3
3.75	106	0	0	485	182	222.5	640	83	110.5
4	120	0	0	551	207	253.1	729	94	125.8

Structural Design

For structural design and engineering of the MHK structures, ORPC conducted a comprehensive review of relevant codes and standards review for structural steel construction, rigging, welding, cathodic protection, and offshore oil and gas (Table 3.8.5) and identified failure criteria (Table 3.8.6).

Table 3.8.5. *Codes and standards applicable to OCGen® device*

Applicable Codes and Standards	
ABS B&US Guide	Buckling of offshore structures
API RP-2A-WSD	Materials, joint design, welding methods, corrosion & CP
AISC 14th Edition	Steel design, bolts, slip-critical connections
ASME BPVC Section VIII	Pressure vessel design, materials, welding inspection
ASME BPVC Section XI	Pre-qualified welding procedures
ASME B30	Rigging fixtures, hardware, slings, chain
AWS D1.1	Pre-qualified welding procedures
NACE SP-0176	Coatings and design of passive cathodic protection
DNV RP-C202	Buckling of cylindrical shells
DNV RP-C205	Structural drag, vortex induced vibrations (VIV)

Table 3.8.6. *Failure criteria for the OCGen®*

Failure Criteria (Steel)	
Shell Buckling Factor	4.0
Member Axial Buckling	API RP-2A-WSD
Allowable von-Mises Stress	0.60 x Fy
Rigging & Lifting Lugs	ASME B30
Fatigue at TYK joints	API RP-2A-WSD
Cross Flow VIV	$3 < V_R < 16$

Vortex-induced vibration (VIV) in a structure was considered as failure due to accelerated fatigue, noise and vibration; additional dynamic forces were not considered in the static analysis. VIV due to cross flow is assessed according to practices set forth in DNV-RP-C205. The reduced velocity, V_R, was calculated and compared to the failure range. When assessing V_R, consideration was also given to the Reynolds Number and the presence of flow spoilers such as strakes or other members in close proximity. Cross-flow VIV on tubular structural members has been ruled out, with $V_R < 1.0$ due to the short length, small diameter, and characteristic FSV at the site. However, rigid body VIM on the mooring system due to shedding from the elliptical fairing may merit analysis; it was outside the scope of DNV RP-C205 and methods described herein. Other references or methods need to be sought for making the VIM assessment.

Design for buckling was a key feature of the buoyancy pod shell due to a net external hydrostatic pressure load arising from either an exclusion or failure of a pressure-compensation system. The buoyancy pod shell used internal ring-tee stiffeners to meet the buckling criterion. Though external stiffeners were not initially considered due to the increased drag, the same ring-tee stiffeners met the buckling criteria if located externally (Figure 3.8.5).

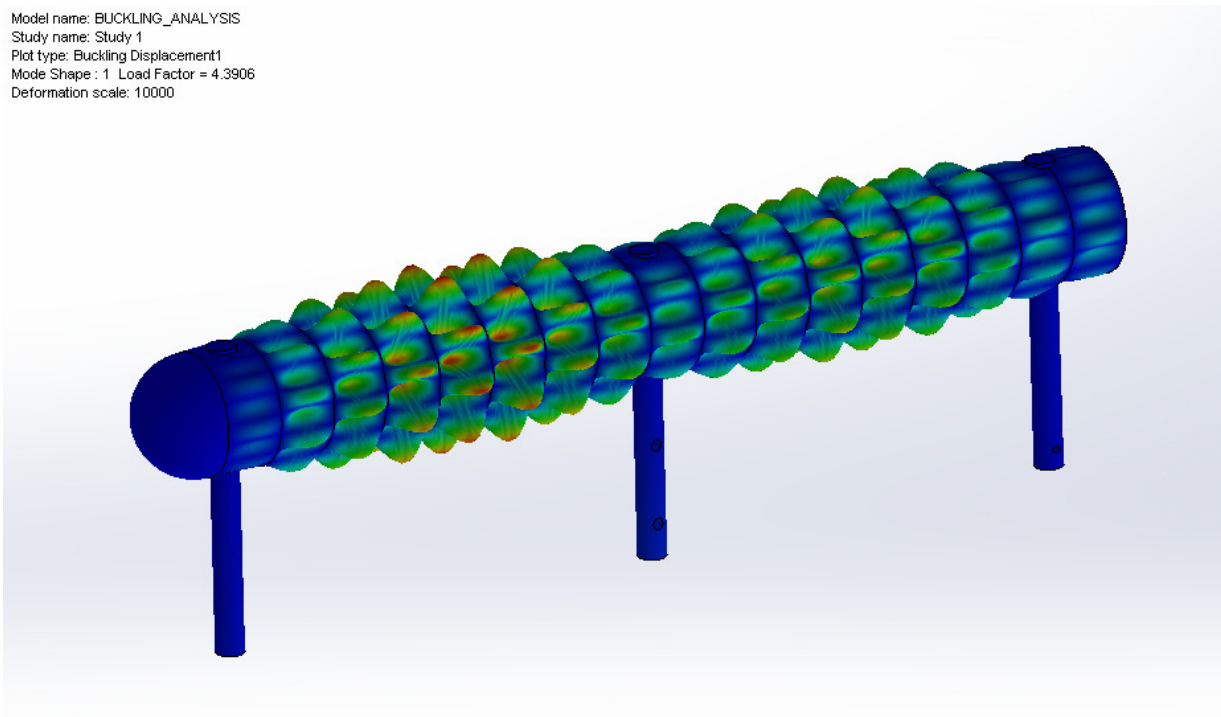

Figure 3.8.5. Buckling of the OCGen® buoyancy pod

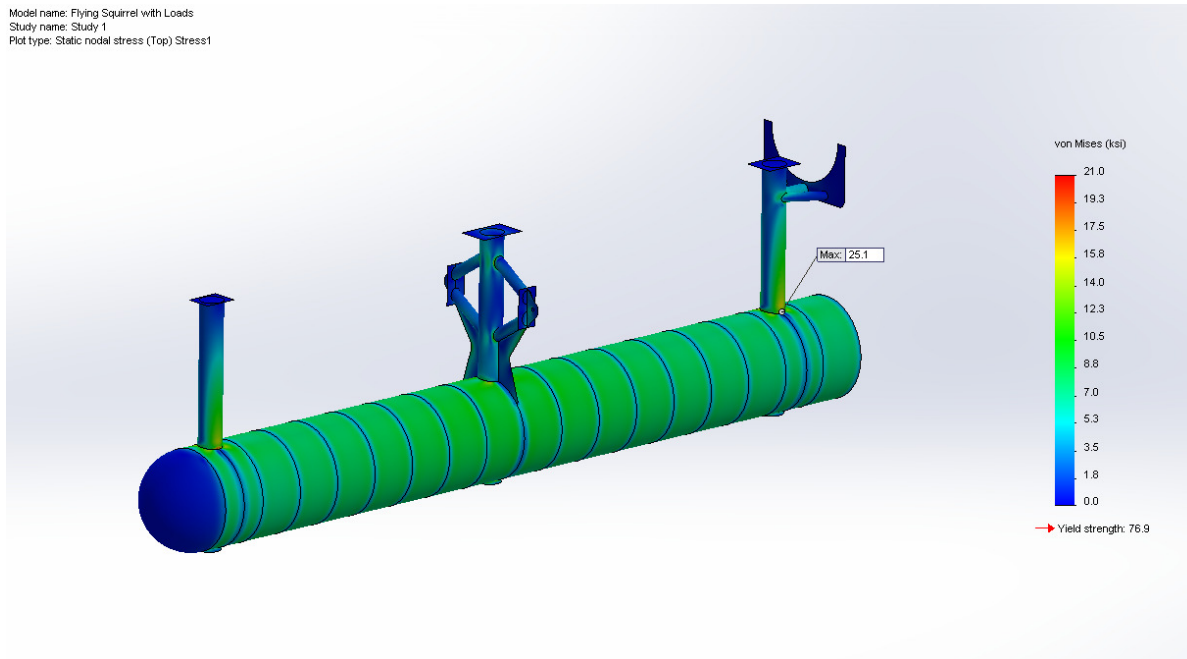

Figure 3.8.6. Von-Mises Stress for OCGen® buoyancy pod with turbines free-spinning

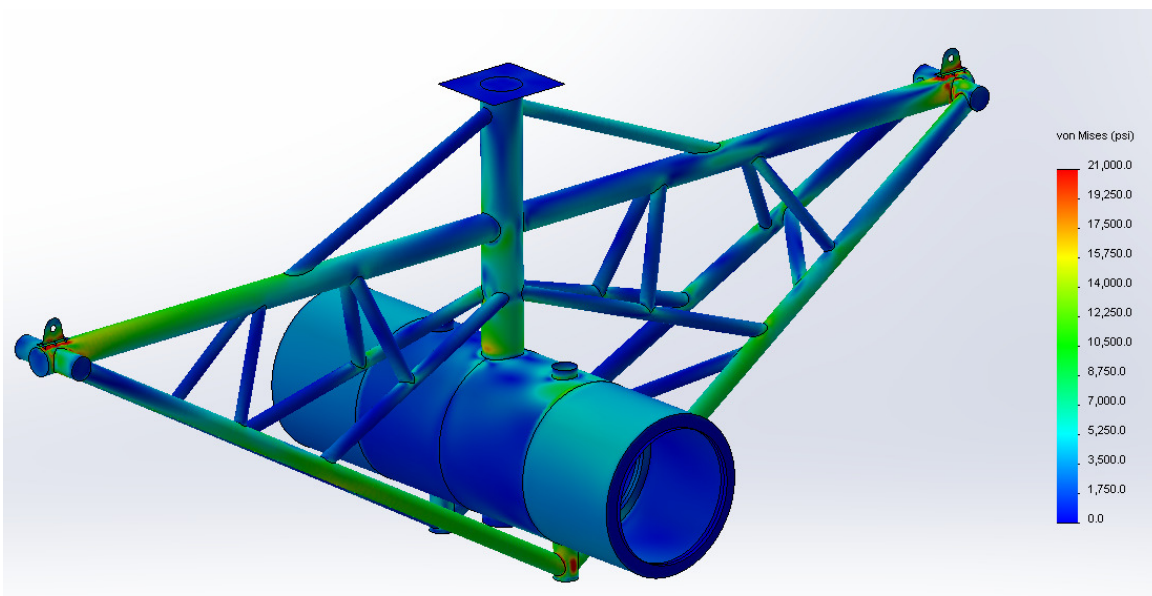

Figure 3.8.7. Von-Mises Stress results for turbines free spinning – mooring line attachment spreader

Fatigue of steel members was not rigorously assessed for the OCGen® pod; though fatigue does need to be assessed due to the oscillatory loading of the turbines and a design life requirement of approximately 20 years. Given an average rotor speed of 40 RPM, the turbines could impart approximately 1E9 stress alternations to the steel structure. However, the alternating component of stress is likely to be small, (< 20% of mean stress), and the mean stress is likely to be well below the allowable stress for most of the time (>75% of operating time) (Figure 3.8.6 and Figure 3.8.7)

Assessment of the effects of a failure of a single mooring line on the full scale OCGen® were not completed as part of this work. However, such an assessment was made for the prototype system. Findings for that work indicated that the mooring loads at the remaining connections would increase and impart additional stresses to the structure. These additional stresses were not expected to lead to failure of the structure. As for the remaining mooring lines, these were sized such that they were capable of accepting the additional loads resulting from failure of a single line, although inspection and potential replacement of all lines would be required after retrieval.

OrcaFlex Model

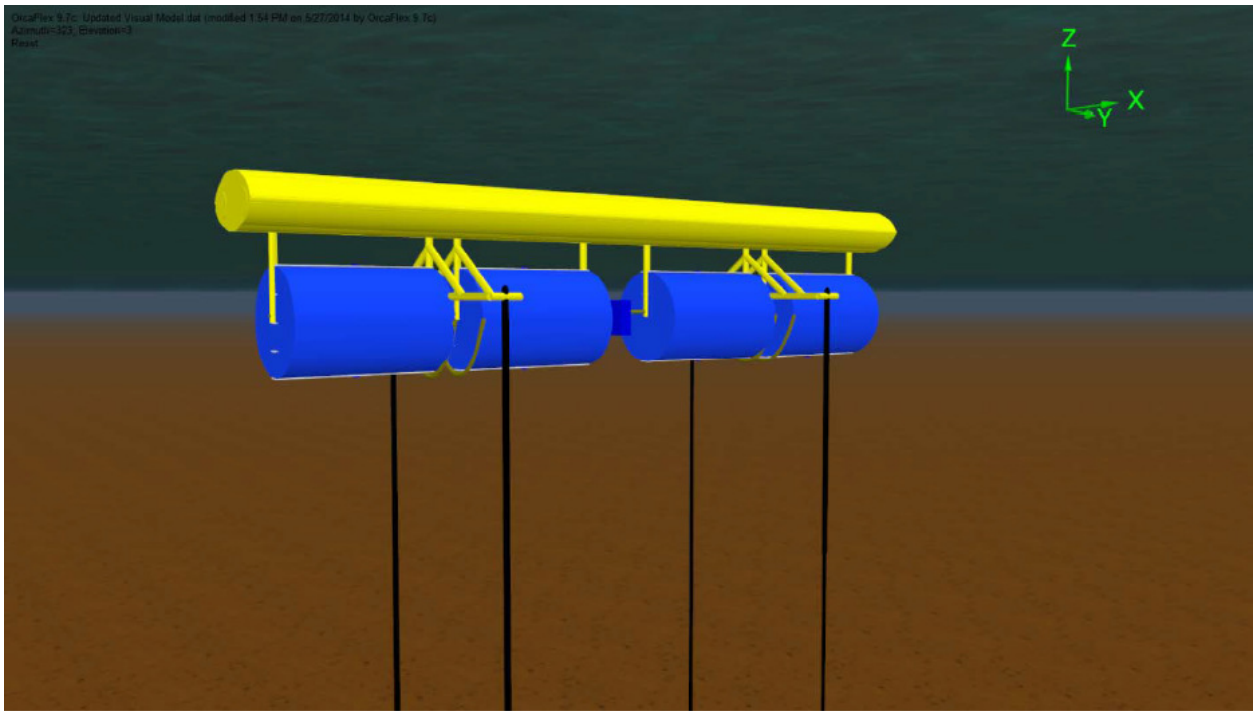

Figure 3.8.8. OrcaFlex model of the full scale OCGen® Power System

Initial models of the mooring lines utilized double braid nylon with an estimated EA value of 2400 kN (Figure 3.8.8). Due to the long length of the mooring lines as compared to the prototype OCGen® Cobscook Bay deployment, the large amount of elastic stretch obtained from the nylon double braid allowed the turbine to take a substantial amount of pitch due to uneven loads between the forward and aft mooring lines. It was determined that for the deeper water at the full scale OCGen® sites, the stiffness of the lines would need to be increased. Increasing the stiffness may be performed by using a stiffer line such as polyester, or using a combination of chain and synthetic line. For this analysis, a polyester double braid mooring line was selected to provide an increased stiffness. The elasticity calculated from the product data elongation curves was estimated at 4,400 kN (Table 3.8.7).

Table 3.8.7. *Mooring line properties for full scale OCGen® system in Western Passage*

Mooring Rope				
Type	Polyester, Double Braid			
	Metric		U.S.	
Diameter	276	mm	3.5	in
Length (Structure to seabed)	90.5	m	297	ft
Weight in Air	5.91	Kg/m	8.79	lb/ft
Weight in Water	1.5	Kg/m	2.23	lb/ft
Break Strength	1549	kN	348,000	lb
Spliced Break Strength (0.9 x MBS)	1394	kN	313,200	lb
Maximum Operating Load	286.5	kN	64,400	lb
FoS (MBS)	4.9	-	4.9	

A design goal was to balance mooring line tensions throughout all operational cases. The vertical position of the mooring line spreader was critical, because the locked and free spinning design cases have disparate loadings, and the ideal vertical location of the spreader was different for each case. The vertical location of the spreader was picked to balance the fore and aft mooring line loads in these cases to avoid very high stresses and slack mooring lines. The vertical position that gives the best load balancing will always be located between the axis of the turbine and the axis of the buoyancy pod.

OrcaFlex models were used to investigate potential mooring line fouling in the turbines or structure and adjustments made to the mooring line attachment points as a result of this analysis (Figure 3.8.9). Earlier models of the system used chain moorings, in shallow water (24-m). The results from this model showed that it was necessary to spread the connection points forward and aft to prevent the mooring lines from contacting the turbine. The device has a fairing on the buoyancy module which effectively acts as a wing, producing lift as the pitch angle increases. This increased the overall vertical force acting on the device and tended to reduce the diving= effect, as the current speed increased. Keeping the device from diving deeper prevented the mooring lines from interfering with the turbines, which occurred at large mooring declination angles. The mooring connection points were adjusted, bringing the mooring connection points closer together and higher. Multiple combinations of line stiffness and connection point spacing may be considered for future refinement of the device. It should be noted that the lift generated by the buoyancy module was the driving force that allowed the mooring line connection points to be shifted closer to the Y-axis. The fairing lift coefficients have a strong influence on the pitch rotation and offsets of the device and should be verified in future modeling efforts. It should also be noted that the added lift also considerably increased the mooring tension due to the increase in vertical force.

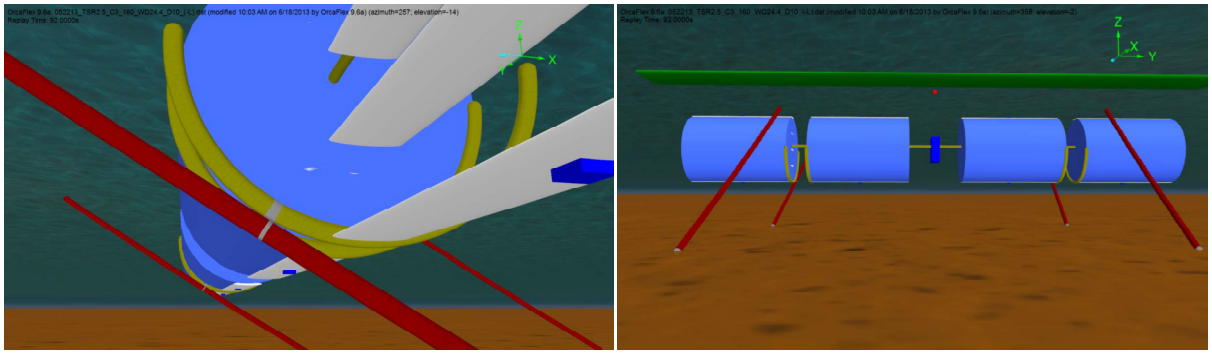

Figure 3.8.9. OrcaFlex model showing potential interference of mooring line with turbines and/or TGU structure

The attachment points were changed from 6.6 m forward and aft of midships to 4.6-m forward and aft of midships. The vertical position of the attachment was raised by .3-m to a position 1.52-m above the turbine drive line.

The OrcaFlex calculated mooring line tension is provided in Table 3.8.8 for the maximum current speed under two current headings directions as well as the baseline 0 current case. The line tension was taken at the top end of the line, at the connection point to the turbine structure, where the maximum tension will occur in the line. The +L and –L cases represented positive and negative turbine lift. Turbine lift direction changed as the flow direction changed from ebb to flood, but this was a relatively minor effect. The maximum mooring line tension found was 286.5 kN, and occurred in both forward lines under a head-on current, with a TSR of 0.

This case also experienced the highest amount of pitch resulting in an increased lift force and larger difference in tension between forward and aft lines, both of which are the driving factors contributing to the higher line tension.

Table 3.8.9 provides the displacement of the model in the X, Y, and Z directions referenced from the starting position of the model, as well as the rotations about the origin of the model. The results showed only a slight variation in rotation in roll and yaw. The maximum pitch angle was nearly 8°. For the most extreme case of a 20° offset current, the yaw of the model is approximately 1°. The maximum roll was less than 1°. The maximum movement in the X direction was 70.7 m, resulting in a forward mooring line angle of 44.2° from horizontal.

Table 3.8.10 provides the maximum mooring loads acting on the anchor connection point. The mooring tensions are separated into vertical and horizontal components for use in the anchor design.

The mooring line size was based on maximum tension load from the mooring analysis. The synthetic fiber mooring lines should operate under a maximum tension of approximately 20% of minimum breaking strength (MBS). Material selection for the line will be dependent on the amount of stretch required from the line, and so will depend on the depth of the deployment. In shallow water deployments nylon lines will be most probably selected in order to provide the required degree of compliance. The issues of water absorption related to nylon, while strength may be reduced, do not appear to have a significant effect on this application. For deeper installations, the use of alternative materials for mooring lines would most likely be necessary.

VIV is more likely to occur for longer mooring lines than for the shorter lines considered previously. It will probably be necessary to equip the mooring lines for deeper deployments with mooring line strakes, or other VIV inhibiting technology.

Table 3.8.8. *OCGen® mooring line tensions – Western Passage*

				Line Tension (kN)				Mooring Line Declination Angle from Horizontal			
TSR	Lift	speed	Dir	Upstream		Downstream					
-	+/-	m/s	Deg	PF	SF	PA	SA	PF	SF	PA	SA
0	-	3	180	**286.50**	**286.50**	229.52	229.52	72.49	72.49	73.14	73.14
2.5	+L	3	180	240.16	240.16	224.32	224.32	54.36	54.36	54.40	54.40
2.5	-L	3	180	267.76	267.76	222.73	222.73	56.08	56.08	56.25	56.25
4	+L	3	180	227.22	227.22	219.10	219.10	44.20	44.20	44.17	44.17
4	-L	3	180	258.48	258.48	**230.19**	**230.19**	48.89	48.89	48.85	48.85
0	-	3	160	274.99	279.45	220.08	224.43	71.94	72.04	72.63	72.71
2.5	+L	3	160	239.21	237.27	223.38	221.41	53.93	54.15	54.01	54.24
2.5	-L	3	160	260.67	263.48	217.04	219.82	55.49	55.49	55.66	55.64
4	+L	3	**160**	228.23	225.26	219.67	216.70	43.92	44.10	43.92	44.10
4	-L	3	**160**	254.78	254.95	227.27	227.41	48.36	48.43	48.32	48.39
0	-	0	-	116.65	116.65	116.65	116.65	90.00	90.00	90.00	90.00

Table 3.8.9. *OCGen® TGU rotation and translation – Western Passage*

				Rotation (Local Axis)			Net Translation Relative to Base Position		
TSR	Lift	speed	Dir	Roll	Pitch	Yaw	X	Y	Z
-	+/-	m/s	Deg	Deg	Deg	Deg	(m)	(m)	(m)
0	-	3	180	0.00	-7.80	0.00	-34.31	0.00	-3.59
2.5	+L	3	180	0.00	-2.58	0.00	-59.39	0.00	-18.50
2.5	-L	3	180	0.00	-6.97	0.00	-57.11	0.00	-16.47
4	+L	3	180	0.00	-1.54	0.00	-70.68	0.00	-29.37
4	-L	3	180	0.00	-4.83	0.00	-65.72	0.00	-23.71
0	-	3	160	-0.53	-7.49	0.74	-33.58	10.32	-4.10
2.5	+L	3	160	-0.50	-2.35	0.95	-56.60	19.13	-18.84
2.5	-L	3	160	-0.24	-6.83	-0.02	-55.06	17.75	-17.15
4	+L	3	**160**	-0.41	-1.38	0.71	-67.20	22.48	-29.58
4	-L	3	**160**	-0.25	-4.67	0.28	-62.93	20.69	-24.31
0	-	0	-	0.00	0.00	0.00	0.00	0.00	0.00

Table 3.8.10. *OCGen® mooring block loads – Western Passage*

				Mooring Loads at Seabed (Global Axes)											
TSR	Lift	speed	Dir	PF			SF			PA			SA		
-	+/-	m/s	Deg	Fx	Fy	Fz	Fx	Fy	Fz	Fx	Fy	Fz	Fx	Fy	Fz
0	-	3	180	118.7	0.0	-262.2	118.7	0.0	-262.2	98.9	0.0	-208.5	98.9	0.0	-208.5
2.5	+L	3	180	159.3	0.0	-181.5	159.3	0.0	-181.5	149.8	0.0	-168.7	149.8	0.0	-168.7
2.5	-L	3	180	170.2	0.0	-208.4	170.2	0.0	-208.4	144.3	0.0	-171.4	144.3	0.0	-171.4
4	+L	3	180	175.2	0.0	-146.7	175.2	0.0	-146.7	169.4	0.0	-141.0	169.4	0.0	-141.0
4	-L	3	180	185.6	0.0	-181.8	185.6	0.0	-181.8	166.9	0.0	-160.5	166.9	0.0	-160.5
0	-	3	160	111.8	-35.1	-250.2	112.7	-35.6	-254.6	93.0	-29.1	-198.7	94.1	-29.6	-203.0
2.5	+L	3	160	151.3	-51.4	-179.7	149.6	-51.1	-178.7	142.3	-48.0	-167.2	140.6	-47.6	-166.0
2.5	-L	3	160	159.7	-51.8	-201.1	161.3	-52.3	-203.4	135.4	-44.0	-165.5	137.0	-44.5	-167.8
4	+L	3	160	167.3	-56.2	-146.7	164.9	-55.6	-145.1	161.5	-54.0	-140.8	159.1	-53.4	-139.2
4	-L	3	160	175.2	-57.8	-177.6	175.1	-57.9	-178.0	157.7	-52.0	-157.1	157.6	-52.1	-157.3
0	-	0	-	0.0	0.0	-117.9	0.0	0.0	-117.9	0.0	0.0	-117.9	0.0	0.0	-117.9

OrcaFlex was used to determine the natural frequency of the overall system. The natural frequency was calculated for the model in two static state cases, no current and 3.0 m/s at 180°. The frequency of the first 10 modes of oscillation is provided in Table 3.8.11.

The shortest period of the flow variations provided in the analytical current model is 60s. The longest modal period calculated for oscillation of the moored structure was 22.73s. The natural period of the structural response was less than half of the shortest expected period of variation in the current; therefore, ORPC does not expect dynamic amplification of the oscillations of the turbine due to resonance with the current variations. For turbulent flows with shorter periods, ORPC expected that the length scale will be small enough so as not to affect the entire structure simultaneously.

Table 3.8.11. *OCGen® modal analysis results*

	No Current		1.5 m/s @180 deg		3.0 m/s @180 deg	
	Period	Frequency	Period	Frequency	Period	Frequency
Mode	(s)	(Hz)	(s)	(Hz)	(s)	(Hz)
Mode 1	22.73	0.044	22.10	0.04526	16.65	0.06007
Mode 2	22.71	0.04404	22.08	0.04528	16.64	0.06009
Mode 3	22.48	0.04448	20.87	0.04791	10.72	0.09328
Mode 4	3.84	0.26049	3.87	0.25863	3.95	0.25329
Mode 5	3.63	0.27532	3.67	0.27239	3.70	0.27043
Mode 6	1.66	0.60094	1.73	0.57941	1.95	0.51173
Mode 7	1.61	0.6213	1.60	0.62619	1.19	0.84113
Mode 8	1.61	0.6213	1.59	0.62802	1.19	0.84353
Mode 9	1.61	0.6213	1.58	0.63389	1.18	0.84702
Mode 10	1.61	0.6213	1.56	0.64091	1.17	0.85296

The Orcaflex model was analyzed through a dynamic simulation using a 6.25 hour current time series. The analytical flow time series is plotted in Figure 3.8.10. Figures 3.8.11 through Figure 3. 8.13 show the results of the mooring tension of the forward and aft lines. As the current direction being at 180°, the tension in the starboard lines matches the port lines. The results showed that the line tension and motion of the turbine closely follow the change in current speed; that there was no substantial increase in mooring tensions due to the effects of dynamics, and therefore no substantial increase in turbine motion; and that there was a lag of approximately 4-sec between the change in current speed and the mooring tension response. The 4-sec lag is small compared to the 60- sec period of the current oscillation, and is equivalent to 0.42-radians. The results showed no indication of an amplification of response of the system due to the time varying current speed.

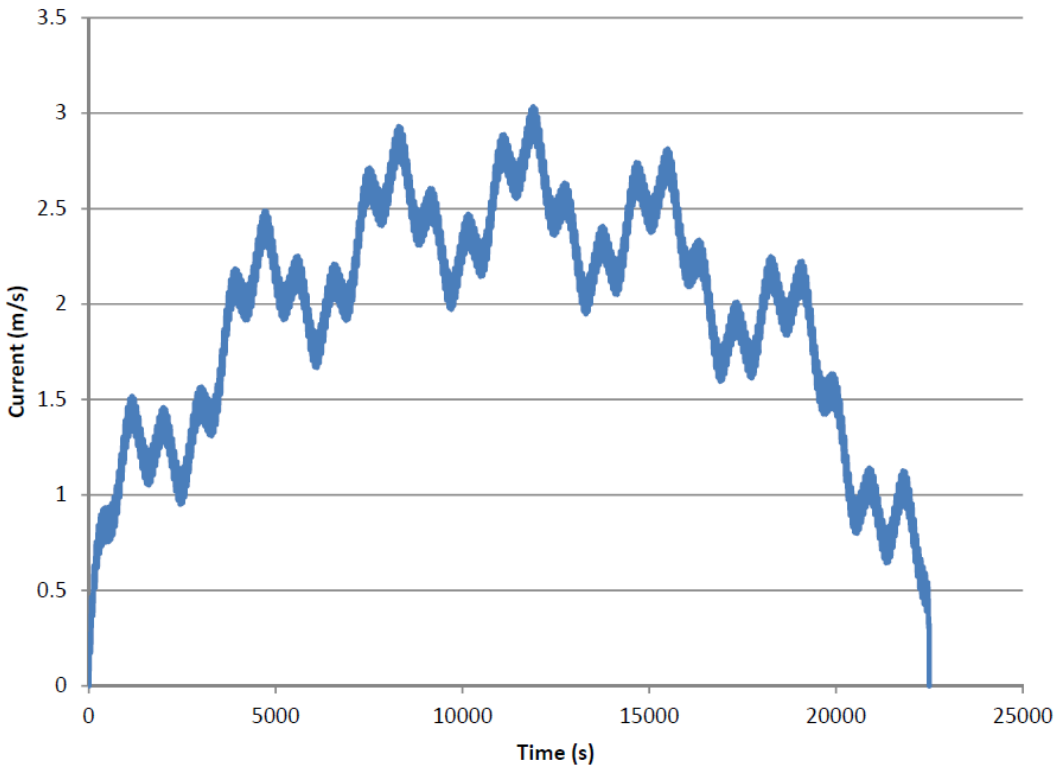

Figure 3.8.10. OrcaFlex model flow speed input

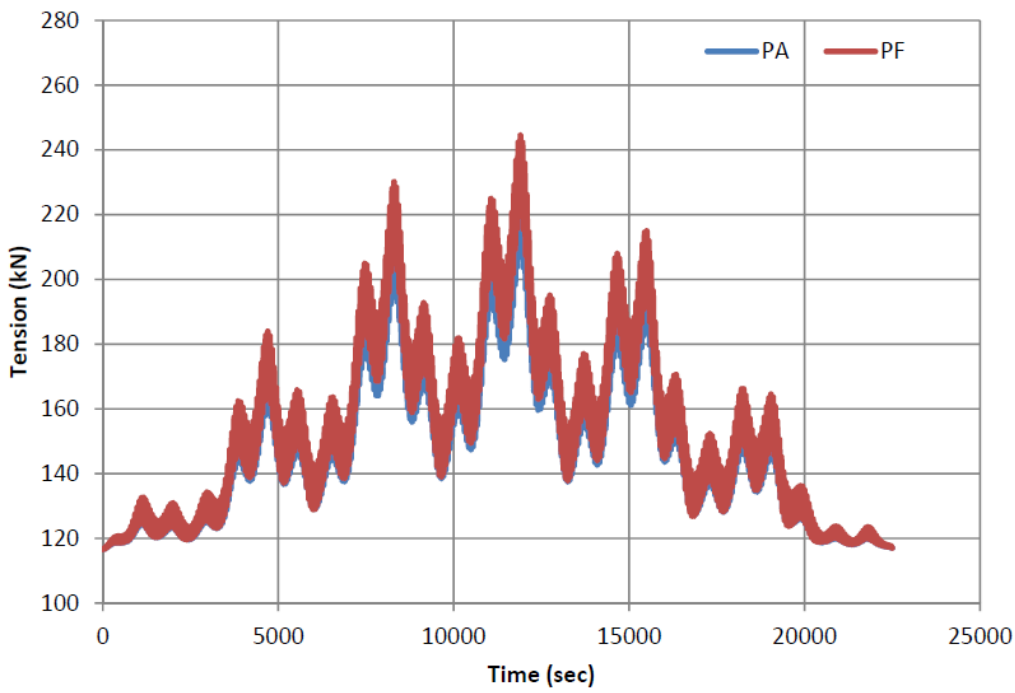

Figure 3.8.11. OrcaFlex model outputs for port mooring line tensions. Fore and aft tensions overlay each other as the flow is from straight ahead.

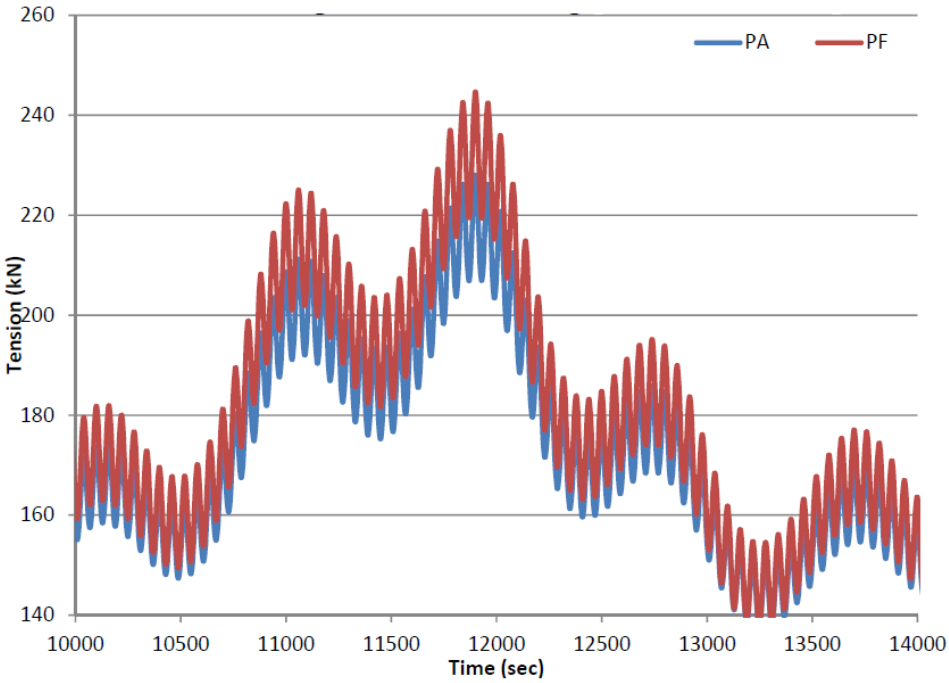

Figure 3.8.12. OrcaFlex model outputs for port mooring line tensions for a subset of time. Fore and aft tensions overlay each other as the flow is from straight ahead.

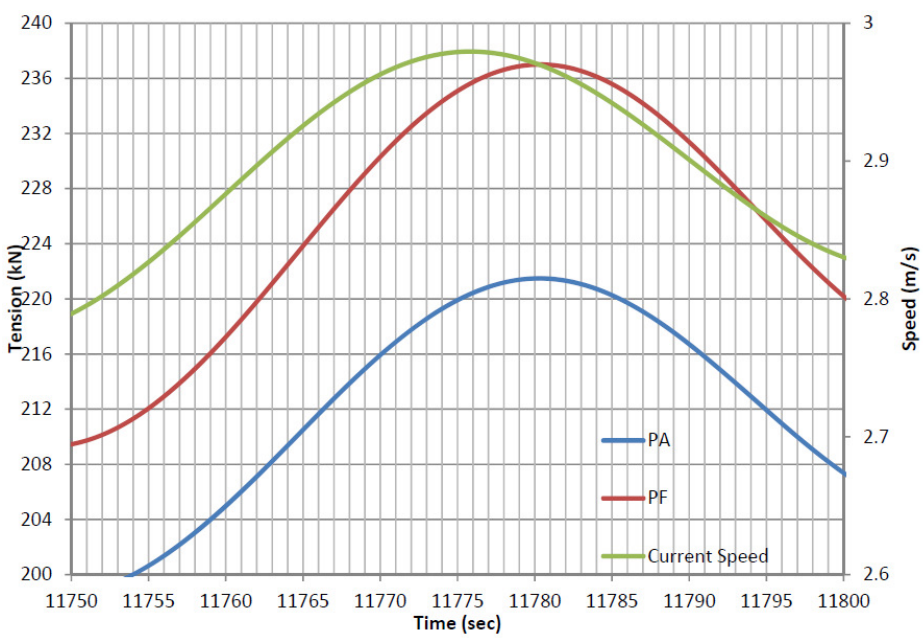

Figure 3.8.13. OrcaFlex model outputs for port mooring line tensions compared to input current speed. Fore and aft tensions overlay each other as the flow is from straight ahead. The small difference is due to numerical rounding errors in the model. The phase lag between input current and tension response is approximately 4 seconds.

Mooring Blocks

For a taut leg mooring, the anchor types to choose from included types of gravity anchor, or piles or pins, either driven or drilled and grouted into the seabed. The soil data available suggested that there is a thin layer of gravel over top a layer of bedrock. Ideally, any pile would need to be secured to the bedrock layer.

The long term effects of biofouling on the gravity based anchor systems have not been fully evaluated, but the expectation is that biofouling will not result in degration of the materials (concrete and steel), and that the additional loads die to bio-accumulation will be small as the water speeds at the seafloor are low. However, the additional weight of accumulated materials will affect the retrieval process, as the lifting requirements will be increased.

The gravity anchors can be designed for the site using mooring loads from Table 8.10. Loads for the full scale mooring are approximately three times those of the prototype moorings, due to both the increase in structure size, but also due to the increase in design water speed. Since these anchors are rather heavy and may be difficult to move, and because the bathymetry of the Western Passage site is so variable, alterative anchoring techniques are worth evaluating.

SMD-BORD has capabilities for developing machinery for subsea installation of piles in many types of bottom substrates. However, it is very important to have detailed bottom information for proper anchor and machinery design. Layers of loose gravel can be very challenging to drill through. A thick layer of gravel may require excavation in order to secure an anchor to the bedrock below. If the substrate consists of a mixture of gravel and soil, drilling may still be possible.

SMD-BORD has an anchor design that is the shape of a hollow cylinder. The drill bit itself is left in the seabed and becomes the anchor. Once drilled into the seabed, grout is injected to secure it. SMD also designs innovative machinery for installing subsea piles.

Sample calculations for various pile sizes for the SMD-BORD design for a Western Passage deployment are presented in Table 3.8.12.

Table 3.8.12. *Pile capabilities for the SMD-BORD system*

Pile diameter (m)	2.0	1.5	0.6
Pile wall thickness (m)	0.075	0.060	0.020
Pile length (m)	10.0	9.0	2.5
Pile weight in air (Tonne)	52.0	26.0	1.4
Horizontal Moment Capability (Tonne m)	3,700	1,810	30
Vertical Load Capability (Tonne)	691	420	45

Marine Micro-Pile Technology is another company that has developed an anchor system involving multiple small diameter pin piles used to secure a foundation to the seabed by drilling and grouting

them in to the substrate.[18] A concept drawing of the micro-pile technology as applied to the OCGen® concept is shown in Figure 3.8.14 and Figure 3.8.15.

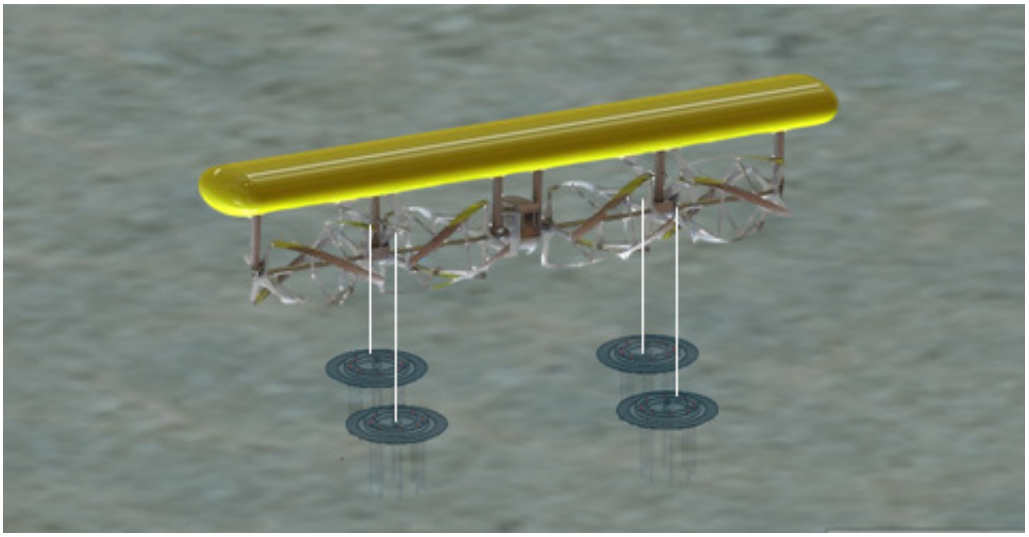

Figure 3.8.14. Marine Micro-Pile Technology as applied to the OCGen® TGU

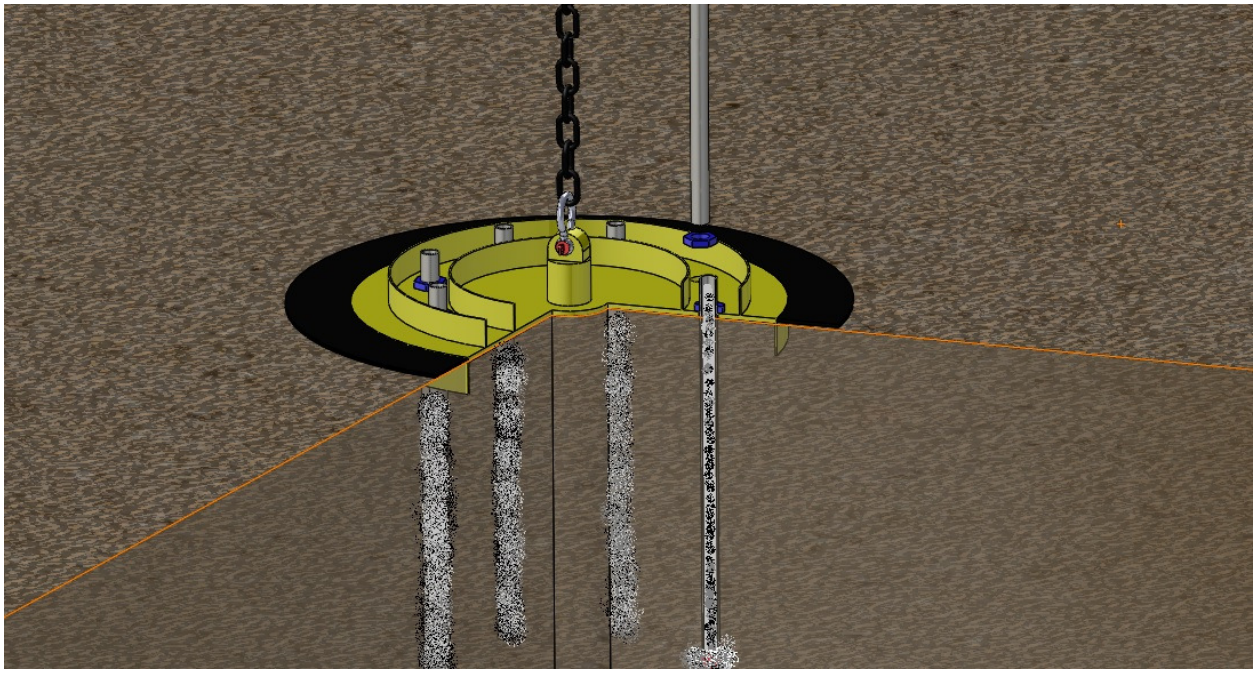

Figure 3.8.15. Marine Micro-Pile Technology view of the pin piles and retaining plate.

[18] Sound & Sea Technology, Inc. (2012, November 9) Advanced Anchoring Technology. Final Technical Report, U.S. Department of Energy, OSTI: EE0003632

Either of these anchor types may be appropriate for the conditions present in Western Passage. Further exploration, including geotechnical sampling would provide the data necessary for properly designing an anchor.

Problems Encountered
None

Departure from Planned Methodology
None

Assessment of Impact on the Project Results

Design of the commercial, full-scale prototype was developed. Based on additional inputs received from the work performed in Task 7, some additional work is required to fully complete the full scale design. In particular, detailed design of the connection points between the mooring blocks and the mooring line needs to be reassessed in the light of the abrasion of the mooring line found at this connection during the deployment. Additional consideration is also need for the mooring line sheathing material in order to ensure maximum abrasion resistance.

4. PRODUCTS

4.1 Publications

<u>Master's Thesis</u>

DuBuque, G. (2011). *A Lumped Parameter Equilibrium Model of a Submerged Body with Mooring Lines* (Unpublished master's thesis). University of Washington, Seattle, Washington.

Fabien, B. The Static Equilibrium of a Submerged Body with Slack Mooring, in L. Dai & R. Jazar (Eds.), *Nonlinear Approaches in Engineering Applications*. New York, NY: Springer, 2012 (pp. 211-236).

Nichol, T. (2014). *Numerical Modeling of Compliant-Moored System Dynamics with Applications to Marine Energy Converters* (Unpublished master's thesis). University of Washington, Seattle, Washington.

Nichol, T., Dubuque, G., & Fabien B. (2014, April). Dynamic modeling of compliant-moored submerged systems with applications to marine energy converters. 2nd Marine Energy Technology Symposium, Seattle, WA.

<u>Public Press</u>

ORPC's tidal energy system successfully proves its performance. (2014, November 4). *Offshorewind.biz.* Retrieved from http://www.offshorewind.biz/2014/10/30/ orpcs_tidal_energy_system_ successfully_ proves_its_performance

ORPC taps tidal sweet spot. (2014, November 5). *ReNews.biz.* Retrieved from http://renews.biz.78575/ ORPC-taps-tidal-sweet-spot/

Ling, K. (2014, November 11). Energy Technology: Cruel sea, scarce cash hinder quests to harness ocean's might. Retrieved from http://www.eenews.net/stories/1060008679

Ling, K. (2014, November 13). Energy Technology: Calloused hands steer voyage to clean power's new world. Retrieved from http://www.eenews.net/stories/1060008840

4.2 Website

The following websites reflect the results of this project:

- ORPC's website: http://www.orpc.co/content.aspx?p=h3jCHHn6gcg%3d
- Facebook: https://www.facebook.com/pages/Ocean-Renewable-Power-Co/207103839024

4.3 Networks or Collaborations

- OES Annex IV
- OES Annex V
- TC114
- Maine Tidal Power Initiative
- OREC
- NHA
- E2 Tech Council
- MOWI
- New England Clean Energy Council

4.4 Technologies

OCGen® Power System

4.5 Inventions

ORPC filed U.S. Provisional Application 61/506,445, Dynamic Lift System for Underwater Turbine (filing date 07/11/2011; expired 07/11/2012).

4.6 Other Products

Presentations

McEntee, J. (2014, October 30). OCGen® Module Mooring. American Society of Naval Engineers. Portland, ME

McEntee, J. & Johnson, N. (2014, November 13). OCGen® Prototype Testing. Maine Ocean and Wind Industry Initiative.

Technical Poster

OCGen® Module Mooring Project: Proving the technical and economic viability of a fast-water mooring system for tidal and ocean current hydrokinetic devices. International Conference on Ocean Energy. Halifax, NS. (2014, November 4).

5. COMPUTER MODELING

Specifics of computer models and techniques are included in the individual task descriptions above.

6. LESSONS LEARNED

Lessons learned during the Project are summarized below by Task:

- Task 1
  - CFD is not yet appropriate as a rapid iteration design tool.
  - FAVOR techniques may be superior to RANS or LES codes for large scale simulations, but will probably be inadequate for applications where boundary layer effects are significant.
  - While rapid design iterations will still be performed using other techniques, the CFD analyses could be used to validate the final design, before construction and deployment. This will become a more viable approach as computer resources become less constricting and CFD tools become more efficient.

- Task 2
  - The lumped systems modeling approach may have utility if the user interface is developed.

- Task 3
  - Commercial modeling codes offered the potential for widely validated codes, a significant user base, and easy to use interfaces.
  - A significant level of expertise was required for proper use of these codes. Multiple variable inputs were not particularly clearly defined and were typically estimates based on prior experience.

- Task 4
  - Scale modeling efforts offered the ability to rapidly iterate through various model arrangements.
  - The results were more useful in a qualitative sense rather than quantitative.
  - Correlation of scale model results with analytical models was an intensive effort and focused on the model scale physics rather than the full scale physics. Issues of Reynolds number scaling versus other types of scaling will confound the effort to scale all aspects of the physical behavior.
  - Scale model testing was perhaps best utilized by a combination of initial analyses and concurrent model testing. Some amount of modeling will limit the number of test options, and scale model testing will confirm that the analyses have qualitative basis, providing validation before moving onto detail design.

- Task 5
  - Accuracy of geophysical investigation limited the utility of comparing multiple surveys to determine effects of any installation. The ability to discriminate difference properly required changes in the order of meters in depth. These large changes are not likely in small MHK installations.

- Task 6
    - A tension leg mooring system for a fully submerged body benefited from the presence of compliance in the mooring lines, as this allows for a degree of imprecision in placing the mooring blocks while retaining relatively even loads in the mooring lines.
    - The use of gravity moorings offers benefits to a project design as it is inherently less sensitive to variation in the subsea soil conditions. Issue of documentation of multiple designs, inability to produce or procure anchors in any kind of volume for a given project, a significant amount of uncertainty related to the design life for the mooring as each installation is different, and the requirement for developing different inspection procedures for each mooring in a site can be addressed by the use of a single gravity type mooring.

- Task 7
    - Sufficient operating experience was obtained for owners to develop bid specifications that were sufficient for contractors to be able to offer fixed price contract terms for various aspects of the work. This limits financial risks for technology and project developers.
    - Instrumentation redundancy is highly beneficial in subsea applications. The use of multiple instrument suites, powered by different power supplies, and reporting data in different manners, reduces the risk of a loss of data due to a failure of an instrument. ORPC would recommend that programmatic funding be dedicated to the development of a standardized instrumentation suite capable of sustained data collection and storage for MHK applications.

      Existing efforts at various DOE funded laboratories are attempting to address this particular issue. Significant progress has been made with the Modular Ocean Instrumentation System at NREL, and with Florida Atlantic University's (FAU) Southeast National Marine Renewable Energy Center (SNMREC) work on MIMOSA. ORPC would suggest that these instrumentation packages and standards be promulgated more widely, and that perhaps it be suggested by DOE that use of these existing packages be considered in any funded DOE MHK program.

    - Data gaps occurred during deployment as the data acquisition system required power from shore to function. Development of an autonomous data logging system would be beneficial.
    - ORPC would recommend that DOE consider assisting awardees with data collection and analysis plans prior to deployments. Assistance could be provided directly by National Laboratories.
    - Corrosion remains an area of concern and greater attention needs to be paid to details of bolted joints, or any other electrically isolated components subject to corrosion failure. Because the corrosion issue was allowed to pass through the design process, it raises other questions related to engineering process.
        - Risk identification and control is necessary for these innovative deployments. The institutional use of FMEAs and HAZOP analyses should be encouraged. Support for such analyses may be available from the national laboratories, and if

so, it would be beneficial for projects to utilize those services for the specific cases.
  - Outputs from these analyses will potentially identify modes of failure which may require specific monitoring.
  - Given the above, it is necessary to point out that all innovative projects like this cannot, by definition, be totally successful in all aspects. Monitoring all potential failure modes would be expensive and would potentially overwhelm a project budget.
  - In addition, ORPC believes that one or more failures should be expected in order for learning to occur. In the absence of failure, all that may be proven is that the system is overdesigned and the failure points are unknown.

- Task 8
  - Design of a full scale OCGen® device and mooring system can be achieved to a significant level of detail and can then be improved based on results and lessons learned from this Project, along with ORPC's Advanced Controls project (DE-EE0006397) and Power Take Off project (DE-EE0006398), leading to a final design of a full scale power OCGen® Power System that could be built, installed and benchmark tested by the end of 2016.

7. PLANS TO ADDRESS LESSONS LEARNED

The design tools created and designs developed, the data collected and analyzed, as well as the lessons learned, are a critical step in ORPC moving forward with the final design, procurement, building, deployment and benchmark testing of a full scale OCGen® Power System.

Subject to obtaining sufficient funding, ORPC plans to build, install and test a full scale OCGen® device and mooring system in 2016 at its FERC licensed Cobscook Bay site in Maine utilizing the existing infrastructure from the Cobscook Bay Tidal Energy Project, which was partially funded by DOE. This infrastructure includes the subsea power and data connection pod and cables to shore and the on-shore station with interconnection to the Emera Maine power grid. These assets are maintained on a regular basis by ORPC in anticipation of such a benchmark testing project.

The analytical tools best suited for design of subsea mooring systems include commercial mooring codes such as OrcaFlex and others. These well validated codes have proved useful and have been validated by this Project for use in this application. They will continue to be used in final design of the full scale OCGen® device and mooring system.

Instrumentation and data reliability issues will be addressed moving forward by the development of a suite of standalone data loggers and recorders capable of limited time autonomous operation. This will address data gaps noted during deployment, retrieval, and during times when network connectivity was insufficient to transmit data to shore.

As the design of the OCGen® Power System becomes more mature with validation of basic concepts, the engineering work will move from benchmark testing deployments to longer term commercial deployments. In this process, reliability of the systems will become the critical factor. To ensure reliability, the quality of the design process must improve and this will occur with the use of structured

engineering approaches including the use of Work Breakdown Structures, Product Development Roadmaps, formal use of Failure Modes and Effects Analysis, and other engineering tools. These approaches to designing commercial products are already being implemented in ORPC's work.